THE HIND LIMB ANATOMY AND LEAPING BIOMECHANICS OF GIBBONS (HYLOBATES)

This thesis is the result of my own work. The material contained in the thesis has not been presented, nor is currently being presented, either wholly or in part for any other degree or other qualification.

Thesis submitted in accordance with the requirements of the University of Liverpool for the degree of Doctor of Philosophy by

Anthony J. Channon

May 2010

This thesis is dedicated to my grandfather, Francis 'Trevor' Preece, who made me laugh with practically every word he said. His kind nature and magnetic personality made it impossible for me not to love him more every time I visited my 'red granddad'.

Acknowledgements

Like any major project this thesis reflects the work, time, effort and patience of many individuals and without their input I am sure it would have never made it this far. I must start by thanking Evie Vereecke, who not only conceived the premise of the project, but appointed me to the post. Her quiet, thoughtful approach, deep wisdom and passion for research turned out to be the perfect antidote to my fast and relentless chattering, which at times must have been near intolerable. Very literally, without her support and guidance throughout this project, it simply could never have happened.

Michael Günther and Robin Crompton provided an astounding literary knowledge and sprinkled scientific brilliance throughout this thesis. They changed my approach to solving biological problems, encouraging me to consider the ecological context in which the animal exists, where before I considered only the physics its body was subject to. In short, they transformed me from a biomechanist into a biologist. They also provided day to day supervision for me for the final 18 months of the project, without ever expressing anything but happy enthusiasm. Again, without them, it is hard to see how this project could have ever been completed.

Much of the experimental work presented here depended on animals (both living and dead) being available for experimentation. Dissection material was kindly provided by the Royal Zoological Society of Antwerp and the National Museums of Scotland. Access to live gibbons for our leaping experiments was granted by the Wild Animal Park, Planckendael, Belgium. Never have I met a more willing and enthusiastic staff of zoo keepers than here. They happily provided the solutions to all of the inherent problems with zoo based studies, with almost no administrative tape in a friendly and personal manor. I also thank the University of Liverpool and the Royal Society for funding and the opportunity to teach undergraduates throughout my degree.

Kristiaan D'Août was critical during the installation of our experimental equipment and was kind enough to turn away as he laughed at my custom made leaping apparatus. He added valuable insight to several of the chapters of this thesis, and proved an entertaining conference roommate and a good friend.

Of course, the successful completion of this kind of work also relies on the support of the family and friends whose shoulders we seek to lean upon when things aren't going well and this is no exception. My friends provided critical down time, bought beers, and suffered my ranting without protest, they are too numerous to list but worthy of special mention are Todd Pataky, Mary Blanchard, Philip Cox and Andrew Preston (who, along with Todd, also provided formidable squash opposition).

Old friends who visited me and provided sofas and beer when I visited them, even when I bored them to tears with what I was doing at work included: Steven Light, Steven Peck, Steven Johnson, Graham Ferridge and Roger Garner.

My mother and father have given unwavering support and love throughout my life. I change my mind about almost everything most days and I thank them for endless patience and entertaining all of my ideas, regardless of how hare brained they were. They are my life 'supervisors' and this thesis is as much a product of their support and patience as it is my work.

Finally, I have to thank my girlfriend. Sarah is the net that stops me from falling but which frees me to soar and her love is why I go home at night. Amazingly, even while wearing her 'knowing' smile, she has no idea how brilliant she truly is, or lucky I am.

Anthony J. Channon

Table of Contents

List of Figures 6

List of Tables 13

Chapter 1 : Introduction 14

Gibbon Locomotor Biomechanics 14

Hind limb functional anatomy 17

Leaping as a locomotor mode 19

Gibbons as leapers 22

Chapter 2 : Mechanical constraints on the functional morphology of the gibbon hind limb 25

Abstract 25

Introduction 26

Materials and Methods 28

Subject data 28

Scaling and functional muscle groups 28

Muscle PCSA and fascicle length 33

Tendon function 35

Results 36

Descriptive anatomy 36

Hind limb muscle volume 38

Muscle PCSA and fascicle length 42

Tendon anatomy 42

Discussion 46

Gluteus superficialis and adductor magnus 46

Muscle volume: Adaptations for vertical climbing, orthograde clambering and leaping? 46

Functional implications of the gibbon's hind limb anatomy 47

Tendon anatomy: Elastic energy storage or ideal mass distribution? 50

Interspecific differences 51

Conclusion **53**

List of abbreviations **53**

Chapter 3 : Muscle moment arms of the gibbon hind limb: implications for hylobatid locomotion. **55**

Abstract **55**

Introduction **56**

The functional importance of muscle moment arms 56

Methods of measuring moment arms 57

Why use cubic splines? 58

Muscular properties of the gibbon hind limb 59

Materials and Methods **60**

Subject data 60

Moment arm measurements 60

Curve fitting 62

Fascicle strain model 64

Hind limb kinematics 66

Results **67**

Muscle moment arms 67

Fascicle strain model 71

Discussion **73**

Muscle function 73

Large MAs for fine control, small MAs for angular velocity and elastic energy storage 78

Comparison of techniques, spline versus polynomial 80

Assessment of the fascicle strain model 81

Conclusions **82**

List of Abbreviations 83

Chapter 4 : The Biomechanics of Leaping in Gibbons. 85

Abstract 85

Introduction 86

Materials and Methods 88

Equipment and experimental setup 88

Limb kinematics 91

Biomechanical parameters 92

Statistical Analyses 94

Results 94

Leap types 94

Joint kinematics 97

Centre of mass movement 104

Impulse 104

Mechanical and kinetic energy 104

Work and power 107

Take-off angle vs. take-off velocity 107

Discussion 107

The biological employment of different leap types 107

Comparisons with other leaping primates 112

Take-off angle 114

Further work 115

Conclusions 116

List of Abbreviations 116

Chapter 5 : The Effect of Substrate Compliance on the Biomechanics of Gibbon Leaps 118

Abstract 118

Introduction 119

Materials and Methods 121

Results 125

Orthograde Leaps: Stiff vs. Compliant pole 125

Pronograde Leaps: Stiff vs. Compliant pole 130

Discussion 134

Leaps from compliant vs. stiff substrates 134

Using elastic energy storage in substrates 137

Wild animals using compliant substrates 139

Future Work 141

Conclusions 143

List of Abbreviations 143

Chapter 6 : Biomechanical analyses of maximally performed gibbon leaps: Results from a field-employable centroid resolution technique. 145

Abstract 145

Introduction 146

Materials and Methods 150

Filming and measurements 150

Post collection analysis 150

Calibration of the enclosure 152

Calibrating each video sequence 152

Biomechanical Parameters 153

Technique validation and sensitivity analysis 157

Results 159

Leap Biomechanics 159

Discussion 162

Leap Biomechanics 162

Assessment of the technique 167

Conclusions 168

List of Abbreviations **169**

Enclosure calibration 169

Video sequence- specific calibration 170

Biomechanical parameters 170

Chapter 7 : General Discussion **172**

Functional morphology: what is the gibbon hind limb specialised for? **172**

What is left to learn? 176

Leaping biomechanics: are gibbons leaping specialists? **177**

The role of substrate compliance in gibbon locomotion 179

What is left to learn? 181

References **183**

Appendices **204**

List of Figures

Figure 1.1. Showing how the centre of mass position, circles for each segment, can be raised from the extended hind limb posture, left (blue), to the flexed hind limb posture (red) during brachiation by leg lift. 16

Figure 1.2. A schematic drawing of a siamang propagating a tree branch before leaping to a lower level. Reproduced from Fleagle (1976). 21

Figure 2.1. Hind limb muscle mass (HLMM) against Body Mass for the individuals where body mass was known. Dashed line shows linear regression. 32

Figure 2.2. Muscle function estimated by position on a graph of PCSA against fascicle length 34

Figure 2.3. Photographs showing the presence of separated (specimen *H. lar* 2) and fused (specimen *S. syn* 1) plantaris muscles. 37

Figure 2.4. The gluteus superficialis muscle, with indication of thigh insertion and tensor fascia lata 37

Figure 2.5. The contribution of each functional group to total hind limb muscle volume and the position of each group on the skeleton. Error bars denote the standard error of the mean. 41

Figure 2.6. Plot of PCSA (scaled to hind limb muscle mass – $HLMM^{2/3}$) against fascicle length (scaled to $HLMM^{1/3}$) for gibbon hind limb muscles. Figure key: Different colours represent different muscle groups; black = knee extensors, red = hip extensors, blue = digital flexors, yellow = adductors, green = hip extensors and knee flexors, mauve = digital extensors, grey = uni-articular knee flexor, cyan = dorsal flexors, pink = plantar flexors, gold = hip rotators, open symbols = bi-articular knee and hip flexors. Different symbols represent different species: cross = siamang, diamond = lar gibbon (white handed gibbon), circle = moloch gibbon, square = pileated gibbon. The red star represents the position of the iliacus muscle from Payne et al. (2006a). 43

Figure 2.7. Estimated safety factors for tendons in the hind limb. (i) denotes an insertion tendon, (o) denotes a tendon of origin. Bars represent the mean of all species. Symbols represent the mean from each species. See Table 2 for muscle name abbreviations. 44

Figure 2.8. Tendon length divided by effective Fascicle Length (EFL, see text for calculation) for all muscles with an appreciable tendon in the hind limb. Bars represent inter-species mean. Symbols represent individual species means. See Table 2 for muscle name abbreviations 45

Figure 2.9. Relative PCSA against relative fascicle length for all non-human ape species (see text for scaling parameters). Data for chimpanzee is from Thorpe et al. (1999), data from bonobo, gorilla and orang-utan are from Payne et al. (2006a).The coloured shapes visualise the position of the muscles of each species. Blue, bonobos; Grey dotted, gibbon; Red, gorilla; Black, Common chimpanzee; Green, orang-utan. 49

Figure 3.1. The apparatus used for data collection. LVDT; Linear voltage displacement transducer. 63

Figure 3.2. The joint angles used in the analyses. 63

Figure 3.3. Decreasing residual sum of squares values for increasing orders of polynomial used to fit data from the rectus femoris (RFe) at the hip. The filled bar represents the least complex model which has an RSS of less than the 5% threshold. 65

Figure 3.4. Scaled moment arms at the hip, for the four specimens. Key: solid yellow line– adductor magnus (AdM), solid red line– gluteus medius (GMe), dashed red line– gluteus superficialis (GSu), solid black line– rectus femoris (RFe), solid grey line– gracilis (Gra), dashed grey line– Sartorius (Sar), solid green line– biceps femoris (BiF), dashed green line– semimembranosus (SeM), dotted green line – semitendinosus (SeT). The vertical black dashed lines indicate the range of joint motion used during jumping (see materials and methods for jumping data collection). 68

Figure 3.5. Scaled moment arms at the knee, for the four specimens. Key: solid black line– rectus femoris (RFe), dotted black line– vastus lateralis, solid grey line– gracilis (Gra), dashed grey line– Sartorius (Sar), solid green line– biceps femoris (BiF), dashed green line– semimembranosus (SeM), dotted green line a– semitendinosus (SeT), solid pink line– gastrocnemius lateralis (GaL), dashed pink line– gastrocnemius medialis (GaM). The vertical black dashed lines indicate the range of joint motion used during jumping (see materials and methods for jumping data collection). 69

Figure 3.6. Scaled moment arms at the ankle, for the four specimens. Key: solid pink line – gastrocnemius lateralis (GaL), dashed pink line– gastrocnemius medialis (GaM), dotted pink line–

soleus (Sol), cyan line– tibialis anterior (TiA). The vertical black dashed lines indicate the range of joint motion used during jumping (see materials and methods for jumping data collection). 70

Figure 3.7. (Previous page) Estimated fascicle strain during the range of motion tested for muscles at the hip (**A**), knee (**B**) and ankle (**C**). Key: adductor magnus (AdM), biceps femoris (BiF), semimembranosus (SeM), semitendinosus (SeT), gluteus medius (GMe), gluteus superficialis (GSu), gracilis (Gra), Sartorius (Sar), rectus femoris (RFe), vastus lateralis (VaL), gastrocnemius lateralis (GaL), gastrocnemius medialis (GaM), tibialis anterior (TiA). 73

Figure 3.8. The differences in predicted MA for polynomial based and spline based techniques for three muscles. Black represents the rectus femoris muscle, green represents the biceps femoris muscle, red represents the gluteus medius muscle. Dashed lines represent the traditional (polynomial based) technique, open circles represent the spline based technique, and solid lines represent a polynomial fitted to the splined data. 79

Figure 4.1. The apparatus setup during data collection. Open diamonds represent digitized points, arcs show joint angles used in the analysis. 90

Figure 4.2. Agreement between centre of mass position from force plate (dashed line) and kinematics (solid line). Star represents the position of the landing pole. Take-off angle is shown in gray. Open star represents the take-off pole position, filled star represents the landing pole position. Filled circle represents the centre of mass position at take-off. 93

Figure 4.3. The four different leap types executed during data collection. 95

Figure 4.4. Examples of the four leap types analyzed in this study performed by three additional captive gibbons. **A**, an orthograde single-footed leap performed by an adult male white-cheeked gibbon (*Nomascus leucogenys*). **B**, a pronograde two-footed leap performed by an adult male white-handed gibbon (*Hylobates lar*, see text for discussion). **C**, an orthograde squat leap and, **D**, a pronograde single-footed leap performed by a juvenile white-handed gibbon. 96

Figure 4.5. The centre of mass positions during the four leap types. Circles, orthograde single-footed leaps; triangles, orthograde two-footed leaps; squares, orthograde squat leaps; diamonds, pronograde single-footed leaps; open star, take-off pole position; filled star, landing pole position. Solid black lines show the mean, dotted gray lines represent standard error of the mean, filled shapes represent the centre of mass position at take-off. 99

Figure 4.6. Take-off (left graphs) and lead (right graphs) hind limb joint angles during stance for the four leap types. (**A**) Orthograde single-footed leaps; (**B**) orthograde two-footed leaps; (**C**) orthograde squat leaps; (**D**) pronograde single-footed leaps. Triangles, ankle; circles, knee; squares, hip. Lines show standard error of the mean; solid, ankle; dashed, knee; dotted, hip. 100

Figure 4.7. Take-off forelimb (left graphs) and lead forelimb (right graphs) joint angles during stance for the four leap types. (**A**) Orthograde single-footed leaps; (**B**) orthograde two-footed leaps; (**C**) orthograde squat leaps; (**D**) pronograde single-footed leaps. Diamonds, shoulder; hexagons, elbow; crosses, wrist. Lines show standard error of the mean; solid, shoulder; dashed, elbow; dotted, wrist. 101

Figure 4.8. Mean impulse during stance for the four leap types, error bars denote standard error of the mean. Black, orthograde single-footed leaps (O1); gray, orthograde two-footed leaps (O2); striped, orthograde squat leaps (OS); white, pronograde single-footed leaps (P1). 105

Figure 4.9. (**A**) Mechanical energy and (**B**) kinetic energy to mechanical energy ratio of the four leap types during stance. Circles, orthograde single-footed leaps; triangles, orthograde two-footed leaps; squares, orthograde squat leaps; diamonds, pronograde single-footed leaps. Solid black lines show the mean, dotted gray lines represent standard error of the mean. 106

Figure 4.10. Mean mass specific net work of the four leap types, error bars denote standard error of the mean. Black, orthograde two-footed leaps; gray, orthograde single-footed leaps; striped, orthograde squat leaps; open, pronograde single-footed leaps. 108

Figure 4.11. Mean mass specific power of the four leap types. Circles, orthograde single-footed leaps; triangles, orthograde two-footed leaps; squares, orthograde squat leaps; diamonds, pronograde single-footed leaps. Solid black lines show the mean, dotted gray lines represent standard error of the mean. 109

Figure 4.12. Take-off angle against take-off velocity, with linear regression (black dashed line). Circles, orthograde single-footed leaps; triangles, orthograde two-footed leaps; squares, orthograde squat leaps; diamonds, pronograde single-footed leaps. 110

Figure 5.1. The experimental setup. Open diamonds show the joint centre digitisation points; filled green diamond shows the pole tip digitisation point. Open outlines show the stiff pole setup; green outlines show the compliant pole setup. 122

Figure 5.2. Schematic representations of the leap types observed. **A**: Orthograde single-footed leaps, **B**: Pronograde single-footed leaps. 127

Figure 5.3. Ground reaction force traces normalised to body weight in the vertical (solid lines) and cranio-caudal (dashed lines) directions during stance phase. Thick lines show the mean, thin lines show standard error of the mean. Lighter colours (grey, pale green) show the stiff pole condition, Darker colours (black, dark green) show the compliant pole condition for **A**: Orthograde leaps and **B**: Pronograde leaps. 128

Figure 5.4A. Stance duration and **B**: Impulse (normalised to body weight) in the horizontal and vertical directions during stance phase for Orthograde (O) and Pronograde (P) leaps from the stiff (light colours, grey, light green) and compliant (dark colours, black and dark green) poles. * denotes significance at the $P < 0.05$ level, ** denotes $P < 0.01$, see text for statistical calculations. 128

Figure 5.5. Centre of mass position during orthograde (**A**) and pronograde (**B**) leaps from the stiff (light colours, grey, light green) and compliant (dark colours, black and dark green) poles. Thick lines show the mean, thin lines show standard error of the mean. Solid lines indicate stance phase, dotted lines show centre of mass position after take-off. Images show body posture at take-off. Closed stars show the position of the take-off pole, open stars show the position of the landing pole. Centre of mass position was normalised to the position of the landing pole. 131

Figure 5.6. Potential (plain solid bars) and kinetic (striped bars) energy of the centre of mass normalised to body mass during orthograde (left) and pronograde (right) leaps from the stiff (light colours, grey, light green) and compliant (dark colours, black and dark green) poles. Numbers show % stance phase, 0 denotes the start of stance and 100 denotes take-off. The total bar height represents the mechanical energy of the centre of mass. ** denotes differences in mechanical energy at the $P < 0.01$ significance level, see text for statistical calculations. 132

Figure 5.7. Mass-specific mechanical work done on the centre of mass during orthograde and pronograde leaps from the stiff (light colours, grey, light green) and compliant (dark colours, black and dark green) poles. * denotes differences in mechanical work at the $P < 0.05$ significance level, see text for statistical calculations. 133

Figure 5.8. Mass-specific centre of mass power during stance phase for orthograde (**A**) and pronograde (**B**) leaps from the stiff (light colours, grey, light green) and compliant (dark colours,

black and dark green) poles. Thick lines show the mean, thin lines show standard error of the mean. 133

Figure 5.9. Hind limb joint angles during stance at the hip (**A**), knee (**B**) and ankle (**C**), for orthograde (left) and pronograde (right) leaps from the stiff (light colours, grey, light green) and compliant (dark colours, black and dark green) poles. Thick lines show the mean, thin lines show standard error of the mean. Angle definitions are described further in the text. 135

Figure 5.10. The instantaneous pole stiffness at the moment of peak force for orthograde and pronograde leaps. * denotes differences at the $P < 0.05$ significance level, see text for statistical calculations. 136

Figure 6.1A The enclosure where filming took place and the measurements required for the calibration were taken. Filled white circles show the measurement points. Black underlined text denotes measurements in metres, red text shows leap branch termini. **B**. The 3-D reconstruction of the enclosure after calibration. Black lines show the vertical trunks and horizontal branches, green angles are used in the calibration (see text for details), red open circles show the centroid position for a typical leap, open black circles show the take-off and landing position. Grey lines show the measurements used for the calculation of biomechanical parameters. d indicates the distance between the vertical trunks. The 'β' angles are referenced to the plane perpendicular to the camera (i.e. when the branch was perpendicular to the camera $\beta_{BRANCH} = 0°$), shown by the grey translucent box. **C**. derivation of the calibration coefficients used in the 3D reconstruction of the enclosure, see text for coefficient calculations. Angles shown in red are 90°. 151

Figure 6.2A White outlines used to attain the centroid position. Open red circles show the centroid position throughout a typical leap, filled red circles show the centroid position for each white outline. Filled white circles show the position at take-off and landing. **B**. The calibrated position of the centroid and the parameters used in the calculation of theoretical kinetic energy requirements (see text for details). Circle representation as in A. Open box indicates preparatory countermovement. Inset, enlargement of boxed area showing counter movement during push-off of squat (red circles) and two-footed (black circles) leaps. 154

Figure 6.3. Black open circles, vertical centre of mass (CoM) position attained from outline based method vs. attainment from forceplate based method from Channon et al. (In Press). Solid line shows a gradient of 1 (i.e. a perfect match), black dashed line shows the gradient of a linear regression on the data (0.88, $P < 0.0005$). Grey open squares (shown on secondary x and y axes),

show vertical centre of mass position of video 2 vs. the same video analysed a second time. Grey dashed line shows the gradient of a linear regression on the data (0.98, $P < 0.0005$). 158

Figure 6.4. Body posture during a typical two-footed leap (A) and a squat leap (B). Timings in seconds are relative to take-off. 160

Figure 6.5A.Open circles, observed vs. minimum theoretical velocity take-off angle for this study; filled circle, data from Channon et al. (In Press), error bars denote standard error of the mean. Dashed line shows a regression of the data from only this study (gradient = 0.73, $P = 0.13$), dotted line includes data from Channon et al. (In Press) in the regression (gradient = 0.85, $P < 0.0005$). Solid line shows a gradient of 1. **B**. Observed vs. minimum theoretically required take-off velocity from this study. Dashed line shows a regression of the data (gradient = 0.54, $P = 0.03$). Solid line shows a gradient of 1. 160

Figure 6.6. Estimates of body (primary y-axis) and propulsive muscle mass (secondary y-axis) specific power during squat leaps in this study. Time 0.00 denotes take-off. Solid line and open circles show the mean, dashed lines show the standard error of the mean. 161

Figure 6.7. Observed and theoretical estimates of body mass-specific total energy for the whole leap (**A**) and mean power during take-off (**B**) under different theoretical scenarios (see materials and methods for calculations). Error bars denote standard error of the mean, boxes show homogenous subsets identified using Tukey's HSD post hoc tests (where $P < 0.05$ is deemed significant). Subsidiary y-axis on B is propulsive muscle mass specific power. 163

Figure 6.8. The centre of mass position during the take-off of video two with the arms present (filled circles) and removed (open circles), solid lines join equivalent frames. Schematics show the section removed (in black) during the 'arms removed' analysis. Timings are relative to take-off. Inset graph, mass specific mechanical energy change (ΔME_M) and mean power during push-off for each condition. 164

Figure 7.1. Vertical ground reaction force traces from human walking (black solid line), human running (black dotted line), bonobo walking (blue solid line) and gibbon bipedalism (grey dashed line). Reproduced from Crompton et al. 2008 and Lieberman et al. 2010. 174

List of Tables

Table 2.1. Details of the 11 gibbon cadavers used in this study. 29

Table 2.2. Functional muscle groups, their constituent muscles and abbreviations (Abr.). The plantaris muscle was inconsistently present and was not included in the analysis (see text); the Iliopsoas was not available for dissection and was also excluded from the analysis. 30

Table 2.3. Mean ($\bar{x}$) anatomical measurements with standard deviations (σ) for each species. 39

Table 3.1. Details of the four cadavers used in this study. 61

Table 3.2. Muscles for which no MA data could be collected 61

Table 4.1. Results of Analysis of Variance and Tukey's HSD post hoc tests for homogenous subsets on inter-leap type differences in biomechanical variables. The groupings were significant at the 95% confidence level ($P < 0.05$). Std Er., standard error of the mean. 98

Table 5.1. (Following page) Statistical comparisons of leap types on stiff and compliant substrates. P-value denotes the significance of a Kruskal-Wallis test between substrate types, where a value of 0.05 or less is deemed significant (significant differences are shown in bold). 128

Table 5.2. Pole stiffness at the moment of peak force application for each leap type. P-value denotes the significance of a Kruskal-Wallis test between leap types, where a value of 0.05 or less is deemed significant (significant differences are shown in bold). 136

Table 6.1. Input parameters used when calculating kinetic energy requirements for the three theoretical leap scenarios and the measured kinetic energy used during the leap (see text for details and Fig. 6.2B for parameter definitions). 156

Table 6.2. Total leap energies and mean powers for the measured and calculated theoretical scenarios. See text and table 1 for definitions and calculations of parameters. 163

Chapter 1: Introduction

By Anthony J. Channon

With contributions from Evie E. Vereecke

Anthony Channon wrote this chapter, Evie Vereecke edited it and provided advice on its content.

The body of this thesis focuses on the functional morphology of the gibbon hind limb and the biomechanics and ecological relevance of leaping as a locomotor mode for gibbons. This introduction should serve to brief the reader on the evolutionary and biomechanical context in which gibbons are placed. Methods and results of detailed investigations into the functional morphology of the gibbon hind limb are presented in Chapters 2 and 3. Leap biomechanics of free ranging, captive gibbons are discussed in Chapters 4 to 6. The thesis concludes with a brief summary discussion compiling the previous chapters' findings and evaluating them in a broader scientific context.

Gibbon Locomotor Biomechanics

Gibbons are small (~5 – 10 kg) apes distributed sparsely throughout the rainforests of south-east Asia (IUCN, 2008). They represent the only extant lineage of 'lesser apes' (Hylobatidae), consisting of four genera, *Hylobates*, *Bunopithecus*, *Nomascus* and *Symphalangus*. Their evolutionary and biomechanical interest stems from their unusually high reliance upon the suspensory locomotor mode, brachiation or 'arm-swinging' the hylobatian model of the evolution of human upright bipedal walking (Tuttle, 1981), and their close phylogenetic relationship with modern humans (gibbons are included in the super family Hominoidea). Gibbons also have an unusual body plan compared with other apes (and, indeed, primates), whereby the limb segments are elongated in comparison to the length of the trunk (Jungers, 1985; Payne et al., 2006a). While many primate species 'arm-swing' gibbons are likely the only true brachiation specialists and it is, by far the most dominant locomotor mode, comprising 50-75% of locomotor bouts observed in wild gibbons (Fleagle, 1976; Gittins, 1983; Sati and Alfred, 2002). Detailed biomechanical studies have likened the centre of mass mechanics occurring during gibbon brachiation to pendular movements (Fleagle, 1974; Preuschoft and Demes, 1984), revealing a highly efficient transfer

between potential and kinetic energies. The importance of hand release and grasp timings have been shown to be crucial to the energetic efficiency of brachiation, where the smooth trajectory of the centre of mass is achieved through collision avoidance (Bertram et al., 1999; Usherwood and Bertram, 2003). The dominance of brachiation is doubtless related to the characteristic elongation of the gibbon forelimbs, where longer forelimbs facilitate a greater magnitude of potential energy recovery (i.e. increasing the arc length of the swing) and give a larger range of possible pendular shortenings than do shorter forelimbs (Preuschoft and Demes, 1985; Bertram and Chang, 2001). Longer forelimbs could also reduce the relative muscle forces necessary for powering brachiation (Preuschoft and Demes, 1985; Chang et al., 2000), by increasing the centre of mass velocity through pendular motion. Interestingly, the length of the gibbon forelimb scales with negative allometry i.e. larger gibbons possess relatively shorter forelimbs (Jungers, 1985). In larger gibbon species (e.g. siamang, *Symphalangus syndactylus*), forelimb length is probably limited by the strength of the digital flexor muscles (Preuschoft and Demes, 1985; Michilsens et al., 2009) since their force production capacity is approximately proportional to body mass raised to the power $\frac{2}{3}$, meaning that body mass increases relatively quicker than the force available to support it (Alexander et al., 1981; Alexander, 1985; Preuschoft and Demes, 1985). By using fore limb length as a denominator, several of the indices used to describe the morphology of limb segments disguise the gibbons' relatively long hind limbs (Tuttle, 1972). Indeed, the long hind limbs have been hypothesised to be benefit the powering of brachiation through leg lift (Fleagle, 1974), similar to the method used by a child to power a playground swing. In this scenario, the gibbon flexes the hip and knee joints at the bottom of the swing reducing the effective pendulum length, and consequently increasing velocity (since the period of swing, $t \approx 2\pi\sqrt{[l/g]}$, where l, is pendulum length and g is the gravitational constant, Fig. 1.1). While some potential adaptations to this mode can be identified in the hind limbs (e.g. long fascicled hip flexors, giving a wide range of motion, Payne et al., 2006a; Channon et al., 2009), the specialised musculature within the thigh and shank is doubtless primarily adaptated to hind limb supported locomotion.

Gibbons are known to utilise a wide range of hind limb supported locomotor modes including pronograde clambering and climbing (which can also be fore-limb powered, Isler, 2005), bipedal, tripedal and quadrupedal walking and leaping (Fleagle, 1976; Gittins, 1983; Sati and Alfred, 2002; Vereecke et al., 2006a). Locomotor data for wild siamang suggest that climbing is the predominant mode used during feeding, both in terms of proportion of bouts (74%) and distance travelled (638 m/km, Fleagle, 1976). During travel, however, brachiation is the dominant

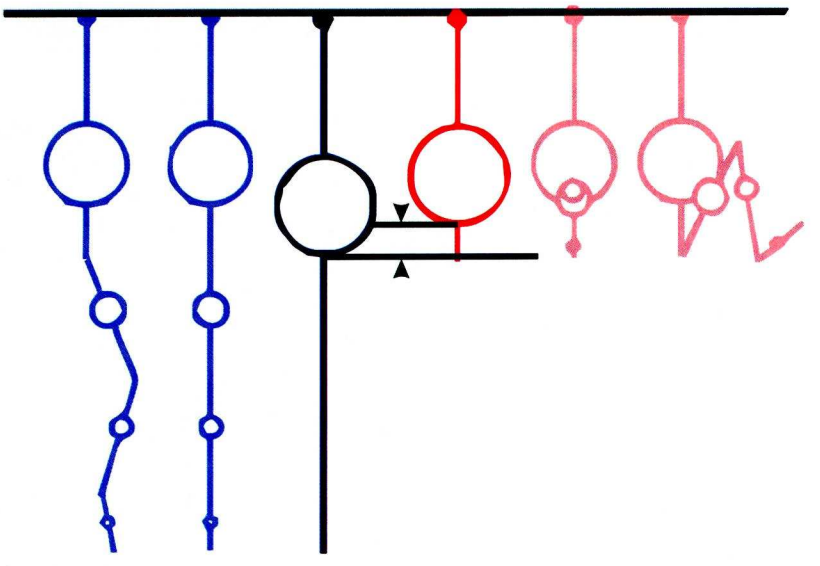

Figure 1.1. Showing how the centre of mass position, circles for each segment, can be raised from the extended hind limb posture, left (blue), to the flexed hind limb posture (red) during brachiation by leg lift.

locomotor mode comprising 51% of bouts and accounting for 623 m/km of travel. Sati and Alfred (2002) found similar trends for hoolock gibbons (*Bunopithecus hoolock*), with climbing being dominant (42% of bouts) during feeding, and brachiation dominant during travel (76% of bouts). Of the hind limb dominated locomotor modes, bipedal walking is the best studied biomechanically. Using an instrumented walkway in a wild animal park environment, Vereecke et al. (2006b) demonstrated that, except at very low speeds, gibbon bipedalism is characterised by a spring-mass type 'bouncing gait', where the potential and kinetic energy of the centre of mass are in phase (Cavangna et al., 1977; Alexander, 1984), yet without an aerial phase. This 'bouncing' pattern is usually only seen in running animals, with an aerial phase (where no limbs are in contact with the substrate). Walking bipeds, by contrast, traditionally utilise an 'inverted pendulum' style gait, where potential and kinetic energy are out of phase (Alexander, 1996). Thus, Vereecke and colleagues (2006b) suggested that defining gaits using the proportion of time each limb spends contacting the ground throughout the stride (known as duty factor), could lead to erroneous assumptions about the centre of mass mechanics being utilised by the animal. An analysis of the ankle kinematics revealed that elastic energy storage and recovery during bipedalism was not likely to occur in the well developed Achilles tendon of the triceps surae, but may be rather more likely in the patellar tendon of the quadriceps femoris muscle group. A later follow up study (Vereecke and Aerts, 2008), found that elastic energy storage and recovery could occur in the plantar ligaments and tendons of the digital flexor musculature, via the mid-tarsal break. The mechanical distinction between human walking and the bipedalism observed in gibbons (inverted pendulum in humans vs. spring mass in gibbons) lead Crompton et al. (2008) to eschew Tuttle's (1981) hylobatian model of the evolution of upright bipedalism. Crompton and colleagues instead purported Thorpe et al.'s (2007b) model based on the quadrumanous clambering observed in Sumatran orangutans (*Pongo abelii*) while accessing very fine terminal branches.

Hind limb functional anatomy

The extensive locomotor repertoire utilised by gibbons and the role of the hind limb in all of these modes almost certainly places contrasting pressures on the musculo-tendinous architecture of the hind limb, which is likely further constrained by the requirement for elastic energy storage, and the normal inertial constraints on swinging limbs (Demes and Günther, 1989; Witte et al., 1991; Preuschoft and Günther, 1994; Steudel, 1996; Preuchoft et al., 1998; Schoonaert et al., 2007; Rubenson and Marsh, 2009). While many data are available on the skeletal dimensions of

hylobatid limbs (Steudel, 1982; see Jungers, 1984 for review), very few studies have investigated the musculo-tendinous morphology of these species. Vereecke et al. (2005) demonstrated that the feet and ankle myology of gibbons and bonobos (*Pan paniscus*) are relatively similar, when compared to human feet, with the ape feet being more adept for a range of locomotor modes compared to the 'stiff' human foot, which is highly specialised for upright bipedalism. Conversely, in a comparative anatomical study (Payne et al., 2006a) found that the gibbon and human hind limbs shared similar muscle architecture and overall morphology when compared to other ape species, indicating some adaptation of the gibbon hind limb for elastic energy storage and/or inertia minimisation (Isler et al., 2006). While both of these studies added valuable anatomical data from an under-represented taxon, the numbers of specimens and represented species were low (Vereecke et al., 2005, *H. lar* [n = 2], *Nomascus leucogenys* [1]; Payne et al., 2006a, *H. lar* [1]). Clearly then, there is a shortage of quantitative muscle and tendon architecture data from gibbon hind limbs, which could aid our understanding of the adaptations of the hind limb to the range of locomotor modes the gibbon utilises. Such data are also crucial for estimating the musculoskeletal forces produced by individual muscle groups within the locomotor system, which in turn are a pre-requisite for accurate dynamic computer models of gibbon locomotion (e.g. Sellers et al., 2005), which can provide valuable insights into the dynamics and evolution of gibbon locomotion. Chapter 2 presents muscle and tendon architecture data from 11 gibbons (from four species), representing the largest anatomical dataset of lesser apes, with analyses focused on functional muscle specialisation and the identification of likely elastic energy stores within the hind limb.

An important determinant of muscle function is the moment arm through which the muscle acts (Biewener, 1989; Pandy, 1999; Eng et al., 2008). The moment arm is defined as the perpendicular distance between the joint centre of rotation and the line of action of the muscle in question (Spoor and Van Leeuwen, 1992). All other things being equal, large moment arms minimise the muscle force required to rotate the joint, but require larger magnitude contractions for a given angular displacement (i.e. rotation). The opposite is true of small moment arms, i.e. they give relatively large angular displacements at the cost of a higher force requirement (i.e. they allow high velocity, low force movements). The moment arm is a direct determinant of both joint torque and available range of limb motion, calculated from muscle force and contraction distance, respectively. Because of their functional significance, detailed functional morphology investigations should include moment arm data. The only available gibbon hind limb moment arm data are from Payne et al. (2006), who noted that the moment arms in the gibbon hind limb were

relatively small when compared to other apes. These data were obtained from a single white-handed gibbon (*H. lar*), and the authors acknowledged that further data are crucial to confirm the patterns they observed. Chapter 3 presents moment arm data from a selection of hind limb muscles from four gibbon specimens (representing three different species), collected using a novel approach based on the commonly utilised tendon travel technique (Spoor and Van Leeuwen, 1992). This novel approach likely minimises the subjectivity of curve selection and uses a cubic spline based curve to describe the data, reducing the error associated with polynomial based techniques. In isolation, moment arm data can be difficult to contextualise, so I make some functional comparisons with published ape data (from Payne et al., 2006b) using a comparable technique. I also present a simple geometric fascicle strain model, to estimate the required fascicle contraction for an observed range of motion from free ranging gibbons, aiding our understanding of the relationship between muscle moment arm and muscle function. I aim to identify which muscles are associated with specific locomotor modes and which are 'generalists'.

Leaping as a locomotor mode

In comparison to cursorial galloping, leaping represents a slow and energetically expensive locomotor mode (Gunther et al., 1991). Yet, for arboreal animals, living in a fragmented environment with large gaps to cross, it likely represents an invaluable method of traversing the canopy. For high canopy dwellers such as gibbons, leaping across a gap is energetically less expensive than climbing to the base of a tree, crossing the gap terrestrially and climbing back up again. In addition, predation risk is lower during leaping than during over-ground travel. During powerful movements such as leaping, however, the flexible tree branches present a challenge for arboreal leapers because the high reaction forces generated during the leap deflect the branch, wasting energy (Fleagle, 1976; Alexander, 1991). To minimise this deflection, Western tarsiers (*Tarsius bancanus*) have been observed to utilise substrates which minimise the proportion of force directed along the weaker axis of the branch, by using more inclined branches for larger leaps (Crompton et al. In press). Given the costly and challenging nature of arboreal leaping, it might be expected that specialised leapers utilise take-off angles that minimise the kinetic energy (and hence power) requirements of a leap. For a horizontal leap (i.e. with no height loss) a take-off angle of 45° requires the least kinetic energy, yet, among a group of leapers only the most specialised leaper, the mohol bushbaby (*Galago moholi*), was observed to use this 'optimum' take-off angle at all leap lengths, while the other, less specialised, leapers (e.g. Garnetts galago,

Galago garnettii; mouse lemur, *Mirza coquereli* and ring-tailed lemur, *Lemur catta*) only used a 45° take-off angle during maximal leaps (Crompton et al., 1993). The authors hypothesised that energy minimisation may not be the primary criterion while leaping for the less specialised leapers, citing shorter flight times and more unpredictable trajectories (aiding predation avoidance) as potential benefits of take-off angles below 45° (Crompton et al., 1993; Crompton and Sellers, 2007).

An alternative to avoiding the energy wasted during branch deflection is to utilise the elastic strain energy stored within the branch to power the leap. Human divers are capable of this when diving from a spring board. The energy stored in the board during the propagations prior to the take-off is returned during the push-off phase by the diver, helping to power the dive (Kooi and Kuipers, 1994; Cheng and Hubbard, 2004). Despite field observations reporting 'branch pumping' by siamang before a leap (Fleagle, 1976, Fig. 1.2), to date no such mechanism has been demonstrated outside of humans. To best recover the energy stored in the branches, the 'push-off' should be timed to coincide with the recoil of the branch, however, detailed biomechanical studies on strepsirrhine vertical leapers indicate that the leap is not timed effectively for energy recovery. Demes et al. (1995) used a combination of free ranging animals and laboratory recordings from an instrumented pole to investigate the effect of compliance on the leaps of several *Propithecus*, *Indri* and *Hapalemur* species, finding that the animals leapt prior to the recoil of the pole, noting instead that "...force is wasted deflecting the pole". Johnston (1980) showed that pigtailed macaques (*Macaca nemestrina*) increased the magnitude of joint extension when making ascending leaps from a compliant substrate, indicating a compensation mechanism for the compliance of the substrate, rather than utilising its energy storage capacity. Thorpe et al. (2007a) were able to successfully demonstrate useful energy recovery from vertical trunks during gap crossing by wild Sumatran orangutans. The authors used video recordings to show that the energy required to sway vertical trunks enough to cross gaps in the forest is likely less than that required to climb down, cross the gap terrestrially and climb back up again, while also reducing predation risk. Yet, during powerful movements such as leaping useful elastic energy storage and recovery in the external environment (i.e. branches) is yet to be demonstrated for non-human species. Alexander (1991) hypothesised that branches with the required material properties to execute this behaviour are unlikely to exist in the arboreal ecomorph.

Figure 1.2. A schematic drawing of a siamang propagating a tree branch before leaping to a lower level. Reproduced from Fleagle (1976).

Gibbons as leapers

Gibbons are very adept leapers, yet, detailed biomechanical studies on gibbon leaping are lacking. Field reports suggest that, during travel, leaping accounts for 15-25% of locomotor bouts in agile and hoolock gibbons (*H. agilis* and *Bunopithecus hoolock*, respectively) and 6% in siamang (Fleagle, 1976; Gittins, 1983; Sati and Alfred, 2002). Leaps are predominantly conducted from, and to, fine terminal branches, landing in trees below the take-off site. Wild gibbons are known to use climbing to ascend and leaping to descend, with leaps conducted "...always from a higher to a lower level..." (Fleagle, 1976, Fig. 1.2). Gibbons may be limited to leaping downwards by the compliance of the fine terminal branches used as take-off substrates. Leaps with vertical height gain require higher take-off velocities (Crompton and Sellers, 2007) and higher propulsive forces, and hence induce greater branch deflection. While 'pumping in place' on a substrate before a leap could be perceived as a method of energy storage within the branch, Fleagle (1976) reports that the hind limbs provide "...very little thrust." and that "at take-off, siamang appear to pull forward with their arms.", suggesting that wild gibbons opt to minimise force wasted on the branch, rather than usefully store energy in it.

Detailed biomechanical data are required to further enhance our understanding of gibbon leaping and the mechanics and ecological context of arboreal leaping as a whole. These data are necessary to better assess the types of leaps that gibbons use and why, as well as the likelihood of useful energy storage in the branches of their habitat. Comparisons with other, more specialised, leapers (such as indriids, galagos and tarsiers) are needed to yield insight into the evolution of, and limitations imposed upon leaping by, the gibbons' unusual body plan (with elongated arms and legs), as well as furthering our understanding of wild gibbons' purported preference for descending leaps. Because maximal leaps likely elicit maximal musculoskeletal performance, biomechanical data from long leaps are a requisite for comparative studies between the musculoskeletal performance of gibbons and other primates. Scholz et al. (2006) hypothesised 'superior muscle properties' in vertically leaping bonobos, while Aerts (1998) purported the use of a power amplifying mechanism in *Galago senegalensis*. Maximal leap data are required to identify or dismiss similar mechanisms in the gibbon locomotor system.

The lack of detailed biomechanical data of wild gibbon leaping is attributable to their high canopy habitus and extremely timid nature. Gibbon sightings are rare in the wild (McClure, 1964), and biomechanical analyses require unobstructed filming conditions and/or data logging equipment to be placed upon the animal (Sellers and Crompton, 1994, 2004; Byrnes et al., 2008; Pfau et al.,

2009). Unobstructed sights for filming where distances can be readily calibrated are rare (Thorpe and Crompton, 2005) and unlikely to be in the forest canopy (where, by definition vegetation is extremely dense), where gibbons spend ~60% of their waking time (Gittins, 1983). Similarly, fitting body mounted data loggers to gibbons almost certainly requires sedation of the animal because of their extremely shy character (McClure, 1964). This would be dangerous and stressful for the individual and is likely to further endanger already seriously threatened taxa (IUCN, 2008). Thus collecting quantitative leaping data from wild gibbons is difficult. However, free ranging gibbons are commonly found in wild animal parks and zoos which allow easier installation of apparatus and a more controlled environment for data collection. Such data are usually required to be collected spontaneously during voluntary bouts, ensuring the gibbon is locomoting in its preferred mode. Also, while gibbon mortality is undesirable, captive animal deaths present an opportunity to collect biomechanical and anatomical data from the same individual. Nevertheless, collecting biomechanical data (via a forceplate or similar apparatus) from a large number of individuals remains challenging due to their monogamous pair dwelling nature, hindering statistical analyses. In addition, interaction with the animals is not often allowed in zoos, precluding the use of body mounted data loggers. Further, the enclosure can limit locomotor performance (e.g. in the case of leaping) and working in a public zoo, while maintaining public access, also has some constraints.

Chapter 4 presents the first detailed biomechanical data from leaping gibbons. I identify biomechanically distinct leap types and relate this to the ecological context in which they might be utilised. In Chapter 5 I present data from gibbons leaping from a compliant pole and investigate whether energy is usefully stored and recovered during the leap, and to what extent, the leap biomechanics differ between stiff and compliant substrates. Chapter 6 introduces a novel technique for recording biomechanical data from maximally leaping, free ranging gibbons, quickly and cost effectively. I use the data to identify the take-off parameters, calculate the musculoskeletal performance, and assess the effect the gibbons' unusual morphology might have on the leap.

This thesis contributes valuable data on the functional morphology of the gibbon hind limb, aiding our understanding of the evolution of gibbons and primates as a whole, while also furthering our understanding of the functional morphology of habitually arboreal animals, and the limits imposed upon it by the habitat. My predominant research questions based around functional morphology are: what is the gibbon hind limb specialised for? And: what can its functional morphology tell us

about the way in which arboreal animals, which maintain a wide locomotor repertoire, specialise their locomotor apparatus? I also present detailed leap biomechanics of gibbons from a variety of substrates, which contributes to the understanding of primate evolution and ecology, locomotor biomechanics, muscle mechanics and neural control. My central biomechanics related research questions are: how go gibbons attain such impressive leaping performance? How is leaping specialised in gibbons for the ecological context in which they are placed? And can gibbons usefully store and recover elastic energy from compliant substrates during leaping?

Chapter 2: Mechanical constraints on the functional morphology of the gibbon hind limb

By Anthony J. Channon

With contributions from: Michael M. Günther, Robin H. Crompton and Evie E. Vereecke.

I dissected the specimens, analysed the resulting data and wrote the manuscript. Evie Vereecke assisted with dissections and provided funding for specimen collection. Michael Günther and Robin Crompton edited the chapter and advised on its content.

A version of this chapter has been published in the Journal of Anatomy

A. J. Channon, M. M. Günther, R. H. Crompton and E. E. Vereecke (2009). Mechanical constraints on the functional morphology of the gibbon hind limb. *Journal of Anatomy* **215**, (4):383-400.

Abstract

Gibbons utilise a number of locomotor modes in the wild, including bipedalism, leaping and, most of all, brachiation. Each locomotor mode puts specific constraints on the morphology of the animal; in some cases these may be complementary while in others they may conflict. Despite several studies of the locomotor biomechanics of gibbons, very little is known about the musculoskeletal architecture of the limbs. In this study, I present quantitative anatomical data of the hind limb for four species of gibbon (*Hylobates lar, H. moloch, H. pileatus, S. Symphalangus syndactylus*). Muscle mass and fascicle lengths were obtained from all the major hind limb muscles, physiological cross-sectional area (PCSA) was calculated and scaled to remove the effect of body size. The results clearly indicate that, for all the species studied, the major hip, knee and ankle extensors are short-fascicled and pennate. The major hip and knee flexors, on the other hand, are long-fascicled, parallel muscles with relatively small PCSAs. I hypothesise that the short-fascicled muscles could be coupled with a power amplifying mechanism, and are predominantly useful in leaping. The long-fascicled knee and hip flexors are adapted for a wide range of joint postures and can play a role in flexing the legs during brachiation.

Introduction

Gibbons possess a large locomotor repertoire which includes quadrupedal walking and leaping (Fleagle, 1974; Gittins, 1983; Vereecke et al., 2006a), and three sub-modes of torso-orthograde suspensory locomotion: vertical climbing, orthograde clambering and brachiation (categories follow Hunt et al., 1996 and Thorpe and Crompton, 2005, 2006). Of these, brachiation is the most common in the wild, with between half and three-quarters of all locomotion conducted in this way (Fleagle, 1974; Gittins, 1983). Because of the diversity of locomotor modes used by gibbons, the hind limb is likely to be under varying mechanical demands, to which its anatomy is likely to be adapted.

Quantitative anatomical data on primate, and particularly human, hind limbs are abundant (for humans: Alexander and Vernon, 1975; Friederich and Brand, 1990; Fukunaga et al., 2001; for other apes: Thorpe et al., 1999, 2004, Vereecke et al., 2005; Payne et al., 2006a; for other primates: Sigmon and Farslow, 1986). However, quantitative data on hind limb anatomy of whole gibbon cadavers is limited to a single specimen from which Payne et al. (2006a) made comparisons with the great apes in an evolutionary context. Vereecke et al. (2005) made comparisons between the lower leg and foot of humans, bonobos and gibbons, based on detailed dissections of bonobo and gibbon feet. Although both studies gave a good insight in the comparative anatomy of the ape hind limb, the number of gibbon species and specimens included was very limited (Vereecke et al., 2005, n=3 from two species; Payne et al., 2006a, n=1, *Hylobates lar*). To get a better insight into gibbon morphology and locomotion a more extensive quantitative anatomical dataset of gibbon hind limb anatomy is needed.

A number of anatomical studies on various mammals have highlighted how gross anatomy can provide insight into muscular force production (Close, 1972; Alexander and Vernon, 1975; Maughan, 1983; Brand, 1986) and locomotor specialisation. Payne et al. (2005) dissected fresh cadaveric hind limbs from seven horses and used macroscopic anatomical measurements (fascicle length, muscle mass etc.) and published values of maximum isometric stress and contraction velocity to estimate force production in the muscles and tendon stress during locomotion. In agreement with Alexander and Vernon (1975), Alexander (1977), and Alexander et al. (1981), they noted a proximal-distal decrease in muscle volume and fascicle length with a simultaneous increase in tendon volume. Payne et al. (2006a) dissected apes from a number of species (bonobo, gibbon, gorilla and orang-utan), using similar techniques to Payne et al. (2005), and combined this with data on humans and chimpanzees from Thorpe et al. (1999). Muscle architecture data was

shown to scale approximately allometrically (as predicted by Alexander, 1977). It was reported that the gibbon was the only ape with a substantial Achilles tendon, and hypothesised that it may be beneficial in returning elastic energy in bipedalism (a hypothesis which was substantiated by Vereecke et al., 2006b). The authors also noted that there was less 'tapering of the limb distally' in the African apes, relating this to a need to grasp with the feet.

Muscle architecture data on smaller cursorial quadrupeds (hares and greyhounds; Williams et al., 2007, 2008) also pointed to a prominent distal decrease in muscle volume and fascicle length, linked to an increase in tendon volume. Muscle architecture and muscle moment arm data from a range of cadaveric Macropodoidea (kangaroos and wallabies; Bennett and Taylor, 1995; McGowan et al., 2008) suggest that muscle force scales allometrically with size, but that tendon stress is larger in larger animals, reducing safety factor (see below) and imposing a limit on body size for animals heavily dependent on elastic energy storage for efficient locomotion. The authors use these data to show that large (~250kg) extinct kangaroos were 'likely very limited in locomotor capacity'. More recent studies have used sophisticated imaging techniques to gain insight into in-situ musculoskeletal properties (Miller et al., 2008).

The role of the hind limb in hind limb-dominated locomotion, such as bipedalism and leaping, is quite obvious. It is also likely, however, that it plays a role in powering brachiation through 'leg lift', by which brachiating animals can convert metabolic energy to mechanical energy by lifting the legs during a swing (Preuschoft and Demes, 1984; Bertram and Chang, 2001; Usherwood and Bertram, 2003). This mechanism can be compared to a human using a playground swing, where lifting the legs at the bottom of the arc increases the height of the subsequent swing.

It has long been recognised that the shape (morphometry) of the limbs has a profound effect on the limb's centre of mass and so is an important factor in powering brachiation. Morphometry is also important for hind limb dominated locomotion since swinging the limb forward incurs a metabolic cost, due to the inertia of the limb itself. This cost can be reduced if the limb is made to swing closer to its natural pendular frequency (NPF, for a historical review and analysis of measurements of inertial properties see Steudel, 1990, 1996; Preuschoft and Witte, 1991; Preuschoft et al., 1992; Isler et al., 2006; Schoonaert et al., 2007). Shorter pendula swing more rapidly (since NPF = $1 \div [2\pi\sqrt{l/g}]$, where π and g are constants and l is pendulum length), so animals which swing their limbs faster than the NPF may gain some benefit by decreasing the effective length of their limbs. This reasoning has been cited as the explanation for a proximo-distal decrease in limb muscle mass observed for many animals (see above), particularly those

with long or rapidly moving limbs such as cursorial mammals (dogs: Steudel, 1990; horses: Payne et al., 2005; greyhounds: Williams et al., 2008).

By utilising many of the techniques seen above this study will quantify gibbon hind limb muscle architecture and investigate how the limb is employed to cope with an extensive locomotor repertoire. Several previous studies (Thorpe et al., 1999; Payne et al., 2005, 2006a; Williams et al., 2007, 2008) did not take into account pennation angles when taking anatomical measurements because the angles were small, could not be measured accurately and likely had little influence on physiological cross-sectional area. In my study, however, I will take pennation angles into account.

Materials and Methods

Subject data

The material used in this study comprises 11 gibbon cadavers of known age and sex (Table 2.1). Specifically: I employed three white-handed gibbons (*Hylobates lar*: L1-3), two pileated gibbons (*H. pileatus*: P1-2), two moloch gibbons (*H. moloch*: M1-2) and four siamang (*Symphalangus syndactylus*: S1-4). All specimens were frozen until required for this study and were eviscerated prior to dissection. Specimens were obtained from The Royal Zoological Society of Antwerp (L1, L3, S2) and The National Museums of Scotland, Edinburgh (L2, P1-P2, M1-M2, S1, S3-4). Most cadavers were eviscerated during post-mortem examination, and body mass (prior to evisceration) was not available for all specimens. Therefore, hind limb muscle mass (HLMM) was used to normalise the animals for size. Unfortunately, the iliopsoas muscle was unavailable for dissection, because of its use in a prior study, and was not included in any of the analyses. Data from Payne et al. (2006a) were used to indicate where the iliacus muscle (part of the iliopsoas and an important hip flexor) would be positioned on a graph of PCSA against fascicle length (see below and Table 2.1).

Scaling and functional muscle groups

The data were normalised assuming geometric similarity (Alexander et al., 1981; Thorpe et al., 1999; Payne et al., 2006a; Williams et al., 2008). Because of post-mortem evisceration, body mass was unavailable for some subjects and so HLMM was used as a normalising factor. Masses

Table 2.1. Details of the 11 gibbon cadavers used in this study.

Specimen	*H.lar* 1	*H.lar* 2	*H.lar* 3	*H. pileatus* 1	*H. pileatus* 2	*H. moloch* 1	*H. moloch* 2	*S. syn.* 1	*S. syn.* 2	*S. syn.* 3	*S. syn.* 4	*H. lar* 4*
Sex	M	M	F	M	F	M	M	F	F	F	M	F
Age at death	6	26	22	41	25	19	-	36	-	9.4	> 10	16
Mass at death (kg)	6.3	10.6	6.5	5.2	-	5.8	-	11.6	12.5	8.5	10.1	4.6
HLMM (kg)	0.49	0.65	0.40	0.39	0.27	0.32	0.43	0.78	0.76	0.38	0.81	0.22
Femur Length (cm)	20.1	22.0	20.5	21.0	20.5	19.6	20.5	21.5	19.0	21.5	20.3	18.3
Tibia Length (cm)	19.2	18.8	16.9	18.5	19.0	17.1	19.8	21.4	21.2	20.9	19.1	15.8
Foot length (cm)	-	8.8	8.8	8.5	8.4	8.0	8.7	9.8	9.3	11.1	9.9	10.2
Abbreviation	L1	L2	L3	P1	P2	M1	M2	S1	S2	S3	S4	-

HLMM – Hind limb muscle mass. Fields where information was unavailable are denoted by a dash. *_H. lar_ 4 is taken from Payne et al. (2006a). All specimens were obtained post-autopsy and declared free of communicable diseases, although cause of death was not provided to us. Specimens were examined to verify that they were free from any musculoskeletal anomaly.

Table 2.2. Functional muscle groups, their constituent muscles and abbreviations (Abr.). The plantaris muscle was inconsistently present and was not included in the analysis (see text); the Iliopsoas was not available for dissection and was also excluded from the analysis.

Thigh			Shank		
Group	**Constituent muscles**	**Abr.**	**Group**	**Constituent muscles**	**Abr.**
Hip Extensors	Gluteus superficialis	GSu	Plantarflexors	Gastrocnemius lateralis	GaL
	Gluteus medius	GMe		Gastrocnemius medialis	GaM
	Gluteus minimus	GMi		Soleus	Sol
Adductors	Adductor magnus	AdM		Tibialis posterior	TiP
	Adductor longus	AdL	Dorsiflexors	Tibialis anterior	TiA
	Adductor brevis	AdB	Digital Flexors (and Plantar flexors)	Flexor tibilais	FlT
	Pectineus	Pec		Flexor fibularis	FlF
	Quadratus femoris	QuF	Digital Extensors (and Dorsiflexors)	Extensor hallucis longus	EHL
Knee Extensors	Rectus femoris	ReF		Extensor digitorum longus	EDL
	Vastus lateralis	VaL	Everters (and Plantarflexors)	Peroneus longus	PeL
	Vastus intermedius	VIn		Peroneus brevis	PeB
	Vastus medius	VMe			
Hip Rotators	Obturator internus	ObI			
	Obturator externus	ObE			
	Piriformis	Pir			
Knee Flexors and Hip extensors (Hamstrings)	Semitendinosus	Set			
	Semimembranosus	Sem			
	Biceps femoris (both heads)	BFL/S			
Bi-Articular Knee & Hip Flexors	Gracilis	Gra			
	Sartorius	Sar			
Uni-Articular Knee Flexor	Popliteus	Pop			

were scaled directly to HLMM, lengths to $HLMM^{1/3}$ and areas to $HLMM^{2/3}$. HLMM correlated significantly with body mass for the subjects where body mass was known (linear regression P=0.002, Fig. 2.1).

For part of the analysis, muscles were categorised into functional groups, which are given in Table 2.2, together with the used abbreviations for the hind limb muscles used in the analyses. A weighted harmonic mean was used to calculate group averages of fascicle length, this technique takes each muscles mass into account when calculating a mean (for a more detailed description see: Alexander et al., 1981; Thorpe et al., 1999; Payne et al., 2006a).

Anatomical measurements

Hind limb muscles were removed systematically and measurements of isolated muscles were taken. Measurements of mass were taken to the nearest 0.1 g, using an electronic scale (Radwag, Poland, accurate to 0.01 g), while measurements of length were taken to the nearest 0.1 mm using a set of digital Vernier callipers (Mitutoyo, UK, accurate to 0.01 mm). Measurements included: muscle tendon unit (MTU) mass and MTU length, muscle belly length and mass.

The muscle was then cut along its tendon in order to determine the orientation of the muscle fascicles and the length of internal tendon. Fascicle length was measured at three points along the muscle belly and the mean was calculated. Photographs of pennate muscles were taken using a digital camera (Nikon D40) so that the pennation angle (θ) could be measured using custom written software (National Instruments LabVIEW 8.2). Pennation angle was measured at ten points along the muscle belly (to account for internal variation) and the mean was calculated. For muscles with an external tendon, the tendon was removed and a uniform section of known length was weighed, this weight was divided by section length and the density of mammalian tendon (=1.12 g cm^{-3}; Ker et al., 1988) in order to estimate cross-sectional area (CSA). Tendon length was measured from its most proximal fibres (in the muscle) to its most distal fibres (insertion on the bone). Muscle function was estimated from the position of the muscle on the skeleton and its line of action.

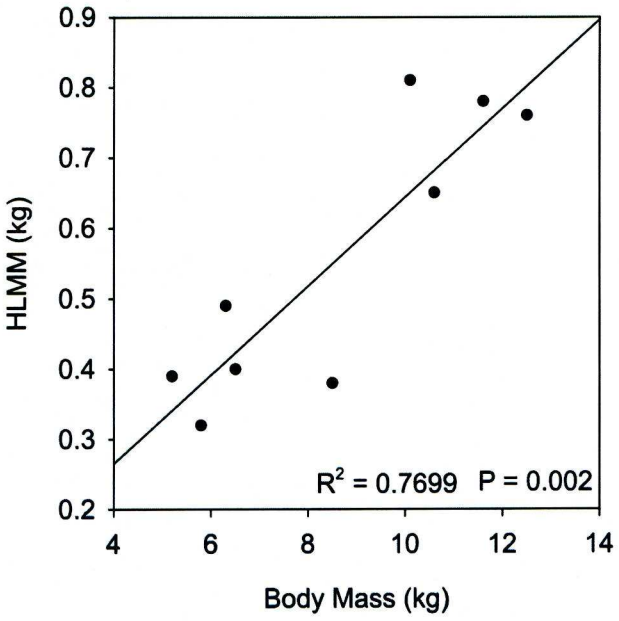

Figure 2.1. Hind limb muscle mass (HLMM) against Body Mass for the individuals where body mass was known. Dashed line shows linear regression.

Muscle PCSA and fascicle length

The physiological cross-sectional area (PCSA) of a muscle is affected by its pennation angle (Alexander, 1968, Burkholder et al., 1994; Thorpe et al., 1999; Payne et al., 2006a). It can be directly related to maximum isometric force (F_{MAX}) generating capacity by multiplying it by the maximum isometric stress of vertebrate skeletal muscle (=0.3 MPa; Wells, 1965; Fukunaga, 2001; Medler, 2002). Although this method is commonly used in functional anatomy it should be noted that the value of maximum isometric stress has been shown to vary between muscles of mammalian species (0.1-0.3Mpa, Medler, 2002; Hiroyuki et al., 1996) and so caution should be taken when making hypotheses based on estimations of F_{MAX}.

PCSA was estimated using:

$$PCSA = (Cos\theta \times m) \div (\rho \times l)$$

Where m is the muscle belly mass, ρ is muscle density (= 1.06 g cm^{-3}; Mendez and Keys, 1960) and l is the muscle fascicle length. Previous studies (Thorpe et al., 1999; Payne et al., 2006a) have observed that pennation angles are close to, 20° in most ape limb muscles, suggesting that θ has little effect on the PCSA (since $Cos[20°] \approx 1$). However, pennation angle was included in my calculation of PCSA because the pennation angle of many gibbon hind limb muscles exceeded, 20° (maximum θ = 39°, implying a 22% reduction in PCSA) which was considered substantial enough to be taken into account.

Muscle function can be estimated by the position of the muscle or muscle group on a graph of PCSA against fascicle length (Fig. 2.2; also: Williams et al., 2008). Muscles at the top of the graph, with high PCSA, can produce high levels of force (since PCSA is directly related to F_{MAX}). Maximum contraction distance is proportional to fascicle length, so muscles on the right hand side of the graph, where FL is high, can contract over a wide range of motion. Muscles with both high PCSA and long fascicles (i.e. large volume) are capable of producing high levels of work (force x distance) in a given time period. Contraction velocity, and therefore power (since power = work ÷ time) can also be said to increase with fascicle length (Zajac, 1989), but only where all other variables are fixed e.g. of two muscles with identical physiological properties but different lengths and volumes (i.e. the same PCSA), the longer muscle should contract more rapidly (and hence produce more power) since they have a greater number of sarcomeres in series (Zajac, 1989, 1992). In reality however, muscle fibre type has a much greater influence on contraction velocity, and a myriad of other factors have a profound effect on muscle power output

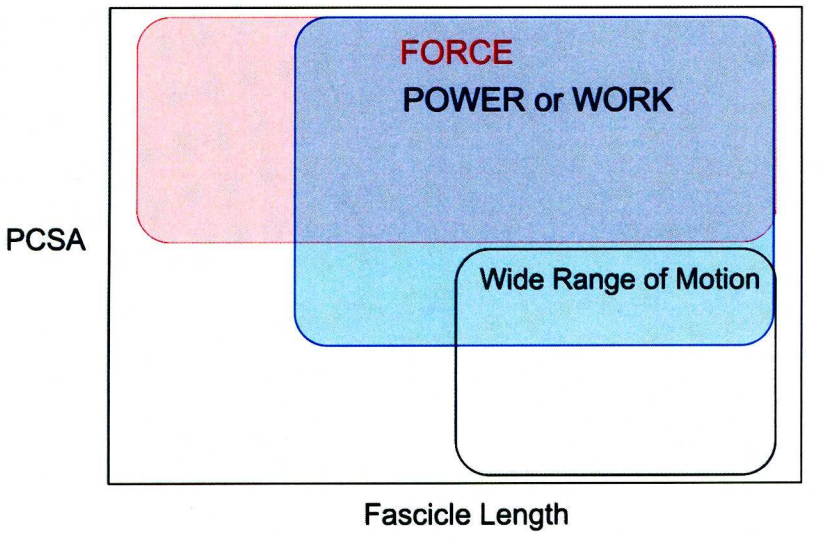

Figure 2.2. Muscle function estimated by position on a graph of PCSA against fascicle length

(activation pattern: Biewener, 1998b, muscle fibre type; Altringham and Johnston, 1990; Widrick et al., 1996 architectural gear ratio and pennation angle; Alexander, 1996; Azizi et al., 2008).

Muscles on the bottom right hand side of the graph, with low PCSA and high FL, produce a modest force over a wide range of motion. Finally, the function of muscles on the bottom of the left hand side of the graph (low PCSA, short fascicles) is debatable. Their function may be related to the stabilisation of joints (Williams et al., 2008), or they may be used for precision movements, or it may simply be that this is the 'default' position of unspecialised muscle and muscles specialised for force, power or work deviate from this.

Tendon function

The function of a tendon can be estimated from its gross morphology, where long thin tendons are indicative of elastic energy storage ('compliant' muscle tendon unit), and short thick tendons imply greater MTU contraction distances and therefore work (i.e. 'stiff' MTUs; Ker et al., 1988; Williams et al., 2007; McGowan et al., 2008). Safety factor is an index which links the force producing capabilities of the muscle to the force resisting capabilities of the tendon. MTUs with a large PCSA to tendon cross-sectional area (TCSA) ratio can place the tendon under large amounts of stress, eliciting large tendon strain and therefore enabling elastic energy storage. MTUs with a relatively smaller PCSA to TCSA ratio have a lower propensity to stretch the tendon and, hence, are less likely to be associated with elastic energy storage. Safety factor gives an indication of how close the tendon comes to rupture when the muscle undergoes F_{MAX}. A safety factor of one implies that if the muscle contracts with F_{MAX} this will be just enough to cause the tendon to fail while a safety factor of two suggests that F_{MAX} is half the force required to rupture the tendon, etc. I estimated the safety factor as follows:

Safety Factor = (TCSA x Max. Tendon Stress) ÷ (PCSA x Max. Iso. Stress)

= Max. Tendon Force ÷ F_{MAX}

Where maximum tendon breaking stress is 100 MPa (again, this value has been shown to vary between species; Pollock and Shadwick, 1994), and maximum isometric stress of skeletal muscle is 0.3 MPa (Wells, 1965; Medler, 2002).

A second estimate of tendon function can be made by devising a ratio of tendon length (TL) against fascicle length (FL). Muscles with long fascicles and short tendons possess a large amount of control over the tendon since the fascicles can negate any tendon strain by muscular contraction. In this context, muscles with low tendon length to fascicle length ratios can be termed 'stiff'. MTUs with short fascicles and long tendons (high TL:FL) are less able to contract to negate tendon strain because of the relatively shorter fascicles. These MTUs can be termed 'compliant' and are more likely to be associated with elastic energy storage. The TL to FL ratio was calculated using:

Tendon Length ÷ (Fascicle Length x Cosθ) = TL:EFL

By including the pennation angle (θ) in my results I calculate an 'Effective Fascicle Length' (EFL) by which I divide tendon length to give a tendon length to effective fascicle length ratio (TL:EFL). In muscles with parallel fibres θ was 0.

Results

Descriptive anatomy

There were few qualitative differences in organisation of the hind limb musculature between the different species and between individuals of the same species. One obvious variation was the presence of a plantaris muscle, which was either absent (4 of 11 specimens), completely or partially fused with the lateral head of the gastrocnemius (5/11) or completely separate (2/11, Fig. 2.3). When present, the thin tendon ran at the medial side of the Achilles tendon and inserted separately on the posterior side of the tuber calcanei.

The gluteus superficialis (called gluteus maximus in humans) was irregularly shaped and had fascicles which were orientated in different directions relative to the insertion tendon (Fig. 2.4). The muscle had a thin, sheet-like origin, originating on the posterior side of the gluteus medius, across the width of the ilium. It became progressively thicker around the hip joint. A small portion of the belly inserted with an internal tendon onto the greater trochanter, another small part passed down the lateral side of the hip until the proximal end of the femoral diaphysis where in some specimens it was associated with a thickened fascia, probably homologous to the tensor fascia lata in humans. Most of the muscle belly passed posterior to the hip and inserted directly

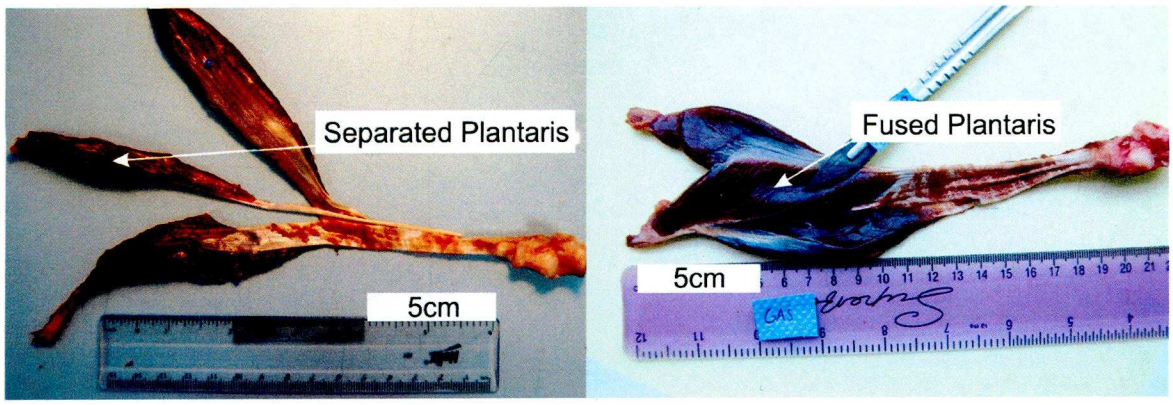

Figure 2.3. Photographs showing the presence of separated (specimen *H. lar* 2) and fused (specimen *S. syn* 1) plantaris muscles.

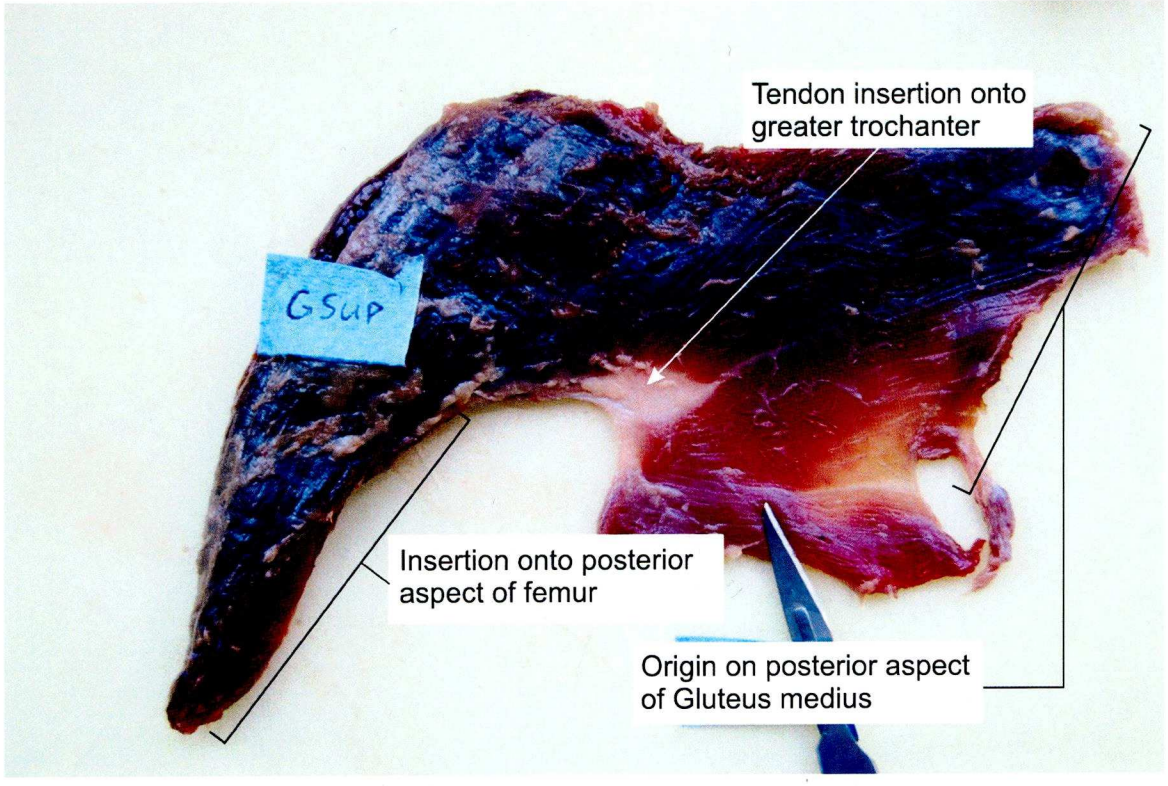

Figure 2.4. The gluteus superficialis muscle, with indication of thigh insertion and tensor fascia lata

onto the posterior aspect of the femur, without a tendon.

The adductor muscles were fused to varying degrees in all the specimens, making identification and separation difficult. The adductor longus was quite distinct and the easiest to identify, while the adductor brevis was very difficult to identify as a separate muscle and was therefore treated as part of the adductor magnus in the analyses.

A detailed qualitative description of the hind limb anatomy of gibbons has been published previously (Bischoff, 1870; Kanagsuntheram, 1952; Sigmon and Farslow, 1986; Vereecke et al., 2005), and I refer to those publications for a full anatomical description of the gibbon hind limb musculature. Mean anatomical data is presented for each species in Table 2.3 and Appendix 2.1.

Hind limb muscle volume

The gluteals (hip extensors), adductors and quadriceps (knee extensors) muscles made up the majority of the hind limb muscle volume (HLMV), together accounting for 58 ± 4% of the total volume (Fig. 2.5). The lar and moloch gibbons both had larger quadriceps than gluteals (lar: 29% *vs.* 23% of HLMV; moloch: 26% *vs.*, 19% of HLMV for quadriceps *vs.* gluteals respectively), a trend not seen in the pileated gibbon or the siamang (pileated: 19% *vs.* 22% of HLMV; siamang: 14% *vs.* 21% of HLMV for quadriceps vs. gluteals respectively). There were few other inter-specific differences in muscle volume make up.

The adductor group was the third largest functional muscle group in all the species, despite including the adductor magnus which was the largest single hind limb muscle (regardless of whether it was fused with the other adductors) in all species (14.6 ± 0.2% of HLMV). The largest muscle group on the distal limb segment was the plantarflexor group (9.8 ± 1.4% HLMV), consisting of the triceps surae. The other muscle groups on the shank made up 5% or less of HLMV.

Table 2.3. Mean ($\bar{x}$) anatomical measurements with standard deviations (σ) for each species.

	H. lar						*H. pileatus*					
Muscle	Fascicle length (cm)		θ (°)		PCSA (cm^2)		Fascicle length (cm)		θ (°)		PCSA (cm^2)	
THIGH	$\bar{x}$	σ	$\bar{x}$	σ	$\bar{x}$	σ	$\bar{x}$	σ	$\bar{x}$	σ	$\bar{x}$	σ
Gluteus superficialis	9.7	0.3	-	-	6.0	1.3	8.1	0.5	-	-	4.4	0.4
Gluteus medius	3.8	0.7	24.6	-	8.3	1.2	3.8	0.2	27.6	-	6.1	1.1
Gluteus minimus	2.8	0.3	-	-	2.5	1.3	3.2	-	-	-	2.1	-
Pectineus	4.8	0.2	p	p	0.6	0.2	5.1	0.4	p	p	0.5	0.0
Obturator internus	2.2	0.8	30.9	-	3.3	1.1	1.3	0.1	-	-	4.5	0.3
Obturator externus	4.0	3.4	-	-	2.0	1.1	2.0	-	-	-	2.2	-
Piriformis	4.2	0.4	28.5	-	1.4	0.1	2.7	0.1	-	-	1.8	0.1
Adductor magnus	13.9	1.7	29.1	5.8	4.6	1.3	12.5	0.9	-	-	3.2	1.3
Adductor longus	8.0	0.6	22.8	-	0.7	0.2	9.8	2.9	-	-	0.9	0.4
Adductor brevis	9.0	-	p	p	1.1	-	5.6	-	p	p	0.6	-
Quadratus femoris	3.4	0.6	p	p	1.4	0.4	3.3	-	p	p	0.7	-
Rectus femoris	3.9	0.3	21.0	0.3	3.9	0.3	3.2	0.2	17.2	0.1	2.8	0.2
Vastus medialis	4.6	-	25.5	0.3	3.8	-	3.4	0.1	21.8	-	6.5	2.6
Vastus intermedius	3.6	0.8	25.9	4.9	10.0	1.5	3.0	-	17.5	-	10.9	-
Vastus lateralis	4.3	0.5	30.7	5.3	11.9	1.4	3.2	0.1	22.3	3.8	10.3	2.4
Gracilis	19.2	0.9	p	p	0.5	1.4	16.9	4.2	p	p	0.4	0.0
Sartorius	21.4	1.7	p	p	0.7	0.8	21.5	1.1	p	p	0.4	0.1
Semimembranosus	11.3	1.8	29.4	-	0.7	0.1	9.0	0.3	18.2	-	0.9	0.1
Semitendinosus	18.0	2.3	p	p	0.8	0.2	16.5	4.3	p	p	0.5	0.1
Biceps femoris (Long head)	7.6	2.9	p	p	1.1	0.1	7.5	0.3	p	p	1.0	0.1
Biceps femoris (Short head)	3.8	1.2	-	-	1.7	0.3	4.1	-	15.3	-	1.0	-
SHANK												
Tibialis anterior	4.4	1.2	26.1	10.8	1.6	0.2	3.3	0.0	12.9	-	1.5	0.1
Extensor digitorum longus	4.9	2.2	15.7	2.3	0.8	0.2	4.3	0.3	16.1	-	0.7	0.1
Extensor hallucis longus	5.5	1.1	14.6	2.4	0.4	0.0	5.8	0.3	-	-	0.3	0.0
Peroneus longus	1.9	0.1	23.5	4.0	2.6	0.2	1.6	0.7	18.4	-	1.5	1.0
Peroneus brevis	1.5	0.2	24.9	-	0.9	1.2	1.4	0.2	-	-	0.9	0.2
Soleus	2.6	0.1	27.7	0.3	3.4	0.3	2.6	0.2	23.0	5.4	1.7	0.2
Gastrocnemius medialis	3.0	0.4	27.4	-	3.5	1.0	3.0	0.4	-	-	2.0	0.3
Gastrocnemius lateralis	3.4	0.1	-	-	4.3	0.3	3.2	0.0	26.6	-	3.2	0.4
Tibialis posterior	1.7	0.4	20.2	-	3.1	0.7	1.3	0.7	27.9	-	3.7	0.9
Flexor tibialis	2.9	0.4	21.8	-	1.8	0.6	2.3	0.9	17.3	1.1	1.6	0.8
Flexor fibularis	3.8	0.2	30.1	2.0	4.5	1.1	3.8	0.2	23.3	2.7	3.1	0.2
Popliteus	1.6	0.2	29.9	-	1.7	0.2	1.4	0.1	24.3	3.2	2.0	0.3

Table 2.3 continued

Muscle	*H. moloch*						*S. Syndactylus*					
	Fascicle length (cm)		θ°		PCSA (cm^2)		Fascicle length (cm)		θ°		PCSA (cm^2)	
THIGH	$\bar{x}$	σ	$\bar{x}$	σ	$\bar{x}$	σ	$\bar{x}$	σ	$\bar{x}$	σ	$\bar{x}$	σ
Gluteus superficialis	7.4	1.6	-	-	5.2	0.3	9.0	3.2	-	-	9.3	4.1
Gluteus medius	3.6	1.4	29.1	5.0	5.8	0.7	4.2	1.1	28.4	4.3	10.1	1.3
Gluteus minimus	3.3	1.4	-	-	1.7	1.1	4.0	1.5	20.5	3.5	2.0	0.9
Pectineus	4.2	0.4	p	p	0.5	0.3	6.2	0.4	p	p	1.0	0.1
Obturator internus	1.8	0.0	-	-	2.6	1.4	3.1	0.4	35.7	5.3	3.6	1.3
Obturator externus	1.8	0.4	-	-	2.2	0.3	3.1	0.4	30.9	0.4	3.6	0.7
Piriformis	4.2	0.5	-	-	0.8	0.3	3.9	1.3	-	-	1.9	0.5
Adductor magnus	10.9	1.5	24.7	-	4.1	0.3	12.2	0.8	32.3	3.7	6.7	2.0
Adductor longus	7.5	0.3	-	-	0.6	0.0	8.9	1.3	-	-	1.2	0.2
Adductor brevis	6.2	-	p	p	0.3	-	7.4	1.2	p	p	0.9	0.8
Quadratus femoris	3.6	0.0	p	p	0.9	0.3	4.8	1.1	p	p	1.6	0.6
Rectus femoris	3.0	0.9	24.7	7.6	2.8	0.2	5.0	0.4	18.9	7.4	4.0	1.3
Vastus medialis	4.3	2.4	-	-	3.4	1.2	4.6	1.5	18.5	3.6	4.8	1.5
Vastus intermedius	3.4	-	-	-	4.6	-	3.8	0.4	22.4	-	12.3	3.3
Vastus Lateralis	4.1	1.2	21.2	1.1	5.5	3.3	5.0	0.5	27.3	8.1	9.7	1.6
Gracilis	16.1	2.2	p	p	0.5	0.0	19.6	2.0	p	p	1.0	0.5
Sartorius	18.9	0.6	p	p	0.6	0.1	20.8	1.3	p	p	1.0	0.4
Semimembranosus	8.2	1.9	26.1	-	0.9	0.0	9.9	1.0	23.9	5.0	1.3	0.5
Semitendinosus	14.0	0.3	p	p	0.8	0.1	17.4	2.9	p	p	1.5	0.6
Biceps femoris (Long head)	8.5	1.9	p	p	1.0	0.0	9.0	2.0	p	p	1.9	0.9
Biceps femoris (Short head)	3.6	0.5	-	-	1.2	0.0	6.8	3.3	-	-	1.5	1.0
SHANK												
Tibialis anterior	3.0	0.2	24.6	-	1.8	0.4	4.5	1.4	20.9	2.9	3.1	0.8
Extensor digitorum longus	3.7	0.1	17.7	-	0.8	0.2	5.8	1.2	15.8	4.6	1.0	0.4
Extensor hallucis longus	5.2	0.1	-	-	0.3	0.0	5.4	1.3	17.3	5.5	0.6	0.3
Peroneus longus	1.7	0.5	19.6	-	2.2	0.1	3.2	0.7	21.2	2.5	2.8	1.0
Peroneus brevis	1.2	0.2	-	-	1.4	0.2	2.0	0.5	20.7	1.6	1.5	0.7
Soleus	2.3	0.3	24.8	-	3.0	0.5	3.3	0.4	23.2	0.9	4.9	1.5
Gastrocnemius medialis	3.2	0.1	25.3	1.1	1.8	0.6	3.9	0.6	24.9	-	4.9	1.8
Gastrocnemius lateralis	3.6	0.0	22.5	-	2.7	0.8	4.1	1.0	-	-	5.9	0.8
Tibialis posterior	1.6	0.3	-	-	2.8	0.0	2.7	1.3	28.4	12.6	3.4	1.0
Flexor tibialis	2.5	1.2	20.5	-	1.1	0.2	4.7	1.9	21.3	2.2	2.5	1.3
Flexor fibularis	4.2	0.8	-	-	2.3	0.9	5.9	0.5	24.6	1.8	3.4	0.8
Popliteus	1.2	0.2	32.4	-	1.8	0.4	2.6	1.9	19.8	4.6	3.1	1.2

p, parallel fibred muscle

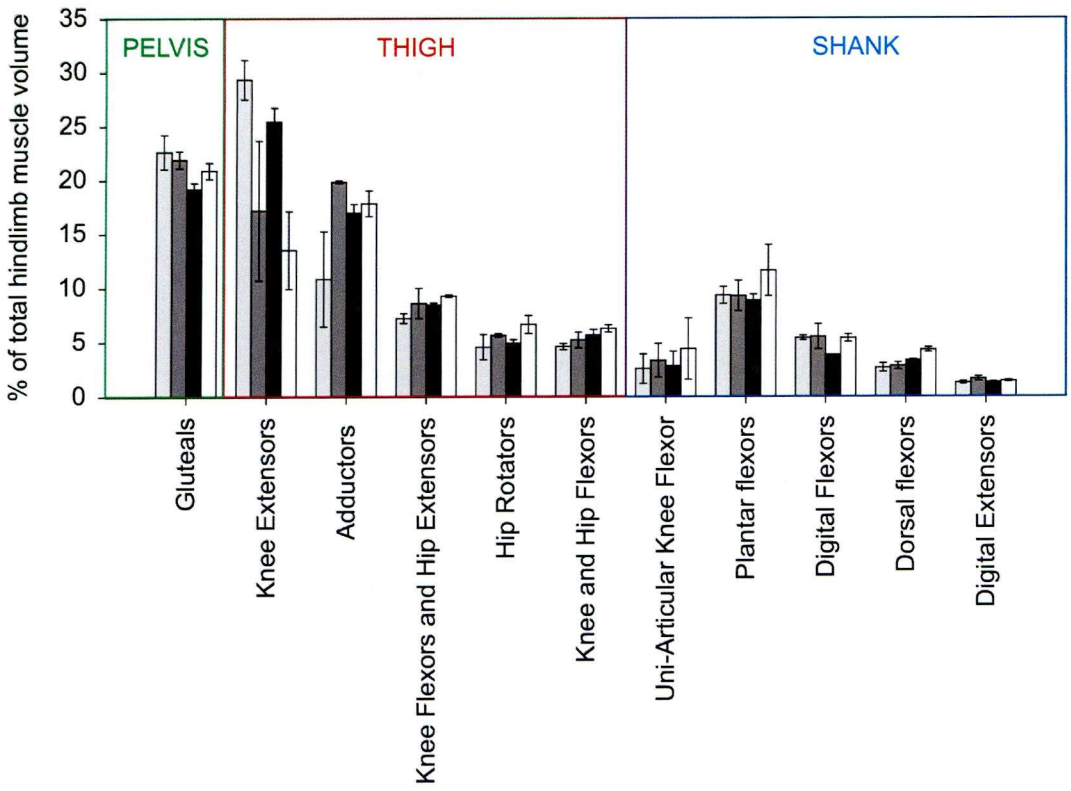

Figure 2.5. The contribution of each functional group to total hind limb muscle volume and the position of each group on the skeleton. Error bars denote the standard error of the mean.

Muscle PCSA and fascicle length

The gibbon hip extensors (gluteals) and knee extensors (quadriceps) showed a relatively higher PCSA and relatively shorter fascicles than the other functional muscle groups of the hind limb (Fig. 2.6). The knee extensors of the siamang had a relatively lower PCSA than the other gibbon species, suggesting that the quadriceps of the siamang have a lower propensity for force production. The muscles with the longest fascicles were the bi-articular knee and hip flexors (i.e. sartorius and gracilis) which had a small PCSA. There were no muscles with both high PCSA and long fascicles. The majority of muscle groups (plantarflexors, dorsiflexors, knee flexors, digital flexors, hip rotators and digital extensors) had short fascicles and relatively small PCSAs, putting them on the lower left hand side of figure 2.6.

The iliacus muscle taken from Payne et al. (2006a) had relatively short fascicles and an intermediate PCSA, positioning it at the middle/left-hand side of the graph (red star, Fig. 2.6).

Tendon anatomy

The tendons of the hind limb muscles of gibbons display a range of safety factors, implying varying tendon function throughout the hind limb (Fig. 2.7). The knee flexors and hip extensors (SeM and SeT), dorsal flexors (TiA), digital extensors (EDL and EHL) and digital flexors (FlT and FlF) all had safety factors above 4 (SeM = 6.4; SeT = 11.4; TiA = 6.6; EDL = 13.5; EHL = 9.8; FlT = 4.1; FlF = 6.0). Tendons with lower safety factors include the patellar tendon of the quadriceps (Pat. = 2.2) and the Achilles tendon of the triceps (Ach. = 3.1), as well as the tendon of origin of the soleus (2.9) and the tendon of insertion of TiP (3.1). The safety factor was highly variable between species, and no pattern was observed suggesting one species had consistently higher or lower safety factors than any other.

Generally, MTUs on the pelvis and thigh had TL:EFL ratios of around or less than 1 (Fig. 2.8). There was one notable exception to this: the quadriceps had relatively longer tendons and more pennate and shorter fascicles than other muscles on the thigh (e.g. adductor magnus), giving a higher TL:EFL ratio (inter-specific means of 3.87, 3.84, 4.36 and 3.12 for ReF, VMe, VIn and VaL respectively *vs.* 0.88 inter-specific mean for all other thigh muscles). Muscles on the distal limb segment (shank and foot) had higher TL:EFL ratios than MTUs on the hip and thigh (inter-specific

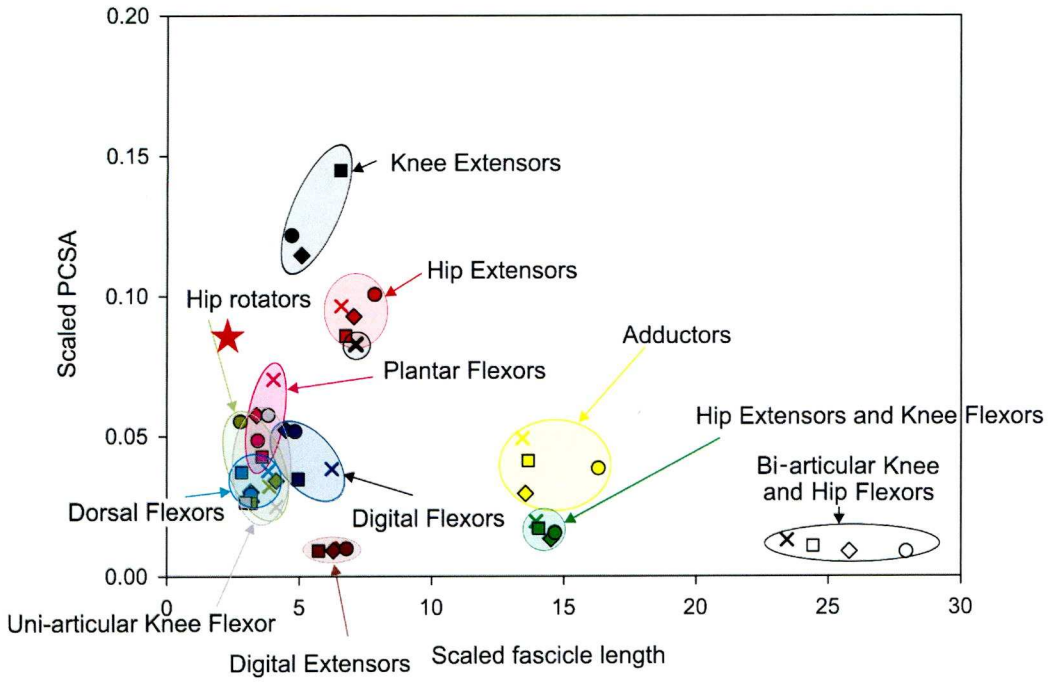

Figure 2.6. Plot of PCSA (scaled to hind limb muscle mass – $HLMM^{2/3}$) against fascicle length (scaled to $HLMM^{1/3}$) for gibbon hind limb muscles. Figure key: Different colours represent different muscle groups; black = knee extensors, red = hip extensors, blue = digital flexors, yellow = adductors, green = hip extensors and knee flexors, mauve = digital extensors, grey = uni-articular knee flexor, cyan = dorsal flexors, pink = plantar flexors, gold = hip rotators, open symbols = bi-articular knee and hip flexors. Different symbols represent different species: cross = siamang, diamond = lar gibbon (white handed gibbon), circle = moloch gibbon, square = pileated gibbon. The red star represents the position of the iliacus muscle from Payne et al. (2006a).

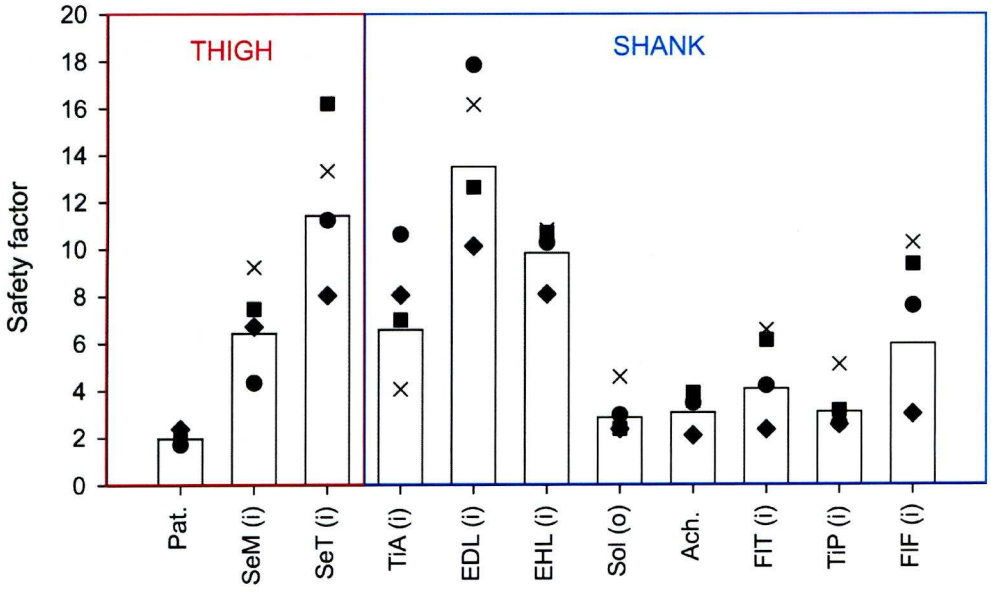

Figure 2.7. Estimated safety factors for tendons in the hind limb. (i) denotes an insertion tendon, (o) denotes a tendon of origin. Bars represent the mean of all species. Symbols represent the mean from each species. See Table 2 for muscle name abbreviations.

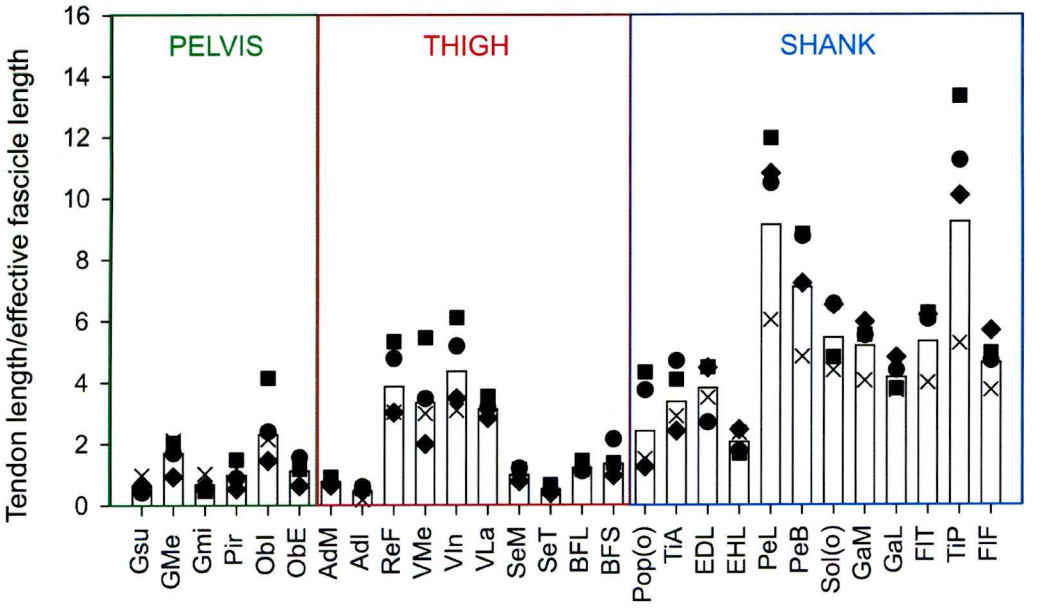

Figure 2.8. Tendon length divided by effective Fascicle Length (EFL, see text for calculation) for all muscles with an appreciable tendon in the hind limb. Bars represent inter-species mean. Symbols represent individual species means. See Table 2 for muscle name abbreviations

mean for all muscles: Pelvis, 0.88; Thigh, 1.99; Shank, 5.15). The highest TL:EFL ratios were seen in tibialis posterior and peroneus longus (inter-specific means of 9.23 and 9.13, respectively).

Discussion

Gluteus superficialis and adductor magnus

The morphology of the gluteus superficialis was similar to that described by Sigmon and Farslow (1986) and Stern (1972), where the authors correlated specific regions of the muscle with human equivalents (for example the presence of a pars tensorica is hypothesised as an equivalent of tensor fascia lata). The gibbon's gluteus superficialis had a similar morphology to that of the African great apes (Sigmon and Farslow, 1986; Payne et al., 2006a). Because the muscle is made up of several functional parts with varying fibre orientations, its function is likely to be diverse. The position of the muscle in gibbons (i.e. mainly posterior to the hip joint) suggests that its main role is hip extension, although it may also play some role in abduction and/or stabilising the hip joint, because it also covers the lateral aspect of the hip joint.

The high degree of fusion in the adductor muscles observed in most of my gibbon specimens has not been described by other authors (Sigmon and Farslow, 1986; Payne et al., 2006a). All the adductor muscles appear to perform the same role (thigh adduction) and probably work together, allowing varying degrees of fusion.

The unpredictability of the presence of a plantaris muscle in gibbons has also been documented by other authors (Sigmon and Farslow, 1986; Vereecke et al., 2005). This muscle is known to be vestigial in many ape species (Sigmon and Farslow, 1986). The plantaris is as a dedicated plantarflexor and inverter of the foot, yet its small size and variable presence suggest it is of minor importance for foot motion.

Muscle volume: Adaptations for vertical climbing, orthograde clambering and leaping?

The gluteals, quadriceps and adductors made up the majority of hind limb muscle volume of gibbons. Having large (voluminous) muscles in these areas might give insight into the specialisation of the gibbon hind limb. Gluteals and quadriceps are hip and knee extensors

respectively, which might be important in several activities such as bipedalism, vertical climbing, and leaping. The volume of muscle dedicated to knee and hip extension in the gibbon is likely to be useful for some or all of these activities. Moreover, having a large proportion of muscle mass situated proximally (hip and thigh) will minimise the inertia of the swinging limb during locomotion, thus reducing metabolic work (Steudel, 1996 and see below for further discussion).

Adductor muscles are traditionally associated with keeping the limbs underneath the body (Alexander, 1996). During vertical climbing and orthograde clambering the limbs are often outside of the projection of the body's centre of gravity. Therefore, arboreal animals should possess enlarged adductor muscles to cope with the increased muscular demand of such activities (Preuschoft, 2002; Isler, 2005). In gibbons, in which these modes form up to 35% of locomotion (Fleagle, 1976), the adductors made up a similar proportion of the HLMV as reported for other non-human apes (gibbons inter-specific mean = 16.4 ± 5.5% HLMV, bonobos =, 18.5%, chimpanzee =18.8%, gorilla = 22.5%, orang-utan = 16.7%; data on great apes from Thorpe et al., 1999 and Payne et al. 2006a), suggesting that limb adduction has a similar importance across the non-human apes. Humans have significantly smaller adductor muscles (≈7% of HLMV, based on estimates from Thorpe et al., 1999 and assuming that each hind limb in humans makes up, 19% of total body mass; Zihlman, 1992), which is likely associated with osteological adaptations to bipedal walking e.g. bicondylar or valgus angle of the knees (i.e. medio-distal inclination of the femur, Jones et al., 1992).

Functional implications of the gibbon's hind limb anatomy

The hip and knee extensors' short-fascicled, large-PCSA anatomy implies that the muscles are suitable for high muscular force production, but not for contracting over a long distance. It is possible that gibbons use high levels of force (as distinct from power) for a number of activities, including the dissipation of energy during landing. In this case, the muscles have to work eccentrically to decelerate the gibbon during landing, reducing the magnitude of the forces associated with landing, although my estimations suggest that the patellar tendon would be close to rupture during maximal eccentric loading (see '*Tendon anatomy: Elastic energy storage or ideal mass distribution?*' and Westing et al., 1991; Demes et al., 1999). Yet, the short-fascicled large PCSA hip and knee extensors may still be able to produce high levels of power at the joint by means of a power amplifying mechanism, as observed in several primate genera (galago: Aerts,

1998; bonobo: Scholz et al., 2006). Power amplifiers usually take one of two forms: some galagos are very proficient leapers and use a tendinous mechanism, where the patellar tendon stores elastic strain energy during pre-stretch, which is released rapidly prior to push-off, amplifying power generation (Alexander, 1995; Aerts, 1998). Bonobos utilise short-fascicled hip and knee extensors (Payne et al., 2006a) coupled with small muscle moment (lever) arms at the hip and knee joints (Payne et al., 2006b) to turn relatively small fascicular contractions into relatively large joint movements (see also Alexander, 1995; Fukunaga et al., 2001). Recent research has shown that bonobos (*Pan paniscus*) are expert leapers, and it is suggested that they use this 'amplifying' mechanism for propulsion generation in leaping (Scholz et al., 2006). My results indicate that gibbons, which are also very able leapers (Fleagle, 1976; Gittins, 1983), have hip and knee extensors which fall into similar positions on a PCSA against fascicle length graph as bonobos (Fig. 2.9). This leads us to hypothesise that both gibbons and bonobos may use a similar mechanism, coupling their short-fibred, large PCSA hip and knee extensors to short muscle moment arms, in order to enhance leaping performance. It is interesting to note that none of the other apes, of which none are remarkable jumpers, have hind limb muscles with similar relative PCSAs as the bonobo or gibbon. Also, although all the published data (Fig. 2.9) are scaled in the same way as my gibbon data, these take no account of pennation angle, meaning that the gap between the gibbon's and bonobo's relative PCSA is likely exaggerated, which further strengthens my hypothesis.

Within gibbons, the knee extensors of the siamang have a relatively smaller PCSA than those of other gibbons (Fig. 2.6). If knee extensors are indeed used to power leaping in gibbons this would suggest that siamang are less adept or less frequent leapers than the other gibbon species. In support of this, field reports (Fleagle, 1976) indicate that siamang spend indeed proportionally less time leaping than other species of gibbon (6% vs. 15% for lar gibbons; see '*Inter-specific Differences*' for further discussion).

The bi-articular hip and knee flexors (gracilis and sartorius) in gibbons have relatively longer fascicles than those of any of the non-human ape species (Fig. 2.9), which may reflect a higher propensity for positioning the hind limb in a wider range of postures. The gibbons' rapid locomotion through an unstable three-dimensional environment may mean that being able to move the limbs over a wide range of motion has advantages in reaching a branch and avoiding a fall. They are also vertical climbers and orthograde clamberers; it is likely that limb placement is highly variable during this form of locomotion and long-fascicled muscles should provide some

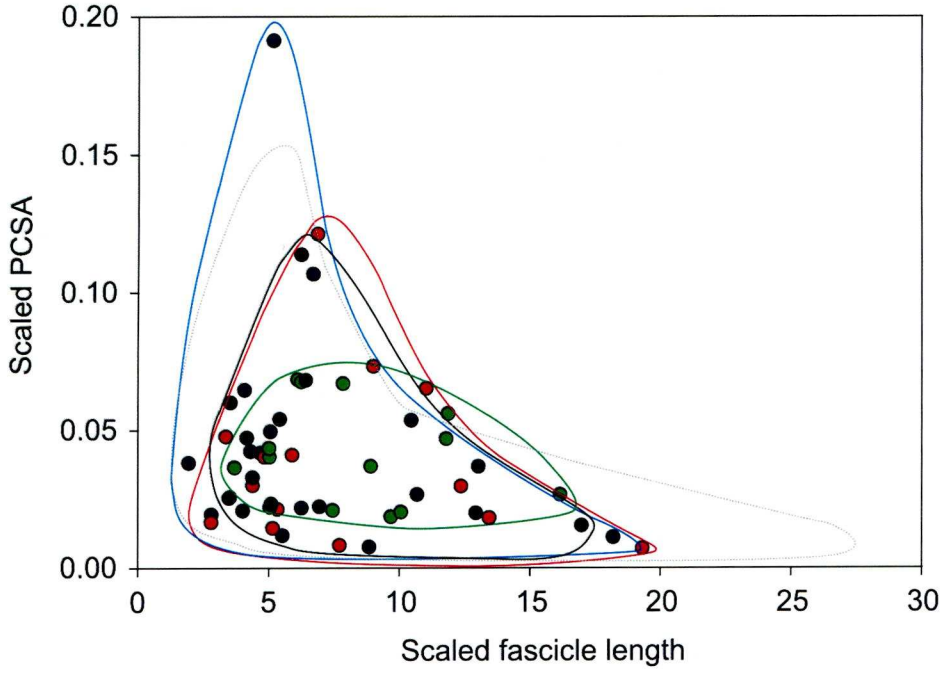

Figure 2.9. Relative PCSA against relative fascicle length for all non-human ape species (see text for scaling parameters). Data for chimpanzee is from Thorpe et al. (1999), data from bonobo, gorilla and orang-utan are from Payne et al. (2006a).The coloured shapes visualise the position of the muscles of each species. Blue, bonobos; Grey dotted, gibbon; Red, gorilla; Black, Common chimpanzee; Green, orang-utan.

aid to this. Indeed, the long-fascicled, low-PCSA muscles of the hind limb of orang-utans (where orthograde clambering is a major activity, Thorpe and Crompton, 2005, 2006) have been attributed to varied limb placement during orthograde clambering by Hunt and colleagues. (1996) and Payne and colleagues (2006a), although when scaled to mass$^{1/3}$ the fascicle lengths do not seem extraordinary in comparison to other ape species (Fig. 2.9). Hind limb position is also thought to be important in powering brachiation (Bertram and Chang, 2001) where 'leg-lift' raises the centre of mass during the swing phase, resulting in an increase in mechanical energy or a reduction in collisional energy loss on the next swing (Usherwood and Bertram, 2003). Long-fascicled muscles allow a greater range of hind limb motion, enabling a greater upward displacement of the body's centre of mass during the swing and a greater mechanical energy benefit for brachiating gibbons. Hip flexors likely play an important role in this leg-lift. However, data on a major hip flexor, the iliopsoas, was not available which means that I have underestimated the mass of muscle used to flex the hip and the force involved in these movements. Published data indicate that the iliacus (part of the iliopsoas) is short fascicled with a large PCSA in comparison with the other hip flexors (i.e. Rectus femoris, Sartorius, Gracilis), suggesting the muscle is unlikely to increase the range of motion of the hip significantly but that it will increase the amount of force available for leg lift (Fig. 2.6).

Tendon anatomy: Elastic energy storage or ideal mass distribution?

Overall, the tendons in the distal hind limb segment were relatively longer (with respect to fascicle length; high TL:EFL) than those in the proximal limb segment (Fig. 2.8 and Appendix 2.1). Longer tendons allow muscle force to be transmitted to the distal limb without the burden of extra muscle mass placed distally, which is detrimental to efficient locomotion (through increased limb inertia; Steudel, 1996). Long tendons also allow short-fascicled muscles to produce force more efficiently by combining isometric muscle contraction with tendon strain, thus keeping the muscle fascicles at optimum length for efficiency (Alexander, 1996). The thickness of tendons with respect to PCSA is shown by the safety factor, where relatively thick tendons have a high safety factor and thinner tendons have a lower safety factor.

One method of power amplification for muscles is the sudden release of elastic energy previously stored in a tendon (Alexander, 1995; Aerts, 1998), and safety factor can be used to estimate

whether this is likely to be the case. The safety factors of the tendons in the gibbon hind limb varied greatly, suggesting different functions (Fig. 2.7). The lowest safety factor, and hence highest potential tendon stress, was found for the patellar tendon, suggesting it may be used for elastic energy storage. As the patella tendon is associated with the knee extensors (quadriceps), a low safety factor in this tendon supports the hypothesis that leaping maybe powered by a tendinous mechanism. This hypothesis is further supported by the relatively long tendons and relatively short fascicles of the vasti and rectus femoris (Fig. 2.8), suggesting a relatively 'compliant' MTU. Interestingly, my estimations of safety factor are based on maximum isometric stress which may be exceeded during eccentric loading (e.g. during cyclical locomotion or landing), further reducing safety factor (Ker et al., 1988; Westing et al., 1991) and potentially making the patellar tendon vulnerable to rupture under high eccentric loads.

The perceived 'compliance' (based on a high TL:EFL) of the MTUs in the distal hind limb could simply be a by-product of minimising inertia in the distal limb. By using the TL:EFL in combination with safety factor I can gain some insight into whether or not the distal MTUs may be used to store elastic strain energy or are merely a by-product of limb inertia optimalisation. The Achilles tendon in gibbons has a very low safety factor and a high TL:EFL ratio, which is due to the remarkably long length of the Achilles tendon in gibbons compared to that of other non-human apes (Payne et al., 2006a; Vereecke and Aerts, 2008). A compliant triceps MTU may play a number of roles during gibbon locomotion including energy storage during bipedalism or leaping (Vereecke et al., 2006b; Vereecke and Aerts, 2008). Alternatively, it may be used to transfer force to the distal limb from the powerful vasti, as in *Galago senegalensis* (Aerts, 1998). It is difficult to know from gross anatomy alone what the function of the Achilles tendon is, especially as it is likely to have a variety of roles given the gibbon's extensive locomotor repertoire. However, the large PCSA of the triceps surae suggests a significant role in hind limb dominated locomotion. Further data on tendon properties (Young's modulus, ultimate tensile strength etc.) and muscle fibre type are needed to yield further insight into the triceps' role in power production, force transfer and weight support.

Interspecific differences

The few studies investigating locomotor behaviour of wild gibbons (Whitmoor, 1975; Fleagle, 1976; Gittins, 1983) indicate that there are few inter-specific differences in locomotor repertoire,

which could explain why only few inter-specific differences in myology were observed in my study. One notable difference was the smaller mean PCSA of the knee extensors of the siamang compared to other gibbon genera. The volume of the knee extensor muscles of siamang was less than the volume of hip extensor muscles, a pattern also observed in the pileated gibbon, but not in the lar gibbon nor moloch gibbon. Like siamang, pileated gibbons spend relatively little time leaping (ca. 5% of their locomotor time; Whitmoor, 1975), yet, pileated gibbons had the highest PCSA in their knee extensor muscles of any of my subjects. This suggests that quadriceps PCSA might not be as good an indicator of leaping frequency as muscle volume, although my sample size is too small to draw any definite conclusions about this. Of the gibbons in my sample, those which spend a greater proportion of time leaping (lar gibbons and moloch gibbons; Fleagle, 1976) had a large muscle volume dedicated to knee extension, and those which spend proportionally less time leaping (siamang and pileated gibbons; Whitmoor, 1975; Fleagle, 1976) had less muscle volume associated with knee extension.

The lack of significant inter-specific differences in the locomotor anatomy of my population could also be attributable to the limited sample size and age of the specimens. Although this was the largest sample number in any quantitative myological study on gibbons to date (11 individuals), the sample number for each species was still relatively low for the purpose of addressing inter-specific variation (4 siamang, 3 lar gibbons, 2 pileated gibbons and 2 moloch gibbons). Hence the primary aim of this study was not to investigate inter-specific differences in myology, but to quantify the general anatomy of the gibbon hind limb and link it to the major locomotor modes utilised by these species. The small inter-specific differences that were noted indicate that the presented anatomical data are valid for all studied gibbon species and I would expect all hylobatids present a similar hind limb musculature as quantified in this study.

All of my animals were kept in captivity, and the area in which they lived is small compared to their natural home range (Milton and May, 1976), so it is likely that they were not as physically active as wild animals. Since all of my cadavers were captive animals it is probable that they were subject to similar limitations of activity. At least four of my specimens were over 25 years old (three were of unknown age) and it is likely this has some effect on the absolute values of some muscle masses, although none died of musculoskeletal pathologies. Unfortunately, these are unavoidable limitations when working with endangered species (i.e. the gibbons represented in this study are specified as endangered or critically endangered on the IUCN Red List, IUCN, 2008), as specimens are very difficult to obtain. I would like to underline that, due to these

limitations, the provided anatomical data are very valuable as they provide a quantitative database of the hind limb musculature of the gibbon. Such databases are valuable tools for a number of studies investigating comparative anatomy, evolutionary biomechanics and human evolution.

Conclusion

This study has investigated how the gibbon hind limb may cope with the varying mechanical demands placed upon them by the gibbon's varied locomotor repertoire. The short-fascicled, high PCSA hip and knee extensors are likely to play a role in leaping, potentially via a power amplifying mechanism using the relatively compliant patellar tendon, while the long-fascicled knee and hip flexors, enable a wide range of limb positions for support and centre of mass position. Further analyses of moment arms and tendon properties, as well as kinematics and kinetics of gibbon locomotion are needed to provide further evidence of this hypothesis.

List of abbreviations

EFL- Effective Fascicle Length

F_{MAX} - Maximum isometric force

FL – Fascicle Length

HLMM – Hind Limb Muscle Mass

HLMV – Hind Limb Muscle Volume

m – Mass

MTU – Muscle Tendon Unit

NPF – Natural Pendular Frequency

ρ – Density of muscle (1.06 gcm^{-3})

PCSA - Physiological Cross-Sectional Area

TCSA – Tendon Cross-Sectional Area

TL – Tendon Length

θ – Pennation angle

Chapter 3: Muscle moment arms of the gibbon hind limb: implications for hylobatid locomotion.

By Anthony J. Channon

With contributions from: Robin H. Crompton, Michael M. Günther and Evie E. Vereecke.

I dissected the specimens, designed the analysis technique, analysed the data and wrote the manuscript. Evie Vereecke assisted with data collection, provided funding for specimen collection and edited the chapter. Robin Crompton and Michael Günther edited the manuscript and advised on its content.

A version of this chapter has been published in the Journal of Anatomy

A. J. Channon, R. H. Crompton, M. M. Günther and E. E. Vereecke (2009). Muscle moment arms of the gibbon hind limb: implications for hylobatid locomotion. **216**, 4, 446-462

Abstract

Muscles facilitate skeletal movement via the production of a torque or moment about a joint. The magnitude of the moment produced depends on both the force of muscular contraction and the size of the moment arm used to rotate the joint. Hence, larger muscle moment arms generate larger joint torques and forces at the point of application. The moment arms of a number of gibbon hind limb muscles were measured on four cadaveric specimens (1 *Hylobates lar*, 1 *H. moloch* and 2 *Symphalangus syndactylus*). The tendon travel technique was used, utilising an electro-goniometer and a linear voltage displacement transducer. The data were analysed using a technique based on a differentiated cubic spline and normalised to remove the effect of body size. The data demonstrated a functional differentiation between voluminous muscles with short fascicles having small muscle moment arms and muscles with longer fascicles and comparatively smaller physiological cross-sectional area having longer muscle moment arms. The functional implications of these particular configurations were simulated using a simple geometric fascicle strain model which predicts that the rectus femoris and gastrocnemius muscles are more likely to act primarily at their distal joints (knee and ankle, respectively), because they have short fascicles.

The data also show that the main hip and knee extensors maintain a very small moment arm throughout the range of joint angles seen in the locomotion of gibbons, which – coupled to voluminous, short-fascicle muscles - might help facilitate rapid joint rotation during powerful movements.

Introduction

The functional importance of muscle moment arms

Muscles contribute to skeletal movement by exerting moments about joints. The magnitude of a joint moment is dependent on the activation level of the muscle, its contractile properties (fascicle length, fibre type, pennation angle, physiological cross-sectional area [PCSA]) and its moment arm at the joint (Zajac, 1992). The muscle moment arm (MA) is defined as the shortest perpendicular distance between the joint centre of rotation (CoR) and the line of action of the muscle tendon unit (Németh and Ohlsén, 1985; Rugg et al., 1990; Spoor and Van Leeuwen, 1992). Larger MAs are associated with larger joint moments (since, Moment = F x MA) but slower contraction velocities (since: Angular velocity = Tan-1 [ΔContraction distance / MA] / time; see also Lieber and Friden, 2001). Because of these relationships, muscles with long fascicles are not necessarily associated with large ranges of motion or rapid joint rotation (McClearn, 1985; Gans and Gaunt, 1991; Lieber and Frieden, 2001), and neither are short-fascicled muscles inherently associated with slow angular joint velocity (e.g. short-fascicled muscles can rotate joints rapidly utilising a small MA). These force- and contraction-velocity modulating capacities of MAs illustrate the important influence of MAs on muscle function.

Clearly, data on MAs represent crucial information when estimating muscle function and predicting muscle forces and moments, and are thus essential to obtain a full insight into the functional morphology of an animal (Gans and Gaunt, 1991; Zajac, 1992; Pandy, 1999; Azizi et al., 2008). In addition, accurate MA data can be used in musculoskeletal modelling to predict the magnitude of joint moments and hence ground reaction forces produced by virtual models (Crompton et al., 1996; Kramer, 1999; Sellers et al., 2005; Hirasaki et al., 2006; Sellers and Manning, 2007). Such computational models are a very powerful and promising tool for understanding locomotor evolution and performance, yet they rely heavily on the availability of accurate anatomical data.

Methods of measuring moment arms

Muscle moment arms can be measured in a number of ways. Traditional methods include the direct measurement of the MA as the distance between the line of action of the muscle-tendon unit and the joint CoR (McClearn, 1985; Németh and Ohlsén, 1985; Graichen et al., 2001; Meershoek et al., 2001). However, the position of the joint CoR can change during flexion and extension due to the irregular morphology of skeletal joints (e.g. the knee joint). Use of the tendon travel technique is often favoured because it requires no direct knowledge of the joint CoR, although this is implied through the calculation of joint angle (see Pandy, 1999 for implications of changes in the CoR on MA measurements), it is also relatively cost effective (Visser et al., 1990; Thorpe et al., 1999; Payne et al., 2006b; Williams et al., 2007). By measuring the joint angle and the amount of tendon travel that the muscle-tendon unit undergoes and subsequently differentiating the tendon travel against angular excursion curve, an estimate of MA can be made. Tendon travel is traditionally measured using threads or cords attached to the muscle belly and running through loops which represent the muscle's insertion or origin. Tags on known reference points and scales are used to calculate the absolute travel distance. Photographs are taken (although video recordings can be used as well) at different stages through the flexion-extension cycle of the joint and the images are digitised to yield joint angle and tendon travel. A polynomial curve is fitted, and then differentiated, to give MA (Visser et al., 1990; Thorpe et al., 1999; Payne et al., 2006b). Dissection is an unavoidable requirement of traditional techniques to ascertain an accurate measurement of the muscle's line of action or tendon travel. The dissection of deeper musculature related to the study muscle can change the MA of the study muscles through the elimination of wrapping effects (Murray et al., 1995; Ackland and Pandy, 2009). When using more advanced methods, such as magnetic resonance imaging (MRI; Rugg et al., 1990; Spoor and Van Leeuwen, 1992) and computed tomography (CT) MAs can be measured on living or undissected specimens. These imaging methods have the advantage of measuring the MAs in situ i.e. the MA of the muscle tendon units (MTUs) in their actual configuration and so conserve muscle wrapping effects and the effects of sesamoid bones on joint morphometry (Delp et al., 1994; Murray et al., 1995, Pandy, 1999; Krevolin et al., 2004). Further, these techniques allow the analysis of moment arms in different planes, especially applicable at the shoulder and hip joints, where circumduction occurs (Garner and Pandy, 2001; Ackland and Pandy, 2009). Non-invasive imaging techniques are, however, subject to the limitation of lacking complete determination of joint CoRs (a

parameter not required for the tendon travel technique), although mathematical analysis of surface geometry can be used to estimate the CoR position within a given confidence interval (Yamaguchi and Zajac, 1989; Wretenberg et al., 1996; Pandy, 1999; Sheehan, 2007). An optimisation based approach can be used to ascertain instantaneous joint axes in dynamic systems (Caravaggi et al., 2009). Other limitations of these techniques include the expense of the apparatus involved and/or time-consuming and technically difficult analyses. The tendon travel technique, on the other hand, is relatively straightforward, inexpensive and fast, allowing multiple specimens to be tested. Its reliability is limited by the accuracy of approximation of the site of the origin or insertion and of the estimated line of action of the muscle (due to the need for dissection) and the accuracy of digitisation of the photographs. Further, the shape of the MA curve is heavily dependent on the type of curve used to fit the raw data (see below). Agreement between MRI and tendon travel techniques is generally good, although for some muscles it can differ substantially (Spoor and Van Leeuwen, 1992, attributed this to a number of reasons including tension in accessory muscles causing changes in MA of the object muscle). Pandy (1999) provides a comprehensive review of moment arm measurement techniques, derivation mathematics and sources of error.

In this study, I use a modified tendon travel technique based on cubic spline functions to ascertain the MAs of hind limb muscles in gibbons, using cadaveric material.

Why use cubic splines?

Traditionally, MAs have been derived from differentiation of polynomial approximations of the tendon travel-joint angle relationship. However, the type of curve used to fit this data has a marked bearing on the parameters of the curve which describes the MA: i.e. if a quadratic function is used to approximate the tendon travel-joint angle relationship, the shape of the MA curve will be linear, whereas it will be constant when a linear function is used. The decision to opt for a quadratic or higher order function is often based on 'visual' best fit or on R2 values, which have not proven to be very accurate (Angliletta, 2006). One way of avoiding this problem is to use a mathematical spline.

Cubic splines use a third-order polynomial to interpolate between data points, providing a smooth curve (Reinsch, 1967; Craven and Wahba, 1978; Hou and Andrews, 1978; Späth and Meier, 1988). Splines of varying complexity are used throughout scientific research and are favoured for allowing large data sets to be smoothed without susceptibility to Runge's phenomenon (where

high-order polynomials approximate extreme regions of the data more poorly than lower order alternatives; Reinsch, 1967; Späth and Meier, 1988).

Muscular properties of the gibbon hind limb

As mentioned above, quantitative anatomical data on mechanically relevant parameters are often lacking for ape species, especially for the lesser apes. Although several functional anatomical studies have been conducted on the gibbon hind limb (Sigmon and Farslow, 1986; Vereecke et al., 2005; Payne et al., 2006a), to date, there is only one study presenting detailed MA data, based on a single white-handed gibbon specimen (*Hylobates* lar; Payne et al., 2006b).

Gibbons are highly agile apes, capable of traversing gaps in the forest canopy of up to 15 m by leaping or brachiating (Fleagle, 1974; Fleagle, 1976; Gittins, 1983). Their locomotor repertoire also includes bipedalism (walking), climbing and orthograde clambering (Sati and Alfred, 2002; Vereecke et al., 2005, 2006a, b) and this locomotor versatility is likely to place contrasting pressures on the musculoskeletal anatomy of the gibbon hind limb. Recent studies have highlighted how the musculo-tendinous anatomy of gibbons may be suited to performing this range of locomotor activities (Payne et al., 2006a; Channon et al., 2009). The gluteal and quadriceps femoris muscle groups have large physiological cross-sectional areas (PCSAs), and thus can produce high levels of force, but their short muscle fascicles may limit contraction distance and velocity (Zajac, 1992). The hamstrings and long hip flexors (sartorius and gracilis), by contrast, appear suited for producing relatively modest levels of force but over a much greater range of joint motion (although this depends on a plethora of other variables including MA, fibre type and the proximity and properties of surrounding muscles). The distal hind limb is characterised by short-fascicled, highly pennate muscles suitable for high force production (Vereecke et al., 2005; Payne et al., 2006a). Yet, accurate information on the MAs of the hind limb muscle groups is needed to better assess the role of these muscles in gibbon locomotion.

In a previous study (Channon et al., 2009) I suggested that the voluminous knee extensor muscles of gibbons may contribute to propulsion generation in leaping when associated with short MAs. In other studies, I have pointed to some potential elastic energy stores in the gibbon hind limb (Vereecke et al., 2006b; Vereecke and Aerts, 2008). Gibbons have very short-fascicled triceps surae with a long and well-developed Achilles tendon (Payne et al., 2006a; Vereecke et al., 2005; Channon et al., 2009) which might act as an elastic energy store during locomotion. Yet, the long

digital flexor and patellar tendons might also function as elastic springs during locomotion (Vereecke et al., 2006b; Vereecke and Aerts, 2008). A detailed understanding of the architectural make-up, the moment arm variation and the functional link between the two is essential to achieve greater insight into the potential adaptations of the gibbon hind limb for energy storage and power production during locomotion.

In this study, I measure the MAs of a selection of gibbon hind limb muscles using a modified tendon travel technique. These data are used in conjunction with data from previous research (Channon et al., 2009) to assess the function of specific muscle groups and their contribution to the range of locomotor modes used by gibbons. In addition, I compare the spline-based technique used here and the traditional, polynomial-based technique to assess the efficacy of the modified methodology for measuring MAs in cadaveric specimens.

Materials and Methods

Subject data

The material used in this study comprises four gibbon cadavers of known age and sex (Table 3.1). Specifically: one white-handed gibbon (*Hylobates lar*), one silvery gibbon (*H. moloch*) and two siamang (*Symphalangus syndactylus*). The relatively small sample analysed here is inevitable when dealing with endangered species (IUCN, 2008), yet the hind limb MA data presented are very valuable as they contribute to a quantitative database of the architecture of the gibbon and enhance our understanding of the quantitative functional anatomy of gibbons (Vereecke et al., 2005; Payne et al., 2006a, b; Channon et al., 2009). The specimens were obtained from The Royal Zoological Society of Antwerp (*H. lar* and one *S. syndactylus*) and The National Museums of Scotland, Edinburgh (*H. moloch* and one *S. syndactylus*) and were kept frozen until required for this study. Cadavers were eviscerated during post-mortem examination, and body mass (prior to evisceration) was hence not available for all specimens. Therefore, segment length was used to normalise MAs to remove the effect of body size, following Alexander (1977; also, see Table 3.1). All specimens died under natural circumstances and none of the specimens exhibited any obvious musculoskeletal pathology.

Moment arm measurements

Table 3.1. Details of the four cadavers used in this study.

Specimen	*H.lar*	*H. moloch*	*S. syndactylus 1*	*S. syndactylus 2*
Sex	M	M	F	F
Age at death	6	19	32	-
Mass at death (kg)	6.3	7.2	12.5	-
Femur Length (cm)	20.5	20.5	21.5	22.7
Tibia Length (cm)	16.9	19.8	21.4	19.8
Foot length (cm)	8.8	8.7	9.8	9.3
Source	RZSA	NMS	RZSA	NMS

Key: RZSA – Royal Zoological Society of Antwerp, NMS – National Museums of Scotland, - indicates that data were unavailable.

Table 3.2. Muscles for which no MA data could be collected

H.lar	*H. moloch*	*S. syndactylus 1*	*S. syndactylus 2*
Tibialis anterior		Gluteus medius	Gluteus medius
		Semimembranosus	

Moment arms were measured using a modified version of the tendon travel technique (Spoor and Van Leeuwen, 1992). A bi-axial electro-goniometer (Biometrics, Gwent, UK) was positioned across the joint, secured using zip ties and connected to a differential thermocouple module and data acquisition (DAQ) base (National instruments, TX, USA, sample frequency: 3 Hz) to measure joint angle. The goniometer gave readings in two perpendicular planes. Modelling the goniometer following the technique of Legnani et al. (2000) allowed the joint angle to be ascertained even when the bases were not parallel (i.e. twisted). Tendon travel was measured using a Linear Variable Differential Transformer (LVDT, Celesco, Chatsworth, CA, USA), which acts like a tensioned drawstring and provides an output voltage linearly correlated to the length of wire drawn from it. The muscle was removed at its origin and a nylon fishing line (strength: 30lb or 13.6 kg; minimal elasticity) was sutured into the muscle belly. The fishing line was passed through a zip tie positioned at the muscle's site of origin, and tied to the free end of the LVDT. The tension maintained on the line by the LVDT was adequate to keep the muscle taut during the experiment. Data from the goniometer and LVDT were collected by separate modules in a DAQ base and using custom-written software in LabVIEW (version 8.2, National Instruments, TX, USA, see Fig. 3.1 for apparatus setup). Five trials per muscle were recorded, where each trial represented distal segment motion from fully flexed to fully extended, and back to full flexion. Hip angle was defined as the angle enclosed between the ventral side of the trunk and the anterior aspect of the femur (range: 7°-178°; Fig. 3.2), knee angle as the angle between the posterior aspect of the femur and the posterior of the calf (7°-202°, the removal of proximal muscles allowed the knee joint to be hyper-extended; it is to be noted that these exceed the in vivo range of joint motion), and ankle angle as the angle between the anterior of the tibia and the dorsum of the foot (16°-171°; Fig. 3.2). For bi-articular muscles, the secondary joint was kept at a constant angle, representative of joint extension (hip ~ 170°, knee ~ 175°, ankle ~160°; cf. Payne et al., 2006b; Thorpe et al., 1999; Williams et al., 2007). Unfortunately, I was not able to collect MA data for all the muscles in all animals due to various reasons, such as damaged muscle bellies (due to skinning by a taxidermist, Table 3.2).

Curve fitting

Tendon travel was plotted against joint angle and a cubic spline was used to smooth the data (National Instruments, LabVIEW 8.2). The spline could be modified by changing a balance parameter, within the boundaries 0 – 1, where 0 smoothed using a linear relationship and 1

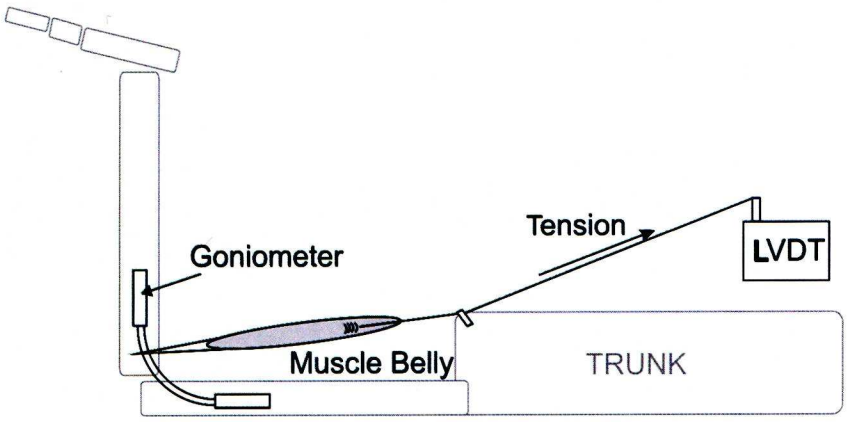

Figure 3.1. The apparatus used for data collection. LVDT; Linear Variable Differential Transformer

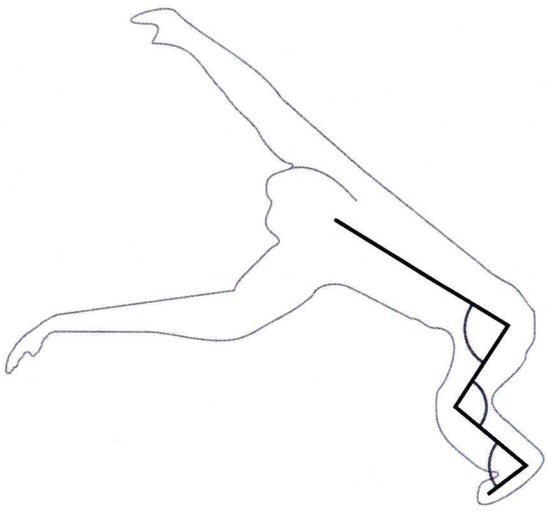

Figure 3.2. The joint angles used in the analyses.

interpolated between the points exactly (see National instruments help files, listed in the bibliography for fitting mathematics). Traditional curve fitting statistics (Jeffrey, 2005; Angilletta, 2006) were not useful in determining which balance parameter should be used, since the large number of degrees of freedom (due to large number of data points per trial) always resulted in a very high significance value ($1 \times 10^{-18} < P < 1 \times 10^{-14}$) regardless of the shape of the curve. Instead, the residual sum of squares (RSS) was used to choose a cubic spline to describe my data. RSS decreases with increasingly complex curves (see Fig. 3.3 for the effect of polynomial complexity on RSS), and I chose the least complex spline curve where the RSS fell within 5% of the sample range, effectively yielding a signal-to-noise ratio of, 19:1. This threshold represented a good compromise between fitting the data accurately and providing a realistically noise-free MA (yet, again, this was difficult to test statistically because of the large number of data points per trial; see Fig. 3.3 for the technique being used to choose a polynomial curve). The splined data was then differentiated to give the instantaneous MA (as a function of joint angle).

One disadvantage of spline fitting is that no F(x) coefficients are given (i.e. no $y = ax^2 + bx + c$ is produced), so it is not possible to calculate the instantaneous MA for a given joint angle. A polynomial curve was therefore fitted to the splined MA data, in order to provide a means of recreating the curves mathematically and allowing comparison with other studies on different species. The polynomial curves were used only for this purpose, while splined data were used exclusively for analysis. The same RSS-based curve fitting technique was used to choose which polynomial I report. For example, in Figure 3.3 a 4th order polynomial is the least complex curve with a RSS value of less than 5% of the signal range, so this curve is chosen. Where a 6th order polynomial was not sufficient to go below this threshold a linear curve is described (Appendix 3.1).

Fascicle strain model

A simple geometric model was used to estimate fascicle strain ($\Delta FL/FL$) during contraction. The role of the model was to estimate the fascicle strain that each respective muscle, with a specific MA and pennation angle (PA), undergoes during flexion or extension through the range of motion tested. Estimating fascicle strain yields insight into muscular function during locomotion by illustrating which muscles are likely to require excessive strain to rotate the joint through the

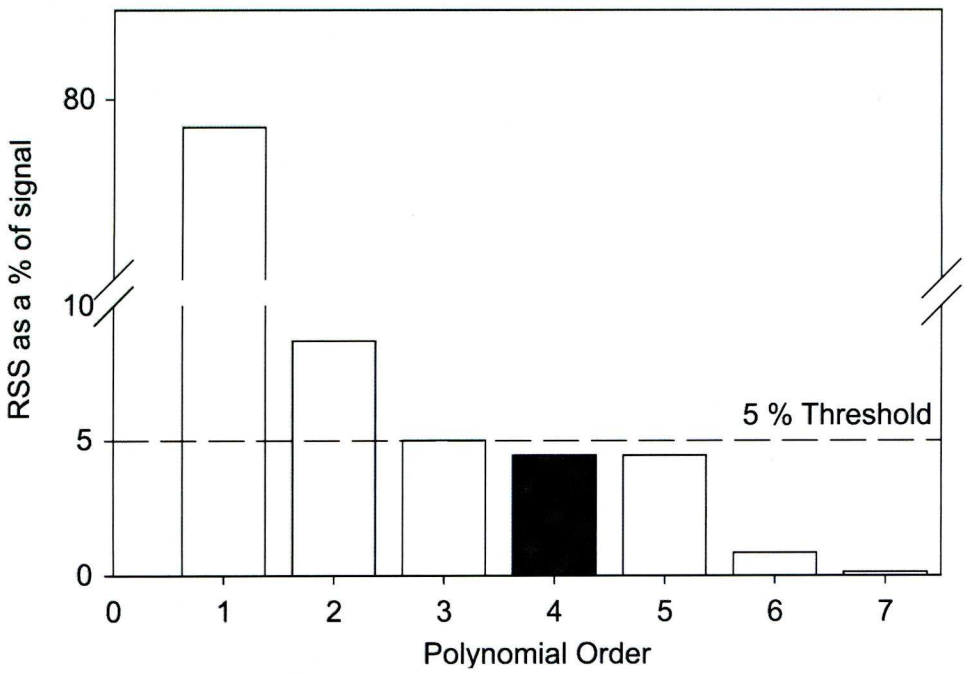

Figure 3.3. Decreasing residual sum of squares values for increasing orders of polynomial used to fit data from the rectus femoris (RFe) at the hip. The filled bar represents the least complex model which has an RSS of less than the 5% threshold.

range of motion seen. It also allows enquiry into the extent to which muscles with short fascicles are compensated by short MAs, to increase joint range and velocity.

The fascicle strain model for a given change in joint angle ($\Delta\theta$) is formulated as:

$$\Delta FL/FL = [(MA \times \text{Tan}\ \Delta\theta) / \text{Cos}(PA)]/FL$$

Since: $\text{Tan}\ \Delta\theta = \Delta FL / MA$, and ΔFL is dependent on the cosine of PA

$$\Delta FL \times \text{Cos}\ (PA) = MA \times \text{Tan}\ \Delta\theta$$

Hence: $\Delta FL/FL = [(MA \times \text{Tan}\ \Delta\theta) / \text{CosPA}]/FL$

The parameters were inserted into the model and the predicted fascicle strain for the range of motion seen during data collection was calculated. The model assumes that the muscle fascicles were at their longest, and fascicle strain= 0, when the joint started its movement. For example, for the vastus knee extensor the model assumes that the fascicles were at their longest when the knee was fully flexed and for the soleus that the fascicles were at their longest when the ankle was maximally dorsiflexed (see also discussion).

Hind limb kinematics

I executed a preliminary kinematic study of squat-jumping (i.e. jumping from a deep crouched position) in a group of captive white-handed gibbons (n=4 gibbons, 12 jumps analysed; Chester Zoo, UK) to measure the actual range of motion of the hind limb joints. Squat-jumping offered the largest range of motion for the hind limb joints and is used here as an example of maximal in vivo range of joint motion. This information is used to estimate the muscle fascicle length ranges during normal activities of gibbons. The (untrained) gibbons were recorded during spontaneous jumping bouts using two orthogonally positioned (one lateral and one frontal) high speed video cameras (125 Hz, AOS Technologies, Switzerland) and the joint centres were digitised using custom written software (National Instruments LabVIEW, TX, USA) to calculate two-dimensional joint angles. The cranial view was used solely to ensure that the jumps were parallel to the field of view of the lateral camera, from which all the joint angles were measured.

The range of motion observed at the hip, knee and ankle during squat jumping was 26° - 158°, 34° - 143° and 58° - 164° respectively (Figs. 4-6). Joint angles are defined as explained above.

Results

Muscle moment arms

At the hip

Semimembranosus (SeM), gracilis (Gra), biceps femoris (BiF), and semitendinosus (SeT) had the largest MAs of the (tested) muscles crossing the hip joint (maximal MA inter-specific mean ± SD: Gra 3.41 ± 0.85cm, SeM 3.41 ± 0.64cm, BiF 3.41 ± 0.21cm, SeT 2.98 ± 0.42cm; scaled MA values are presented in Fig. 3.4). The shape of these moment arm curves was consistent in all specimens, except for the white-handed gibbon, where there was a more-or-less linear relationship between MA and joint angle for the hamstrings instead of the bell-shaped curve that was found in the other specimens. The gluteal muscles had the smallest MAs (maximal MA inter-specific mean ± SD, gluteus superficialis, GSu, 0.85 ± 0.43cm, gluteus medius, GMe, 0.85 ± 0.21cm) of all hip muscles. In all specimens, the MA-joint angle curve of adductor magnus (AdM) crossed the x-axis, implying a change of function from flexion to extension the same phenomenon was also seen for the gracilis in all but one specimen (the silvery gibbon) where it approached but never reached zero (minimum value 0.06). The MA-joint angle curve of GMe also crossed the x-axis in two specimens (silvery gibbon and siamang 1), but the change in function was reversed in the two specimens: in the silvery gibbon the change in function was from flexion to extension and in the siamang it was from extension to flexion. The rectus femoris (RFe) MA varied greatly in magnitude, particularly at the extreme joint angles measured.

At the knee

Gra (4.10 ± 0.78cm) and SeT (3.90 ± 0.78cm) had the largest MAs of the tested muscles crossing the knee joint (Fig. 3.5), the shape of the MA curve for these muscles being broadly similar in all specimens. The hamstrings (BiF, 0.98 ± 0.39cm and SeM, 0.78 ± 0.20cm) and the quadriceps (Vastus lateralis, VaL, 0.05 ± 0.01cm and RFe, 0.78 ± 0.20cm) had the smallest inter-specific mean MAs of the knee joint muscles. The MAs of the two gastrocnemius heads (medius, GaM, 1.17 ± 0.20cm and lateralis, GaL, 1.76 ± 0.39cm) remained small throughout the full range of motion of the knee, and crossed the x-axis at the extreme joint angles in two specimens (siamang 1 and 2), indicating a change of function. The MA-joint angle curve of BiF also crossed the x-axis in two specimens (siamang 1 and the white-handed gibbon), but the change in function was reversed in the two specimens i.e. in the siamang, the change in function was from extension to

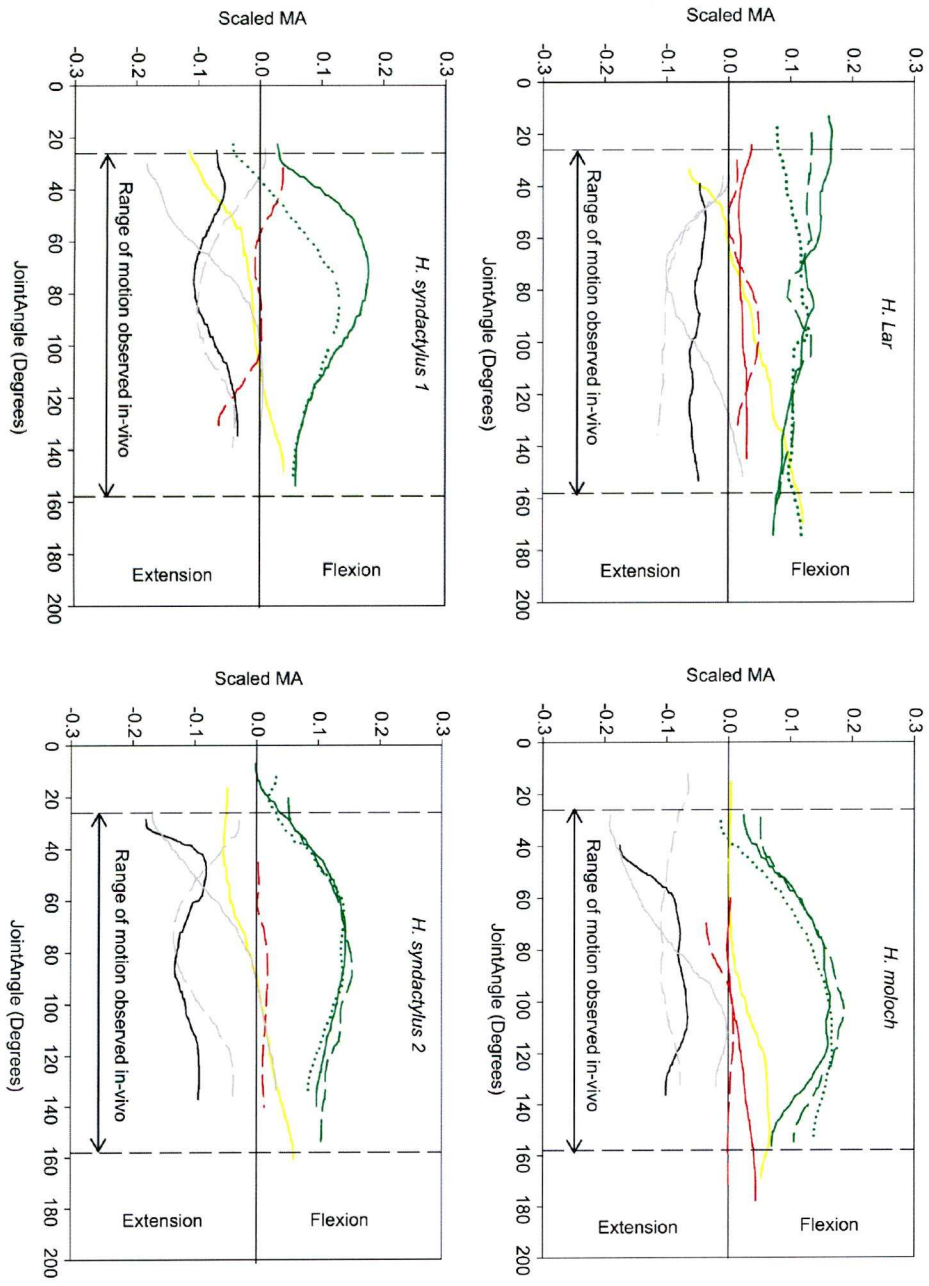

Figure 3.4. Scaled moment arms at the hip, for the four specimens. Key: solid yellow line– adductor magnus (AdM), solid red line– gluteus medius (GMe), dashed red line– gluteus superficialis (GSu), solid black line– rectus femoris (RFe), solid grey line– gracilis (Gra), dashed grey line– Sartorius (Sar), solid green line– biceps femoris (BiF), dashed green line– semimembranosus (SeM), dotted green line – semitendinosus (SeT). The vertical black dashed lines indicate the range of joint motion used during jumping (see materials and methods for jumping data collection).

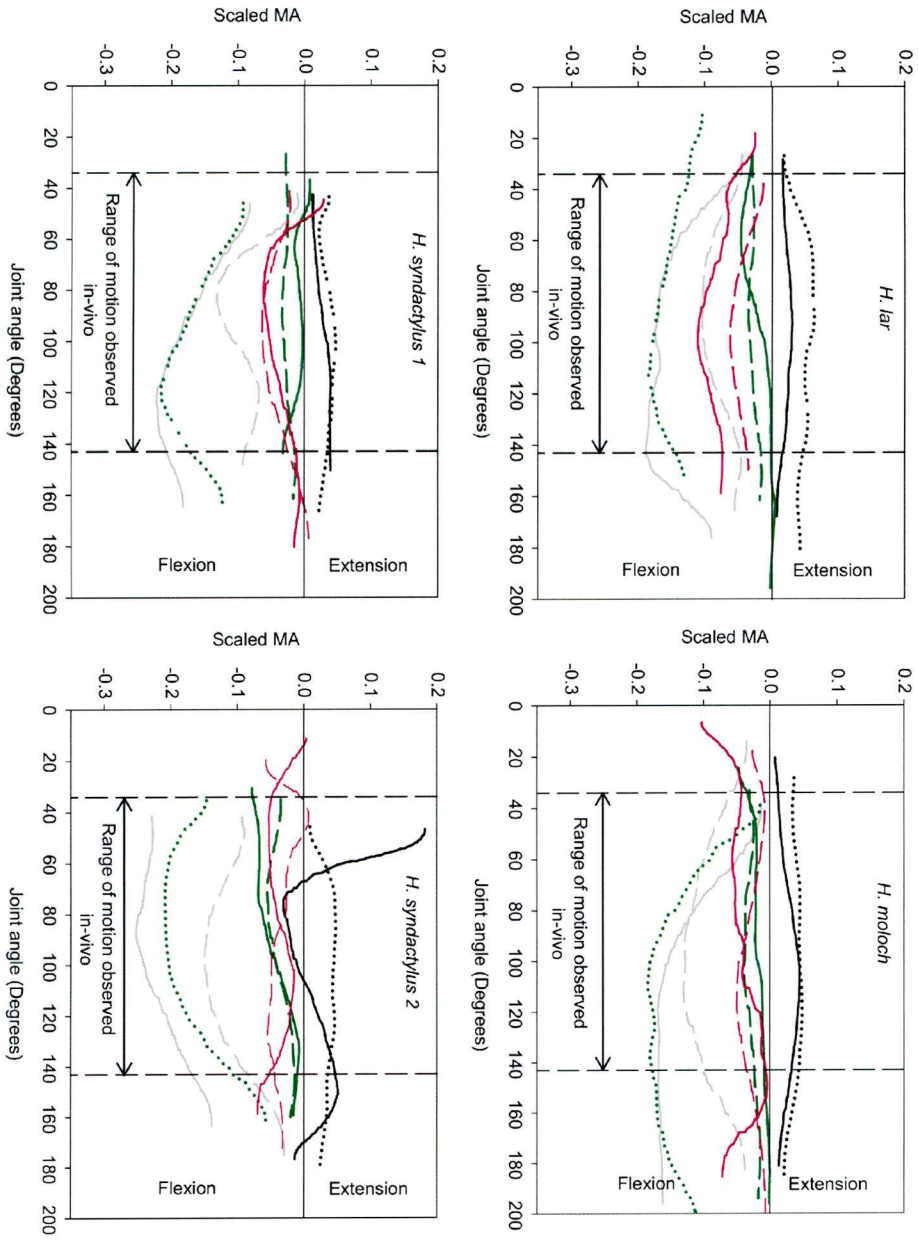

Figure 3.5. Scaled moment arms at the knee, for the four specimens. Key: solid black line– rectus femoris (RFe), dotted black line– vastus lateralis, solid grey line– gracilis (Gra), dashed grey line– Sartorius (Sar), solid green line– biceps femoris (BiF), dashed green line– semimembranosus (SeM), dotted green line a– semitendinosus (SeT), solid pink line– gastrocnemius lateralis (GaL), dashed pink line– gastrocnemius medialis (GaM). The vertical black dashed lines indicate the range of joint motion used during jumping (see materials and methods for jumping data collection).

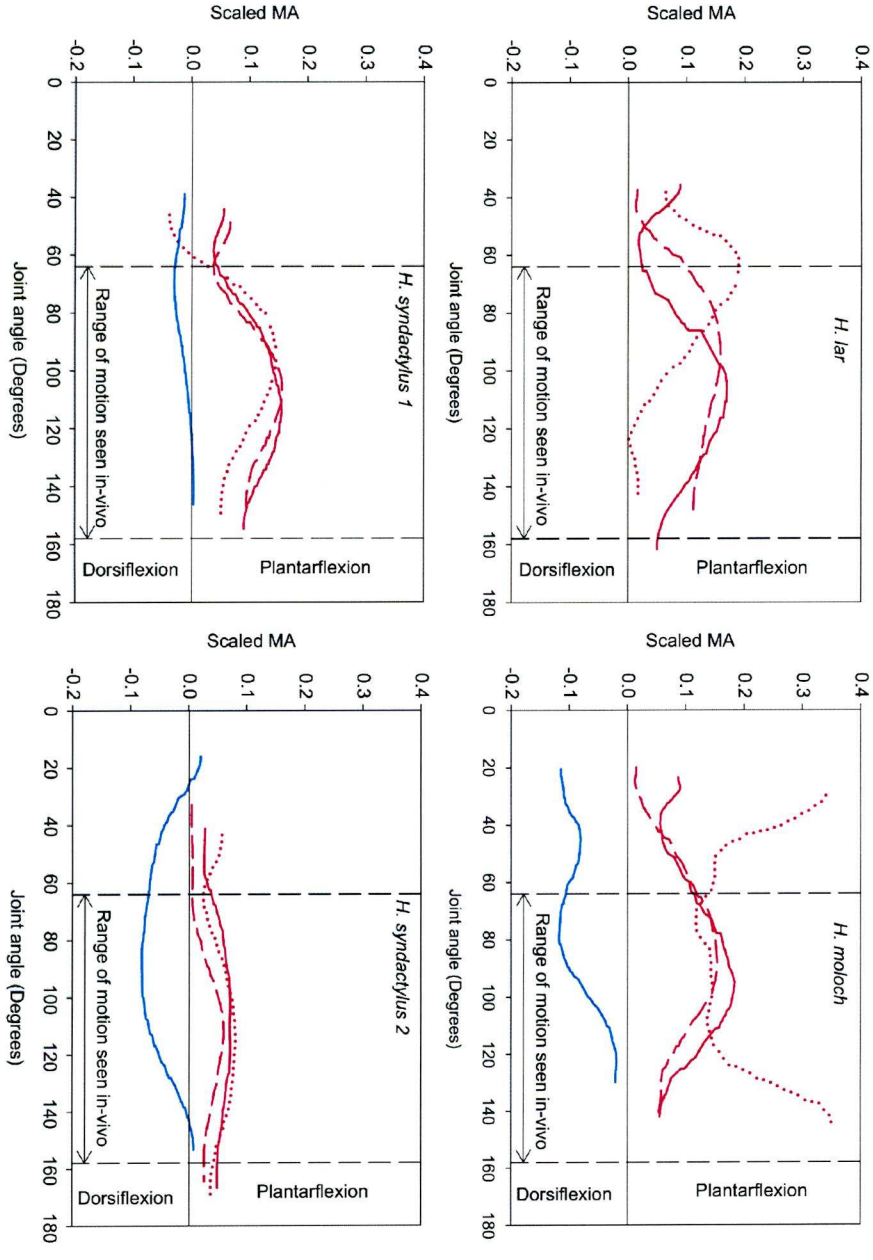

Figure 3.6. Scaled moment arms at the ankle, for the four specimens. Key: solid pink line – gastrocnemius lateralis (GaL), dashed pink line– gastrocnemius medialis (GaM), dotted pink line– soleus (Sol), cyan line– tibialis anterior (TiA). The vertical black dashed lines indicate the range of joint motion used during jumping (see materials and methods for jumping data collection).

flexion and in the white-handed gibbon it was from flexion to extension. The MA-joint angle curve of RFe of siamang 2 was unusually shaped in comparison to the other specimens, especially at extreme joint angles; it was also the only specimen where the MA of RFe at the knee crossed the x-axis.

At the ankle

The soleus (Sol, 1.75 ± 0.92cm, maximal inter-specific mean MA) had the largest MA of the ankle joint muscles (Fig. 3.6), the GaM and GaL had similar MAs throughout the entire range of motion of the ankle joint (1.38 ± 0.46cm and 1.20 ± 0.46cm, respectively). The tibialis anterior (TiA) had the smallest MA (0.74 ± 0.37cm) and crossed the x-axis in two specimens implying that the insertion passed the joint CoR during extreme plantarflexion.

Fascicle strain model

The fascicle strain model estimates how much strain the muscle fascicles must undergo (shortening distance during contraction relative to the fascicle rest length) to move the joint through the observed range of motion. Vertebrate muscle fascicle strain data from in vivo activity is widespread but variable between ~0.20 and ~0.36, depending on the species, activity and measurement technique (Griffiths, 1991; Kawakami et al., 2002; Daley and Biewener, 2003; Lichtwark et al., 2006; Wakeling et al., 2006). Since no fascicle strain data for gibbons are available to date, my estimated strains will be compared to the values shown here.

Muscles at the hip

RFe was predicted to exhibit the largest fascicle strain (0.86 ± 0.25, Fig. 3.7a), although the BiF and SeM were also predicted high strains (0.68 ± 0.11, 0.63 ± 0.05, respectively). The SeT and GMe were predicted to have strains of 0.32 ± 0.09 and 0.24 ± 0.06 respectively. The lowest strains were predicted for Sar, AdM, Gra and GSu (0.16 ± 0.04, 0.15 ± 0.03, 0.12 ± 0.04, 0.06 ± 0.04 respectively).

Muscles at the knee

GaL and GaM were predicted the highest fascicle strains crossing the knee (0.77 ± 0.20, 0.60 ± 0.12, respectively, Fig. 3.7b). SeT, VaL, Gra and RFe were predicted to have strains of 0.46 ±

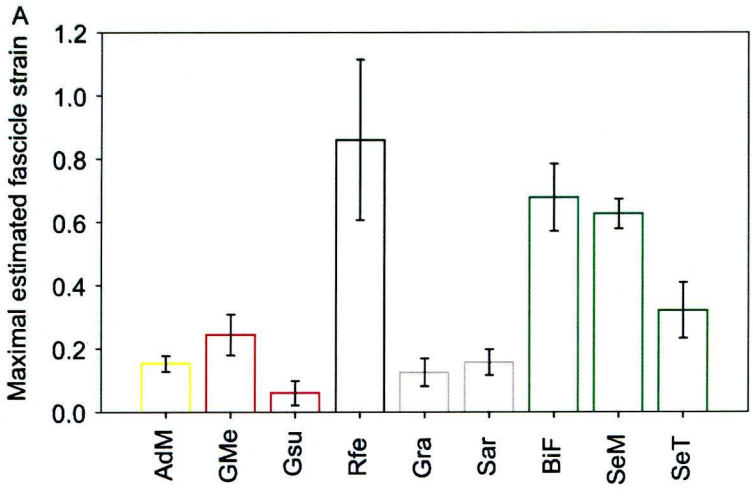
A
Maximal estimated fascicle strain
1.2
1.0
0.8
0.6
0.4
0.2
0.0
AdM
GMe
Gsu
Rfe
Gra
Sar
BiF
SeM
SeT

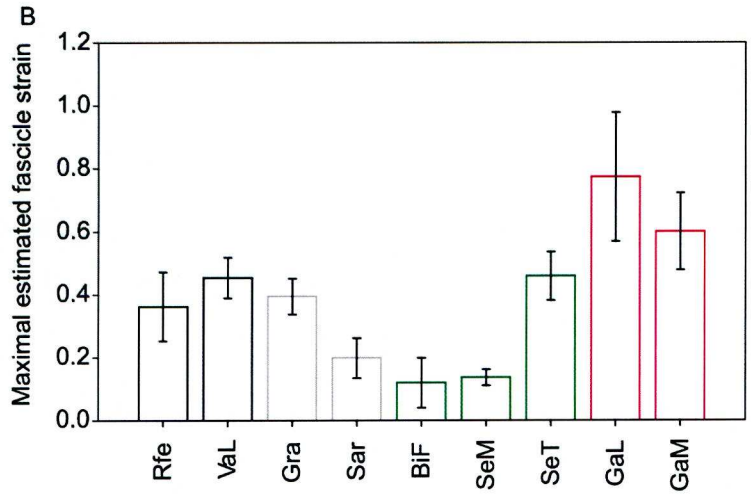
B
Maximal estimated fascicle strain
1.2
1.0
0.8
0.6
0.4
0.2
0.0
Rfe
VaL
Gra
Sar
BiF
SeM
SeT
GaL
GaM

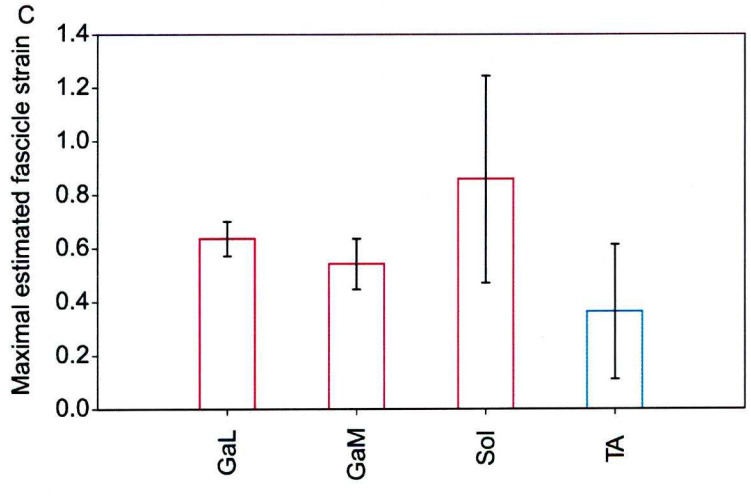
C
Maximal estimated fascicle strain
1.4
1.2
1.0
0.8
0.6
0.4
0.2
0.0
GaL
GaM
Sol
TA

Figure 3.7. (Previous page) Estimated fascicle strain during the range of motion tested for muscles at the hip (**A**), knee (**B**) and ankle (**C**). Key: adductor magnus (AdM), biceps femoris (BiF), semimembranosus (SeM), semitendinosus (SeT), gluteus medius (GMe), gluteus superficialis (GSu), gracilis (Gra), Sartorius (Sar), rectus femoris (RFe), vastus lateralis (VaL), gastrocnemius lateralis (GaL), gastrocnemius medialis (GaM), tibialis anterior (TiA).

0.08, 0.45 ± 0.06, 0.39 ± 0.06 and 0.36 ± 0.01, respectively. The lowest strains were predicted for BiF, SeM and Sar (0.12 ± 0.08, 0.14 ± 0.03 and 0.20 ± 0.06, respectively).

Muscles at the ankle

The highest predicted strains across the ankle were in Sol (0.86 ± 0.39, Fig. 3.7c). GaL and GaM were predicted to have strains of 0.64 ± 0.06 and 0.54 ± 0.09 respectively. The lowest predicted strains were in TiA (0.36 ± 0.25).

Discussion

Muscle function

By combining the MA data with quantitative information about muscle properties from previous studies I can assess the function of different hind limb muscle groups. My fascicle strain model gives additional insight into muscle function by predicting the strains occurring in the muscle fascicles during joint motion. Although this model is quite simple and makes several assumptions (see below), the predicted fascicle strains can be used as rough estimates in evaluating muscle function. In vivo strain values have been published for several animals (cats, Griffiths, 1991; humans, Kawakami et al., 2002; Lichtwark et al., 2006; Wakeling et al., 2006; guinea fowl, Daley and Biewener, 2003; see also above). Predicted strain values that fall outside the reported range of in vivo values are considered 'unrealistic'.

Hip extension

The gluteal muscles had relatively small MAs in all animals tested (Fig. 3.4) and the fascicle strain model estimated that they would undergo moderate fascicle strains during the range of in vivo motion (Fig. 3.7a). Small MAs require large muscle forces to produce high joint torques, but do not require long fascicles for rapid joint rotation (Gans and Gaunt, 1991; Lieber and Friden, 2001; Alexander, 1996). The gluteal muscles of gibbons have been shown to possess a large

PCSA, which is proportional to force production, and short fascicles (Channon et al., 2009). The glutei have MAs of ~0.025 times femur length, i.e. 2–8 times smaller MAs than other muscles crossing the hip, but possess 4-10 times as much PCSA as other muscles crossing the hip (Channon et al., 2009) and are therefore likely to maintain equal or greater moment production capabilities than other hip muscles. Having muscles with a small MA and a large PCSA probably reduces thigh mass, and hence thigh inertia, contributing to efficient locomotion (Witte et al., 1991; Crompton et al., 1996; Steudel, 1996; Schoonaert et al., 2007). This particular muscle architecture enables the production of large amounts of joint power without high thigh muscle mass (as would be the case for long-fascicled, voluminous muscles).

Powerful hip extension is useful for a variety of locomotor tasks including clambering, climbing (Preuschoft, 2002; Isler, 2005) and leaping (Alexander, 1995; Scholz et al., 2006) and the gross architecture of gibbon gluteals is similar to that of the bonobo, a very proficient – yet atypical – leaper (Payne et al., 2006a; Scholz et al., 2006; note however that the studies on bonobos utilised a polynomial based approach and digitised photographic images). My results also indicate that the MAs of the gluteals are relatively smaller in gibbons than in the great apes (except bonobos; Payne et al., 2006b), facilitating increased angular velocity and excursion at the hip (Scholz et al., 2006) for a given distance of muscular contraction (Gans and Gaunt, 1991). There were no outstanding differences in MA of the hip extensors between gibbon species, despite a difference in the prevalence of leaping (~6% locomotor time for siamang vs. ~15% for white-handed gibbons, Whitmoor, 1975). Differences in muscle architecture between species are very subtle (Channon et al., 2009), and inter-specific analyses are hampered by the small sample size analysed here.

The large MAs of the hamstrings at the hip (Fig. 3.4) and the unrealistically high fascicle strains (inter-specific hamstring mean 0.56) predicted by the fascicle strain model (Fig. 3.7a) suggest that, despite the relatively long fascicles (and hence sarcomeres in series) of BiF and SeT, these muscles are unlikely to be involved in powerful hip extension during jumping. This hypothesis is supported by their small PCSA (Channon et al., 2009) which precludes them from producing large amounts of force (although even with a low PCSA large moment production might be achieved thanks to the large MA). Instead, they may be involved in producing a modest hip extension force during bipedalism, as in humans (Hase and Stein, 1999), or may play a fine-tuning or stabilising role during terrestrial locomotion (see below). The advantage of using the glutei instead of the hamstrings as powerful hip extensors is two-fold. First, high muscle powers require large muscle volume, and locating that volume on the femur shaft would increase the limb inertia and hence the

metabolic costs of other (leg swinging) activities such as walking (Witte et al., 1991; Crompton et al., 1996; Steudel, 1996; Schoonaert et al., 2007). Secondly, the hamstrings are bi-articular (see below for how secondary MA might affect estimates of fascicle strain) and during powerful movements such as jumping, extending the hip might (depending on both joint positions) require muscular effort (and hence metabolic energy) from an antagonist (here the knee extensors) to prevent energy wastage through knee flexion (the hamstrings' other role).

Hip flexion

Activities which require hip flexion, i.e. swinging the leg forward during terrestrial locomotion or lifting the legs during brachiation, do not require high levels of muscular force (Bertram and Chang, 2001), but call for a wide range of motion instead. The bi-articular muscles Sar and Gra (which flex both hip and knee) had large MAs (Figs. 4 and 5) which, thanks to their long fascicles, facilitate a large range of motion at both joints as predicted by the fascicle strain model (Figs. 7a,b). This large range of motion is likely useful in achieving the wide range of joint angles used during leg-lift brachiation (Usherwood and Bertram, 2003; Channon et al., 2009) and during quadrumanous clambering, where limb placement is highly variable. They also have very small PCSAs, but can increase torque production by using a large MA. This has the added benefit of decreasing the muscle mass and, hence, the rotational inertia of the thigh, saving metabolic energy during locomotion (Steudel, 1996).

The short fascicles of RFe and relatively large MA lead to unrealistically high strains to obtain the range of hip flexion seen in vivo, as predicted by the model (inter-specific mean, 0.86). This implies that RFe does not act as a primary hip flexor, but is likely synergistic to the other quadriceps muscles (i.e., the vasti) in knee extension (see below).

Thigh adduction

The MA of AdM was small throughout the tested range of hip flexion-extension and presented a change of role from flexion to extension with decreasing joint angle. This is due to a change in position of the muscle's insertion relative to its origin. When the hip joint angle is larger than 90°, the line of action of the muscle suggests that it acts as a flexor (second to an adductor), but when the hip is flexed (0° < hip angle < 90°) its line of action indicates hip extension. However, its main role is undoubtedly thigh adduction (Sigmon and Farslow, 1986). In all specimens, the fascicle strain model predicted low fascicle length changes through the flexion-extension cycle. Since the MA was not measured during adduction-abduction, it is not possible to accurately suggest what

the result in adduction would have been. However, the origin of AdM is approximately circular in shape (it covers the obturator foramen, see also: Sigmon and Farslow, 1986) which makes it unlikely that the MA, and hence the fascicle strain model, would be radically different from the flexion-extension results seen here. Further data are, however, desirable to support or refute this hypothesis.

Knee extension

The fascicle strain model indicates that the short fascicles of RFe are more adept at knee extension than hip flexion. Unpublished work on the fibre type composition of gibbon quadriceps supports this hypothesis: RFe is made up almost entirely of type 2 (both a and b), fast twitch fibres (as in galagos; Ariano et al., 1973) without a significant proportion of type 1 slow twitch fibres (as in humans; Saltin et al., 1977; A.J.C., personal observation). Since type 2 muscle fibres are associated with fast, powerful movements it seems likely that RFe has a primary role in knee extension. In gibbons, RFe probably acts in concert with the powerful vasti to obtain knee extension (although the anatomical approach taken here would not differentiate between the functions of these muscles, since they share an insertion). Muscle volume dedicated to knee extension is likely to be associated with powerful movements, such as jumping and climbing, at both of which gibbons are very proficient (Fleagle, 1974; Gittins, 1983). The voluminous VaL has a small MA at the knee which, according to the fascicle strain model, allows its short fascicles (Channon et al., 2009) to execute the range of knee motion observed in vivo. The other vasti (vastus medialis and v. intermedius) were not measured in this study but are likely to have similar fascicle strain estimates to VaL since they share an insertion, originate from a similar position and have a similar muscle architecture (Channon et al., 2009).

Again, there were no outstanding differences in MA of the knee extensors between gibbon species (see above), likely due in part at least to the small sample size analysed here.

The short fascicle-small MA combination seen in the quadriceps femoris (RFe and vasti) may also facilitate elastic energy storage during locomotion, in the well-developed patellar tendon (Vereecke et al., 2006b). Recent studies on human ankle morphology have suggested that the size of the MA is more important than tendon stiffness in facilitating storage of elastic strain energy in tendons during cyclical locomotor modes, with a small ankle MA leading to enhanced energy storage and recoil, and hence more economical locomotion (Scholz et al., 2008). When

extrapolated to the knee joint, this could mean that the small MA of the quadriceps might, together with appropriate tendon properties, facilitate elastic energy recovery via the patellar tendon.

Knee flexion

All knee flexors located on the thigh had long fascicles, small PCSAs (Channon et al., 2009) and relatively large MAs. The fascicle strain model predicted that none would require unrealistically high strains to flex the knee joint fully. As with hip flexion, activities involving knee flexion do not require large amounts of force production and so it is not surprising that the main knee flexors have neither small MAs nor high PCSAs. Again, having large MAs may allow the long-fascicled muscles to produce relatively larger knee torques while adding relatively little mass to the thigh.

The gastrocnemius was predicted to be a poor knee flexor by the fascicle strain model, which is not surprising since many previous studies have indeed indicated that it is the main ankle plantarflexor in a range of mammalian taxa (Wickiewicz et al., 1983; Alexander, 1995, 1996; Vereecke et al., 2005; Payne et al., 2006a).

Ankle plantarflexion

Interestingly, the triceps surae were predicted to undergo very high muscle strains at the ankle (group average, 0.68). This observation is surprising since the group is considered the primary plantarflexor (see above). It may be that the group is involved primarily in isometric contraction during cyclical locomotion, where elastic energy may be stored in the well-developed Achilles tendon (Vereecke et al., 2006b), as in several other species (Alexander, 1984). A potential candidate for large joint excursion at the ankle is the digital flexor group, which has fascicles of a similar length as the triceps surae but acts via a MA which is probably smaller, given its site of insertion - the insertion tendon passes down the medial side of the calcaneus close to the talocrural joint - and therefore elicits smaller fascicle strains (note that the digital flexor MA was not measured in this study).

Payne et al. (2006b) found that the triceps surae MA at the ankle in gibbons was short but of a comparable size to that seen in other apes. Yet, the mass specific fascicle length of the calf muscles was considerably shorter in gibbons compared to the other apes (1.6 cm for gibbons vs. 2.2 cm inter-specific mean for other apes, Payne et al., 2006a), indicating a functional difference between lesser and great ape species.

Ankle dorsiflexion

The MA of TiA was highly variable between specimens (Fig. 3.6) and, as a result, the fascicle strain estimates also vary widely. It is likely that the presence of retinaculae contributed to the variability of these data even though the retinaculae at the ankle were left intact or reconstructed during data collection. The (superior and inferior) retinaculae reduce the MA of the TiA (and of other muscles running through the retinaculae, e.g. digital flexors and extensors) and avoid 'bowstringing' of the tendons, i.e. prevent the tendon taking a direct line between its origin (on the proximomedial tibia) and its insertion (on the lateral cuneiform of the foot).

Large MAs for fine control, small MAs for angular velocity and elastic energy storage

One could predict that to maximize torque production, long-fascicled muscles will be associated with large MAs, whereas short-fascicled muscles will have small MAs to allow a full range of motion and high angular velocity, yet, my model shows that such a clear correlation between fascicle length and MA is not observed in all muscles. One reason for this could relate to control. In a short-fascicle/small-MA muscle a very small change in fascicle length elicits a large change in joint position. If, however, a large MA is used (for the same fascicle length), the movement is smaller and a finer degree of control is possible. This may be especially advantageous if the muscles are involved in stabilisation (rather than realising a large range of motion), or if there are synergists that can help elicit extreme joint angles (as with RFe when acting at the hip).

In gibbons, the short-fascicled/small-MA muscles may use short fascicles to reduce the amount of muscle mass on the hind limb and reduce locomotor cost. By reducing fascicle length, muscles can increase PCSA (and hence propensity for force production) with no penalty in limb inertia. The trade-off of having short fascicles is that range of motion and angular joint velocity (limiting work and power respectively) may be compromised, but using a small MA increases the range of motion and angular joint velocity.

Short fascicles and small MAs may also be advantageous for eliciting strain and hence elastic energy storage in tendinous tissues (Scholz et al., 2008). Channon et al. (2009) showed that the major tendons in the gibbon hind limb (Achilles and patellar) are both associated with short-fascicled muscle groups (triceps surae and quadriceps femoris respectively). Short-fascicled muscles with long, well-developed tendons are often associated with elastic energy storage, where the muscle fascicles act mainly isometrically, eliciting tendon strain and elastic energy storage. Here I found that the quadriceps femoris possesses a small MA and short fascicles coupled in

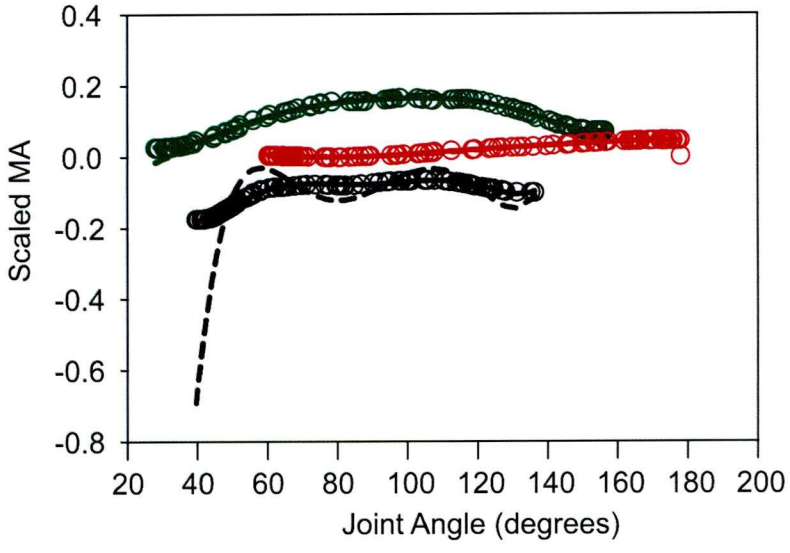

Figure 3.8. The differences in predicted MA for polynomial based and spline based techniques for three muscles. Black represents the rectus femoris muscle, green represents the biceps femoris muscle, red represents the gluteus medius muscle. Dashed lines represent the traditional (polynomial based) technique, open circles represent the spline based technique, and solid lines represent a polynomial fitted to the splined data.

series with a well-developed tendon (patellar) and so is a likely candidate for elastic energy storage during gibbon locomotion. The short-fascicled triceps surae had a relatively large MA and appeared to require relatively high fascicle strains to elicit a large range of motion. The substantial Achilles tendon associated with the group may also be used as an elastic energy store. This would explain the short-fascicled nature of the triceps surae, since during cyclical locomotion the muscle fascicles could act isometrically, storing strain energy in the tendon. Further biomechanical studies into tendon properties and gibbon locomotor kinematics are required to enhance our understanding of these mechanisms during the different locomotor modes of gibbons.

Comparison of techniques, spline versus polynomial

The differences in MAs obtained with the traditional, polynomial-based technique and the spline-based technique were inconsistent between individual muscles and specimens (Fig. 3.8). In some muscles, the two methods predicted very similar MAs (Fig. 3.8: gluteus medius); whilst in others (Fig. 3.8: rectus femoris) there were large differences, particularly at extreme joint angles, leading to MAs which fluctuate excessively and/or increase in magnitude to a size I would consider unrealistic given my knowledge of the joint geometry. This is likely attributable to fitting a polynomial to the large and varied dataset and then differentiating the resulting curve. The differentiation stage amplifies the small inflections made by the original function, resulting in unrealistically high MA values. Fitting a polynomial directly to the spline gave a very close fit, which deviated little at extreme values; the coefficients of these polynomials are given in Appendix 3.1.

The cubic splines used in this investigation produced MA curves which were at least as feasible, given the basic joint geometry, as their polynomial counterparts, and in many cases the cubic spine method gave more feasible results. Polynomial interpolation is particularly susceptible to erratic behaviour at the extremes of the data set (as seen in Fig. 3.8: RFe). This tendency, termed Runge's phenomenon (Epperson, 1987), is caused by the high sensitivity of high-order polynomials to small changes in the dependent variable (in this case tendon travel).

One of the disadvantages of smoothing by spline interpolation is that there is no definitive curve output; i.e. an F(x) is not produced. Having a definite function has several advantages: the curve

can be reproduced exactly, y can be calculated for a given x, and curves can be compared more easily. The output of a spline function is a vector of y-coordinates for the x-coordinate input vector. I have presented polynomial functions approximating the spline smoothed data to yield an approximate F(x), to allow others to replicate the curves produced by my spline functions for comparison with other studies only (Appendix 3.1).

Without re-analysing the raw data it is difficult to estimate the effect that the use of spline-fitting would have on the results of past studies which used polynomial interpolation. Many previous studies used digitised photographs to attain tendon travel and so the number of data points per trial was much lower than in this study ($n \sim 10\text{-}30$, compared with $n = 150$ per trial), so that polynomial approximation may have behaved less erratically. When data from this study are compared to Payne et al.'s (2006b) study of gibbon moment arms the results are mixed, with some muscles comparable in shape and magnitude to the previous study (RFe at the hip, VaL, BiF, SeT, Gra, GaM and GaL across the knee), some muscles comparable in magnitude only (AdM, SeT across the hip, SeM across hip and knee), some in curve shape only (GSu, GMe), and some not comparable in either attribute (BiF at the hip). It can be argued that MAs derived through MRI or CT may be more accurate (Rugg et al., 1990; Spoor and Van Leeuwen, 1992; Wretenberg et al., 1996), since they allow the avoidance of dissection damage to the muscle's line of action and direct measurement of the joint CoR (and hence joint angle). They are however expensive to perform and require technical expertise and complex analyses to yield usable results. The tendon travel technique, however, is intuitive, simple and cost effective. My modifications to it do not change any of these properties; the equipment used was of modest value, and the analysis can be performed in many basic computer packages. The most pertinent advantages of the technique outlined here are its repeatability (by removing subjective measurements in digitising and curve fitting) and plasticity (by changing the curve fitting parameters or thresholds). These characteristics make the modified tendon travel technique a favoured method of MA derivation when using cadaveric material.

Assessment of the fascicle strain model

The simple model presented here combines MA and muscle architecture data and attempts to estimate fascicle strain in vivo, but there are several sources of error associated with my model's calculation of fascicle strain. The measurement of initial (resting) fascicle length is taken from

cadaveric gibbon muscles, and so may not be identical to in vivo resting length. However, to obtain the best possible estimates, the specimens were slowly defrosted at room temperature before dissection and exhibited no obvious muscle tension in the form of rigor (Jungk et al., 1967). A second potential source of error is that the model does not account for the effect of secondary MA on fascicle strain for bi-articular muscles, several of which exhibited unrealistically high strains. I used fixed and consistent secondary joint angles during measurements, yet there is likely to be some unaccountable change in primary MA (and hence fascicle strain) with secondary joint angle. MacFadden and Brown (2007) quantified the effect of secondary joint angle on primary MA in cats and found quite substantial effects for bi-articular muscles. My model also assumes there is no change in pennation angle during contraction, yet, several studies have shown pennation angle to vary between, 18° and 30° during contraction of mammalian muscle, which would however only reduce the model's denominator from 1 to 0.95–0.87, and thus have little effect on the majority of strain estimates (Lichtwark and Wilson, 2005; Azizi et al., 2008; McGowan et al., 2008). My fascicle strain estimates were calculated using joint angle attained during the MA data collection and there is likely to be a small error associated with this (see above). Finally, my model assumes fascicle homogeneity throughout the muscle belly and recent studies have shown this not to be the case (Carroll et al., 2008). My model predicted fascicle strains in excess of what I would consider feasible for several muscles. Despite these limitations, I believe that the model is adequate to estimate muscle function, even if numerical values of fascicle strain are not exact. A more complex version of the model, e.g. with incorporation of force-strain data, could provide additional insight and might indicate that muscles use short MAs to allow them to remain at an optimal length for longer, or otherwise explain the results shown here.

Conclusions

This study shows that the gibbon hind limb displays a functional specialisation of the muscles to different locomotor tasks. The hip and knee extensor muscles - with large PCSAs coupled to small MAs - are likely advantageous for powerful movements such as leaping and climbing. Conversely, the slender hip and knee flexors - with large MAs and long fascicles - are probably useful in providing a wide range of limb placement for support or for leg lift during brachiation. Muscles with short fascicles coupled to long MAs may represent a method of increasing control during precise limb placement. The triceps surae and quadriceps femoris muscle groups may

provide some means of storing elastic energy in the substantial Achilles and patellar tendons respectively. Additional in-depth biomechanical studies could further elucidate the relationship between morphology and locomotor biomechanics in gibbons.

List of Abbreviations

AdM – Adductor magnus

BiF – Biceps femoris

CoR – Centre of rotation

CSA – Cross sectional area

ΔFL – Change in fascicle length

$\Delta\theta$ – Change in joint angle

EMA – Effective mechanical advantage

GaM – Gastrocnemius medialis

GaL – Gastrocnemius lateralis

GMe – Gluteus medius

Gra – Gracilis

GSu – Gluteus superficialis

LVDT – Linear Voltage Displacement Transducer

MA – Muscle moment arm

MRI – Magnetic resonance imaging

MTU – muscle-tendon unit

PA – Pennation angle

PCSA – Physiological cross sectional area

RFe – Rectus femoris

Sar – Sartorius

SeM – Semimembranosus

SeT – Semitendinosus

Sol – Soleus

TiA – Tibialis anterior

VaL – Vastus lateralis

Chapter 4: The Biomechanics of Leaping in Gibbons.

By Anthony J. Channon

With contributions from: Robin H. Crompton, Michael M. Günther and Evie E. Vereecke.

I designed, built and installed the data collection equipment, collected and analysed the data and wrote the manuscript. Evie Vereecke assisted with installation and provided funding for travel and equipment purchase. Robin Crompton and Michael Günther edited the manuscript and advised on its content.

A version of this chapter has been published in the American Journal of Physical Anthropology

A. J. Channon, R. H. Crompton, M. M. Günther and E. E. Vereecke (In press). The biomechanics of leaping in gibbons.

Abstract

Gibbons are skilled brachiators but they are also highly capable leapers, crossing distances in excess of 10 m in the wild. Despite this impressive performance capability, no detailed biomechanical studies of leaping in gibbons have been undertaken to date. I measured ground reaction forces and derived kinematic parameters from high-speed videos during gibbon leaps in a captive zoo environment. I identified four distinct leap types defined by the number of feet used during take-off and the orientation of the trunk, orthograde single-footed, orthograde two-footed, orthograde squat and pronograde single-footed leaps. The centre of mass trajectories of three of the four leap types were broadly similar, with the pronograde single-footed leaps exhibiting less vertical displacement of the centre of mass than the other three types. Mechanical energy at take-off was similar in all four leap types. The ratio of kinetic energy to mechanical energy was highest in pronograde single-footed leaps and similar in the other three leap types. The highest mechanical work and power were generated during orthograde squat leaps. Take-off angle decreased with take-off velocity and the hind limbs showed a proximal to distal extension sequence during take-off. In the forelimbs, the shoulder joints were always flexed at take-off, while the kinematics of the distal joints (elbow and wrist joints) were variable between leaps. It is possible that gibbons may utilize more metabolically expensive orthograde squat leaps when a safe landing is uncertain,

while more rapid (less expensive) pronograde single-footed leaps might be used during bouts of rapid locomotion when a safe landing is more certain.

Introduction

Biomechanical studies on leaping in primates have mostly focused on specialized leapers from the primate sub-order Strepsirrhini (non-tarsier prosimians), particularly the Lemuridae, Indriidae and Galagidae. Such studies (including: Demes and Günther, 1989; Preuschoft et al., 1996, 1998; Aerts, 1998; Crompton and Sellers, 2007) have revealed functional relationships between leaping performance, body mass and segment length in primates.

When leaping, larger animals are limited by muscle force, since force is proportional to length squared while mass is proportional to length cubed (see Alexander et al., 1981; Demes and Günther, 1989; Günther, 1989), and tend to minimize bone stresses by adopting shorter segments and smaller load arms (Biewener, 1989; Preuschoft et al., 1998; Scholz et al., 2006). Indeed, Demes et al. (1999) demonstrated that while take-off forces are higher in larger animals, relative forces decrease with increasing body size. Smaller animals, however, require maximization of impulse (force*time) to reach the required take-off velocity and so possess long distal segments to facilitate longer contact times at take-off (Preuschoft et al., 1998). Remarkably, despite a particularly forelimb-dominated locomotor repertoire, gibbons actually have long hind limbs in comparison to other non-human ape species (Schultz, 1936; Jungers, 1985), which could be particularly adaptive to maintaining contact with the compliant, deflecting branches, from which 67-85% of gibbon leaps are performed (Fleagle, 1976; Gittins, 1983; Sati and Alfred, 2002).

Smaller animals can also maximize impulse by increasing the amount of force they apply to the substrate. Aerts (1998) demonstrated the use of a power amplification mechanism in *Galago senegalensis* to achieve extremely high ground reaction forces during leaping. It was suggested that energy is stored in the tendon of the vastus muscle during a period of pre-stretch prior to the leap; when released, this energy is transferred to the long distal segments via the bi-articular muscles of the thigh and calf, generating power for the leap.

Specialized leapers are able to coordinate body segmental kinematics to maximize leap distance (e.g. use of the tail to manipulate CoM rotation etc.; Demes et al., 1991, 1995, 1999; see also: Preuschoft et al., 1998) and have a body build which places the centre of gravity along the take-

off trajectory (Crompton and Sellers, 2007; Crompton et al. In press). However, field and laboratory research into optimal leaping strategies for a number of specialized and less specialized leapers suggests that theoretical optima (based on expectations from ballistic science) may be utilized only during near maximal leaps even in the most specialized leapers (Crompton et al., 1993, In press; Linthorne et al., 2005). Other factors, such as support type or available support density, may have a greater influence on leaping performance (Warren and Crompton, 1997; Crompton and Sellers, 2007; Crompton et al. In press).

Leaping is an essential mode of locomotion for arboreal animals in a wide range of animal taxa. The often fragmented nature and height of forest canopy means that crossing gaps using powerful leaps is often more energy efficient than climbing down, crossing the gap terrestrially, and then climbing back up again (Sellers, 1992; Crompton et al. In press). The largest Asian ape, the orangutan, has been shown to require an order of magnitude less energy when crossing gaps by swaying compliant supports than would be required to cross them by coming to the ground and climbing up again (Thorpe et al., 2007a) while also reducing risks from ground dwelling predators (tigers in Sumatra, or the clouded leopard in Borneo). Leaping would serve equally well in terms of predator avoidance. Of course, there are risks involved in leaping: landing forces are typically higher than take-off forces when using stiff substrates (Preuschoft, 1985; Günther, 1989), suggesting potential for injury. However, this trend is reversed for compliant substrates, i.e. lower landing forces than take-off forces (Demes et al., 1995, 1999).

The exclusively arboreal lifestyle of gibbon requires an extensive locomotor repertoire to exploit their three dimensionally complex environment. Gibbons use quadrupedalism, bipedalism and leaping (Fleagle, 1976; Gittins, 1983; Vereecke et al., 2006a) as well as several modes of orthograde suspensory locomotion: vertical climbing, orthograde clambering and brachiation (categories follow Hunt et al., 1996 and Thorpe and Crompton, 2005, 2006). Of these, brachiation is the most common in the wild (comprising 50-75% locomotor time; Gittins, 1983) and best studied (Fleagle, 1974; Bertram et al., 1999; Bertram and Chang, 2001; Usherwood and Bertram, 2003; among others). These studies have shown that flexion of the long (muscular) forelimbs (16-17% of total body mass; Michilsens et al., 2009) allows the centre of mass (CoM) trajectory to be modified during brachiation, while the hind limbs (15-20% of total body mass; Isler et al., 2006) can be flexed to shorten the gibbons' effective pendular length, improving overall economy (Bertram et al., 1999; Usherwood and Bertram, 2003).

Despite the domination of forelimb-suspensory locomotion including brachiation in the gibbon locomotor repertoire, the hind limbs should not be considered simply as transferable ballast. Recent anatomical studies have shown that the hind limbs have a great propensity for muscular power production and elastic energy storage in substantial tendinous structures (Vereecke et al., 2005, Channon et al., 2009). Biomechanical studies of gibbon bipedalism have demonstrated the potential for energy storage and return in these tendinous structures and/or in the 'mid-tarsal break' (the concave flexing of the dorsal foot) seen in great apes (Vereecke et al., 2006b; Vereecke and Aerts, 2008; DeSilva, 2009). Channon et al. (2009) hypothesized that the powerful hip and knee joint extensor musculature found in gibbons is an adaptation to powerful leaping. Indeed, wild gibbons commonly utilize leaping as locomotor mode (5-25% locomotor time; Fleagle, 1976; Gittins, 1983; Sati and Alfred, 2002) and are able to cross distances in excess of 10 m in a single leap (Gittins, 1983; mean distance leapt by siamang, ~4 m; Fleagle, 1976). It is possible, therefore, that the extensive hind limb musculature and long hind limb length of gibbons is an adaptation to this mode and type of locomotion. Despite the scientific interest surrounding gibbons, both from evolutionary and biomechanical perspectives, and their impressive leaping performance, to date, no biomechanical study has been conducted on this important locomotor mode.

This study investigates the biomechanics of leaping in gibbons from a stiff substrate, with the aim of elucidating the underlying mechanism enabling the impressive leaping performances seen in wild gibbons. Further, this study represents an opportunity to investigate leaping in an unstudied primate with unusual body proportions. As such, it aims to identify mechanisms and adaptations in gibbons that contrast with leaping animals with a more typical body plan, reflecting this specialization.

Materials and Methods

Equipment and experimental setup

Data were collected during 24 spontaneous leaps from an adult female white-cheeked gibbon (*Nomascus leucogenys*, age: 6 years, mass: 8.7 kg) in the Wild Animal Park, Planckendael (Belgium). A wooden pole was rigidly fixed to a strain gauge forceplate (AMTI, OR6-7, Watertown, MA, USA) and positioned at the entrance to the indoor partition of the gibbon enclosure (Fig. 4.1). Force and moment data in vertical (F_Z, M_Z, respectively), cranio-caudal (F_X,

M_X) and mediolateral (F_Y, M_Y) directions (forces) and axes (moments) were collected at 500 Hz using a National Instruments (NI, Austin, Texas, USA) USB data acquisition module and custom-written software in National Instruments LabVIEW (version 8.2). The leaps were simultaneously recorded using two orthogonally positioned (lateral and cranio-caudal views) high-speed video cameras (AOS, X-Pri,

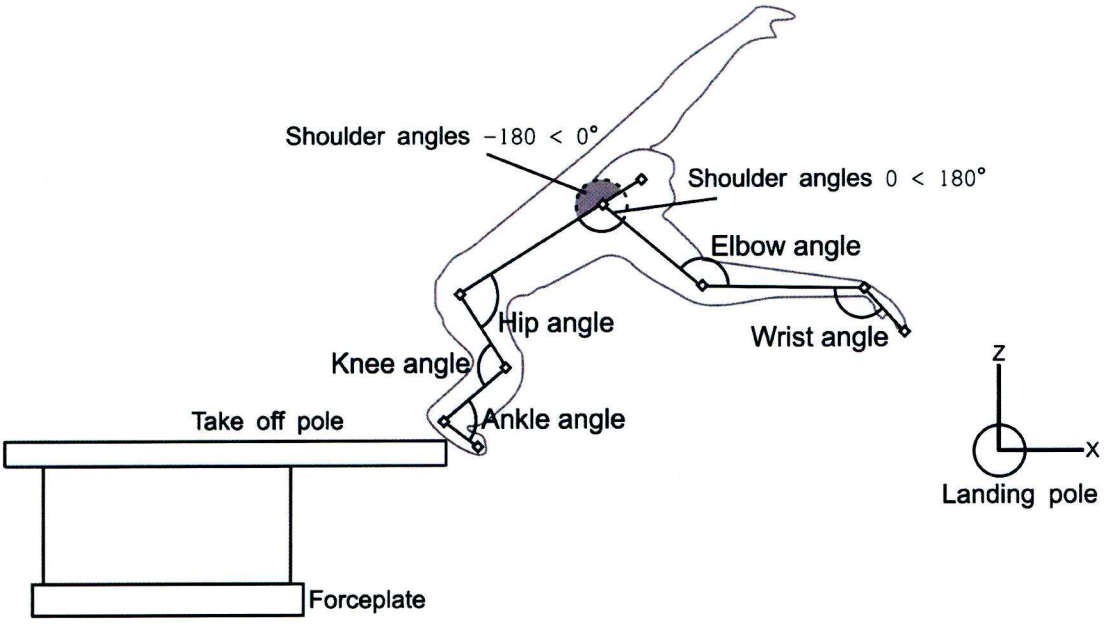

Figure 4.1. The apparatus setup during data collection. Open diamonds represent digitized points, arcs show joint angles used in the analysis.

Baden Dättwil, Switzerland) at 120 Hz. The lateral view was used for kinematic analysis while the cranio-caudal view was used to ensure that the leaps were executed orthogonally to the lateral view camera. The forceplate and cameras were synchronized using an external trigger. Voluntary leaps were recorded during morning and evening feeding sessions when the animal was drawn repeatedly over the pole, outside and inside, using food incentives. No direct interaction with the animal was allowed as stipulated by the zoo regulations, and all recorded leaps were thus executed spontaneously by the gibbon while moving around in its large enclosure. Leaps of an adult male white-cheeked gibbon were also recorded (in the same enclosure) but were not included in the analysis due to the low sample size, and observations were taken of two white-handed (*Hylobates* lar) gibbons leaping in a separate enclosure. Although not quantitatively analyzed, these leaps were qualitatively similar to the female gibbon (see results and discussion).

Limb kinematics

Approximations of 15 anatomical landmarks (i.e. left and right toe, ankle, knee, elbow, wrist and fingertip and hip, shoulder and ear at one side) were digitized in 2D from the lateral view videos using custom written software (NI, LabVIEW, 8.2, see Fig. 4.1, open diamonds for landmarks). Joint angles were defined as follows; Ankle joint angle, between the dorsum of the foot and the anterior of the shank; knee joint angle, between the posterior of the thigh and the posterior of the calf; hip joint angle, between the anterior of the trunk and the anterior of the thigh; wrist joint angle, between the palmar surface of the hand and the anterior of the forearm; elbow joint angle, between the forearm and the anterior of the upper arm; shoulder joint angle, between the anterior of the trunk and the posterior of the upper arm (Fig. 4.1, arcs). The shoulder joint is the only joint that is capable of circumduction, and an angle of 0° at the shoulder joint was defined as when the arm is directly in line with the trunk and inferior to the shoulder. Positive angles (0 - 180°) at the shoulder joint occur when the arm is anterior to the trunk (i.e. shoulder joint flexion), negative joint angles (-180 - 0°) occur when the arm is posterior the trunk (i.e. shoulder joint extension), at 180° and -180° the arm is held vertically, directly in line with the trunk, with the shoulder inferior to the arm (Fig. 4.1). Joint angles during take-off were smoothed using a cubic spline and resampled to the duration of the stance phase of the take-off foot. For the analysis, the limbs were categorized into (1) the take-off hind limb, the last hind limb to have contact with the pole; (2) the lead hind limb, the opposing hind limb to the take-off hind limb; (3) the take-off forelimb, the

ipsilateral forelimb to the take-off hind limb; and (4) the lead forelimb, the ipsilateral forelimb to the lead hind limb.

Stance phase was defined as the period from when the take-off foot touched down until the take-off foot left the pole, when take-off occurred.

Biomechanical parameters

The ground reaction force data were filtered using a bi-directional Butterworth filter (cut-off 10 Hz, 3rd order) and used to calculate acceleration (a_X, a_Z), velocity (v_X, v_Z), CoM position (S_X, S_Z), potential and kinetic energy (PE and KE) and impulse during stance. Vertical (F_Z) and fore-aft forces (F_X) were included in the analysis, medio-lateral forces were small and unpredictable, so were ignored in my analyses.

Horizontal and vertical accelerations (a_X and a_Z, respectively) were calculated as follows: $a_X = F_X/m$, $a_Z = g + F_Z/m$. This was integrated over stance time to yield centre of mass (CoM) velocity in horizontal (v_X) and vertical (v_Z) directions, the resultant velocity (v_R) was calculated using Pythagoras' theorem ($v_R^2 = v_X^2 + v_Z^2$). The initial velocity (v_0; used as the constant, when integrating acceleration with respect to time) was found using the path matching method of McGowan et al. (2005, see also, Daley et al., 2005 and Williams et al., 2009). The CoM velocity was then integrated to yield CoM position. Segmental inertial properties from a study by Isler and colleagues (2006) were combined with the segmental positions from the digitized video, and moments were resolved to give an initial CoM position in horizontal and vertical directions. CoM position (S_X and S_Z) was calculated throughout the trial from force traces and kinematics (as detailed above) and a good agreement between the two was found (Fig. 4.2). CoM position was standardized between trials to the position of the landing pole, which was set as the origin (0, 0). Impulse was calculated as the integral of force throughout the take-off hind limb stance time.

Potential ($PE = mgS_Z$) and kinetic ($KE = mv_R^2/2$) energies were calculated from force traces, resampled to take-off foot stance time and summed to give mechanical energy ($ME = KE + PE$). Work (W) was calculated as the net change in mechanical energy ($\Sigma\Delta ME$) and Power (P) as the derivative of work over stance time (dW/dt), after calculation, both were resampled to take-off

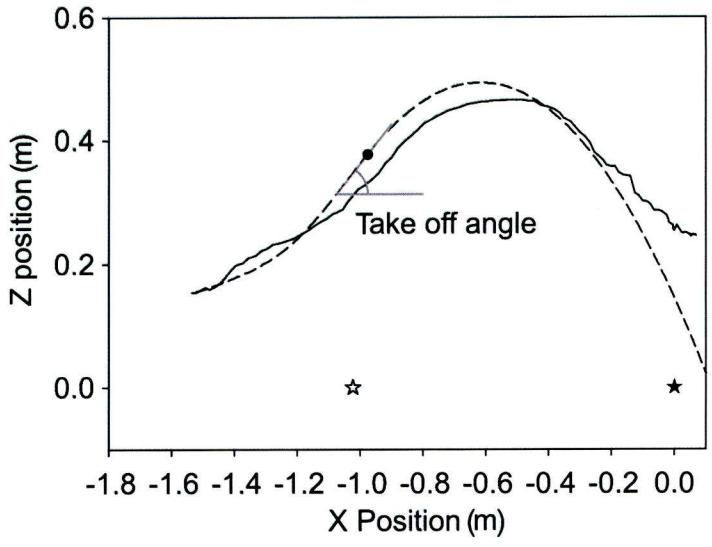

Figure 4.2. Agreement between centre of mass position from force plate (dashed line) and kinematics (solid line). Star represents the position of the landing pole. Take-off angle is shown in gray. Open star represents the take-off pole position, filled star represents the landing pole position. Filled circle represents the centre of mass position at take-off.

foot stance time. Work and power were normalized to body mass of the animal to give mass specific work and power (W_M and P_M, respectively).

Take-off angle to the horizontal (x-axis of Fig. 4.2) was calculated using the CoM path derived from force recordings, by differentiating the CoM trajectory (dS_Z/dS_X) for the five samples prior to take-off (this was felt to be representative of the take-off angle) and finding the mean angle to horizontal (see above and Fig. 4.2). Take-off velocity was derived from the force data (see above).

Statistical Analyses

Analysis of variance (ANOVA) and Tukey's HSD post-hoc tests were used to distinguish biomechanical variables between leap types (using SPSS, Systat software, Germany). A linear regression of take-off velocity against take-off angle was conducted (using Sigmaplot 11, Systat software, Germany) for each leap type individually and with all leap types pooled. P-values of less than 0.05 were considered significant. The results of these analyses are shown in Table 4.1.

Results

Leap types

Four distinct leap types were recorded during data collection: orthograde single-footed leaps (9/24), orthograde two-footed leaps (3/24), orthograde squat leaps (7/24) and pronograde single-footed leaps (5/24, Fig. 4.3). These leap types were also observed in other free-ranging gibbons at the park, yet were not included in the biomechanical analysis (see discussion). Still frames of each leap type are presented in Figures 4.3 and 4.4.

Orthograde single-footed leaps were performed as a smooth continuation of the gibbon's bipedal locomotion on top of the pole, with one full bipedal stride prior to the take-off stance phase. During the take-off stance phase (mean stance phase duration ± SE, 0.28 ± 0.02 s), the take-off hind limb extended rapidly and both shoulder joints flexed, raising the arms. The lead hind limb passed the take-off hind limb during the take-off stance phase and was used as the primary landing limb. The trunk remained orthograde (trunk angle > 45° to horizontal at take-off) throughout the leap.

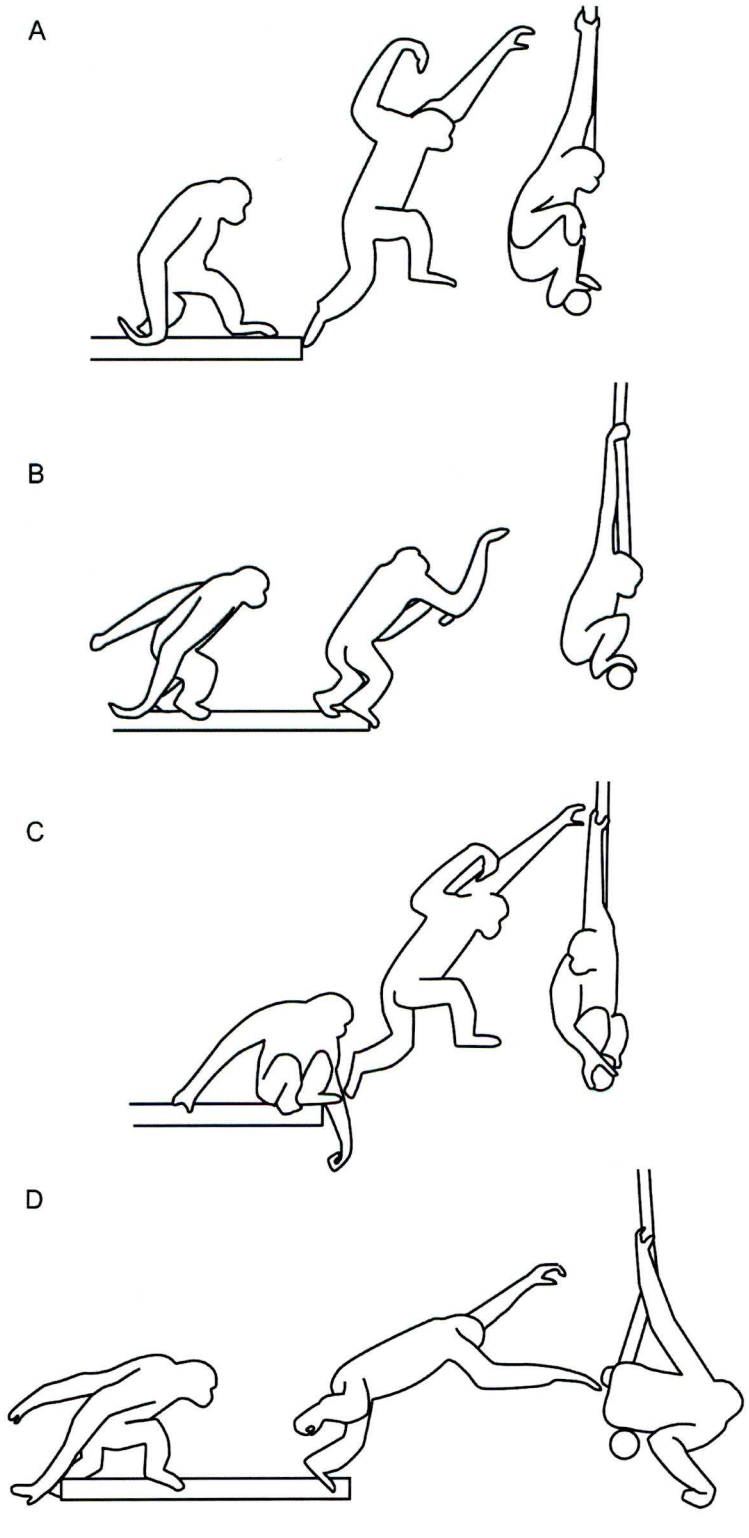

Figure 4.3. The four different leap types executed during data collection.

Figure 4.4. Examples of the four leap types analyzed in this study performed by three additional captive gibbons. **A**, an orthograde single-footed leap performed by an adult male white-cheeked gibbon (*Nomascus leucogenys*). **B**, a pronograde two-footed leap performed by an adult male white-handed gibbon (*Hylobates lar*, see text for discussion). **C**, an orthograde squat leap and, **D**, a pronograde single-footed leap performed by a juvenile white-handed gibbon.

Orthograde two-footed leaps were preceded by one full bipedal stride on the mounted pole. Immediately prior to the take-off stance phase (duration 0.30 ± 0.03 s), the would-be lead hind limb took a half stride and was positioned next to the take-off hind limb, causing a disjointed transition to take-off (unlike the case in orthograde single-footed-leaps; this is reflected in the shallow trough in the CoM position, Fig. 4.5). Both legs extended simultaneously and landing was executed either by one hind limb (n=1/3) or both limbs simultaneously (2/3). Again, the shoulder joints flexed during the take-off stance phase, raising the arms before take-off.

Orthograde squat leaps began with the gibbon sitting, hind limbs fully flexed, stationary on the mounted pole. From this position, the gibbon turned to face the direction of travel and extended both legs simultaneously, while flexing the shoulder joints and raising the arms. The gibbon landed on one or both hind limbs simultaneously. The take-off hind limb was continuously in contact with the pole throughout the trial (prior and during take-off) and so no meaningful stance phase duration could be calculated.

Pronograde single-footed leaps were preceded by a single bipedal stance phase prior to the take-off stance phase (i.e. one half of a stride). The trunk was more pronograde (trunk angle < 45° to horizontal at take-off) throughout the leap, than in the orthograde leap types. During the take-off stance phase (duration 0.20 ± 0.02 s), both forelimbs reached forward while the take-off hind limb flexed extended rapidly. The gibbon leapt past ('overleapt') the landing pole, using the forelimbs to grasp a nearby rope and swing to the floor ~0.5 m beyond the landing pole.

Joint kinematics

There was a proximo-distal extension of the take-off hind limb during take-off stance in all leap types, where the hip joint began extending prior to the knee joint, which in turn was followed by ankle joint extension (Fig. 4.6). The take-off hind limb hip joint extended continuously throughout stance. The range of take-off hind limb hip joint angles for all leap types was greater for orthograde squat (mean ± SE°, 108 ± 12°) than orthograde two-footed (76 ± 5°) and pronograde single-footed (77 ± 3°) leaps, while hip joint angles during orthograde single-footed leaps (94 ± 3°) were somewhere in between both groups (Fig. 4.6, Table 4.1). For orthograde single-footed, orthograde two-footed and pronograde single-footed leaps, the take-off hind limb knee joint was first flexed before beginning extension prior to 50% stance (% stance of minimum knee joint angle: orthograde two-footed, 37%; orthograde single-footed, 45%; pronograde single-footed,

Table 4.1. Results of Analysis of Variance and Tukey's HSD post hoc tests for homogenous subsets on inter-leap type differences in biomechanical variables. The groupings were significant at the 95% confidence level ($P < 0.05$). Std Er., standard error of the mean.

		Orthograde single-footed			Orthograde two-footed			Orthograde squat			Pronograde single-footed		
		Mean	Std. Er.	Group	Mean	Std. Er.	Group	Mean	Std. Er.	Group	Mean	Std. Er.	Group
Range of Take-off Limb Angles	Hip	93.94	3.21	1,2	76.29	4.85	1	107.65	11.71	2	77.36	3.34	1
	Knee	62.32	3.80	1	58.36	12.67	1	100.88	5.93	2	49.56	2.42	1
	Ankle	67.84	2.85	1	65.00	17.74	1	68.00	5.95	1	74.74	5.51	1
	Shoulder	127.59	10.39	1,2	134.90	59.22	1,2	40.64	17.23	1	175.64	24.14	2
	Elbow	95.41	5.61	1,2	143.50	60.07	2	57.74	7.87	1,2	103.19	9.54	1,2
	Wrist	55.72	6.37	1,2	131.64	84.79	2	33.60	5.38	1	92.78	4.58	1,2
Range of Lead Limb Angles	Hip	100.91	8.21	1	66.63	9.74	1	66.73	21.76	1	106.60	28.27	1
	Knee	66.80	7.85	1	66.63	9.74	1	64.30	20.47	1	117.74	28.88	1
	Ankle	81.65	5.76	2	47.73	6.50	1	44.34	7.94	1	85.40	4.75	2
	Shoulder	94.51	20.80	1,2	71.93	10.92	1	180.42	47.16	2	60.08	8.70	1
	Elbow	92.34	14.11	1,2	100.08	9.67	2	119.63	22.81	2	35.39	5.36	1
	Wrist	92.46	34.98	1	59.20	8.50	1	60.04	8.74	1	64.09	12.70	1
CoM	Start	0.20	0.01	2	0.12	0.04	1	0.13	0.03	1,2	0.19	0.01	1,2
	Displacement	0.22	0.04	1,2	0.21	0.01	1,2	0.30	0.01	2	0.11	0.01	1
Impulse	Z	39.51	1.44	1,2	50.35	0.26	2,3	60.51	0.40	3	28.81	0.78	1
	X	4.67	4.53	1	6.47	7.96	1	16.83	4.30	2	7.43	2.36	1
Take off ME		85.90	5.46	1	81.27	6.37	1	79.56	3.60	1	82.03	2.74	1
Take off KE:ME		0.31	0.02	1	0.34	0.05	1	0.29	0.01	1	0.44	0.01	2
Work		3.83	0.69	1	4.40	0.44	1,2	6.36	0.34	2	2.68	0.29	1
Peak power		25.71	2.65	1	32.07	5.88	1	71.06	2.04	2	21.18	0.58	1
Take off angle		25.58	2.49	2	30.67	2.80	2	34.46	2.81	2	12.46	0.79	1
Take off velocity		2.47	0.12	1,2	2.51	0.22	1,2	2.28	0.02	1	2.88	0.07	2

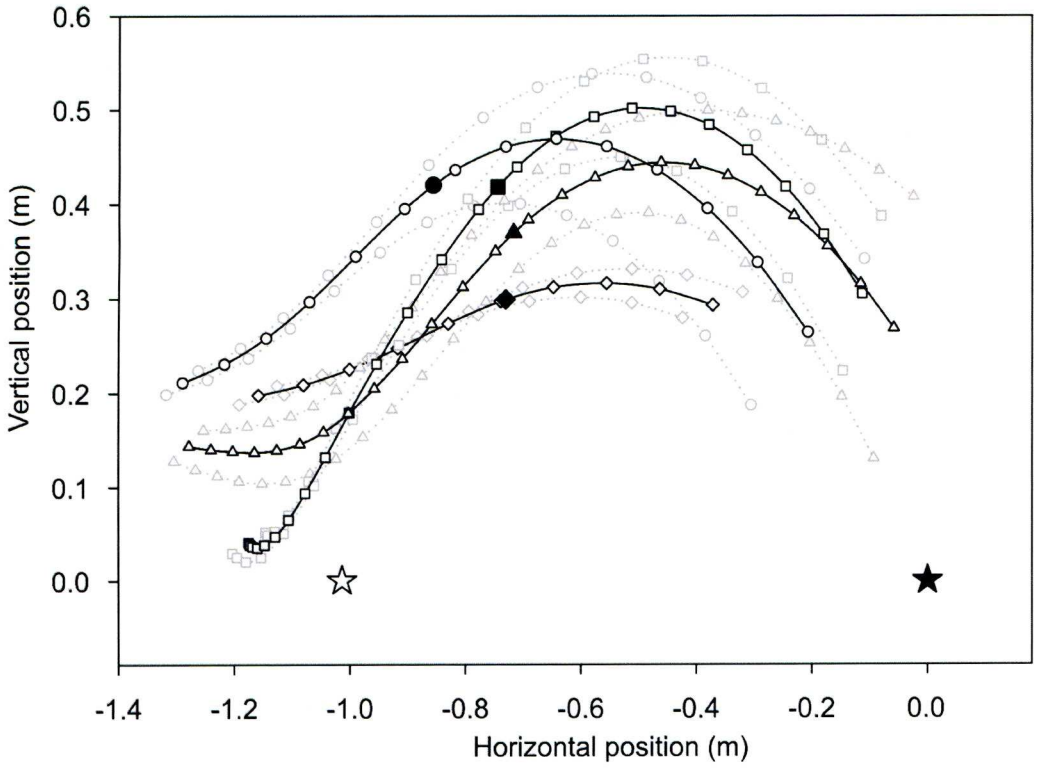

Figure 4.5. The centre of mass positions during the four leap types. Circles, orthograde single-footed leaps; triangles, orthograde two-footed leaps; squares, orthograde squat leaps; diamonds, pronograde single-footed leaps; open star, take-off pole position; filled star, landing pole position. Solid black lines show the mean, dotted gray lines represent standard error of the mean, filled shapes represent the centre of mass position at take-off.

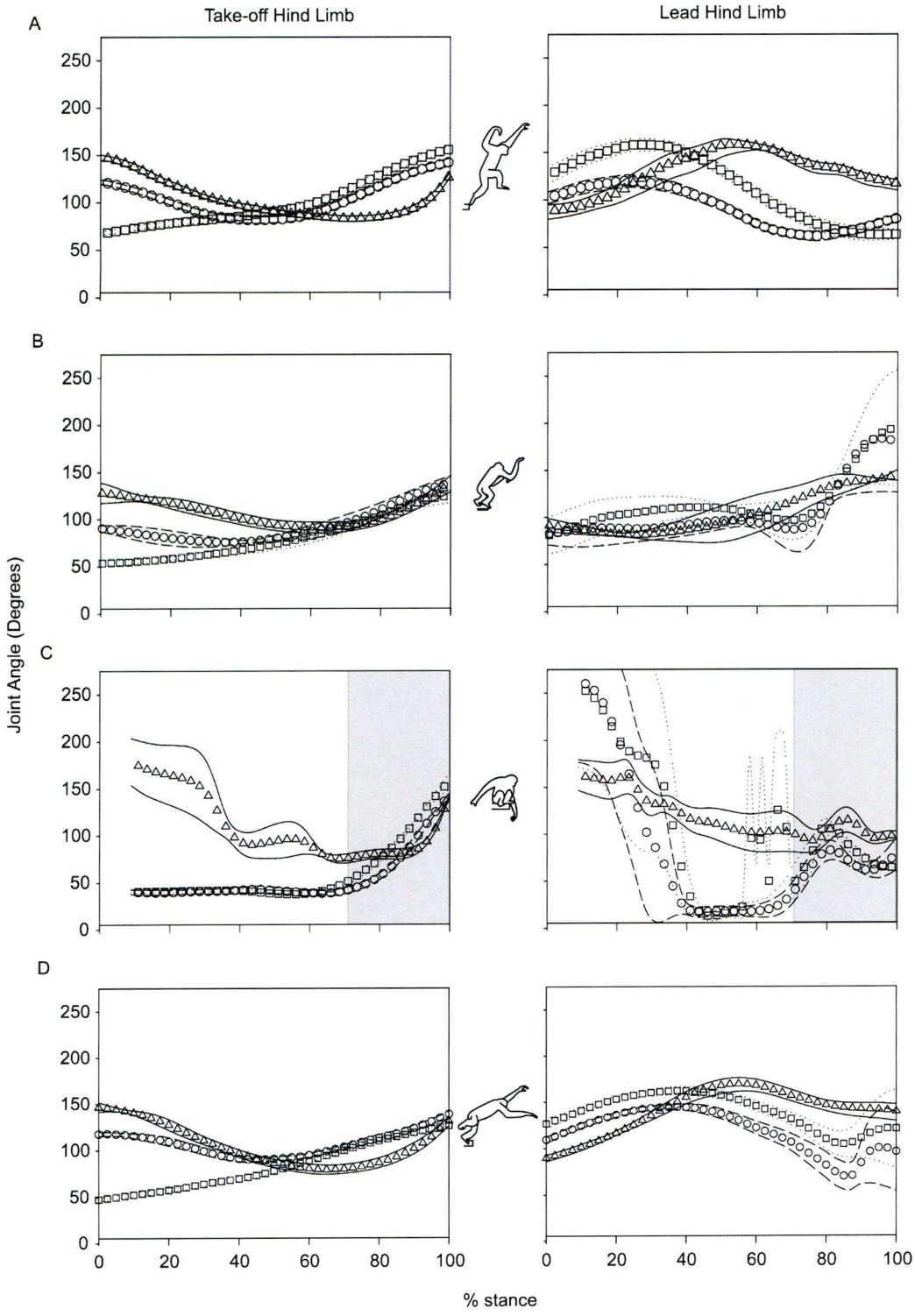

Figure 4.6. Take-off (left graphs) and lead (right graphs) hind limb joint angles during stance for the four leap types. (**A**) Orthograde single-footed leaps; (**B**) orthograde two-footed leaps; (**C**) orthograde squat leaps; (**D**) pronograde single-footed leaps. Triangles, ankle; circles, knee; squares, hip. Lines show standard error of the mean; solid, ankle; dashed, knee; dotted, hip.

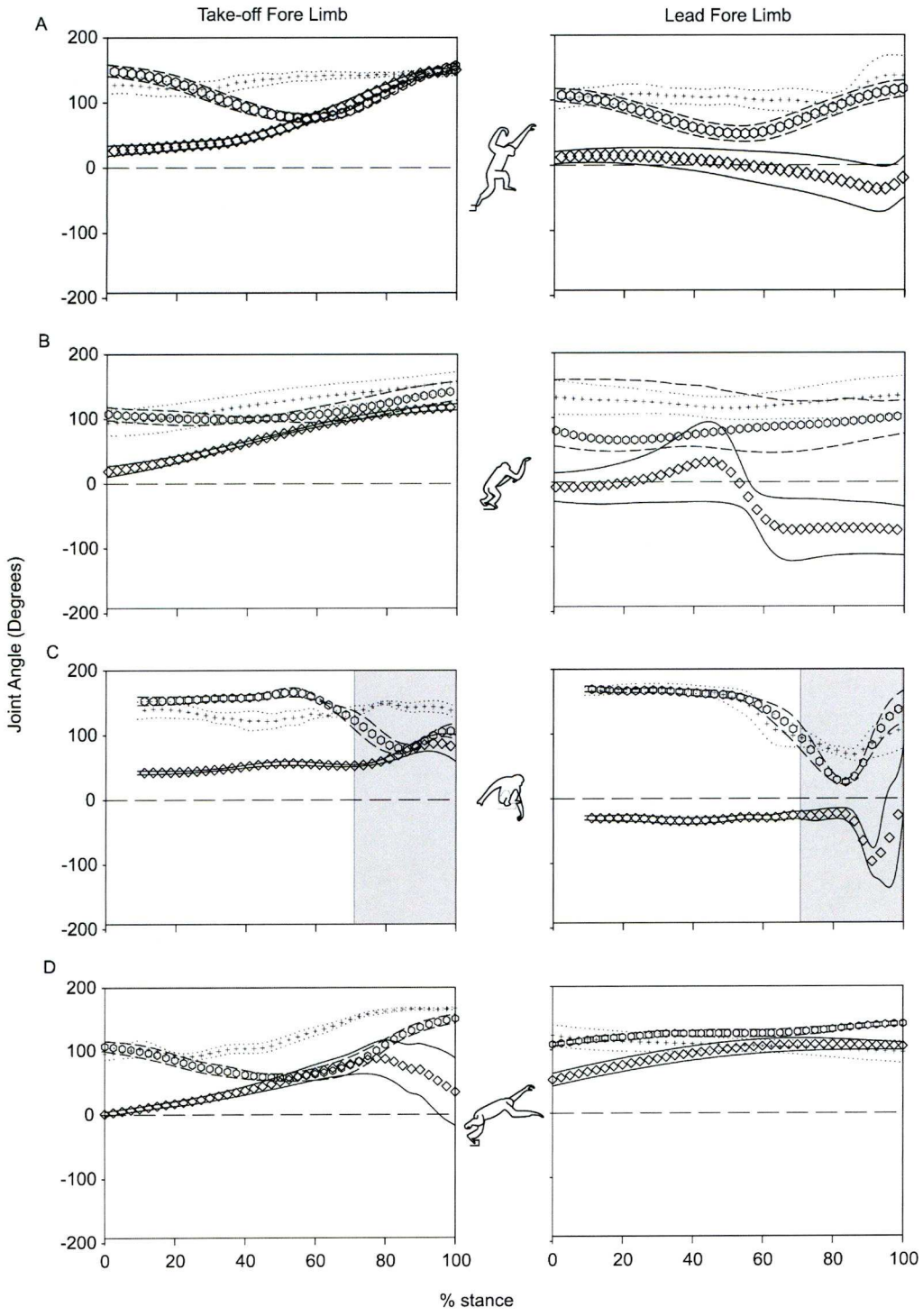

Figure 4.7. Take-off forelimb (left graphs) and lead forelimb (right graphs) joint angles during stance for the four leap types. (**A**) Orthograde single-footed leaps; (**B**) orthograde two-footed leaps; (**C**) orthograde squat leaps; (**D**) pronograde single-footed leaps. Diamonds, shoulder; hexagons, elbow; crosses, wrist. Lines show standard error of the mean; solid, shoulder; dashed, elbow; dotted, wrist.

46%). In orthograde squat leaps, the knee joint was deeply flexed at the beginning of stance time (39 ± 4°) and extended in the second half of stance (note that the region considered in the analysis is shown by the shaded translucent boxes on Figs 4.6c and 4.7c; see discussion). The take-off hind limb knee joint underwent a larger angular excursion during orthograde squat leaps (101 ± 6°) than during the other leap types (orthograde single-footed, 63 ± 4°; orthograde two-footed, 58 ± 13°; pronograde single-footed, 50 ± 2°; Table 4.1). During orthograde single-footed, orthograde two-footed and pronograde single-footed leaps, the take-off hind limb ankle joint was first flexed before beginning extension at approx. 65% stance (% stance of minimum ankle joint angle; orthograde two-footed, 66%; pronograde single-footed, 66%; orthograde single-footed, 72%). Orthograde squat leaps began with the ankle joint in a dorsiflexed position (75 ± 4°). All leap types demonstrated a similar take-off hind limb ankle joint angular excursion (orthograde single-footed, 68 ± 3°; orthograde two-footed, 65 ±, 18°; orthograde squat, 68 ± 6°; pronograde single-footed, 75 ± 6°, Table 4.1).

The angular excursions of the lead hind limb ankle joint were statistically different between orthograde single-footed (82 ± 6°) and pronograde single-footed leaps (85 ± 5°, Table 4.1) and orthograde two-footed (48 ± 7°) and orthograde squat leaps (44° ± 8°) . Lead hind limb angles for the hip and knee joints were statistically indistinguishable between leap types. In orthograde single-footed and pronograde single-footed leaps, the lead hind limb hip joint underwent a period of extension at the beginning of stance (maximum hip joint angle; pronograde single-footed, 162 ± 5°, 39%; orthograde single-footed, 158 ± 7°, 27%, Fig. 4.6) before flexing until just before take-off (minimum hip joint angle; pronograde single-footed 104 ± 13°, 86%; orthograde single-footed, 63 ± 6°, 94%). The lead hind limb knee joint angles of orthograde single-footed and pronograde single-footed leaps mirrored this (maximum knee joint angle, % stance - minimum knee joint angle, % stance; pronograde single-footed, 144 ± 4°, 38% - 69 ± 15°, 87%; orthograde single-footed, 120 ± 7°, 24% – 61 ± 5°, 77%). The lead hind limb ankle joint angles of orthograde single-footed and pronograde single-footed leaps peaked later in stance than the hip and knee joints and showed no late stance extension (maximum ankle joint angle, % stance; pronograde single-footed, 169 ± 7°, 56%; orthograde single-footed, 158 ± 6°, 54%).

In orthograde two-footed and orthograde squat leaps, lead hind limb angles were highly variable. In orthograde two-footed leaps, the lead hind limb hip joint extended throughout most of stance before flexing slightly, then extending from approximately 70% stance until take-off. The knee joint mirrored this almost exactly, while the ankle joint flexed only slightly at the beginning of

stance before extending from 26% stance until take-off. In orthograde squat leaps, the lead hind limb hip joint extended during push-off then flexed again before take-off, a pattern also observed at the knee joint. The ankle joint began extending later in stance than the hip and knee joints (76% for ankle vs. 60% for knee) and flexed again before the end of take-off hind limb stance (Fig. 4.6).

The shoulder joint of the take-off forelimb showed a gradual extension throughout stance (Fig. 4.7a). The angular excursion of the take-off shoulder joint during orthograde squat leaps (41 ± 17°) was smaller than during pronograde single-footed leaps (176 ± 24°; Table 4.1), with orthograde single-footed (128 ± 10°) and orthograde two-footed (134 ± 60°) leaps demonstrating intermediate shoulder joint angle values. The take-off forelimb elbow joint flexed during the beginning of stance before extending from approximately mid-stance to take-off (Fig. 4.7b). The angular excursion of the take-off forelimb elbow joint was similar during all leap types (Table 4.1). The take-off forelimb wrist joint maintained a flexed posture throughout take-off and leap. The angular excursion of the take-off forelimb wrist joint was larger during orthograde two-footed (132 ± 85°) leaps than orthograde squat (34 ± 5°) leaps, with orthograde single-footed (56 ± 6°) and pronograde single-footed (93 ± 5°) leaps demonstrating wrist joint angle values in between (Table 4.1). The contralateral forelimb angles were highly variable between and within leap types. In all leaps types, the lead forelimb upper arm was in line with the body and inferior to the shoulder (i.e. hanging down; shoulder joint angles close to zero degrees, Fig. 4.1) during early stance, then the shoulder joint flexed gradually (going through positive joint angles, pronograde single-footed, Fig. 4.7) or extended gradually (passing through negative joint angles, orthograde single-footed, orthograde two-footed and orthograde squat, Fig. 4.7). The angular excursion of the lead forelimb shoulder joint during orthograde squat leaps (180 ± 40°) was higher than for orthograde two-footed leaps (72 ± 11°), with orthograde single-footed (95 ± 21°) and pronograde single-footed leaps (60 ± 9°) spanning both groups. The kinematics of the lead forelimb elbow joint were also highly variable, either exhibiting the 'U'-shaped curve seen in the take-off forelimb elbow joint (orthograde single-footed, orthograde squat), or remaining constant throughout stance (orthograde two-footed, pronograde single-footed). The angular excursion of the lead forelimb elbow joint during orthograde squat (120 ± 21°) and orthograde two-footed (100 ± 10°) leaps was higher than for pronograde single-footed leaps (35 ± 5°), with orthograde single-footed leaps (92 ± 14°) spanning both groups (Table 4.1). The lead forelimb wrist joint angle remained approximately constant in pronograde single-footed and orthograde two-footed leaps (between 90 – 130°), but extended at the end of stance in orthograde single-footed (89% stance)

and orthograde squat (85%) leaps. The range of lead forelimb wrist joint angles was similar in all leap types (Table 4.1).

Centre of mass movement

The CoM (S_Z) position started lower in orthograde two-footed (0.12 ± 0.04 m) than orthograde single-footed (0.20 ± 0.01 m) leaps, with orthograde squat (0.13 ± 0.03 m) and pronograde single-footed (0.19 ± 0.01 m) leaps spanning both groups (Fig. 4.5, Table 4.1). CoM displacement prior to take-off was higher in orthograde squat leaps (0.30 ± 0.01 m, Fig. 4.5) than pronograde single-footed leaps (0.11 ± 0.01 m), with orthograde single-footed (0.22 ± 0.04 m) and orthograde two-footed leaps (0.21 ± 0.01 m) spanning both groups (Table 4.1). Take-off occurred at similar horizontal positions of the CoM for all of the leaps types.

Impulse

Horizontal impulse was highest during orthograde squat leaps (16.83 ± 4.3 Ns; Fig. 4.8) and similar in the other three leap types (orthograde two-footed, 6.47 ± 0.26 Ns; pronograde single-footed, 7.43 ± 2.36 Ns; orthograde single-footed, 4.67 ± 1.44 Ns). Vertical impulse was higher in orthograde squat leaps (60.51 ± 4.30 Ns) than orthograde single-footed (39.51 ± 4.53 Ns) and pronograde single-footed leaps (28.81 ± 2.36 Ns). Vertical impulse values during orthograde two-footed leaps (50.35 ± 7.96 Ns) were situated in between both groups (Fig. 4.8, Table 4.1).

Mechanical and kinetic energy

Mechanical energy (ME) at take-off was (statistically) similar between leap types (orthograde single-footed, 85.9 ± 5.56 J; orthograde two-footed, 81.3 ± 6.37 J; orthograde squat, 79.6 ± 3.60 J; pronograde single-footed, 82.0 ± 2.74 J, Fig. 4.9a, Table 4.1). The KE:ME ratio was higher at take-off in pronograde single-footed leaps (range: 0.42 ± 0.00 at 8% stance to 0.45 ± 0.01, 85% stance, Fig. 4.9b, Table 4.1) than the other three leap types, which had similar peak KE:ME ratios at take-off (orthograde two-footed, 0.38 ± 0.01 at 82% stance; orthograde single-footed, 0.35 ± 0.01, 80%; orthograde squat, 0.34 ± 0.01, 90%).

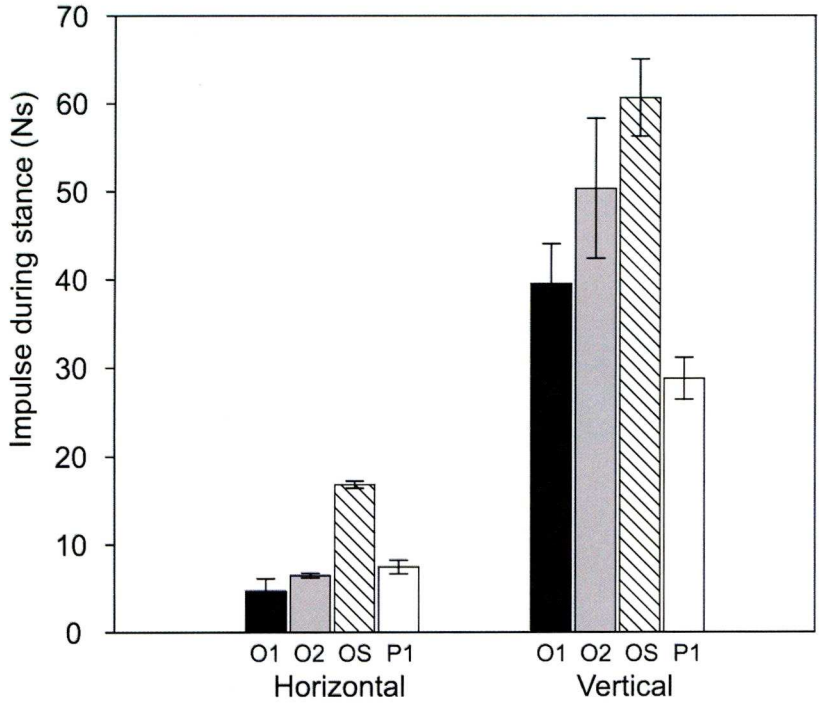

Figure 4.8. Mean impulse during stance for the four leap types, error bars denote standard error of the mean. Black, orthograde single-footed leaps (O1); gray, orthograde two-footed leaps (O2); striped, orthograde squat leaps (OS); white, pronograde single-footed leaps (P1).

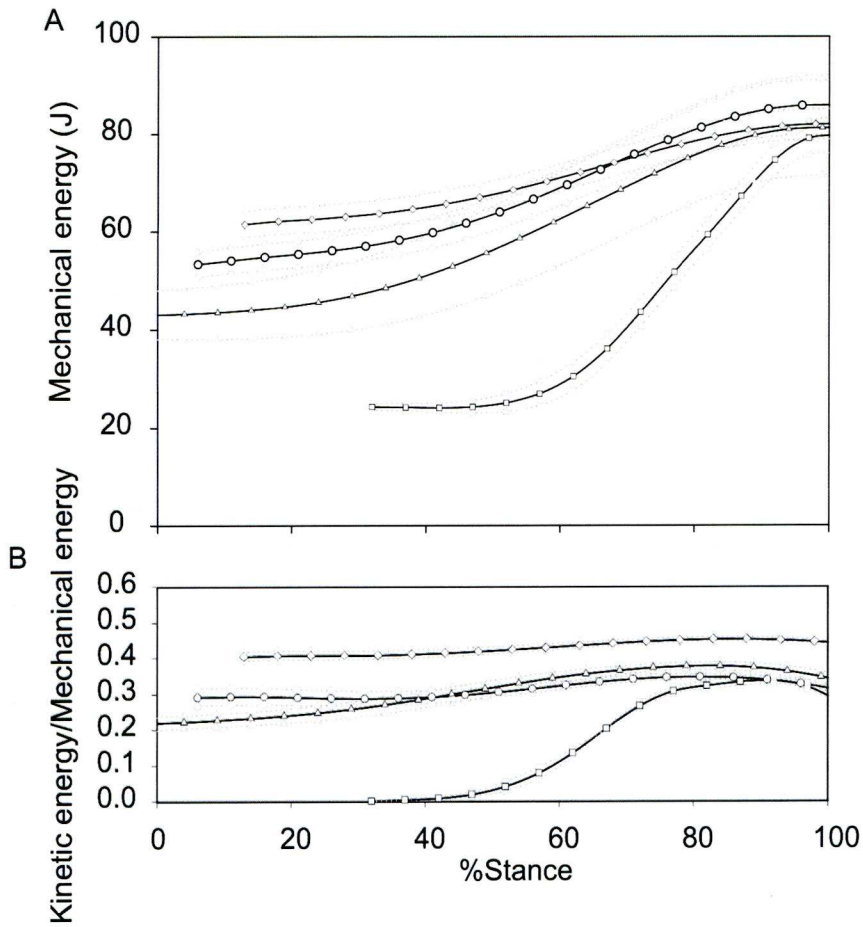

Figure 4.9. (**A**) Mechanical energy and (**B**) kinetic energy to mechanical energy ratio of the four leap types during stance. Circles, orthograde single-footed leaps; triangles, orthograde two-footed leaps; squares, orthograde squat leaps; diamonds, pronograde single-footed leaps. Solid black lines show the mean, dotted gray lines represent standard error of the mean.

Work and power

Mass-specific work (W_M) during the take-off stance phase was higher in orthograde squat leaps (6.36 ± 0.34 Jkg-1, Fig. 4.10), than pronograde single-footed leaps (2.68 ± 0.29 Jkg^{-1}), with orthograde single-footed (3.83 ± 0.69 Jkg^{-1}) and orthograde two-footed (4.40 ± 0.44 Jkg^{-1}) leaps spanning the two groups. Peak mass-specific power (P_M) was highest in orthograde squat leaps (71.06 ± 2.04 Wkg^{-1}, Fig. 4.11, Table 4.1), and similar for the other leap types (orthograde two-footed 32.07 ± 2.8 Wkg^{-1}, orthograde single-footed leaps 25.71 ± 2.65 Wkg^{-1}, pronograde single-footed leaps 21.18 ± 0.58 Wkg^{-1}). Peak PM occurred at between 63 and 75% stance for all leap types.

Take-off angle vs. take-off velocity

Within leap types no significant correlation was found between take-off angle and take-off velocity ($P > 0.5$ for each leap type). When all the leap types were pooled, the relationship between take-off angle (θ) and take-off velocity (v_{TO}) became significant, with take-off angle being negatively correlated with take-off velocity ($v_{TO} = -13.7*\theta + 59$, $P = 0.04$, Fig. 4.12).

Discussion

The biological employment of different leap types

My results indicate that gibbons systematically use (at least) four biomechanically distinct leap types. Given the prevalence of leaping in wild gibbons, and the range of substrates from which leaps are conducted (Fleagle, 1976; Gittins, 1983), I suggest that the choice of leap type will be influenced by specific conditions of the environment (substrate, gap distance, canopy structure, tree level) as well as the socio-ecological context (predator avoidance, food access, playing). It is further likely that the variety of leap types available increases the versatility, and hence adaptive effectiveness of leaping as a locomotor mode.

Orthograde single-footed and orthograde two-footed leaps appear biomechanically similar, with similar levels of muscular power required to complete the leap (Fig. 4.11). These leap types seem to be slower versions of the more rapid pronograde single-footed leaps. It is probable, therefore,

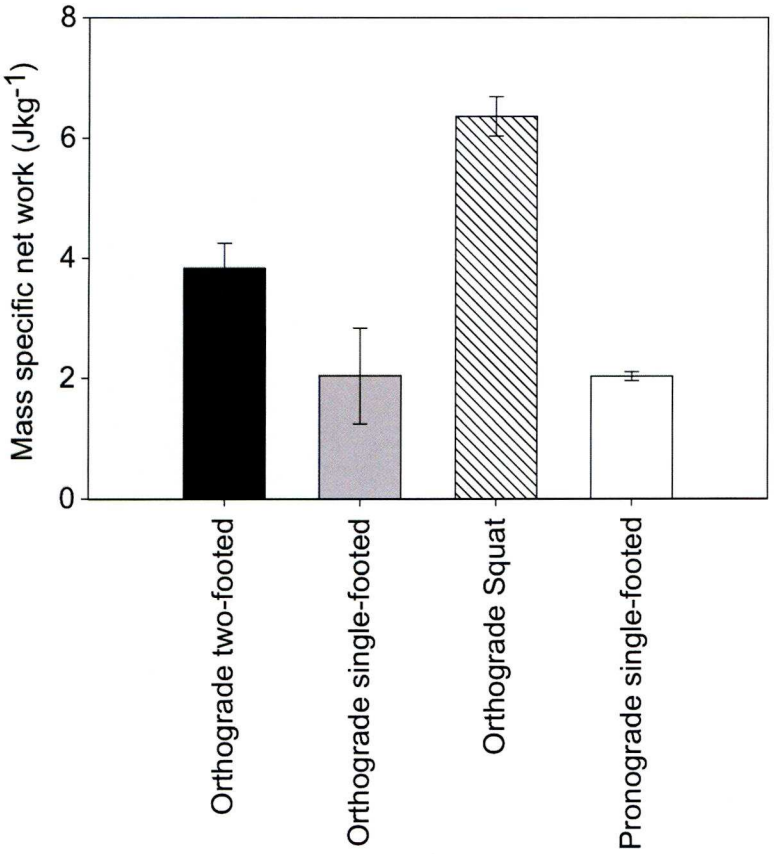

Figure 4.10. Mean mass specific net work of the four leap types, error bars denote standard error of the mean. Black, orthograde two-footed leaps; gray, orthograde single-footed leaps; striped, orthograde squat leaps; open, pronograde single-footed leaps.

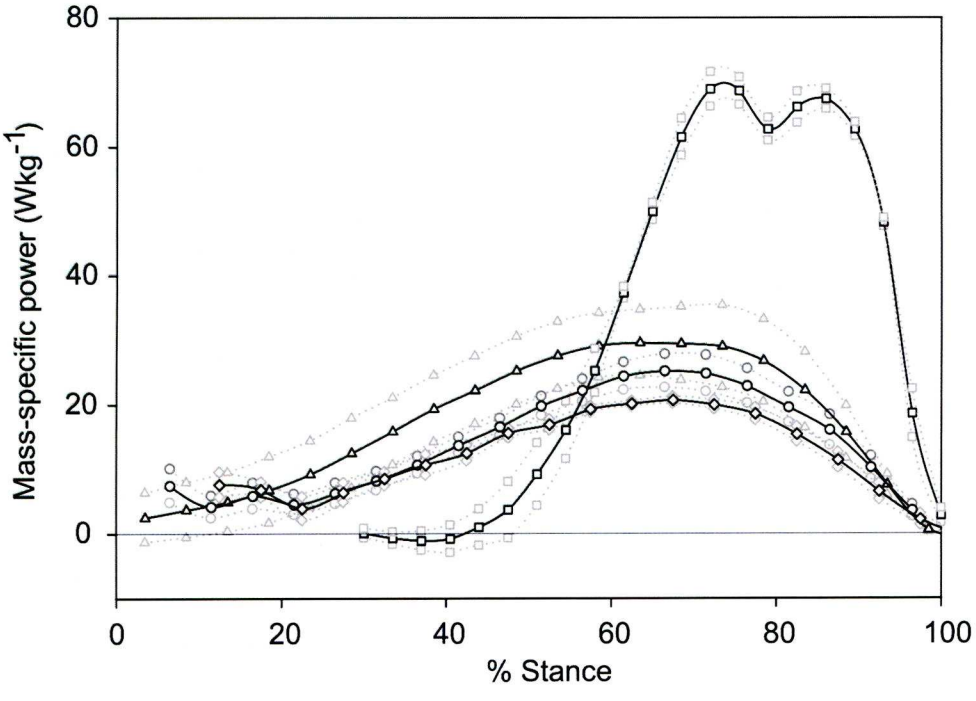

Figure 4.11. Mean mass specific power of the four leap types. Circles, orthograde single-footed leaps; triangles, orthograde two-footed leaps; squares, orthograde squat leaps; diamonds, pronograde single-footed leaps. Solid black lines show the mean, dotted gray lines represent standard error of the mean.

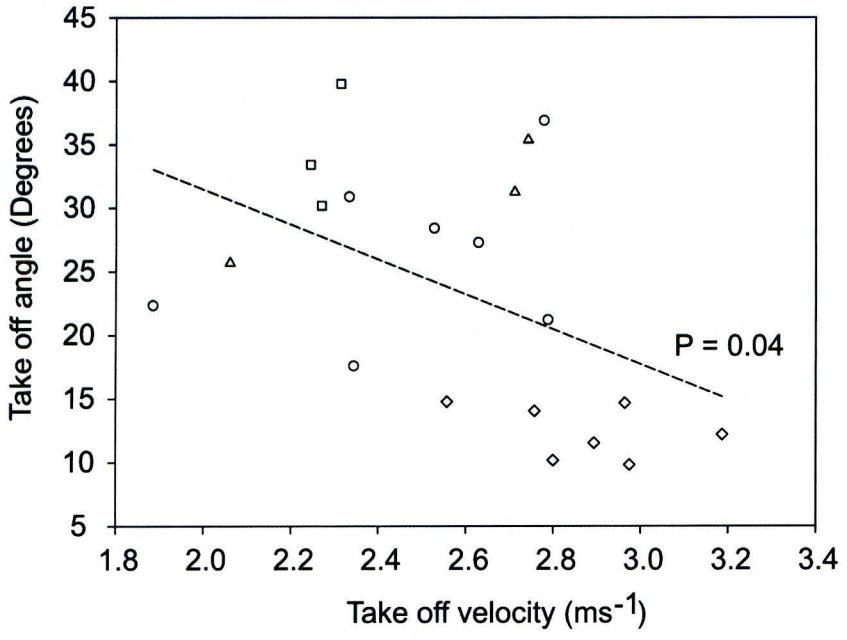

Figure 4.12. Take-off angle against take-off velocity, with linear regression (black dashed line). Circles, orthograde single-footed leaps; triangles, orthograde two-footed leaps; squares, orthograde squat leaps; diamonds, pronograde single-footed leaps.

that orthograde single and two-footed leaps are used for leaping short distances, perhaps between branches of the same tree during feeding, while more rapid pronograde leaps facilitate crossing larger distances. In support of this, I observed two white-handed gibbons (one adult male and one adolescent female) using pronograde single-footed leaps (and pronograde two-footed leaps, a potential 5th leap type) when crossing larger distances (~4 m, AJC, personal observation, Fig. 4.4). Further, when pronograde single-footed leaps were conducted from the instrumented pole, the gibbon rarely landed on the landing pole, opting instead to grasp a nearby rope and land on the far side of the landing pole (i.e. the gibbon 'over-leapt' the gap).

Leap distance is a function of take-off angle (discussed below) and take-off velocity (Crompton et al., 1993; Alexander, 1995), where a more rapid take-off allows a longer leap. The drawback of very rapid leaps is that the energy must be dissipated upon landing. Landing on compliant substrates (in this case a rope) facilitates a lower peak force and reduces the chance of injury (Huang and Li, 2005; Stevens, 2008). Indeed, wild gibbons have been shown to select compliant branches for landing after long leaps (Fleagle, 1976), while a range of prosimians minimized landing force when leaping to a compliant pole (Demes et al., 1995, 1999). It is likely therefore that the rope landings shown by the test subject of this investigation (and, indeed, by the white-handed gibbons mentioned above) after pronograde single-footed leaps act to dissipate energy slowly, reducing injury risk. A pronograde body position during take-off allows a larger proportion of the leap force to be directed along the compression axis of the substrate (if the substrate is horizontal, as here), reducing substrate deflection and potential energy loss (Crompton et al. In press), further purporting the suitability of pronograde single-footed leaps for larger gap crossing.

A disadvantage of pronograde vs. orthograde leaps is that comparatively little height is gained (i.e. take-off angle is reduced) meaning that, for a given horizontal distance, some net potential energy loss is likely. Field observations indicate that wild gibbons often land lower in the canopy than their take-off position, particularly after longer leaps, during travel (Fleagle, 1976; Gittins, 1983). In the experimental setup used in this study, the take-off and landing pole were positioned at the same height, ruling out investigations of the effect of relative level of the landing pole. In a follow up study, it would be interesting to change both the gap distance and level of the landing pole to assess the effect of these factors on leap type. The observations of the free-ranging white-handed gibbons are particularly relevant in this respect.

Orthograde squat leaps were the most costly (in terms of mechanical work and power) leap type measured (Figs. 4.10 and 4.11). Squat leaps demonstrate a wider angular excursion of hip and knee joints during take-off than single-footed leap types, increasing effective leg length, and hence impulse (for a given peak force). Further, using both legs to accelerate the CoM likely allows higher peak forces than a single support limb. It is not surprising, therefore, that squat leaps can be used to cross large gaps, even without any initial kinetic energy (AJC, personal observation). One potential advantage of squat leaps (regardless of trunk orientation) vs. rapid pronograde leaps is safety. Whilst, a rapid approach to a long leap may be advantageous for conserving kinetic energy, when leaping in an unfamiliar environment or when the leap target is partially obscured, squat leaps may offer a more stable starting position for a powerful (and hence well directionally controlled) leap. This is pertinent for a large-bodied canopy dwelling animal, where a fall could result in a serious injury or death (see Schultz, 1956), particularly when rapidly changing direction on thin branches and twigs, which may deflect unpredictably in two dimensions (up/down, left/right). Branch deflection may be useful during squat leaps, however, where 'branch pumping', a technique reliant on a stationary starting position, could facilitate elastic energy return before a leap (Fleagle, 1976), although exploitation of the theoretical energetic advantage of such leaping by branch recoil has yet to be demonstrated for any species.

Comparisons with other leaping primates

The maximal power I found for gibbon leaping (71 Wkg^{-1}) is low compared to other specialized leapers, such as the galago (~540 Wkg^{-1}, albeit using a power amplification mechanism, Aerts, 1998), and seems also to be lower than that of some strepsirrhine leaping primates (Demes et al., 1999). Although no CoM powers were calculated by Demes and colleagues (1999), take-off forces during strepsirhine leaping were typically 6-12 times body weight, while the gibbon data shown here represents forces of 1.5-3 times body weight. The low power values observed in my study are probably due to sub-maximal leaping performance. I recorded leaps with a fixed distance of 1 m, while wild gibbons have been reported to leap distances of 10 m (Gittins, 1983). Take-off forces during such leaping performances are certainly much higher, yet, while maximal performances are easy to obtain in human subjects, they are hard, if not impossible, to record using untrained animals in an experimental setting.

Bonobos have been shown to be proficient leapers and possess a large volume of muscle dedicated to hip and knee joint extension (Payne et al., 2006a, b). Gibbons also have voluminous hip and knee extensors (Channon et al., 2009) and it is therefore probable that leaping in gibbons is conducted via powerful hip and knee joint extension as seen in bonobos (Scholz et al., 2006). This is more likely than a galago-like, ankle joint powered leap (Günther, 1989; Aerts, 1998) since, in addition to the much larger mass of gibbons (~10-15 times the mass of a galago), the distal segments (feet) of gibbons are relatively short (compared to galagos; yet rather long compared to bonobos), which would minimize contact time during an ankle joint powered leap (Bennet-Clark and Lucey, 1967; Alexander, 1995; Preuschoft et al., 1998). Further, smaller leapers (with elongated distal segments) often utilize a 'catapult' style mechanism, storing elastic strain energy and increasing peak force during stationary leaps (Bennet-Clark and Lucey, 1967; Lutz and Rome, 1994; Aerts, 1998; Nauwelaerts and Aerts, 2006). Gibbons, in contrast, use leaps intermittently with bouts of ricochetal brachiation (Fleagle, 1976; Gittins, 1983) and so are less likely to benefit from a catapult style mechanism, which requires a stationary start.

Unlike most specialized leapers, which land predominantly feet first (Günther, 1989; Oxnard et al., 1990; Demes et al., 1995), gibbons use their forelimbs during landing, either to take hold of a rope when touching down with the feet, or to 'vault' over the landing pole during pronograde single-footed leaps. During all of the collected leaps, the forelimbs were held beside or behind the body prior to initiation of the leap and were swung upwards and forwards during take-off (Fig. 4.3), attaining a position in front of the CoM at the end of the leap. This places the hands in front of the body ready to take hold of a landing sub/superstrate. Perhaps crucially, gibbons often switch to brachiating immediately after a leap, utilizing the kinetic energy of the leap to power the initial swing (Gittins, 1983; Bertram and Chang, 2001; Sati and Alfred, 2002). The forward swing of the forelimbs also accelerates the CoM upwards and forwards during the take-off phase, assisting the leap. Observations of white-handed gibbons leaping distances of ca. 4 m (referred to above) indicate indeed that a preparatory arm swing countermovement is used in squat leaps to accelerate the jump. Detailed biomechanical data on such leaps is, however, lacking. Arm swinging has been show to be beneficial to human leaps (Alexander, 1995; Cheng and Hubbard, 2008; Cheng et al., 2008; Hara et al., 2008) and since gibbons have substantially more mass (relative to body weight) located in the forelimbs (approx. 16% body mass, Michilsens et al., 2009) than humans, it is probable that forward movement of the forelimbs assists in powering the leap.

The long fore- and hind limbs of gibbons are doubtless also useful for energy dissipation during landing. Long hind limbs are equally effective for absorbing potentially harmful landing energies and increasing effective limb length during take-off. The specialized, strong and long forelimbs allows gibbons to not only cope with high landing energies, but usefully convert this energy into movement by initiating brachiation immediately after a leap, indeed gibbons are particularly effective at the efficient transition between locomotor modes (Bertram et al., 1999; Usherwood and Bertram, 2003).

Take-off angle

When including all leap types, take-off angle was found to decrease with increasing velocity at take-off (Fig. 4.12, although no statistical difference was found in take-off velocity between leap types, Table 4.1), which was expected, both intuitively and mathematically (Crompton et al., 1993; Crompton and Sellers, 2007). Within leap types, however, there was no significant relationship between take-off angle and take-off velocity (which is probably due to the relatively small number of leaps for each leap type, and the relatively small range of velocities represented), making it difficult to separate the effect of velocity and leap type on take-off angle. The maximum efficiency hypothesis suggests that a take-off angle of 45° should be utilized most often, yet take-off angles of the recorded leaps were all below 45° (9 - 40°). Nauwelaerts and Aerts (2006) showed that optimum take-off angle varies with relative (to body length) leap distance; this effect may be pertinent in my study since the leap distance was not near maximal. Further, a comparison of a specialist strepsirrhine leaper, *G. moholi*, with unspecialized strepsirrhine leapers, including *Otolemur crassicaudatus* and *Lemur catta*, indicated that in all but the specialized leaper, leap angles of 45° are only used for crossing maximal distances (Crompton et al., 1993). For the smallest strepsirrhine leapers, and for small haplorrhines such as *Tarsius* and *Cebuella*, not only leaping locomotion per se, but specifically low leaping trajectories probably do reduce predation risk, as less time is spent in the air and the trajectory may be less predictable (Crompton and Sellers, 2007; Crompton et al. In press). However, Blanchard (2007) found that at Mantadia even *Hapalemur griseus* did not use leaping as a means of predator avoidance, choosing rather to move downwards or remain immobile when threatened by avian predators, but to vocally-mob ground predators, while larger leapers such as Indri and *Propithecus diadema* are likely to approach a predator, except when accompanied by young. Gibbons' large body size and almost completely high-canopy habitus mean that predation risk is unlikely to be high: avian predators are probably

too small to take adults. Since a greater energetic advantage accrues to large leapers than small leapers from using leaping to cross gaps that otherwise would require height change, it thus seems likely that leaping of gibbons serves an energetic rather than predator-avoidance role. Thus, secure landing and obstruction-avoidance are probably the major desiderata influencing leaping performance (see above).

Further work

The leaps recorded and analyzed in this study are representative of the leap types used by other free-ranging gibbons to cross similar or larger distances (compare leaps of ~4 m by white-handed gibbons [see above] and leaps of ~1 m by a male white-cheeked gibbon, shown in Fig. 4.4a), yet due to limitations of the experimental setup detailed biomechanical analyses of these longer leaps were not possible. Collecting force and detailed kinematic data from gibbons is very difficult for several reasons. First, their pair-living sociality (with the exception of Nomascus concolor which is not held in accessible zoos) limits the numbers which can be held in any one zoo. Second, as discussed above, gibbons can leap great distances and creating a safe environment for them to do so makes demands on space in zoos and wild animal parks. Moreover, when working in a captive, free-ranging environment (such as the Wild Animal Park Planckendael), data must be collected opportunistically, as no direct interaction with the (untrained) animals is allowed, ruling out the possibility to record maximal performances. At the same time, however, this approach guarantees that the recorded leaps are spontaneous behaviours and representative of the locomotor behaviour of wild gibbons.

These difficulties mean that all collected force data and subsequent analysis are very valuable. I were able to attain good agreement between CoM movements recorded using forceplate data and those derived from kinematic data (Fig. 4.2), which suggests that video data alone could give reasonable insight into the biomechanics of longer leaps. This opens possibilities for studies in the wild, where maximal performance is far more likely to be observed, and may permit an analysis of the behavioural contexts in which each of the four leap types are employed.

Observation of free-ranging and wild gibbons indicate that leap biomechanics are likely to be affected significantly by distance and leap orientation (i.e. leaping up or down), as well as by substrate compliance (Fleagle, 1976; Gittins, 1982; other: Alexander, 1991; Cheng and Hubbard, 2004; Demes et al., 1995, Crompton and Sellers, 2007). Given the complex three-dimensional

environment that gibbons inhabit, all of these factors are likely to be relevant to the biomechanics and ecology of gibbons and other arboreal leapers, and as such should be the foci of future work.

Conclusions

This study has shown that leaping in gibbons can be categorized into four distinct leap types based on the spatiotemporal characteristics of the limbs and trunk position. Despite the kinematic differences between these leap types, the mechanical energy at take-off and the proportion of kinetic energy was broadly the same for all leap types (thus, dynamically/mechanically the four leap types are similar). Orthograde squat leaps required much greater work and power levels (due to the squatted start position of the animal), while faster pronograde leaps required less work and power as much of the mechanical energy was already present before the take-off phase. My results clearly indicate that the (long) hind limbs are important for propulsion generation (mainly by strong extension of hip and knee joints), whereas the long and heavy forelimbs play a role in securing the landing and potentially act as a means of accelerating the CoM before take-off. My study highlights the importance of the hind limbs in the gibbons' locomotor apparatus, despite the dominance of brachiation as a locomotor mode. Take-off angle is found to decrease with take-off velocity during gibbon leaping, but the effect of varying leap orientation, distance and substrate compliance on leaping biomechanics needs to be addressed in future studies.

List of Abbreviations

a_X – Craniocaudal acceleration

a_Z – Vertical acceleration

F_X – Craniocaudal force

F_Z – Vertical force

KE – Kinetic energy

m – Mass

ME – Mechanical energy

M_X – Craniocaudal moment

M_Z – Vertical moment

PE – Potential energy

P_M – Mass specific power

S_X – Craniocaudal displacement

S_Z – vertical displacement

v_R – Resultant velocity

v_0 – Initial velocity

v_X – Craniocaudal velocity

v_Z – Vertical velocity

W_M – mass specific work

Chapter 5: The Effect of Substrate Compliance on the Biomechanics of Gibbon Leaps

By Anthony J. Channon

With contributions from Michael M. Günther, Robin H. Crompton, Kristiaan D'Août, Holger Preuschoft and Evie, E. Vereecke.

I designed, built and installed the data collection equipment, collected and analysed the data and wrote the manuscript. Evie Vereecke provided funding for data collection, helped with the analysis and edited the manuscript. Kristiaan D'Août assisted with equipment installation and edited the manuscript. Michael M. Günther, Robin H. Crompton and Holger Preuschoft edited the manuscript.

Abstract

The storage and recovery of elastic strain energy in the musculoskeletal systems of locomoting animals has been extensively studied, yet the external environment represents a second potentially useful energy store which has often been neglected. Recent studies have highlighted the ability of orangutans to usefully recover energy from swaying trees to minimise the cost of gap crossing. While mechanically similar mechanisms have been hypothesised for wild leaping primates, to date no such energy recovery mechanisms have been demonstrated biomechanically in leapers.

I used a setup consisting of a forceplate and two high-speed video cameras to conduct a biomechanical analysis of captive gibbons leaping from stiff and compliant poles. I found that the gibbons minimised pole deflection by using different leaping strategies. Two leap types were used: slower orthograde leaps used a wider hip joint excursion to negate the downward movement of the pole, using more impulse to power the leap, but with no increase in work done on the centre of mass. Greater hip excursion also minimised the effective leap distance during orthograde leaps. More rapid, pronograde leaps conversely applied peak force earlier in stance where the pole was effectively stiffer, minimising deflection and potential energy loss. Neither leap type appeared to usefully recover energy from the pole to increase leap performance, but the gibbons demonstrated

an ability to adapt their leap biomechanics best to counter the negative effects of the compliant pole.

Introduction

Animals have long been known to store and recover energy in the elastic structures of the musculoskeletal system (Cavagna et al., 1977; Alexander, 1984; McGowan et al., 2005), economising on muscular work and reducing the cost of locomotion (Alexander, 1991, 1992). For animals moving on compliant substrates, the external environment represents another potentially useful energy store (Alexander, 1995; Demes et al., 1995). Indeed, recent studies have shown that orangutans utilise the slow sway of tree trunks to minimise the cost of gap crossing (Thorpe et al., 2007a), and that they control excess branch sway through irregular gait patterns and multiple support limb use (Thorpe et al., 2009). Human biomechanics studies show that athletes run faster on tracks with optimum stiffness properties (McMahon and Greene, 1979), while sprung boards and floors are commonly known to increase the jumping performance of divers and gymnasts (Kooi and Kuipers, 1994; McNitt-Gray et al., 1994; Cheng and Hubbard, 2004). Wild white-headed langurs (*Trachypithecus leucocephalus*) and siamang (*Hylobates syndactylus*) have been shown to utilise the damping properties of compliant substrates for dissipating energy when landing after vertical descent (Fleagle, 1976; Huang and Li, 2005; Stevens, 2008), lowering impact forces and the risk of injury (Demes et al., 1995, 1999). Despite field studies reporting that "In preparation for a leap, a siamang often acquires momentum by 'pumping in place on a branch'" (Fleagle, 1976), useful elastic energy storage in the substrate by non-human animals during powerful movements such as leaping has not been demonstrated to date. Biomechanical studies on sifaka (Propithecus sp., a vertical clinger and leaper) concluded that energy spent deforming the substrate was not recovered on take-off, increasing the metabolic cost of leaping (Demes et al., 1995). Further, tarsiers executing long leaps actively select wider diameter take-off substrates with orientations that best direct the leaping force along the long axis of branches, suggesting that they are actively seeking to avoid branch deflection and energy loss (Crompton et al. in Press).

A likely barrier to utilising substrate compliance during rapid, powerful movements is the stiffness and resonant frequency of the substrate (Alexander, 1991; Cheng and Hubbard, 2004; Ahlborn et al., 2006). When an animal leaps from a compliant substrate, such as a branch, the magnitude of deflection is proportional to the substrate's stiffness. Since the animal is in contact with the substrate, it loses potential energy proportional to the deflection. In a leaping animal, leg

extension contributes equal energy to substrate deformation and to centre of mass acceleration, hence stiffer substrates - which deflect less for a given force (i.e. input energy) - minimise potential energy loss of the centre of mass. The resonant oscillation frequency of the substrate is dependent on its stiffness, mass moment of inertia and the force applied to it (Jeffrey, 2005). An oscillating beam (or substrate) undergoes alternating periods of descent and ascent, where one period of descent and one period of ascent represent one oscillation. In order to most effectively utilise the energy stored in the substrate, leg extension, or push-off, should occur during the final period of ascent before take-off (Cheng and Hubbard, 2004). Therefore, slower oscillations (lower natural frequencies) require longer periods of leg extension and consequently lower forces, hindering leap performance.

The problem of substrate stiffness (and indirectly, resonant frequency) is a pertinent one for elastic energy recovery in locomoting animals. The most common natural sprung compliant substrates (as distinct from purely damping substrates which do not recoil noticeably, such as rotting branches or tree trunks, or wet soil) are living wooden branches and trunks and the animals most likely to encounter such substrates are habitually arboreal. Due to the fragmented nature of forest canopies, habitually arboreal animals must cross (often large) gaps between trees frequently, which they can do in a number of ways including tree swaying by larger animals (Thorpe et al., 2009) and gliding and leaping in smaller animals (Demes et al., 1991; Crompton et al., 1993; Byrnes et al., 2008). 'Branch pumping' observed in wild siamang (Fleagle, 1976) before a leap may be a mechanism to utilise the energy stored in the branch for propulsion. However, most gap crossing leaps are conducted from fine terminal branches (Fleagle, 1976; Gittins, 1983; Crompton et al., 1993; Sati and Alfred, 2002), with low resonant frequencies (McMahon and Kronauer, 1976) making efficient energy storage and recovery during leaping from terminal branches unlikely (Alexander, 1991). Indeed, wild sifaka were shown to take-off at the 'wrong' time for efficient energy return from thin branches (Demes et al., 1995).

Another significant effect of substrate compliance is unexpected perturbation. Many arboreal animals move rapidly through the forest canopy, and presumably lack the time to test the compliance of each branch before use. Branch failures by fracture or buckling have been observed in field studies, e.g. in leaping of *Otolemur crassicaudatus* and *Tarsius bancanus* respectively (RHC, pers. obs.), but observations are not frequent enough for statistical analysis. Even on familiar routes (during travel arboreal primates often follow specific routes or 'Jungle highways', McClure, 1964). Branch material properties may be highly dependent on foliage, water content or

interaction with other trees (McMahon and Kronauer, 1976). Since a mistake could result in serious injury or death (Schultz, 1956; Bramblett, 1967; Buikstra, 1975; Lovell, 1978), it seems probable that rapidly moving arboreal animals possess some mechanism(s) for coping with the perturbation effects (unexpected or otherwise) of compliant substrates. Data on arboreal animals dealing with such perturbation is lacking but the problem is undoubtedly real. McClure (1964) reported a siamang that "...misjudged the strength of a dead limb [branch]...and it plunged 25 or 30 feet into a crown below and continued without hesitation". Laboratory studies of running guinea fowl suggest that the rapidity of perturbation may require that such responses are passive (i.e. do not require central nervous system activity, Biewener and Daley, 2007).

In this study I compare the biomechanics of gibbons leaping from stiff and compliant substrates. Although renowned as specialist brachiators (Fleagle, 1974; Bertram et al., 1999), recent studies have highlighted that gibbons possess anatomical and biomechanical adaptations to execute hind limb powered movements such as leaping (Channon et al., 2009, 2010, In press). Gibbons commonly utilise leaping for, 20-25% of their locomotor activity (Fleagle, 1976; Gittins, 1983; Sati and Alfred, 2002) and regularly leap from thin terminal branches during travel and feeding (Kappeler, 1984; Sati and Alfred, 2002). Further, this study is the first to examine locomotion on compliant substrates by lesser apes, which is particularly relevant in light of recent findings on the locomotion of the orang-utan (a great ape, Thorpe et al., 2007a).

This study investigates the leaping mechanics of gibbons, with specific attention to the role and effect of substrate compliance. I hypothesize that gibbons will not be able usefully store and recover elastic energy from the substrate but expect that biomechanical strategies are used to cope with substrate compliance.

Materials and Methods

Voluntary leaps from a stiff (n = 16) and compliant substrate (n = 16) to a nearby landing pole (~1m away) by two white cheeked gibbons (*Nomascus leucogenys*, 1 female, age: 6 years, mass: 8.7 kg and 1 male, age: 38 years, mass: 6.7 kg) were recorded using high-speed video (120 Hz, AOS X-PRI, AOS Technologies, Switzerland). The cameras were positioned orthogonal to each other and recorded lateral and frontal views. The lateral view camera was used for the 2D-biomechanical analysis, while the frontal view camera was used to ensure that leaps were conducted in the plane perpendicular to the lateral camera. Each pole was mounted atop a strain

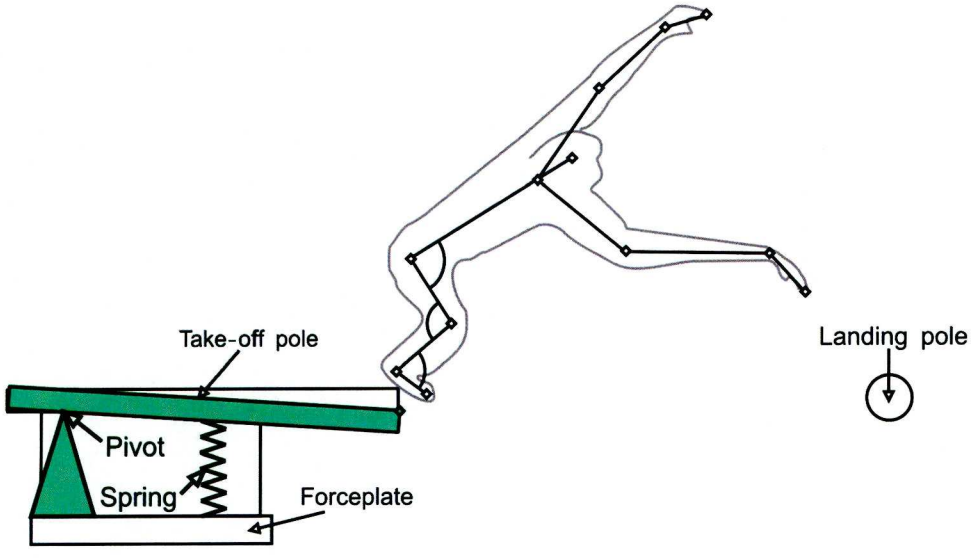

Figure 5.1. The experimental setup. Open diamonds show the joint centre digitisation points; filled green diamond shows the pole tip digitisation point. Open outlines show the stiff pole setup; green outlines show the compliant pole setup.

gauge forceplate (Fig. 5.1, OR6-7, AMTI, Watertown, MA, USA) and the analogue output signals were digitised by a National Instruments data acquisition module (NI, Texas, USA) and collected at 500 Hz using custom written software (LabVIEW 8.2, NI). The forceplate recordings were triggered by a synchronisation pulse from the high speed video cameras, and were thus fully synchronised with the video recordings.

The stiff pole was a cylindrical (80 mm diameter, 1000 mm length) wooden pole, rigidly mounted horizontally to the forceplate. The compliant pole was a stiff horizontal aluminium tube (80 mm diameter, 1000 mm length, 2.3 kg mass), fixed at one end to a pivot with the other end free (cf. a cantilever). Four parallel springs (stiffness [k] 7.5 N/mm each, combined 30 N/mm) were mounted at a distance of 285 mm from the pivot on the underside of the pole, and fixed to the forceplate (Fig. 5.1).

In my analyses the compliant pole was modelled as a mass-less beam attached to a frictionless pivot. To validate this assumption I compared the pole tip position based on the forceplate traces and manually digitised from the high-speed video. I used craniocaudal (X), mediolateral (Y) and vertical (Z), forces and moments (F_X, F_Y, F_Z, M_X, M_Y, M_Z respectively; the animal moved parallel, from negative to positive, to the X axis of the forceplate, allowing the animal and forceplate to share co-ordinate systems) to calculate the horizontal centre of pressure (CoP_X) position relative to the pivot as:

$CoP_X = [M_Y + (F_X*\alpha)]/F_Z$ where α is a force plate specific constant.

The displacement of the spring (S_{DIS}) was calculated as:

$S_{DIS} = (F_Z*CoP_X)/(S_X*k)$ where S_X is the distance between the spring and the pivot and k is the spring stiffness.

Displacement at the tip (T_{DIS}) as:

$T_{DIS} = (S_{DIS}/S_X)*T_X$ where T_X is the beam length (1 m).

I compared the tip displacement of the compliant pole calculated from forceplate data and digitised video for each trial using a linear regression (SPSS 17, Systat software, Germany). The mean gradient was close to 1 (0.97 ± 0.23 [s.d.]), the regression was highly significant (mean R^2 = 0.95, mean $P < 0.0005$) and the unloaded resonant frequency of the pole was high (~30Hz) suggesting that my model is sound.

Anatomical landmarks representing the toes, ankles, knees, hips, shoulders, elbows, wrists, fingers and head were digitised manually from the high speed video (Fig. 5.1). Hind limb joint angles were defined as ankle: the internal angle made by a line joining the toe ankle and knee (between the dorsum of the foot and the anterior of the shank); knee: the internal angle made by a line joining the ankle, knee and hip joints (between the posterior of the shank and posterior of the thigh), and hip: the internal angle made by a line joining the knee, hip and shoulder (between the anterior surface of the thigh and the anterior surface of the trunk, Fig. 5.1). Hind limb joint angles were resampled to the final stance phase before take-off (i.e. 0% stance, when the take-off limb touched the pole to 100% stance when the take-off foot left the pole, at take-off), using a cubic spline based interpolation algorithm in LabVIEW.

Forces were resampled to the duration of the final stance before take-off (hereafter: stance), and normalised to body mass, to remove the effect of body size. Mediolateral forces were small, and out of plane with the camera, and were omitted from my analyses (i.e. they were restricted to 2D). Impulse was calculated as the integral of the force-time curve during stance and was normalised to body mass.

Accelerations, resultant velocities (v_R) and centre of mass positions were calculated by dividing force by body mass and double integration of the resulting curve. Boundary (initial) conditions for the integration were attained using a kinematic path-matching technique, where the initial centre of mass position was calculated by combining the positions of the body segments (from digitised video) with published inertial properties (from Isler et al., 2006), and resolving the resulting moments. A more comprehensive description of these commonly utilised methods can be found elsewhere (McGowan et al., 2005; Daley et al., 2006; Williams et al., 2009; Channon et al. In press). Instantaneous centre of mass position was normalised to the landing pole position so that the landing pole was set at the origin (0, 0).

Potential and kinetic energy were summed to give mechanical energy.

ME = potential energy [PE] + kinetic energy [KE]

$PE = m*g*h$ and $KE = 0.5*m*v_R^2$

Where g is gravitational acceleration (9.81 ms^{-2}), h is the vertical height of the centre of mass and m is body mass.

Mechanical work was calculated as the net change in mechanical energy during the final stance phase before take-off. Power was calculated as the derivative of work over time through stance. Work and Power were divided by body mass to yield mass-specific work and power.

As the gibbon travels along the compliant pole, away from the pivot, the moment acting to compress the spring increases and so the combination of pole and spring becomes effectively less-stiff. The instantaneous pole stiffness (k_I), was calculated as:

$k_I = F_Z/S_{DIS}$

Statistical comparisons of biomechanical parameters (listed in Table 5.1) were made between leaps from the stiff and compliant pole. Because of the limited sample size (both in terms of individuals and number of leaps), I opted to use a non-parametric Kruskal-Wallis test, thus avoiding any assumptions of normality or equal variance, where a P-value of 0.05 or less was deemed significant. All statistical calculations were conducted in SPSS 17.

During this study, the gibbons utilised two distinct leap types: orthograde single-footed and pronograde single-footed leaps (Fig. 5.2, See Channon et al. In press for the biomechanics of different leap types used by gibbons). Since these are biomechanically distinct leap types, they were analysed separately here. The female gibbon conducted both leap types from both substrates (9 orthograde leaps from the stiff pole, 2 from the compliant pole, 7 pronograde leaps from the stiff pole, 3 from the compliant pole), while the elderly male only conducted orthograde single-footed leaps from the compliant substrate (11 leaps).

Results

Orthograde Leaps: Stiff vs. Compliant pole

Orthograde leaps from the compliant pole used peak vertical forces that were not statistically different in magnitude to stiff-pole leaps (P = 0.71) but peak force occurred earlier in stance during compliant-pole leaps (P = 0.04, Table 5.1, Fig. 5.3A). The vertical ground reaction force component appeared visually flatter during compliant pole leaps than during stiff pole leaps. Horizontal forces, conversely, were qualitatively and statistically similar between pole types. Stance duration for orthograde leaps was significantly longer when leaping from the compliant pole leaps vs. leaping from the stiff pole (P = 0.04, Table 5.1, Fig. 5.4A). Vertical impulse during

stance was higher in leaps from the compliant pole than from the stiff pole ($P < 0.0005$, Fig. 5.4B, Table 5.1), while horizontal impulse was not significantly different between substrate types. Leap distance (the horizontal distance from the centre of mass at take-off to the landing pole) was

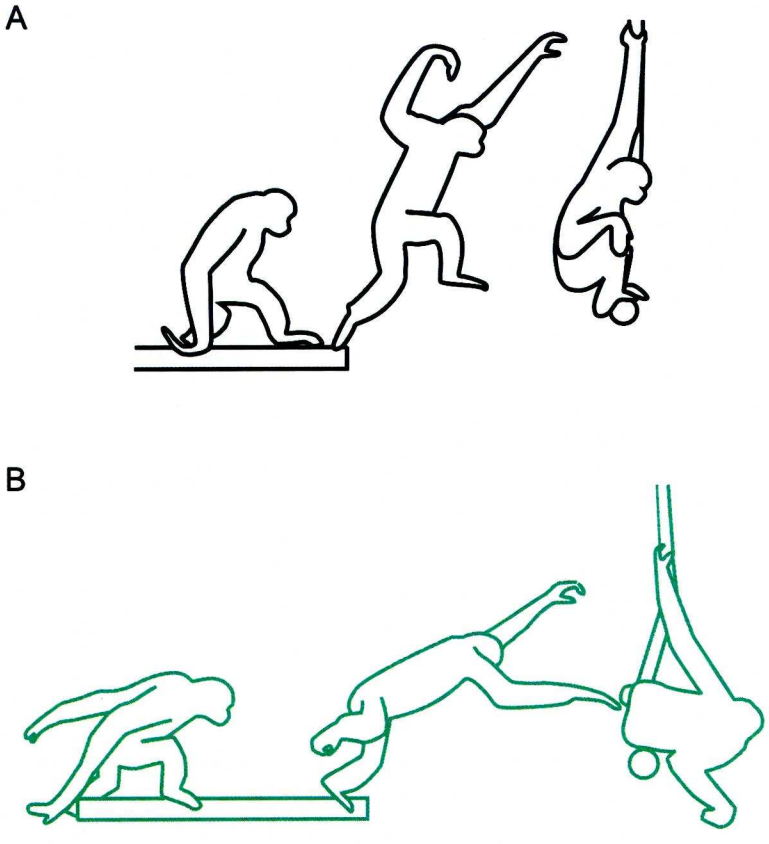

Figure 5.2. Schematic representations of the leap types observed. **A**: Orthograde single-footed leaps, **B**: Pronograde single-footed leaps.

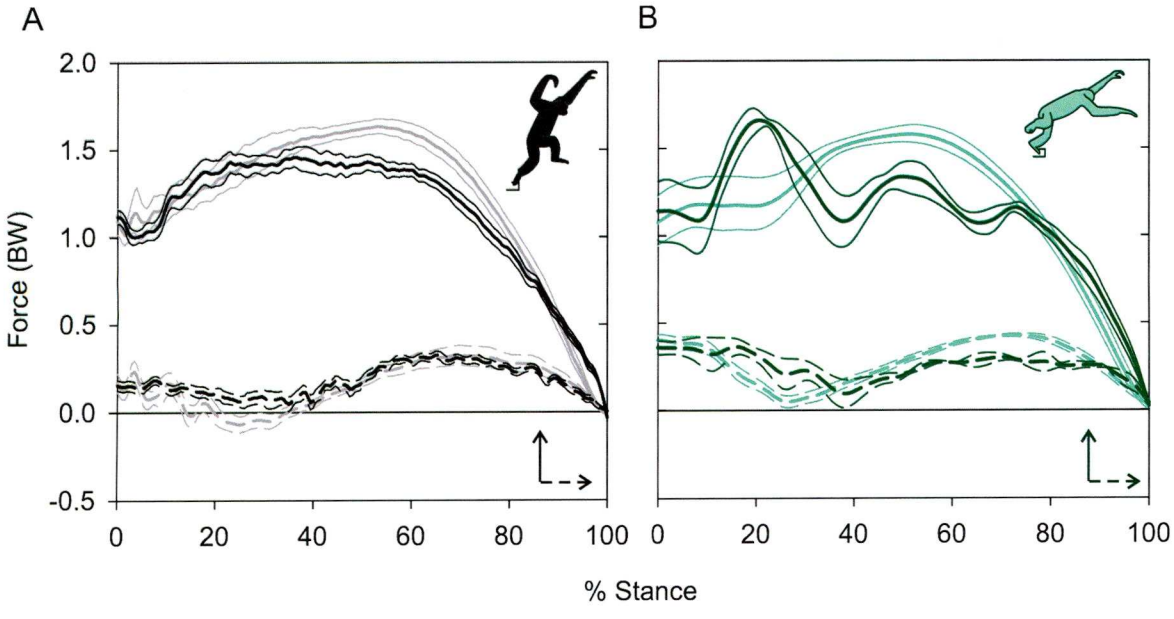

Figure 5.3. Ground reaction force traces normalised to body weight in the vertical (solid lines) and cranio-caudal (dashed lines) directions during stance phase. Thick lines show the mean, thin lines show standard error of the mean. Lighter colours (grey, pale green) show the stiff pole condition, Darker colours (black, dark green) show the compliant pole condition for **A**: Orthograde leaps and **B**: Pronograde leaps.

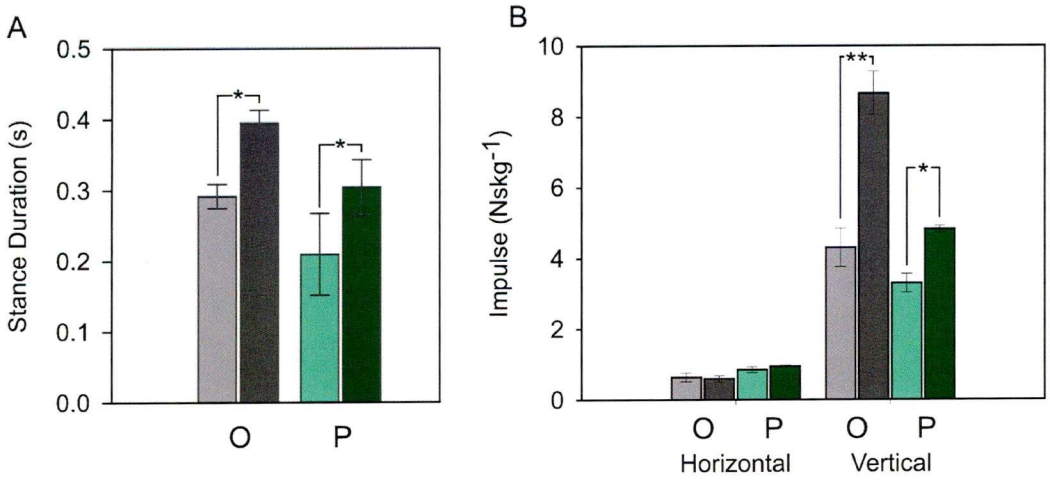

Figure 5.4A. Stance duration and **B**: Impulse (normalised to body weight) in the horizontal and vertical directions during stance phase for Orthograde (O) and Pronograde (P) leaps from the stiff (light colours, grey, light green) and compliant (dark colours, black and dark green) poles. * denotes significance at the $P < 0.05$ level, ** denotes $P < 0.01$, see text for statistical calculations.

Table 5.1. (Following page) Statistical comparisons of leap types on stiff and compliant substrates. P-value denotes the significance of a Kruskal-Wallis test between substrate types, where a value of 0.05 or less is deemed significant (significant differences are shown in bold).

		Figure	Orthograde Mean	Orthograde Std. Er.	Orthograde P-Value	Pronograde Mean	Pronograde Std. Er.	Pronograde P-Value
Peak Fx (body weight)	Stiff	5.3	0.41	0.04	0.71	0.48	0.02	0.21
	Compliant		0.39	0.02		0.41	0.04	
At % Stance	Stiff	5.3	39.39	11.20	0.39	46.50	14.21	0.82
	Compliant		59.92	5.96		31.00	24.08	
Peak Fz (body weight)	Stiff	5.3	1.76	0.07	0.30	1.65	0.06	0.57
	Compliant		1.69	0.05		1.71	0.02	
At % Stance	Stiff	5.3	45.22	6.00	**0.04**	45.07	4.81	0.09
	Compliant		36.31	2.75		22.33	2.35	
Stance duration (s)	Stiff	5.4A	0.29	0.02	**0.04**	0.21	0.02	**0.03**
	Compliant		0.39	0.06		0.30	0.02	
Horizontal Impulse ($Nskg^{-1}$)	Stiff	5.4B	0.64	0.12	0.97	0.85	0.09	0.57
	Compliant		0.59	0.09		0.94	0.03	
Vertical Impulse ($Nskg^{-1}$)	Stiff	5.4B	4.31	0.54	**0.00**	3.30	0.27	**0.02**
	Compliant		8.66	0.61		4.83	0.09	
orizontal centre of mass position at take-off (m)	Stiff	5.5	-0.81	0.05	**0.00**	-0.70	0.04	0.09
	Compliant		-0.38	0.07		0.55	0.09	
inetic energy at 0% stance (J/kg)	Stiff	5.6	2.21	0.27	**0.00**	3.51	0.26	0.14
	Compliant		0.80	0.15		2.63	0.49	
Kinetic energy at take-off (J/kg)	Stiff	5.6	3.66	0.20	**0.00**	4.11	0.21	0.43
	Compliant		1.76	0.24		3.63	0.52	
Potential energy at 0% stance (J/kg)	Stiff	5.6	5.32	0.08	**0.01**	4.97	0.22	0.31
	Compliant		4.10	0.33		5.47	0.31	
otential energy at take-off (J/kg)	Stiff	5.6	8.41	0.61	0.19	6.61	0.18	0.03
	Compliant		6.71	0.60		8.18	0.54	
Mechanical energy at 0% stance (J/kg)	Stiff	5.6	7.53	0.25	**0.00**	8.48	0.44	0.31
	Compliant		4.90	0.38		8.10	0.18	
Mechanical energy at take-off (J/kg)	Stiff	5.6	12.07	0.74	**0.01**	11.71	0.39	0.09
	Compliant		8.48	0.76		12.69	0.21	
Mass specific work (Jkg^{-1})	Stiff	5.7	3.66	0.60	0.84	2.63	0.25	**0.05**
	Compliant		3.74	0.46		3.74	0.16	
Mass specific power (Wkg^{-1})	Stiff	5.8	25.73	2.42	**0.04**	22.32	0.61	0.14
	Compliant		19.08	1.89		20.04	1.41	
At % Stance	Stiff	5.8	60.93	1.09	0.17	64.29	1.91	0.42
	Compliant		57.15	1.72		67.17	3.19	
Hip range of angles (°)	Stiff	5.9	97.46	2.65	**0.00**	80.39	3.32	0.31
	Compliant		135.44	5.13		72.97	3.71	
Knee range of angles (°)	Stiff	5.9	65.44	3.35	**0.03**	53.93	3.47	0.73
	Compliant		75.55	3.20		52.16	3.64	
Ankle range of angles (°)	Stiff	5.9	72.74	3.01	0.23	84.17	5.54	0.73
	Compliant		66.45	4.14		80.68	14.34	

shorter ($P < 0.0005$) for leaps from the compliant pole (0.38 ± 0.07 m) than from the stiff pole (0.81 ± 0.05 m), as take-off occurred nearer the tip of the compliant pole (Table 5.1, Fig. 5.5). Leaps from the compliant pole began more slowly (with less KE, which is proportional to v_R^2, $P < 0.0005$, Fig. 5.6, Table 5.1), with less potential energy ($P = 0.01$, Fig. 5.6) and less mechanical energy ($P < 0.0005$). The centre of mass trajectories (Fig. 5.5A) were qualitatively similar in shape during the stance period, although at take-off the gibbons appeared to reach with fore and hind limbs markedly during compliant pole leaps compared to stiff pole leaps (Fig. 5.5A). The stance phase from compliant pole leaps ended (at take-off) with lower velocity ($P < 0.0005$) and less mechanical energy ($P = 0.01$, Table 5.1, Fig. 5.6). Potential energy at take-off was not significantly different between substrate types ($P = 0.19$, Table 5.1). Mass-specific work done on the centre of mass during stance phase was similar between substrate types ($P = 0.84$, Fig. 5.7). Peak centre of mass power during stance, was not significantly different between leap types, and occurred at a similar point in stance (57 – 61% stance, $P = 0.17$, Fig. 5.8A, Table 5.1). The hip and knee joints underwent a wider angular excursion during the stance phase when leaping from the compliant pole (hip: $P < 0.0005$, knee: $P = 0.03$, Table 5.1, Fig. 5.9), while the ankle joint excursion was not significantly different between substrate type.

Pronograde Leaps: Stiff vs. Compliant pole

Peak vertical force was similar in magnitude but occurred at varying points of stance during leaps from the compliant pole (31 ± 24% stance, Table 5.1, Fig. 5.3B). The vertical ground reaction force component oscillated during the stance period with a noticeable peak early in stance (before 50%, Fig. 5.3B), when leaping from the compliant pole. By comparison the pronograde stiff-pole leaps had a more 'typical' single humped vertical ground reaction force profile. Peak horizontal forces were similar in magnitude and timing for both substrates. Leaps from the compliant pole used a longer stance duration ($P = 0.03$, Fig. 5.4A), and higher vertical impulse ($P = 0.02$, Fig. 5.4B), than leaps from the stiff pole. The centre of mass trajectories between substrate types when pronograde leaping appear qualitatively and statistically similar (Table 5.1, Fig. 5.5B), and in contrast to orthograde leaps, the posture of the gibbons was not noticeably different between substrates when leaping. There were no significant differences in potential, kinetic or mechanical energy of the centre of mass at the beginning or end of stance between substrates (Table 5.1, Fig. 5.6), yet mass-specific work done on the centre of mass was significantly greater when leaping

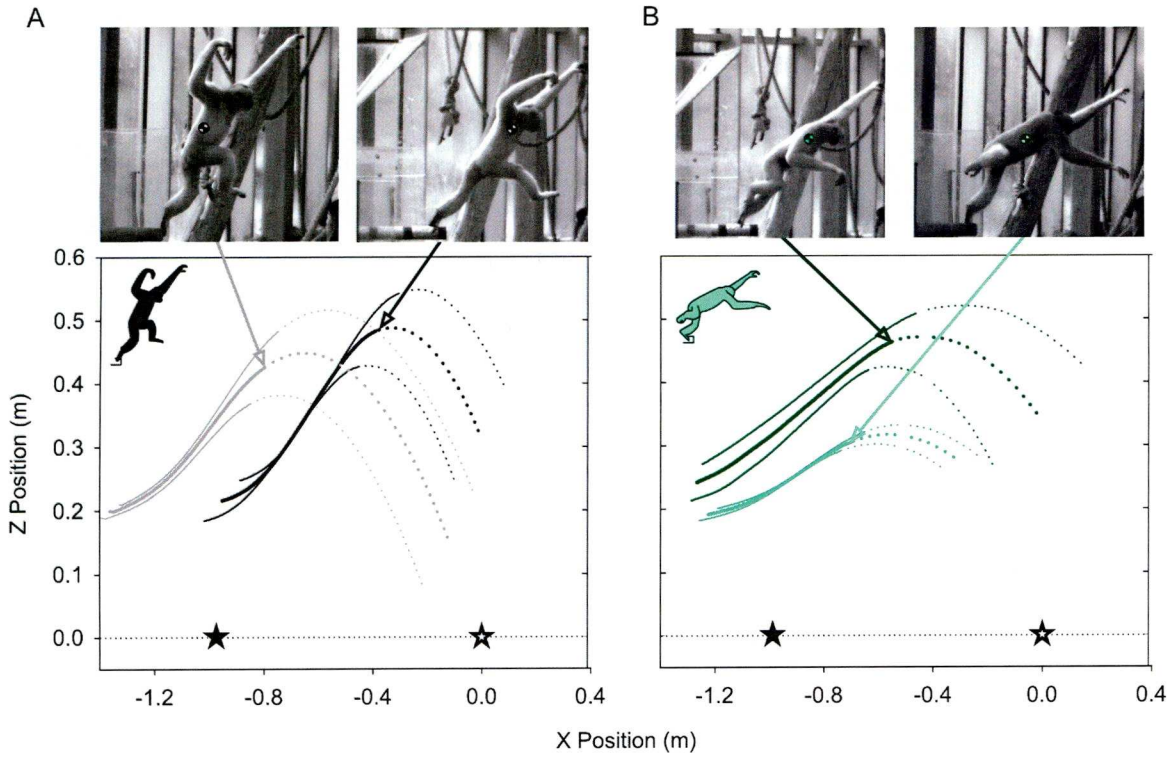

Figure 5.5. Centre of mass position during orthograde (**A**) and pronograde (**B**) leaps from the stiff (light colours, grey, light green) and compliant (dark colours, black and dark green) poles. Thick lines show the mean, thin lines show standard error of the mean. Solid lines indicate stance phase, dotted lines show centre of mass position after take-off. Images show body posture at take-off. Closed stars show the position of the take-off pole, open stars show the position of the landing pole. Centre of mass position was normalised to the position of the landing pole.

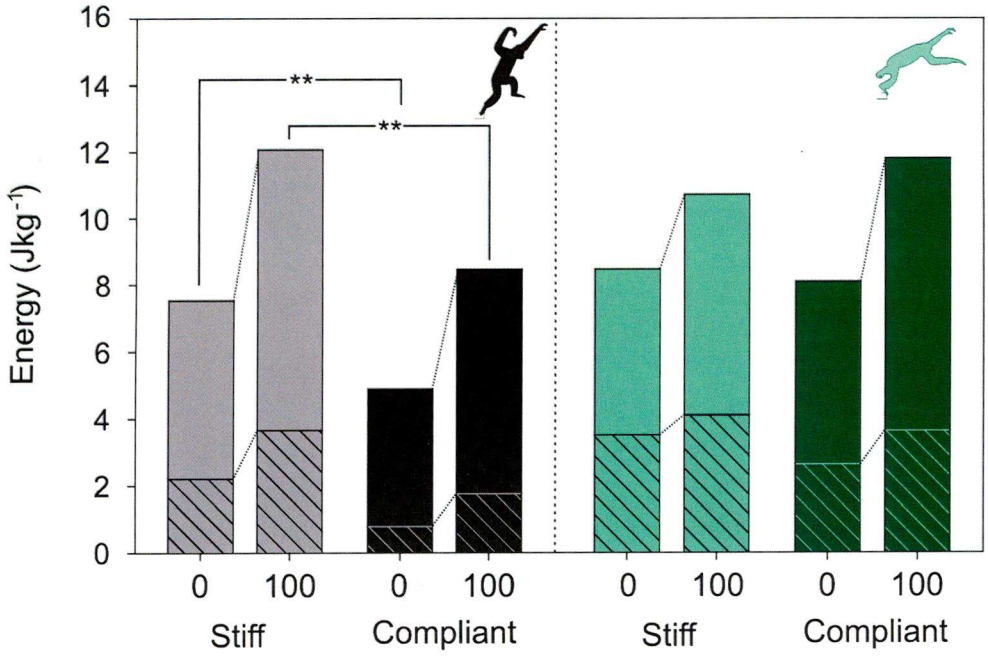

Figure 5.6. Potential (plain solid bars) and kinetic (striped bars) energy of the centre of mass normalised to body mass during orthograde (left) and pronograde (right) leaps from the stiff (light colours, grey, light green) and compliant (dark colours, black and dark green) poles. Numbers show % stance phase, 0 denotes the start of stance and 100 denotes take-off. The total bar height represents the mechanical energy of the centre of mass. ** denotes differences in mechanical energy at the $P < 0.01$ significance level, see text for statistical calculations.

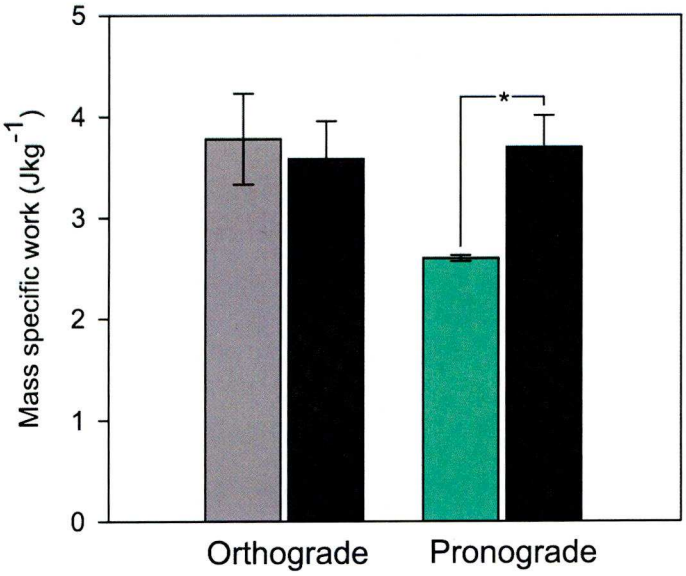

Figure 5.7. Mass-specific mechanical work done on the centre of mass during orthograde and pronograde leaps from the stiff (light colours, grey, light green) and compliant (dark colours, black and dark green) poles. * denotes differences in mechanical work at the $P < 0.05$ significance level, see text for statistical calculations.

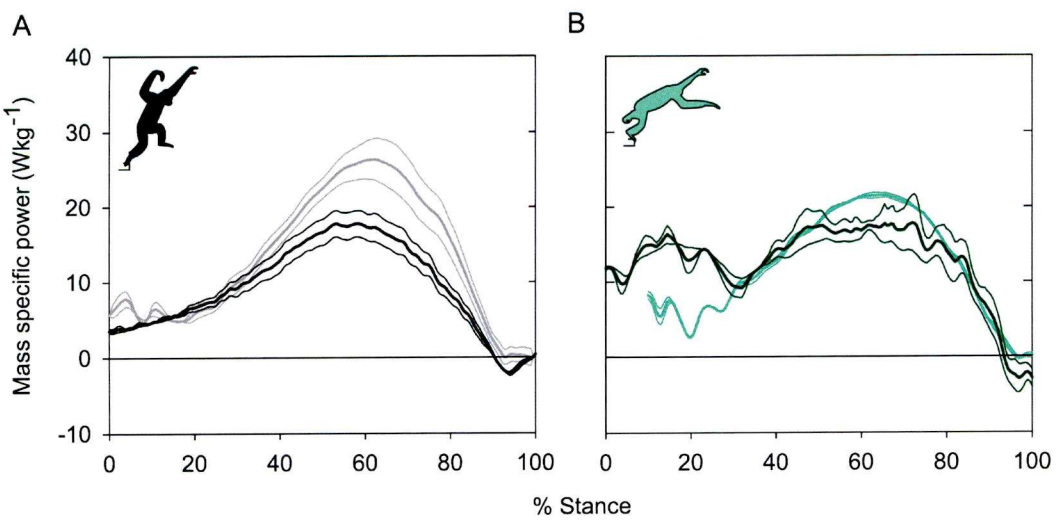

Figure 5.8. Mass-specific centre of mass power during stance phase for orthograde (**A**) and pronograde (**B**) leaps from the stiff (light colours, grey, light green) and compliant (dark colours, black and dark green) poles. Thick lines show the mean, thin lines show standard error of the mean.

from the compliant pole than from the stiff pole (P = 0.05, Table 5.1, Fig. 5.7). Neither, peak centre of mass power magnitude or timing were significantly different between substrate types, but there was an additional power 'peak' at the beginning of stance (~20%, Fig. 5.8B) when leaping from the compliant pole, that was not observed during stiff pole leaps. Hind limb joint angular excursions were (statistically) similar between substrate types (Table 5.1, Fig. 5.9), during pronograde leaps.

Peak force occurred earlier in stance during pronograde leaps, and so the pole was stiffer at the moment of peak force application during pronograde leaps than during orthograde leaps (P = 0.04, Fig. 5.10, Table 5.2, see materials and methods).

Discussion

Leaps from compliant vs. stiff substrates

The gibbons increased the vertical impulse, without increasing peak force, during both leap types when leaping from the compliant pole. This is advantageous since it minimises pole deflection (which is proportional to instantaneous force) and the associated loss in potential energy of the centre of mass. The minimisation of pole deflection in leaping is reflected by the leap types utilised when taking off from a compliant pole. A previous study (Channon et al. In press) showed that gibbons use at least four leap types, of which two were never used on the compliant pole (i.e. orthograde two-footed and squat leaps). These two leap types exhibit higher peak centre of mass powers than the leap types shown here, which points to a preference for low power (and indirectly, force) leap types to minimise the deflection of the substrate. The mechanisms used by the gibbons to maximise impulse without increasing peak force differed between leap types.

The approach taken during orthograde leaps was to leap more slowly, using a (significantly) longer stance time and slower take-off velocity. Pole deflection toward the end of stance during orthograde leaps (Fig. 5.9A) was compensated for by using a more extended hip joint (Fig. 5.9), increasing leg length and minimising potential energy loss by deflection of the pole. Lowering the centre of mass (PE is effectively a measure of centre of mass height, Fig. 5.6) at the beginning of stance was facilitated by increased hip flexion. Flexed hips allow a more 'compliant' gait leading up to the leap, aiding stability and yielding a flatter ground reaction force curve, a mechanism employed by many arboreal primate species (Schmitt, 1994, 1999, 2003, Crompton et al., 1998).

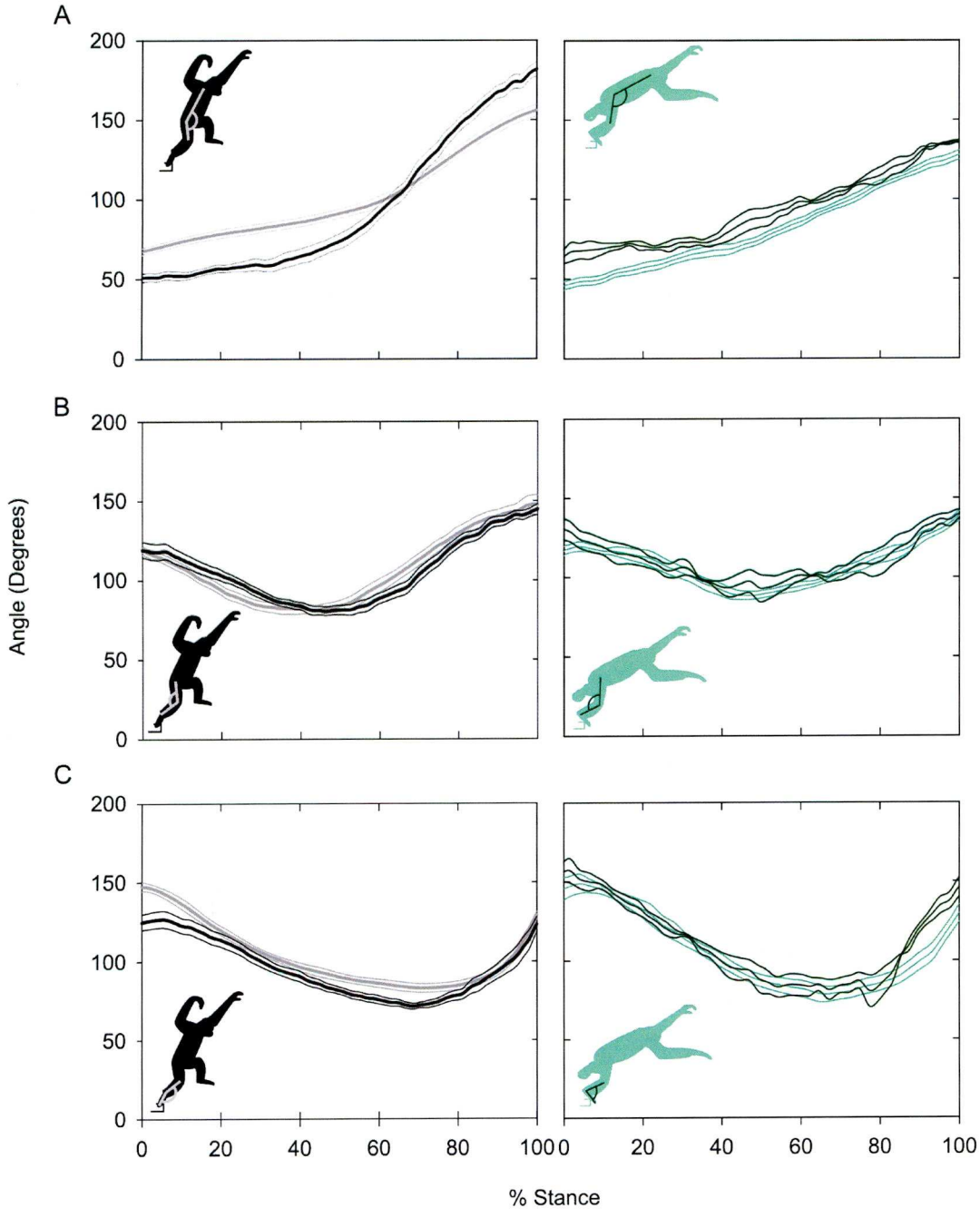

Figure 5.9. Hind limb joint angles during stance at the hip (**A**), knee (**B**) and ankle (**C**), for orthograde (left) and pronograde (right) leaps from the stiff (light colours, grey, light green) and compliant (dark colours, black and dark green) poles. Thick lines show the mean, thin lines show standard error of the mean. Angle definitions are described further in the text.

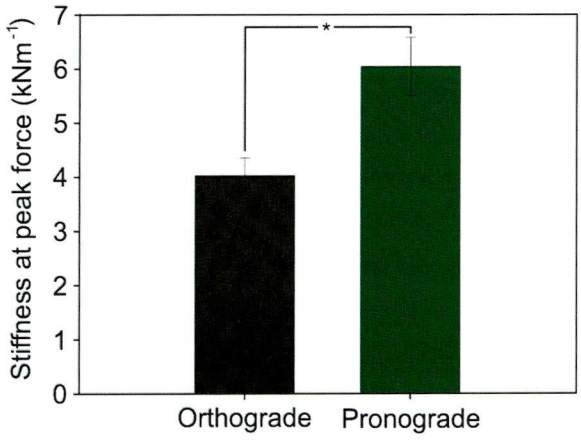

Figure 5.10. The instantaneous pole stiffness at the moment of peak force for orthograde and pronograde leaps. * denotes differences at the $P < 0.05$ significance level, see text for statistical calculations.

Table 5.2. Pole stiffness at the moment of peak force application for each leap type. P-value denotes the significance of a Kruskal-Wallis test between leap types, where a value of 0.05 or less is deemed significant (significant differences are shown in bold).

	Figure	Orthograde		Pronograde		P-Value
		Mean	Std. Er.	Mean	Std. Er.	
Pole stiffness at peak force (Nmm^{-1})	5.10	4.02	0.332	6.04	0.54	**0.03**

A more flexed hip joint also increases the effective amount of leg extension available before take-off, increasing effective leg length during the push-off phase (see above). Like other leapers, gibbons have relatively long hind limbs compared to trunk length (Schultz, 1936; Alexander, 1985; Isler et al., 2006, although the long forelimbs disguise this in some traditional indices such as the intermembral index), which helps to compensate for the downward movement of the pole by allowing force production over a longer time period (Preuschoft et al., 1996), increasing impulse without increasing peak force. A downside of this tactic is that the extra impulse gained compared to stiff pole leaps (Fig. 5.4b) is used deflecting the compliant pole, and not used to accelerate the centre of mass (Figs. 5.5, 5.6, 5.7). The increased hip joint excursion also allows the gibbon to effectively reduce the leap distance by maintaining pole contact until the centre of mass is further toward the landing pole (Fig. 5.5) than when leaping from the stiff pole. This is likely a necessity for safely completing the leap given the reduced amount of kinetic energy available at take-off.

While pronograde leaps used significantly longer stance times when leaping from the compliant pole than from the stiff pole, the kinetic energy of the centre of mass was similar between substrates: i.e. the gibbons did not leap more slowly. The power peak early in stance (~20% stance), accelerated the centre of mass (the peak coincides with peak force, Fig. 5.3), while it was positioned over a relatively stiff (compared to the orthograde leaps) part of the pole. Powering the leap from a stiffer region of the pole, compared to orthograde leaps, minimises vertical deflection, and hence, potential energy loss i.e. the extra power, compared to stiff pole leaps, is converted into centre-of-mass work (see Fig. 5.7) and not spent deflecting the pole, as is the case during orthograde compliant pole leaps, resulting in a net gain in work.

I believe that this preference for powering the leap from a stiffer section of the pole, as well as actively avoiding leap types with higher centre of mass powers, demonstrates a strategy to optimize leaping performance. During data collection the female gibbon changed her leap type from always conducting orthograde leaps to always conducting rapid pronograde leaps, suggesting some conscious learning while using the pole, and a preference for the stiffer section (closer to the pivot) of the pole from which to power the leap.

Using elastic energy storage in substrates

The pole used here was very lightweight, and possessed little rotational inertia and had a high unloaded natural frequency (~30 Hz). These characteristics are more comparable to a springboard that a gymnast might use to vault from, than to a cantilever diving board that a diver might use. This distinction is important because reports of 'branch pumping' of wild gibbons to store energy in the branch before leaping (Fleagle, 1976) are more like the latter, diving board-type, substrate. In this hypothesized scenario, the substrate is massive in comparison to the gibbon and oscillates slowly; as the gibbon pumps the branch it stores increasing amounts of energy in it, which can be used at take-off to propel itself during the leap. This allows the energy from a number of 'pumps' to be released quickly during one leg extension, and so increases power (acting as a power amplifier, Cheng and Hubbard, 2004). This technique is reliant on the substrate having more momentum, and hence larger mass (since, momentum = mass*velocity, and the gibbon is travelling at the same velocity as the branch before push-off) than the accelerating gibbon during leg extension. Without this prerequisite the substrate is deflected away from the gibbon, and potential energy is lost (Alexander, 1991). Conversely, when a gymnast steps on a spring board (which is much less massive than the gymnast) after a run up, the kinetic and potential energy of the falling centre of mass is stored as elastic energy in the springs, and returned when the gymnast undergoes leg extension, in a much more rapid (single) oscillation. This technique relies on the board being able to compress and extend rapidly during the stance phase of the gymnast, requiring little inertia and hence, mass (see, Prassas et al., 2006 for review).

The gibbons in this study did not sit on the pole and propagate its motion before leaping, despite being capable of sitting comfortably on the end of the pole (indicating that the stability of the pole did not prohibit this behaviour). Squat leaps have a stationary start and so seem the most likely leap type to exhibit 'branch pumping' behaviour, yet squat leaps from the compliant pole were not observed in this study. Future field studies should investigate if squat leaping and branch pumping do specifically occur on substrates with a higher rotational inertia and a lower oscillation frequency.

The increased vertical impulse, which is not converted to centre of mass work, the requirement of a wider range of hip joint angles, and the slow take-off speed of the recorded gibbon leaps makes the efficient use of the pole as a gymnastic-style springboard seem unlikely during orthograde leaps. The more rapid pronograde leaps, however, do convert additional impulse into increased mechanical work. Yet, if the gibbons were using the pole like a gymnastic springboard I would expect to see the centre of mass decrease in height (lose gravitational-potential energy) through

the first part of stance as the pole was displaced downwards, storing potential energy in the springs before rising upward until take-off (where the springs return the stored energy as kinetic energy (Kooi and Kuipers, 1994). The centre of mass of the gibbons during pronograde leaping increased in height throughout the stance phase (Fig. 5.5), ruling out the use of the pole in this manner. Further, there was no increase in kinetic energy at take-off, a major leap performance determinant (Crompton et al., 1993) when leaping from a compliant pole, which makes it improbable that the compliant pole increases leap performance by the storage and recovery of elastic energy either via a branch pumping method or by using the pole as a rapidly recoiling springboard.

While this study indicates that the gibbons did not use the substrate compliance as power amplifier, it is the first biomechanical study to highlight the ability of non-human apes to actively modify leaping biomechanics advantageously when using a compliant vs. stiff substrate. Further, my findings highlight peak force (and hence, pole deflection) minimisation during leaping as a desideratum in both the leap types used, with differing techniques employed for each leap type to achieve this.

Wild animals using compliant substrates

As mentioned above, the useful storage of elastic energy in the natural habitat of wild animals during powerful movements is yet to be demonstrated biomechanically. For leaping animals the ideal substrate to utilise such a mechanism would be either: highly compliant, with a low natural frequency, and high inertia and hence, mass (similar to a cantilever diving board) or relatively stiff, with a high natural frequency, and low inertia (like a gymnastic spring board). Yet, tree branches that are highly compliant are generally very thin, and hence lightweight (McMahon and Kronauer, 1976), and so likely provide insufficient momentum against the push off of a large leaper to be useful. Conversely, branches with a high natural frequency are likely too stiff to deflect sufficiently to facilitate useful energy storage. Further, the frictional damping effects of foliage on branch resonance are probably more significant during rapid movements than during the slow branch sway of orang-utans (McMahon and Kronauer, 1976; Thorpe et al., 2007a), slowing branch sway and wasting energy. Like the pole used here, tree branches get progressively less stiff with distance from the trunk (even more so in the wild as diameter decreases towards the tip, which was not the case in my experiment), and so there is a possible optimum distance from

the trunk from which to execute the leap. Field data from leaping gibbons and langurs suggest that most leaps are conducted tree to tree from the terminal branches and twigs of less than 2 cm diameter (Fleagle, 1976; Gittins, 1983; Sati and Alfred, 2002; Huang and Li, 2005), indicating that such optima are not utilised. This is likely because the energy required to leap the increased distance from the optimum position to the target is greater than the energy required to negate the deflection at the branch terminus. Alternatively there may be trade-off between leap cost and safety, where terminal branch leaps allow a better perception of leap distance and potential hazards (predators, obstructions etc.) Unfortunately, such data are currently unavailable. The problem is likely exacerbated for vertical clingers and leapers (Kinzey et al., 1975; Demes et al., 1995), where the stiffest part of the substrate is nearest the ground, reducing the energetic benefits of leaping (Sellers, 1992) and almost certainly increasing predation risk (orang-utans likely utilise canopy level crossings to reduce predation risk: from tigers in Sumatra and clouded leopards in Borneo, Thorpe et al., 2007a). However, vertical leaping ensures that a large proportion of the take-off force is directed down the long (compression) axis of the tree trunk, a property hypothesised to explain the substrate orientation selection of tarsiers (Crompton et al. In press).

The selection of larger-diameter obliquely-angled take-off substrates that minimise forces orthogonal to the branch (and hence branch deflection) by tarsiers (*Tarsius bancanus*) indicates avoidance of the undesirable perturbing properties of compliant branches, rather than an attempt at utilising them for energetic gain (Crompton et al. In press). The gibbons in this study could not avoid the compliant pole, or choose a less compliant alternative. They did, however, modulate the timing of their force production during pronograde leaps to coincide with the centre of mass being positioned over a stiffer region of the pole, again suggesting an active avoidance of the perturbing properties of the pole, rather than using the pole for energetic gain. Together, the two studies suggest that haplorrhine primates at least are capable of selecting substrates for leaping according to their gross mechanical properties. However, demonstrating that active selection is taking place is not trivial under field conditions, as substrate availability and stratum choice must also be factored-in.

The approaches used by the gibbons to minimise pole deflection in this study are theoretically available to all leapers. The method utilised when leaping with orthograde posture (wider hip excursion, minimising leap distance and peak force) is likely most useful for short leaps. My gibbons reduced the effective leap distance from 0.81 m to 0.38 m during orthograde leaping from the compliant pole versus the stiff pole. In this case that represents a 43% reduction in leap

distance, whereas if the leap was 4 m (mean wild-siamang leap distance, Fleagle, 1976) instead of the 1 m used here the leap would be reduced by ~12% ([3.38/3.83]*100). However, even this reduction could be considered significant when a fall could result in serious injury or death (Schultz, 1956; Bramblett, 1967; Buikstra, 1975; Lovell, 1978). Similarly, this technique is likely most effective for larger leapers, with longer legs to further displace the centre of mass horizontally before a leap.

The extra 'power peak' early in stance during the leaps observed here, could easily be replicated by wild animals moving on compliant branches. A notable limitation of my setup was that the gibbons did not have sufficient distance to 'run up' to the leap. Wild animals could run along the stiffer regions of branches for several metres before take-off, adding substantial mechanical energy to the centre of mass, while minimising branch deflection.

A further likely method by which arboreal animals minimise branch deflection is by sacrificing potential energy during the leap. My setup was built to study horizontal leaps without loss of height, but field studies of wild gibbons (Fleagle, 1976; Gittins, 1983) and observations of free ranging captive gibbons (AJC, personal observation, Planckendael Wild Animal Park, Belgium, Chester Zoo, UK and Twycross Zoo, UK) indicate that gibbons often simply run off the end of branches or "...[launch themselves] by pulling with the arms." (Gittins, 1983) and "...leaps are always from a higher to a lower level...Although leaps may extend over, 20m vertically, they rarely cover as far as 10m horizontally" (Fleagle, 1976). These leaps likely have comparatively low vertical acceleration (Crompton et al., 1993) and hence, branch displacement, yet still reach the lower positioned landing target. This hypothesis is supported by field data suggesting that in gibbons, leaping is mainly used to rapidly cross gaps in the forest canopy, while height gains are achieved by climbing (Gittins, 1983).

Future Work

My understanding of the role and utilisation of substrate compliance of wild animals is limited by quantitative field data. While previous field studies (Fleagle, 1976; Gittins, 1983; Günther et al., 1991; Demes et al., 1995; Crompton et al. In press) have greatly enhanced my understanding of the types and frequency of locomotion utilised by arboreal leapers, detailed biomechanical data (centre of mass movements, joint kinematics etc.) are still largely lacking. Knowledge of branch

thickness, animal mass, and distance along the branches that leaps take place greatly aid my estimations of the likelihood of useful energy storage in compliant branches.

Zoo based studies on captive animals allow a more precise quantification of biomechanical variables but space and performance are limited. Arboreal leapers are often capable of leaping many metres and creating a captive (safe) environment in which they can do so is constrained by space and safety in wild animal parks and zoos. Further, eliciting maximal leap performance in captive animals is extremely difficult as direct interaction with the animals is limited if not forbidden completely. The attainment of maximal performance leaps is a significant difficulty for the investigation of compliant substrate use, since it is intuitively more likely that such mechanisms are utilised during longer, more challenging leaps if, indeed, a performance advantage is conferred (e.g. during chasing away rivals or escaping from predators). Technological advances in wireless accelerometry and field video techniques (Sellers and Crompton, 2004; Thorpe et al., 2007a; Byrnes et al., 2008; Pfau et al., 2008, 2009) allow accurate biomechanical measurements to be taken in the wild by free ranging animals, and have a high potential to yield novel and interesting data of maximally performed leaps. Such high-cost leaps are particularly likely to be associated with high rewards: avoidance of predators or access to highly valued resources (e.g. food, mates).

The low mass and inertia of the pole used in this study allowed a simple mass-less model to be employed during the analyses. These properties however, ensured a high resonant frequency and so ruled out 'branch pumping' behaviour by the gibbons. Future studies utilising a range of pole stiffnesses and inertias would shed valuable light on the mechanisms of coping with and utilising substrate compliance in leaping animals.

With reference to muscle mechanics, dealing with compliant substrates is a complex motor task, requiring careful coordination of the neuromuscular system (Cheng and Hubbard, 2004). Human-hopping studies highlight a change in approach with increasing surface compliance (Moritz and Farley, 2005), while Daley and colleagues (2006) used electromyography and tendon strain buckles to demonstrate that perturbations are dealt with passively in running guinea fowl. Such invasive techniques can however not be used on lesser apes (due to ethical considerations including but not limited to conservation, IUCN, 2008). Muscle mechanics studies are thus limited to cadaveric dissections and musculoskeletal models (Channon et al., 2009, 2010).

Small sample numbers are further constraints on working with endangered species, yet, while this limits the statistical power of some analyses, I would like to point out that such rare biomechanical data are equally particularly very valuable as they provide the first quantitative insights into leaping biomechanics and substrate interaction mechanics of lesser apes to date. Leap biomechanics are also likely to be affected significantly by leap distance and orientation (i.e. leaping up or down), as well as by different substrate stiffnesses (gibbons; Fleagle, 1976; Gittins, 1982; other taxa: Alexander, 1991; Cheng and Hubbard, 2004; Demes et al., 1995, Crompton and Sellers, 2007). Given the complex three-dimensional environment that gibbons inhabit, all of these factors are likely to be relevant to the biomechanics and ecology of gibbons and other arboreal leapers. Therefore the foci of future work should be on the attaining data on the relationship between leaping behaviour and substrate use of free-ranging gibbons in their natural environment, and in particular the properties of the leaping substrates used (orientation, diameter, length etc.) and captive- based studies varying the stiffness and inertial properties of the leaping pole better to investigate the limiting properties of branches as useful elastic energy stores.

Conclusions

My data indicate that the gibbons in this study neutralised substrate deflection rather than utilising its energy storage capability. The gibbons employed different techniques to minimise substrate deflection depending on leap type and approach speed. Orthograde leaps used a wider hip joint excursion to compensate for the deflection of the pole and increased the effective leg length over which force could be exerted. The increased hip joint motion also reduced the effective distance of the leap, allowing a longer stance time and slower take-off velocity to be used. More rapid pronograde leaps produced power earlier in stance than during orthograde compliant pole leaps, when the pole is effectively stiffer, minimising deflection and potential energy loss. The gibbons also avoided more powerful orthograde two-footed and orthograde squat leaps, perhaps to minimise pole deflection. Future work investigating maximal leap biomechanics and a wide range of pole stiffnesses would yield further understanding of leap biomechanics and the role of substrate compliance in an arboreal environment.

List of Abbreviations

α – Forceplate specific constant, 0.478

CoP_X – Craniocaudal position of the centre of pressure

F_X – Craniocaudal force

F_Y – Mediolateral force

F_Z – Vertical force

g – Gravitational acceleration ($-9.81 ms^{-2}$)

h – Vertical height of the centre of mass

k – Stiffness

KE – Kinetic energy of the centre of mass

m – Mass

ME – Mechanical energy of the centre of mass

M_X – Craniocaudal moment

M_Y – Mediolateral moment

M_Z – Vertical moment

PE – Potential energy of the centre of mass

S_{DIS} – Vertical displacement of the spring

S_X – Distance between the spring and the pivot point

T_{DIS} – Displacement at the pole tip

T_X – Distance between the pole tip and the pivot (pole length)

v_R – Resultant velocity

Chapter 6: Biomechanical analyses of maximally performed gibbon leaps: Results from a field-employable centroid resolution technique.

By Anthony J. Channon

With contributions from Robin H. Crompton, Michael M. Günther and Evie E. Vereecke.

I designed the experiment and analysis technique, collected and analysed the data and wrote the manuscript. Robin Crompton, Michael Günther and Evie Vereecke edited the manuscript and provided funding for travel.

Abstract

Recording biomechanical performance data on wild or free ranging animals is notoriously difficult and laboratory based studies often struggle to elicit maximal performance. Advances in global positioning and accelerometry technology have yielded valuable insight into the biomechanics and behaviour of several free-ranging and wild species. Yet these techniques still require some interference with the animal, both initially (attaching the unit to the animal) and during the investigated behaviours (i.e. they may affect performance or behaviour). Here I present a video based technique for finding the centre of mass of an animal (in this case gibbons) which is low cost, easy to perform and can be used in the field. This centroid resolution methodology is used to investigate the biomechanics of maximally leaping free-ranging white-handed gibbons in a wild animal park. The technique is proven robust by validating my findings against forceplate data and performing a sensitivity analysis. My data show that the gibbons do not utilise theoretically optimal take-off angles, and suggest that muscle power is unlikely to constrain the leap performance to an overall 'downward' trajectory. Arm-swing countermovement and elastic energy recovery are shown to contribute significantly to powering the leap and the gibbons oriented the trunk to best align it with the compression axis of the take-off substrate, minimising deflection. The non-invasive technique described in this study is a valuable method for collecting

maximal performance field data on species for which accelerometer based techniques are not appropriate.

Introduction

The challenge of recording detailed biomechanical data from free ranging or wild animals is well known. The recent introduction of mobile accelerometry has allowed the collection of data previously unavailable to laboratory based studies (Sellers and Crompton, 2004; Byrnes et al., 2008; Pfau et al., 2008, 2009; Green et al., 2009; Preece et al., 2009; Nagy et al., 2010). In accelerometry-based studies, the accelerometer and mobile data logger or telemetry transmitter are placed as close as possible on an approximation of the animals' centre of mass, accelerations recorded ad libitum, and later associated with activity based on signal characteristics during simultaneously recorded behaviours. Such investigations have added substantial understanding to the biomechanics of free ranging animals and can allow the automated monitoring of animal behaviours. Data collected from free ranging animals often represents performance that is nearer maximal than equivalent studies in a laboratory setting, probably due to space constraints, structural environmental impoverishment (Crompton et al., 1993) or because the animal behaves differently when removed from its natural environment because of reasons such as differences in resource and risk distribution (Britt, 1996). For example, Williams et al. (2009a, b) found that free ranging greyhounds accelerated more than twice as quickly as those in a laboratory study ($10ms^{-2}$ vs. $4.5ms^{-2}$). Using accelerometry to approximate the movements of the centre of mass is, however, not without difficulty. Identifying the centre of mass can be difficult and movements of the limbs may move the centre of mass (to a greater or lesser extent according to the animal's mass distribution) with no change in the accelerometer position, especially when the trunk is elongated. For smaller animals the weight of the accelerometry apparatus, usually comprised mostly of the weight of the battery which powers it, may also affect the animals' locomotor behaviour, e.g. pigeons carrying an accelerometry backpack were unable to execute slow flight due to the increase in effective body mass relative to wing area (AJC, pers. obs.).

Video analyses predate accelerometry based studies by perhaps a century (Muybridge, 1887; Marey, 1894) and represent a potential alternative (or partner) to accelerometry studies (Pelletier et al., 2007; Usherwood, 2008). Attainment of the centre of mass position by video may either be done by digitising a repeatable point on the animal (e.g. a conspicuous mark, or eye) or by

digitising joint centres and resolving moments based on the segments inertial properties. The former (as used in Essner, 2002; Thorpe et al., 2007a; Usherwood, 2008; Legreneur et al., 2010) assumes that the digitised point moves synchronously with the centre of mass (which does not account for limb movement) while the latter is probably more accurate (see, Jayes and Alexander, 1982; Gunther et al., 1991; Sellers and Crompton, 1994; Channon et al. In press), but requires detailed knowledge of both joint position and segmental inertial properties, which may not be available. Using digitised joint positions in combination with known inertial measurements is a common method to obtain centre of mass position attained from forceplate recordings during non-steady state locomotion (McGowan et al., 2005; Daley et al., 2006; Williams et al., 2009a; Channon et al. In press) and so video analyses remain an essential part of laboratory-based biomechanics studies. Video resolution and the animal's morphology can inhibit the accurate digitisation of the joint centres of free ranging or wild animals, where conspicuous or reflective markers (for automatic tracking video system) cannot be attached to the animal. This is particularly pertinent for rapid movements for which high-speed video cameras with high resolution are needed, which are expensive and require artificially high light levels, which may not be practical or may be too intrusive in a natural environment. Further, free ranging and wild observations are often out of plane with the camera (Thorpe et al., 2007a), making the calibration of distances and angles difficult. Here I present a video analysis technique to approximate centre of mass position from free ranging gibbons, which does not require individual joint digitisation or the assumption that a given point is rigidly coupled to the centre of mass and which could be applied to the analysis of a plethora of wild animal species using modestly priced apparatus. Their high forest canopy habitus, rapid movement, and unusual body plan make gibbons an ideal candidate for the evaluation of such a technique.

While renowned as specialist brachiators, wild gibbons undertake a range of locomotor modes (Fleagle, 1976; Gittins, 1983; Sati and Alfred, 2002; Vereecke et al., 2006a). Although the hind limbs have a demonstrable role in powering brachiation (Fleagle, 1974; Bertram et al., 1999; Young-Hui et al., 2000; Bertram and Chang, 2001; Usherwood and Bertram, 2003), they have also been shown to possess anatomical specialisations for hind limb supported locomotor modes such as leaping and bipedalism (Payne et al., 2006a; Vereecke et al., 2005; Channon et al., 2010). Several of these specialisations seem only useful for hind limb supported locomotion, i.e. the well developed Achilles and patellar tendons (Vereecke et al., 2005; Channon et al., 2009) and an energy-storing midtarsal break (Vereecke and Aerts, 2008; DeSilva, 2010).The hind limb muscle architecture of gibbons suggests a propensity for powerful hip and knee extension (Payne et al.,

2006a; Channon et al., 2009), which is likely to be associated with the impressive leaping performance observed in wild gibbons, which are reported to cross gaps of 10m or more (Fleagle, 1976; Gittins, 1983) by leaping.

The leaps of gibbons can be categorised into at least four biomechanically distinct leap 'types' based on the number of feet used during take-off and the orientation of the trunk. Channon et al. (In press) hypothesised that for less challenging leaps (shorter or with an easy to reach landing site), the gibbons use pronograde single-footed leaps, in which the kinetic energy of the gibbon prior to take-off powers the leap, requiring little additional power during the push-off stage. Conversely, more difficult leaps (e.g. longer distance or partially obscured landing site) are executed using more powerful squat leaps, where the stationary start could be advantageous for calculating the leap (and landing) thoroughly before take-off. This study was conducted in a zoo environment and only included short (~1 m) leaps. Biomechanical data of maximal leaps of gibbons thus, remain lacking. Field observations indicate that, 20-25% of all locomotor bouts of wild gibbons are leaps (Fleagle, 1976; Gittins, 1983; Sati and Alfred, 2002), and that many leaps are conducted from a higher to a lower level, usually (in 63% of cases; Gittins, 1983) from fine terminal branches, which deflect under the high forces associated with leaping. This deflection probably limits the horizontal distance of leaps, which are reportedly up to 10m in length (Gittins, 1983, mean distance leapt by siamang ~4m, Fleagle, 1976).

The take-off angle and velocity used during the leap are crucial determinants of leap distance (Crompton et al., 1993; Alexander, 1996; Jeffrey, 2005), a 45° take-off angle offering the furthest horizontal distance for a given take-off velocity, during an effectively flat leap (i.e. the take-off and landing sites are at the same level). Crompton et al. (1993) demonstrated that only the most specialised of leapers, *Galago moholi*, utilised this theoretical optimum at all leap distances, while the less specialised leapers used suboptimal (in terms of kinetic energy minimisation) take-off angles for sub-maximal leaps. Channon et al. (In press) found that gibbons also used suboptimal take-off angles for short leaps and the same is also demonstrable for squirrels (Essner, 2002) and mouse lemurs (*Microcebus murinus*, Legreneur et al., 2010). Crompton and Sellers (2007) hypothesised that low take-off angles might increase velocity and minimise flight time and so aid predator avoidance. Leaping is not a fast mode of locomotion in comparison to cursorial galloping: *G. moholi* achieves a take-off velocity of $5.1ms^{-1}$ (Günther et al., 1991), well below the $\sim 15ms^{-1}$ of a galloping quadruped (Hildebrand and Hurley, 1985), while non-specialised leapers use still lower take-off velocities (gibbon, 3.2 ms^{-1}, Channon et al. In press; squirrel, $2.6ms^{-1}$,

Essner, 2002; mouse lemur, 3.2ms^{-1}, Legreneur et al., 2010). By comparison, during cyclical ricochetal brachiation gibbons have been shown to attain velocities in excess o f 3 ms^{-1} (Bertram et al., 1999; Bertram and Chang, 2000). Thus, it is likely that leaping represents one of the most rapid modes of locomotion available to habitually arboreal animals, where the fragmented environment likely encourages (acyclical) powerful movements to cross large gaps rapidly (Gunther et al., 1991).

In acyclical arboreal locomotion, energy can not only be stored in the elastic elements of the locomotor system (during pre-stretch of muscles and tendons, via a countermovement or specialised anatomical apparatus) but also in the substrate. At take-off, this energy is released very rapidly (by the recoil of elastic structures and the substrate), amplifying muscle power output (Aerts, 1998). Such a power amplification mechanism as seen in bushbabies facilitates the production of much higher powers of the centre of mass than during cyclical locomotion (~800Wkg^{-1}, *G. moholi*, Aerts, 1998, vs. 65Wkg^{-1}, blue breasted quail, Askew and Marsh, 2001) where pre-stretch is impossible. Vertically leaping bonobos (*Pan paniscus*) have been shown capable of producing ~80Wkg^{-1} centre of mass power, with no body countermovement (and hence pre-stretch), perhaps demonstrating exceptional performance of primate skeletal muscle (Scholz et al., 2006). Gibbons produced 71Wkg^{-1} (using a countermovement) during short leaps (~1m, Channon et al. In press), but since these leaps were sub-maximal, it is expected that they are capable of producing much higher centre of mass powers. The arm-swing countermovement by gibbons is likely loads the hind limb musculature eliciting pre-stretch (Alexander, 1992), this is probably very effective given their large forelimbs and highly mobile shoulder joints (Jungers, 1988; Isler et al., 2006; Michilsens et al., 2009). The movement of the arms forwards also increases the velocity of the centre of mass, by translating it forward during the swing.

The objective of this study is to utilise a field friendly image analysis technique to quantify biomechanical parameters during maximally performed gibbon leaps. Using this technique it aims to test the hypotheses that 1) gibbons use suboptimal take-off angles, that do not minimise kinetic energy requirements, and 2) centre of mass power constrains the leap performance to requiring a net loss of height, despite the use of a countermovement.

Materials and Methods

Filming and measurements

A handheld video camera (Sony HDR-SR11E) mounted on a tripod (Manfrotto, Italy) was used to make high definition (HD, 1080 x, 1920 pixels, 25Hz) video recordings of two white-handed gibbons (*Hylobates lar,* one adult male, mass: 7.5 kg, 11 leaps; one juvenile female age: 7 years, mass: 5.5 kg, 11 leaps) as they leapt voluntarily within their outdoor enclosure at the Wild Animal Park Planckendael, Belgium. After filming, measurements were made of the enclosure (Fig. 6.1a) for calibration of the video images. Measurements were made using a laser measure (Bosch PLR-50, for distances <10 m) and a 50 m tape measure (for distances >10 m) and consisted of: the height of both vertical trunks (4.64 m and 6.70 m, Fig. 6.1a), the horizontal distance between the end of each of the take-off and landing branches (shown as 1-5, Fig. 6.1) and the vertical trunk they were attached to, and the distance between the two vertical trunks (indicated as d, on Fig. 6.1a). It was also noted whether each branch was orientated 'toward' or 'away' from the camera.

Post collection analysis

The video sequences were exported from the cameras and converted to uncompressed AVIs using Adobe Premier Elements (Adobe, CA, USA), before being de-interlaced (yielding 50 fields/s) and saved as bitmap image stacks using VirtualDub (www.virtualdub.org). Each field was imported chronologically into Inkscape (Free software foundation, MA, USA), where the Bezier tool was used to trace the outline of the gibbon in each field (examples of outlines shown in Fig. 6.2a). The filled outline was then exported as a binary image. A custom written LabVIEW (Version 8.5, National Instruments, TX, USA) program assigned coloured pixels a weight [m] of 1 and white pixels a weight of 0. The centroid of the resulting shape was found by resolving the moments of each pixel of the image in both horizontal (h) and vertical (v) directions. Thus, the centroid in an image with i rows and j columns has the coordinates (h_{CENT}, v_{CENT}, Fig. 6.2a) where:

$h_{CENT} = \Sigma(h_{ij} * m_{ij})/\Sigma m$ and $v_{CENT} = \Sigma(v_{ij} * m_{ij})/\Sigma m$

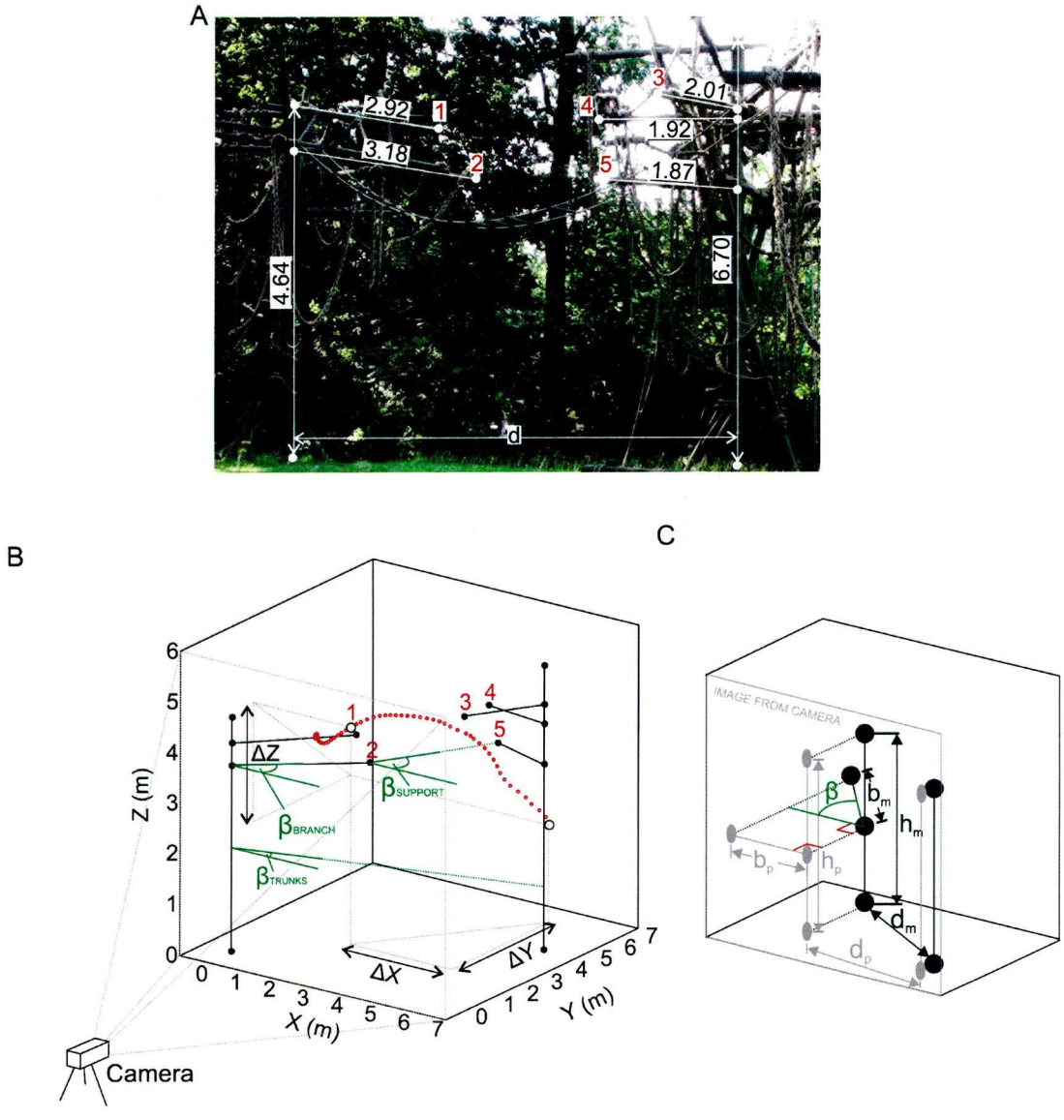

Figure 6.1A The enclosure where filming took place and the measurements required for the calibration were taken. Filled white circles show the measurement points. Black underlined text denotes measurements in metres, red text shows leap branch termini. **B**. The 3-D reconstruction of the enclosure after calibration. Black lines show the vertical trunks and horizontal branches, green angles are used in the calibration (see text for details), red open circles show the centroid position for a typical leap, open black circles show the take-off and landing position. Grey lines show the measurements used for the calculation of biomechanical parameters. d indicates the distance between the vertical trunks. The 'β' angles are referenced to the plane perpendicular to the camera (i.e. when the branch was perpendicular to the camera $\beta_{BRANCH} = 0°$), shown by the grey translucent box. **C**. derivation of the calibration coefficients used in the 3D reconstruction of the enclosure, see text for coefficient calculations. Angles shown in red are 90°.

Calibration of the enclosure

To calibrate the centroid's position in real space a 3-D calibration of the gibbon enclosure was created (Fig. 6.1b). To do this the top and bottom of each vertical trunk and the end (tip) of each branch were digitised from a single video frame. The digitised measurements (in pixels, hereafter designated by subscript 'p') of vertical trunk height (h_p, Fig. 6.1c), horizontal branch lengths (b_p, Fig. 6.1c) and the distance between the vertical trunks (d_p, Fig. 6.1c) were divided by their respective measured values (in metres, hereafter designated by subscript 'm', h_m, b_m, d_m, in Fig. 6.1c) to give a vertical calibration coefficient ($\underline{E}_{VERT}$), individual branch horizontal calibration coefficients (for each branch of interest, 1-5, Fig. 6.1a, $\underline{E}_{BRANCH}$) and an inter-vertical trunk distance coefficient ($\underline{E}_{TRUNKS}$) for the enclosure (hence the '$\underline{E}$' prefix). The horizontal branches were not all positioned orthogonally to the camera, with some of the branches orientated 'toward' the camera (in the Y direction of Fig. 6.1b, branches 3 and 4) and others pointing 'away from' the camera (branches 1 and 2). The angle of orientation in the (horizontal) XY-plane of the horizontal branches from the vertical trunks they were attached to (β_{BRANCH}) and the angle of the trunks from each other (β_{TRUNKS}) relative to a plane perpendicular to the camera (XZ-plane, shown in grey, Fig. 6.1b) was calculated using trigonometry:

$\underline{E}_{VERT}$ (pixels m^{-1}) = h_p/h_m, $\underline{E}_{BRANCH} = b_p/b_m$, $\underline{E}_{TRUNKS} = d_p/d_m$

$\beta_{BRANCH} = Cos^{-1}(\underline{E}_{BRANCH}/\underline{E}_{VERT})$

$\beta_{TRUNKS} = Cos^{-1}(\underline{E}_{TRUNKS}/\underline{E}_{VERT})$

Calibrating each video sequence

Filming took place over several days and the camera was moved regularly, so it was necessary to calibrate each video individually. Because only a single camera was used to make recordings it was impossible to know to what extent the gibbon leapt 'towards' or 'away from' the camera (in the Y direction of Fig. 6.1b). For each video sequence the end of the take-off branch and the end of the nearest branch to the landing position was digitised. The vertical and horizontal distances (δ_p and η_p, respectively, in pixels) between them were divided by the actual distances (δ_m and η_m, calculated from the 3D reconstruction, in meters, Fig. 6.1b) to give the vertical ($\underline{V}_{VERT}$) and horizontal ($\underline{V}_{HORIZ}$) calibration coefficients specific to that video sequence (hence the '$\underline{V}$' prefix). The angle of orientation in the XY-plane between the take-off and landing supports ($\beta_{SUPPORT}$, Fig.

6.1b) relative to a plane perpendicular to the camera (XZ-plane, Fig. 6.1b) was calculated using trigonometry:

$\underline{V}_{VERT} = \delta_p/\delta_m$, $\underline{V}_{HORIZ} = \eta_p/\eta_m$

$\beta_{SUPPORT} = Cos^{-1}(\underline{V}_{HORIZ}/\underline{V}_{VERT})$

The centroid's position in 3-D can be resolved using the 2-D digitised Cartesian coordinates of the centroid (in pixels, h_{CENT}, v_{CENT}), the calibration coefficients specific to each video ($\underline{V}_{VERT}$ and $\underline{V}_{HORIZ}$) and the angle of orientation ($\beta_{SUPPORT}$) between the take-off and nearest landing support. The left-right (X, with reference to the camera, Fig. 6.1b), near-far (Y) and vertical (Z) coordinates of the centroid are:

$X = h_{CENT}*\underline{V}_{HORIZ}*Sin(\beta_{SUPPORT})$

$Y = h_{CENT}*\underline{V}_{HORIZ}*Cos(\beta_{SUPPORT})$

$Z = v_{CENT}*\underline{V}_{VERT}$

This approach assumes that each pixel is square and that the vertical trunks are perpendicular to the ground (i.e. to the X-Y plane, Fig. 6.1b).

Biomechanical Parameters

The centre of mass position was differentiated with respect to time (t) to give velocity and the resultant velocity V_R was found using Pythagoras (Fig. 6.1b):

$V_R = \sqrt{(\Delta X^2+\Delta Y^2+\Delta Z^2)} / \Delta t$

Mass specific kinetic (KE_M) and potential (PE_M) energies were calculated as:

$KE_M = 0.5*V_R^2$

$PE_M = g*Z$, where g is gravitational acceleration (9.81 ms^{-2}).

PE_M was normalised to take-off position (i.e. at take-off $PE_M = 0$).

The take-off angle (φ, Fig. 6.2b) and velocity (U) were calculated as the angle to the horizontal and magnitude of the velocity vector at take-off (following the labelling convention of Crompton

A

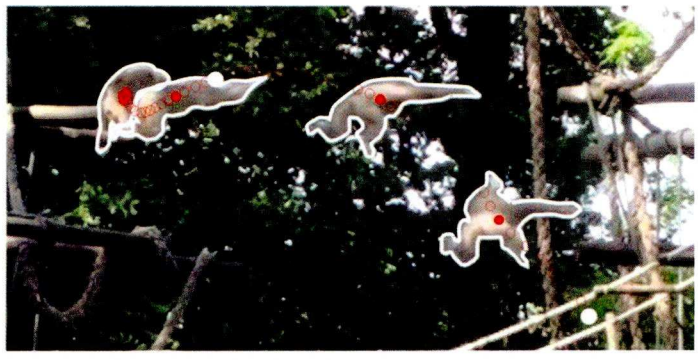

B

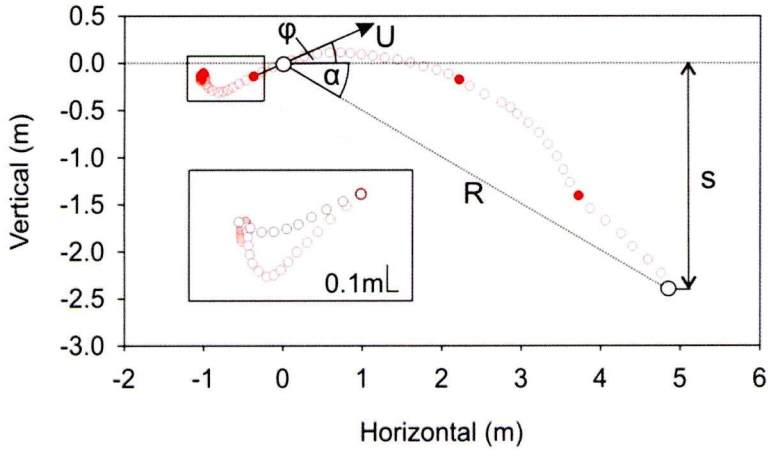

Figure 6.2A White outlines used to attain the centroid position. Open red circles show the centroid position throughout a typical leap, filled red circles show the centroid position for each white outline. Filled white circles show the position at take-off and landing. **B**. The calibrated position of the centroid and the parameters used in the calculation of theoretical kinetic energy requirements (see text for details). Circle representation as in A. Open box indicates preparatory countermovement. Inset, enlargement of boxed area showing counter movement during push-off of squat (red circles) and two-footed (black circles) leaps.

and Sellers, 2007). The leap angle (α) was calculated from the resultant leap distance (R) and the total height loss (S, Fig. 6.2b) between take-off and landing where:

$\alpha = Sin^{-1}(S/R)$

Theoretical estimations of the mass-specific kinetic energy required (KE_M) for three leap scenarios were analysed alongside the measured KE_M (see, Crompton and Sellers, 2007 and Table 1 for KE calculation):

1) $KE_{M\Phi}$, the observed leap distance (R), angle (α) and take-off angle (φ)

2) KE_{Mmin}, observed R and α, but a take-off angle (φ_{min}) which minimised KE_M

3) $KE_{M45°}$, a leap of the observed horizontal distance with no height loss (S = 0) at $\varphi = 45°$

The push-off time (t_{PUSH}) was defined as the period from the start of the final movement toward take-off until the feet left the substrate. The mass-specific energy cost of the leap (ε_M) was the summation of the kinetic energy at take-off (KE_M) and the potential energy loss ($PE_M = S*g$) during the leap:

$\varepsilon_M = KE_M + PE_M$, this approach assumes that KE_M is generated from standstill.

For the kinematic data, maximum instantaneous mass specific power (P_{Mpeak}) was calculated from the derivative of mechanical energy change of the centre of mass ($ME_M = KE_M + PE_M$) during the push-off:

$P_{Mpeak} = dME_M/dt$

Mean mass-specific power (P_{Mmean}) during the push-off was measured from the kinematics and calculated based on the theoretical estimations of KE_M divided by the push-off time:

$P_{Mmean} = KE_M/t_{PUSH}$

To investigate the effect of the forelimbs on leap performance, the contours of the forelimbs were manually 'removed' (blotted out) from the gibbon outline in one video sequence. This sequence was then analysed using the same centroid determination protocol as the other video sequences.

A Kolmogorov-Smirnoff test confirmed the data were normally distributed (P = 0.01). Least squares regressions were used to correlate the observed take off angle (φ) with the minimum

Table 6.1. Input parameters used when calculating kinetic energy requirements for the three theoretical leap scenarios and the measured kinetic energy used during the leap (see text for details and Fig. 6.2B for parameter definitions).

		Parameters				Abbreviations		
Scenario	Calculation	R	α	φ	h	Velocity	Mean power	Total Energy
KE_M	Meas.	Obs.	Obs.	Obs.	Obs.	U	P_{Mmean}	E_M
$KE_{M\Phi}$	Theor.	Obs.	Obs.	Obs.	Obs.	U_Φ	$P_{Mmean\Phi}$	$E_{M\Phi}$
KE_{Mmin}	Theor.	Obs.	Obs.	Minimum KE	Obs.	U_{min}	$P_{Mmean\text{-}min}$	E_{Mmin}
$KE_{45°}$	Theor.	Obs.	0	45°	0	$U_{45°}$	$P_{Mmean\text{-}45°}$	$E_{M45°}$

velocity take-off angle (φ_{min}, which minimised KE_M) and the observed take-off velocity with the theoretically required take-off velocity. Data from a previous study (Channon et al. In press) were included in the take-off angle analyses to represent 'flat' leaps ($\alpha = 0°$).

ANOVAs were used to distinguish between the means of biomechanical variables and a Tukey's-HSD post-hoc analysis was used to distinguish between W_M and P_M for the theoretical scenarios, and identify homogenous subsets within the data. All statistical analyses were conducted in SPSS (version 17, Systat software, Germany), defining significance as $P < 0.05$.

Technique validation and sensitivity analysis

In order to assess the ability of the technique to correctly identify the centre of mass of the animal, a high-speed video recording of a gibbon leaping from a stiff instrumented pole (see Channon et al. In press for experimental setup) was analysed using the outline based centroid resolution technique. The centre of mass position from the outline based technique was compared to the instrumented pole based approach using a least squares linear regression (SPSS 17, Systat). The regression was highly significant ($P < 0.0005$) and the gradient was close to 1 (0.88, Fig. 6.3), a repeatability score (calculated as the intra-class correlation coefficient, Lessells and Boag, 1987) showed that 2% of the variation in the data was attributable to the technique used, suggesting the outline based technique is sound.

To test repeatability of the method, the same video sequence was analysed twice by the same researcher, once at the beginning of the analysis and once at the end (39 days apart). The average residual in interpolated vertical centre of mass position (from equal horizontal position) was 0.02 ± 0.005m (Fig. 6.3). A linear regression showed that the data correlated significantly with a gradient close to 1 ($P < 0.0005$, gradient = 0.98, Fig. 6.3), and a repeatability score showed that less than 1% of the variation in the data was attributable to the video sequence used, suggesting the method is repeatable (see Appendix 6.1 for input and output parameters from each sequence).

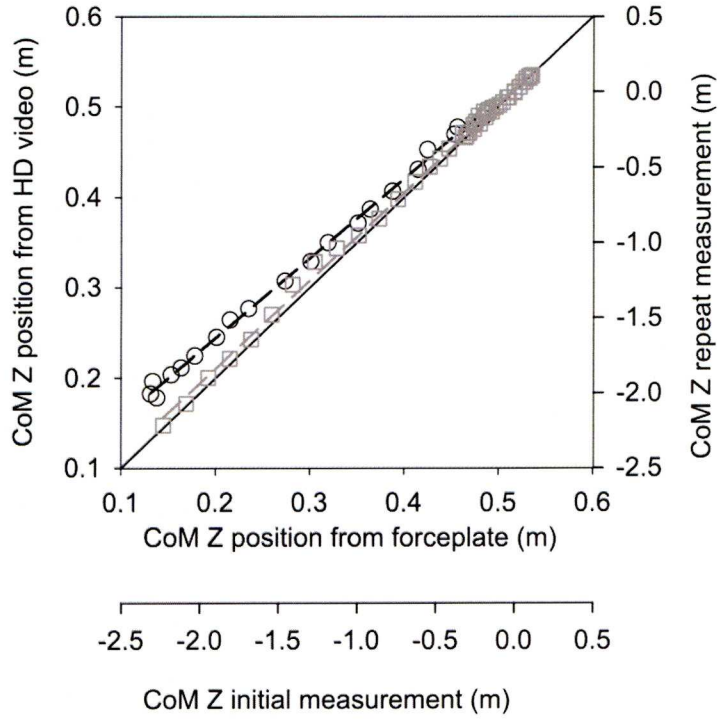

Figure 6.3. Black open circles, vertical centre of mass (CoM) position attained from outline based method vs. attainment from forceplate based method from Channon et al. (In Press). Solid line shows a gradient of 1 (i.e. a perfect match), black dashed line shows the gradient of a linear regression on the data (0.88, $P < 0.0005$). Grey open squares (shown on secondary x and y axes), show vertical centre of mass position of video 2 vs. the same video analysed a second time. Grey dashed line shows the gradient of a linear regression on the data (0.98, $P < 0.0005$).

Results

Leap Biomechanics

The gibbons leapt an average (mean ± SE) resultant (R) distance of 4.40 ± 0.12 m, with a net horizontal distance of 4.15 ± 0.11 m and a leap angle (α) of, 20.6 ± 1.2°. The leaps were conducted as either pronograde two-footed (Fig. 6.4a) or pronograde squat leaps (Fig. 6.4b, following Channon et al. In press). Although the trunk angle could not be calculated (because individual segments were not digitised), visual observations indicated it to be consistently less that 45° to the horizontal (i.e. in a pronograde position) during all leaps (Fig. 6.4b). During both leap types there was a noticeable countermovement before take-off, although this was more pronounced during pronograde squat leaps (Fig. 6.2b). Qualitatively, the squat leaps were performed with the hind limb and trunk in a squatted position, with the back, hip, knee and ankle highly flexed. During push-off the joints extended rapidly until take-off (Fig. 6.4b). In contrast, there was relatively little joint flexion and extension during the pronograde two-footed leaps, which began with a short 'preparatory-leap' (of approximately 1 m) to the take-off branch (Fig. 6.4a). There were, however, no statistical differences between any of the biomechanical parameters measured between leap types, so the data were pooled and not analysed as distinct leap types. The results from each individual were also grouped after a repeatability measure revealed that 'individual' as a variable accounted for only 6 ± 5% of the variation in the dataset (Lessells and Boag, 1987).

The observed take-off angle (φ, 14.5 ± 1.3°) was significantly lower than the take-off angle which minimised the required KE_M for the leap (φ_{min}, 34.7 ± 0.6°, Fig. 6.5a, $P < 0.0005$). A linear regression of the data showed no significant correlation between observed (φ) and minimum velocity (φ_{min}) take-off angles (gradient, 0.73, $P = 0.13$). However, when additional data from a previous study (Channon et al. In press) was included, the regression became significant (gradient, 0.85, $P < 0.0005$). The observed take-off velocity (U, 7.3 ± 0.2 ms^{-1}) was significantly higher than the theoretically required minimum for the observed leap parameters (U_Φ, 5.9 ± 0.2 ms^{-1}, $P < 0.0005$, calculated from $KE_{M\Phi}$, $v_\Phi = \sqrt{[2*KE_{M\Phi}]}$, Fig. 6.5b). A regression showed that observed (U) and the minimum required take-off velocity (U_Φ) were positively correlated, although the gradient was not close to 1 (gradient, 0.53, $P = 0.03$, Fig. 5b).

Peak centre of mass power (P_{Mpeak}) was 260 ± 42.5 Wkg^{-1} and was attained 60 ms before take-off (Fig. 6.6). Peak propulsive muscle mass power, based on the volume of muscle dedicated to hip,

Figure 6.4. Body posture during a typical two-footed leap (A) and a squat leap (B). Timings in seconds are relative to take-off.

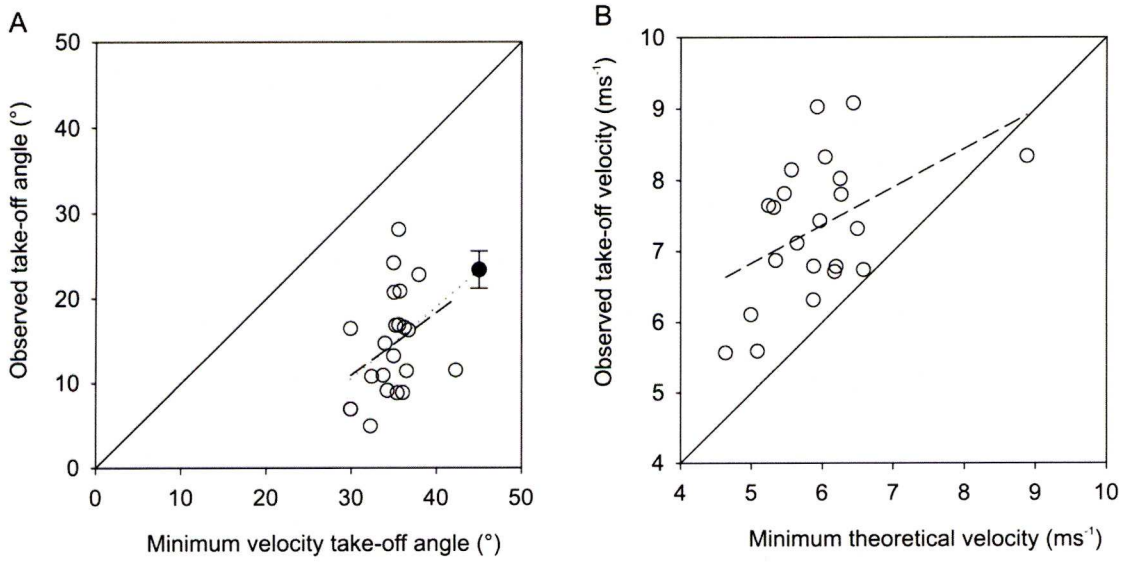

Figure 6.5A.Open circles, observed vs. minimum theoretical velocity take-off angle for this study; filled circle, data from Channon et al. (In Press), error bars denote standard error of the mean. Dashed line shows a regression of the data from only this study (gradient = 0.73, P = 0.13), dotted line includes data from Channon et al. (In Press) in the regression (gradient = 0.85, P < 0.0005). Solid line shows a gradient of 1. **B**. Observed vs. minimum theoretically required take-off velocity from this study. Dashed line shows a regression of the data (gradient = 0.54, P = 0.03). Solid line shows a gradient of 1.

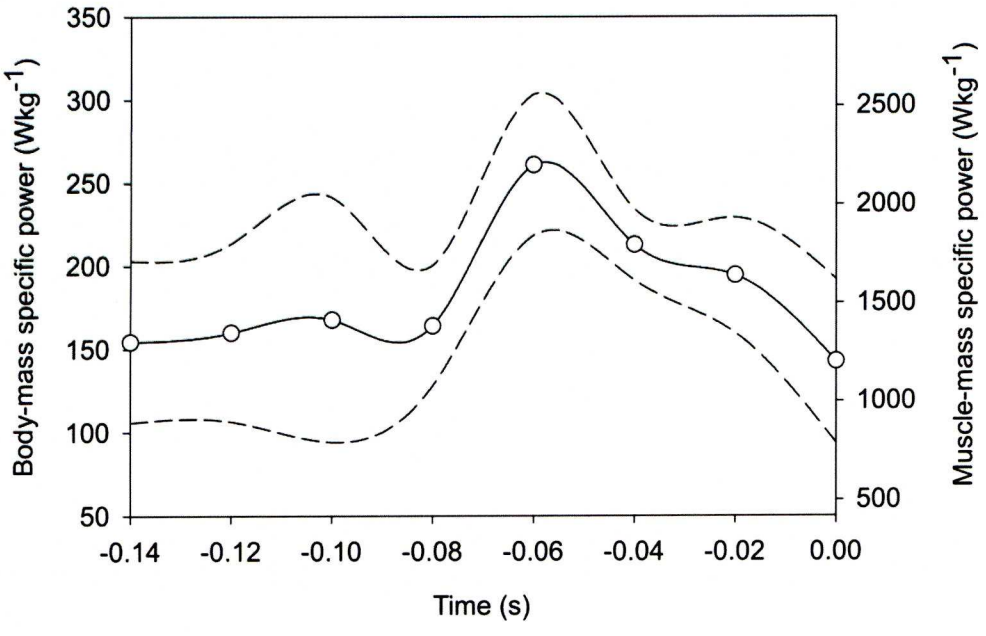

Figure 6.6. Estimates of body (primary y-axis) and propulsive muscle mass (secondary y-axis) specific power during squat leaps in this study. Time 0.00 denotes take-off. Solid line and open circles show the mean, dashed lines show the standard error of the mean.

knee and ankle extension (being 11.9% of body mass; Channon et al., 2009), was 2199 ± 357 Wkg^{-1}. Mean mass specific energy costs of the leap, for each of the theoretical scenarios and their respective groupings (based on Tukey's post-hoc analysis) are shown in Table 6.2 (and on Fig. 6.7a). The mean push-off time was 0.24 ± 0.02 s and the mean centre of mass powers and respective homogenous grouping are presented in Table 2 (and Fig. 6.7b).

The average difference in resultant position of the centre of mass between the 'arms present' and 'arms removed' conditions over the whole leap sequence was 0.11 ± 0.02 m. The maximal difference in horizontal position was 0.28 m, occurring immediately prior to take-off (-0.02 s, Fig. 6.8). Mass-specific work and power during the push-off were higher in the 'arms present' condition than in the 'arms removed' condition (30.7 vs. 21.9 Jkg^{-1} and 85.4 vs. 61.0 Wkg^{-1}; Fig. 6.8).

Discussion

Leap Biomechanics

The gibbons used leap types not previously described by Channon et al. (In press), reorientating the trunk to a more pronograde posture during the take-off. This preference is likely associated with the challenge of longer leaps, which require the trunk to be better aligned with the ground reaction force (GRF) vector (Crompton et al. In press). A pronograde trunk orientation also maximises the proportion of force transmitted along the long (compression) axis of a horizontal branch, minimising vertical deflection (Kinzey et al., 1975; Crompton et al., 1993; Crompton and Sellers, 2007). While no force vectors could be measured in this kinematic analysis, the take-off angle (which is effectively a measure of velocity vector angle) of 14° means that, assuming constant acceleration, 80% of the take-off force is directed along the stronger compression axis of the take-off substrate. This may provide a potential explanation of the gibbons' deviation from a take-off angle which minimised the amount of kinetic energy required for the leap (Fig. 6.5a). Indeed, such criteria for take-off angle selection have been suggested for Western tarsiers (*Tarsius bancanus*, Crompton et al. In press), and the small branch deflection during take-off in the present study (< ~5 cm), supports the hypothesis that maximizing force alignment with the compression axis of the branch determines take-off angle selection.

Table 6.2. Total leap energies and mean powers for the measured and calculated theoretical scenarios. See text and table 1 for definitions and calculations of parameters.

Total Leap Energies (Jkg^{-1})	Mean		SE	Tukey grouping
E_M	34.2	±	1.9	1
$E_{M\Phi}$	31.7	±	1.0	1, 2
E_{Mmin}	27.9	±	0.8	2
$E_{M45°}$	20.4	±	0.5	3
Mean powers (Wkg^{-1})				
P_{Mmean}	89.8	±	9.5	1, 2
$P_{Mmean\Phi}$	82.5	±	7.3	1, 2
$P_{Mmean-min}$	65.0	±	5.0	1
$P_{Mmean45°}$	94.9	±	7.4	2

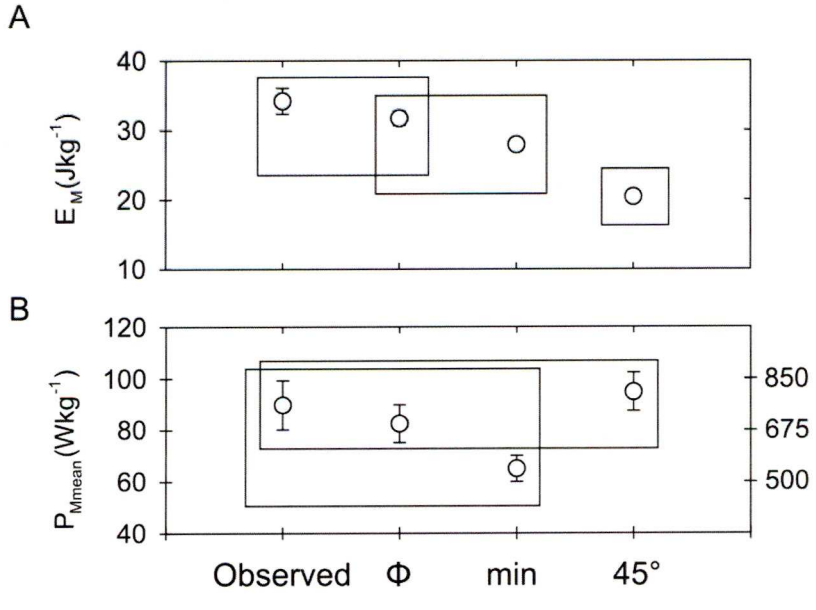

Figure 6.7. Observed and theoretical estimates of body mass-specific total energy for the whole leap (**A**) and mean power during take-off (**B**) under different theoretical scenarios (see materials and methods for calculations). Error bars denote standard error of the mean, boxes show homogenous subsets identified using Tukey's HSD post hoc tests (where $P < 0.05$ is deemed significant). Subsidiary y-axis on B is propulsive muscle mass specific power.

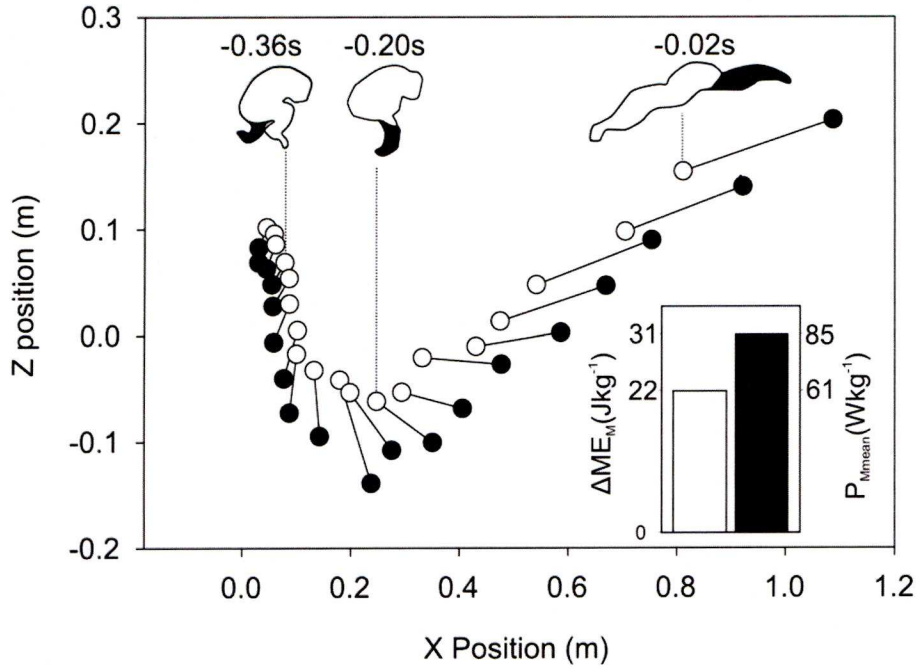

Figure 6.8. The centre of mass position during the take-off of video two with the arms present (filled circles) and removed (open circles), solid lines join equivalent frames. Schematics show the section removed (in black) during the 'arms removed' analysis. Timings are relative to take-off. Inset graph, mass specific mechanical energy change (ΔME_M) and mean power during push-off for each condition.

A lower take-off angle also requires, or by the same token, facilitates, a higher take-off velocity. The take-off velocities observed here (7.3 ± 0.2 ms^{-1}) are substantially higher than observed during gibbon bipedalism (~3.5 ms^{-1}, Vereecke et al., 2006b) and maximal leaping of bushbabies (*Galago moholi*, Gunther et al., 1991). Crompton et al. (1993) hypothesised that low take-off angles could be beneficial as an anti-predation mechanism, where the increased velocity and unpredictable trajectory could serve to avoid predation at the expense of energetic efficiency. Obviously, the captive gibbons in this study were under no risk of predation, but during the leaps they were often chasing one another playfully around the enclosure, so speed as a selective criterion could not be ruled out. Gibbons are unusual among leapers in that they often land with the forelimbs; in this study landing always took place by swinging from a branch or nearby rope. High velocity leaps therefore could power the first swing of brachiation, often undertaken immediately after landing (Gittins, 1983; Sati and Alfred, 2002), which both recovers kinetic energy and dissipates the potentially dangerous landing forces (Demes et al., 1995, 1999). In support of this, the gibbons' take-off velocity was higher than theoretically required, even when the 'sub-optimal' take-off angle is taken into account (Fig. 6.5b). An alternative hypothesis to 'overleaping' the distance is that the gibbons build in a 'safety margin', in case unexpected energy wastage occurs e.g. by branch deflection or breaking, so that take-off velocity unexpectedly slowed during take-off. It is also possible that the gibbons land opportunistically and do not calculate an exact landing position. In support of this, wild white-headed langurs (*Trachypithecus leucocephalus*) have often been observed to leap into large bushes during cliff descent (Huang and Li, 2005; Stevens, 2008) and wild siamang (*Hylobates syndactylus*) have been reported to "...fall into the tree below, apparently grasping available supports with all cheiridia" and "...it is not clear to what extent siamang have specific landing targets for leaps." (from Fleagle, 1976). Thus, it is possible that the 'extra' velocity above the theoretically required minimum allows the gibbon to safely modify its landing target during the leap.

The gibbons in this study always lost potential energy during the leap (i.e. they leapt 'downwards'), meaning that the total cost of the leap (including the work done to recover the loss in potential energy) was significantly higher than if they had executed a flat leap ($\alpha = 0°$) with a 45° take-off angle (Fig. 6.7a). Executing a flat leap would require a higher take-off velocity (and hence, more KE_M), which in the same push-off time, would require a higher mean power. Yet, the mean power observed here was not significantly different from that required for a flat leap (with take-off angle 45°), suggesting that the gibbons were not limited to completing 'downward' leaps by centre of mass power. Indeed the instantaneous (real time) centre of mass power was 2.7 times

higher than that required for the 45° leap, further suggesting that the gibbons could power a flat leap, if desired. The gibbons in this study were often playfully chasing one another during the leaps, which doubtless affected their chosen routes and landing targets. Wild gibbons, conversely, might be expected to perform energy efficient leaps if possible, but field reports suggest that most leaps incur some height loss (Fleagle, 1976; Gittins, 1983). A likely explanation for wild gibbons not using high powered leaps is the energy dissipating effects of the take-off branches (Alexander, 1991). Most leaps are conducted from fine terminal branches, which deflect substantially under load, wasting energy (McMahon and Kronauer, 1976). Powerful (high force) movements exacerbate this effect, and so should be avoided, unless the energy storing capacity of the branch can be exploited gainfully (as in slow moving orangutans, Thorpe et al., 2007a). Despite field reports of branch propagation by wild siamang before a leap (Fleagle, 1976), no such mechanism has been demonstrated during powerful movements to date (Demes et al., 1995), and structural and damping properties of tree branches make this unlikely, exceptional circumstances aside (McMahon and Kronauer, 1976; Alexander, 1991).

The peak centre of mass powers observed here are within the range seen among other primates during non-cyclical locomotion and substantially below the ~800 Wkg^{-1} observed for *Galago senegalensis* (Aerts, 1998). The gibbons did, however, exceed published values of cyclical locomotor modes (e.g. 65 Wkg^{-1} for blue crested quail, Askew and Marsh, 2001), suggesting some energy storage prior to the push-off. The countermovement in both leap types is one likely mechanism used by gibbons (as opposed to the tensioned 'power amplifier' based mechanism used in galagos and frogs; Lutz and Rome, 1994; Aerts, 1998). During the squat leap I found that the arms contributed 29% (8.8 Jkg^{-1}) of the work done on the centre of mass during the push-off and increased mean power by 24.4 Wkg^{-1}. This is likely an underestimate since my technique only allows the removal of sections of the arm which fall outside of the profile of the body. Moreover, human jumping studies have shown the arm-swing countermovement to load the muscles more effectively and stretch tendons before the push-off (Alexander, 1992, 1995), the effects of which could not be quantified using my technique. Estimates of the role of the arms during human vertical jumping suggest that the arms contribute ~22% to centre of mass work during the push-off phase (Cheng et al., 2008). The large mass of gibbon forelimbs relative to body mass compared to humans (~16% vs. ~10% respectively; Clauser et al., 1969; Chandler et al., 1974; Isler et al., 2006; Michilsens et al., 2009), suggest that my findings are feasible (if underestimated) suggesting the forelimbs are major contributors to power production during gibbon leaping. During pronograde two-footed leaps, the arms were also swung forward during push-off,

suggesting a power contribution in this leap type. The countermovement was, however, noticeably reduced in comparison to squat leaps (Fig. 6.2b). The preparatory-leap observed during the two-footed pronograde leaps could facilitate tendon stretch during the landing (of the preparatory-leap) and subsequent energy recovery during the push-off of the leap. Such a mechanism could store the energy from the preparatory-leap in the well developed Achilles, digital flexor and patellar tendons of the hind limb (Vereecke et al., 2005, 2008; Channon et al., 2009), then recover it during the push-off period, contributing power to the leap. The analyses required to test this hypothesis require detailed foot kinematics and so were not possible here, but Vereecke and Aerts (2008) demonstrated the energy storage capacity of the gibbon foot during bipedalism, and have suggested that energy could be stored and recovered from the knee joint during gibbon bipedalism (Vereecke et al., 2006b). Further, a preparatory-leap has been identified in galagos before maximal leaps (Gunther et al., 1991), perhaps related to the same mechanism. The propulsive muscle-mass specific powers calculated here were based on an assumption that only the legs powered the leap and so are certainly overestimates. If the arms are included (as 16% body mass, Michilsens et al., 2009) the peak propulsive muscle mass-specific power falls dramatically (to 935 ± 152 Wkg^{-1}). This value is still substantially higher that muscle mass-specific powers calculated for vertically leaping bonobos (615 Wkg^{-1}, Scholz et al., 2006), where 'superior muscle properties' are hypothesised to yield high muscle powers. It is conceivable that gibbons possess similar myological properties to bonobos, but it is also likely that energy is transferred from other sources such as the back musculature. The back is deeply flexed during the squat leaps and is likely to contribute to powering the leap by extending the trunk (and so accelerating the centre of mass) during the push-off phase. Detailed investigations into the myology of gibbon muscle would help support or reject hypotheses about any 'superior properties' of gibbon muscles, while a detailed inverse dynamics analysis of maximal gibbon leaps (as performed by Scholz et al., 2006, for bonobos) could assess power contributions from the back musculature. Whether via arm-swinging countermovement, or tendon stretching preparatory-leap, the high calculated muscle mass specific powers (Fig. 6.6) strongly indicate that either energy transfer (from the arms and probably back muscles) or recovery (from elastic structures within the body) or more likely both, contribute substantially to powering the leaps observed here.

Assessment of the technique

This study demonstrates a new technique for attaining centre of mass movements of free ranging, leaping animals based on video recordings of the animals' voluntary locomotion. This technique could be utilised in a wide range of locomotor studies, both in captivity or in the wild. Gibbons are a particularly pertinent study subject because the use of body mounted accelerometers is extremely difficult in these species. Gibbons live high up into the forest canopy and unobstructed filming is notoriously difficult as clear sightings are rare (McClure, 1964; Thorpe and Crompton, 2005), yet the parameters quantified in this study only require the take-off to be filmed and the landing position known, partially obscuration of the flight is inconsequential. Further, the calibration of the volume can be done once the behaviour has been recorded (as was the case here). The data collection equipment for this study was light, robust and affordable, making it suitable for field and zoo based studies. Moreover, filming from the ground does not affect the locomotor biomechanics and behaviour of the animals making this a reliable analysis technique. Again, gibbons are pertinent here, because their pair dwelling habit (with the exception of *Nomascus concolor*) and critically endangered status (IUCN, 2008) mean that low sample numbers are an inevitable limitation of gibbon research. However data collection using this technique is fast and requires minimal interference with the animals and their enclosure.

The sensitivity analysis revealed that measurements of instantaneous power were highly variable (Table 2, Fig. 6). This is almost certainly because of the double differentiation from centre of mass position (once to attain KE_M, again to differentiate W_M) which is required. Calculations based on the theoretical scenarios were robust and represent the most repeatable data. Both a higher resolution video camera and a higher frame rate would help alleviate problems with repeatability, although specialist cameras with such facilities are costly and often difficult to transport. The comparison with forceplate derived measurements of centre of mass position showed the technique to be sound.

This technique represents an affordable, accurate and simple method to obtain centre of mass movements of wild and free ranging animals with minimal interference from video recordings. As such it is a useful tool for the study of many wild or captive species where interference with the subject is impractical or undesirable.

Conclusions

This study shows that during maximal leaps, gibbons orientated the trunk better to align it with the force vector, minimising branch deflection. The gibbons utilised low take-off angles and high velocities which may ensure a safe leap and rapid onwards progression by brachiation, and might also allow the identification of landing target during the leap itself. I show that the gibbons are probably not limited by muscle power to perform only leaps with a net height loss, although wild gibbons are likely limited to lower power leaps (than observed here) by branch stiffness, and hence deflection. My results strongly indicate that arm-swing and/or a preparatory-leap probably contribute substantially to powering maximal leaps, given the unfeasibly high muscle specific powers required of a 'legs only' leap. The technique used here facilitates detailed biomechanical measurements to be taken from video recordings with minimal interruption to free-ranging or wild animals, quickly and cost effectively.

List of Abbreviations

Enclosure calibration

b_m – Measured horizontal branch length (m, Fig. 6.1c)

b_p – Digitised horizontal branch length (pixels, Fig. 6.1c)

β_{BRANCH} – The angle of orientation between individual branches with reference to a plane perpendicular to the camera (°, Fig. 6.1b)

β_{TRUNKS} – The angle of orientation of the vertical trunks, with reference to a plane perpendicular to the camera (°, Fig. 6.1b)

d_m – Measured inter-vertical trunk distance (m, Fig. 6.1c)

d_p – Digitised inter-vertical trunk distance (pixels, Fig. 6.1c)

$\underline{E}_{BRANCH}$ – Individual calibration coefficients for branches within the enclosure (pixels m^{-1})

$\underline{E}_{TRUNKS}$ – Inter-trunk distance coefficient for the enclosure calibration (pixels m^{-1})

$\underline{E}_{VERT}$ – Vertical coefficient for the calibration of the enclosure (pixels m^{-1})

h – Horizontal

h_{CENT} – Horizontal coordinate of the centroid (pixels)

h_m – Measured vertical trunk height (m, Fig. 6.1c)

h_p – Digitised vertical trunk height (pixels, Fig. 1c)

v – Vertical

v_{CENT} – Vertical coordinate of the centroid (pixels)

Video sequence- specific calibration

$\beta_{SUPPORT}$ – the orientation of take-off and landing supports from one another, with reference to a plane perpendicular to the camera (°, Fig. 6.1b).

δ_m – Measured vertical distance between take-off and nearest landing support (m)

δ_p – Digitised vertical distance between take-off and nearest landing support (pixels)

η_m – Measured horizontal distance between take-off and nearest landing support (m)

η_p – Digitised horizontal distance between take-off and nearest landing support (pixels)

$\underline{V}_{HORIZ}$ – Horizontal, video sequence-specific, calibration coefficient (pixels m^{-1})

$\underline{V}_{VERT}$ – Vertical, video sequence-specific, calibration coefficient (pixels m^{-1})

X – The calibrated position of the centroid in the left-right plane, referenced to the camera (m)

Y – The calibrated position of the centroid in the near-far plane, referenced to the camera (m)

Z – The calibrated position of the centroid in the vertical plane, referenced to the camera (m)

Biomechanical parameters

α – Leap angle (°, Fig. 6.2b)

ε_M – Mass-specific total energy cost of the leap ($J\ kg^{-1}$)

g – Gravitational acceleration (-9.81m s^{-2})

KE_M – Mass-specific kinetic energy (J kg^{-1})

$KE_{M\Phi}$ – Mass specific kinetic energy for theoretical leap scenario 1 (Table. 1, J kg^{-1})

KE_{Mmin} – Mass specific kinetic energy for theoretical leap scenario 2 (Table. 1, J kg^{-1})

$KE_{M45°}$ - Mass specific kinetic energy for theoretical leap scenario 3 (Table. 1, J kg^{-1})

ME_M – Mass-specific mechanical energy (J kg^{-1})

P_{Mmean} – Mass-specific mean power (W kg^{-1})

P_{Mpeak} – Peak mass-specific centre of mass power (W kg^{-1})

PE_M – Mass-specific potential energy (J kg^{-1})

φ – Take-off angle (°, Fig. 6.2b)

φ_{min} – Take-off angle which required the minimum theoretical velocity (°)

R – Resultant leap distance (m, Fig. 6.2b)

S – Net height loss during the leap (m, Fig. 6.2b)

t – Time (s)

U – Take-off velocity (m s^{-1}, Fig. 6.2b)

V_R – Resultant velocity (m s^{-1})

t_{PUSH} – Push-off time (s)

Chapter 7: General Discussion

By Anthony J. Channon

With contributions from Evie E. Vereecke.

I wrote the manuscript and Evie Vereecke edited it and advised on its content.

This thesis has examined the functional anatomy and leaping biomechanics of gibbons, this general discussion section serves to unite the preceding Chapters and substantiate my findings into a broader scientific context.

Functional morphology: what is the gibbon hind limb specialised for?

In Chapter 2 I demonstrated that gibbons appear to have several specialised functional muscle groups within the hind limb, consistent across species. Pennate, high PCSA muscles are probably involved in powerful movements such as leaping and rapid climbing, while the parallel fascicled, low PCSA knee and hip flexors facilitate a wide range of motion and limb positions, which are presumably valuable in the complex and unpredictable environment that gibbons inhabit. The fascicle strain model (presented in Chapter 2) showed that the rectus femoris is probably more adept at knee extension that hip flexion, perhaps indicating an adaptation for producing high forces across the knee joint. Overall the gibbon hind limb has a PCSA vs. fascicle length 'profile' similar to that of bonobos (Fig. 2.9), which are considered locomotor generalists (Aerts et al., 2000; D'Août et al., 2004). The varied and extensive locomotor repertoire of both wild and captive gibbons (Fleagle, 1976; Gittins, 1983; Sati and Alfred, 2002; Vereecke et al., 2006a) implies that gibbons too, are generalists, at least when referring to hind limb supported locomotion, since the gibbon forelimb is undoubtedly specialised for brachiation. The gibbon hind limb, then, could be considered a generalist whole, made up of specialist parts, a Swiss army knife-type apparatus with specific tools (muscle groups) for specific tasks (locomotor modes). Yet, as I noted in Chapter 2, differing locomotor modes likely place contrasting strains on the same muscles. Thus, there is almost certainly some compromise in morphology to maintain an ability to perform a variety of tasks at an acceptable level, selecting against the very specialised apparatus seen in highly specialised animals such as *Galago senegalensis* (Stevens et al., 1972; Aerts, 1998). Indeed,

D'Août et al. (2004) found that bonobos (*Pan paniscus*) likely compromised performance (in terms of speed or efficiency) in one locomotor mode to maintain the ability to perform the full range of modes.

This compromise in musculoskeletal adaptation can be compensated for, to some extent, by modifying locomotor biomechanics to best suit the morphology present (although in fact, the behaviour and anatomy probably evolve in tandem). I showed (in Chapter 6) that gibbons utilised the arms and back in a substantial countermovement to power maximal leaps. I hypothesised that this technique both translated the centre of mass more rapidly (increasing velocity) and loaded the tendons of the hind limb, storing elastic energy in them, that could be recovered during the push-off stage. The most likely candidate tendons for this mechanism are the patellar, Achilles and digital flexor tendons of the hind limb, which have relatively low safety factors (Fig. 2.7). The same tendons were hypothesised to store elastic energy during gibbon bipedalism, allowing a mechanically effective 'bouncing' gait (Vereecke et al., 2006b; Vereecke and Aerts, 2008) to be efficient. The vertical ground reaction force profile produced during gibbon bipedalism is thus more akin to human running than walking (Fig. 7.1, Vereecke et al., 2006b; Crompton et al., 2008; Lieberman et al., 2010). Gibbons probably opt to use running-like mechanics at walking speeds because their muscular anatomy does not allow the hip and knee joints to be extended simultaneously, so a stiff-legged inverted pendulum type gait is not possible, making a 'bouncing' gait the next most mechanically efficient alternative. This alternative is reliant on the energy storage capacity of the well developed tendons of the gibbon hind limb, a trait shared only with humans in the ape lineage (Payne et al., 2006a). Bonobos, who are also very adept leapers, by comparison do not posses well developed hind limb tendons (Vereecke et al., 2005; Payne et al., 2006a), did not utilise a countermovement when leaping maximally (Scholz et al., 2006), although it is very likely that they utilise a countermovement in some situations, and their walking mechanics are characterised by a flat (trapezoidal) vertical ground reaction force profile indicating a more energetically expensive compliant, bent-hip bent-knee gait (Fig. 7.1, Crompton et al., 1998; D'Août et al., 2004; Sellers et al., 2005). Thus, the mechanics of gibbon and bonobo bipedal locomotion differ according to their morphology. This statement lends the question: Why don't bonobos possess well developed hind limb tendons, as gibbons do? One factor could be control.

Muscle tendon units with relatively long tendons compared to the length of the muscle fascicles are often highly pennate, to allow sufficient numbers of muscle fascicles in parallel to serve the force production requirements the muscle (Alexander, 1992; Biewener, 1998a, b; Azizi et al.,

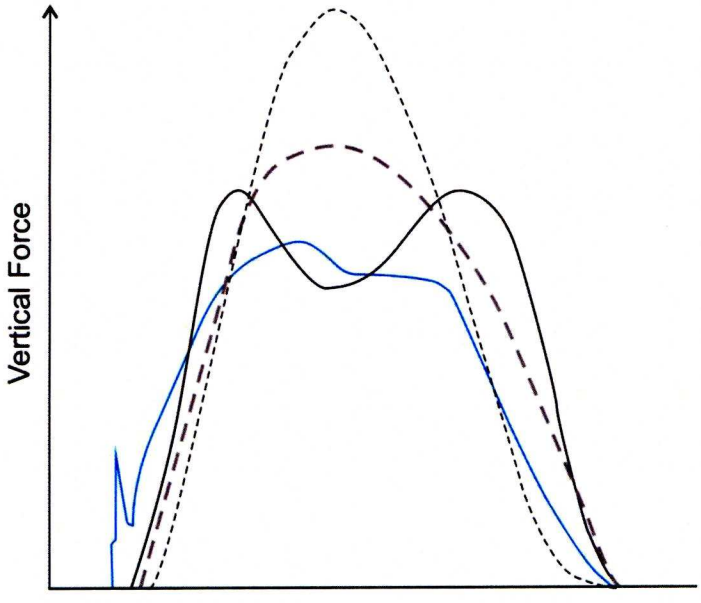

Figure 7.1. Vertical ground reaction force traces from human walking (black solid line), human running (black dotted line), bonobo walking (blue solid line) and gibbon bipedalism (grey dashed line). Reproduced from Crompton et al. 2008 and Lieberman et al. 2010.

2008). Pennate muscle fascicles are generally shorter and contain fewer sarcomeres in series which reduces their propensity for shortening (Medler, 2002). Consequently, pennate muscles offer a more narrow range of motion than do parallel muscles of equal volume, this can be exacerbated by fibre rotation during contraction (Zajac, 1989, 1992; Azizi et al., 2008). Further, muscles produce force most effectively at specific range of sarcomere lengths (Hill, 1968), having more sarcomeres in series therefore allows the muscle to work most effectively over a wider range of motion, increasing control over the limb. Bonobos undertake a large proportion (80-90%, Doran, 1993) of locomotor bouts using hind limb supported locomotion, and so the hind limbs are likely adapted for high levels of muscular control, particularly given their arboreal habitat.

In an arboreal habitat, the locomotion of larger animals is characterised by slow climbing, bridging and suspensory behaviours requiring a wide range of limb positions (e.g. quadrumanous clambering, Doran, 1993; Thorpe and Crompton, 2005; Thorpe et al., 2007b), while smaller animals utilise leaping to a greater extent (Gunther et al., 1991; Crompton et al., 1993; Sellers and Crompton, 1994). Thus, for bonobos, a high level of force over a wide range of limb postures is likely strongly selected for, especially in light of the potential danger of a fall. Gibbon locomotion conversely, is characterised by rapid bouts of brachiation, interspersed with bipedalism, climbing and leaping (Gittins, 1983; Sati and Alfred, 2002). The gibbons' smaller size compared to bonobos (5-10 kg vs. 30-35 kg) almost certainly reduces branch deflection nearer the base of branches. This, coupled to their greater dependence on suspensory locomotion probably reduces the importance of both exact hind limb placement and the ability to produce high levels of force throughout the range of limb positions. For gibbons, which are more likely to leap across gaps in the canopy than to bridge between supports (Fleagle, 1976), the ability to store energy in the tendons of the hind limbs that can be recovered during bouts of bipedalism atop branches or leaping, is likely highly advantageous. Given the gibbons' dependence on forelimb suspensory locomotion and its role in landing - gibbons are unusual among arboreal leapers in that they often land with the forelimbs - it is intuitive that gibbon forelimbs should contain muscles able to produce force over a wide range of motion, especially in light of the importance of fall avoidance (Schultz, 1956). Michilsens et al. (2009) showed that, indeed, much of the forelimb musculature possesses long fascicles, with a range of PCSAs, indicating a propensity for control over a wide range of motion.

I conclude that the gibbon hind limb is a generalist whole, composed of (musculo-tendinous) specialist units, allowing a diverse locomotor repertoire, necessary for negotiating the three-dimensionally complex environment, that gibbons inhabit.

What is left to learn?

Our understanding of the functional morphology of gibbons and of apes as a whole are undoubtedly enhanced by the data presented here (Chapters 2 and 3), but there are some key variables that remain to be quantified and some crucial limitations that need to be addressed.

A third key determinant of muscle function, alongside muscle architecture and moment arm, is the muscle fibre type (Eng et al., 2008). Knowledge of the fibre type distribution of gibbon hind limbs would aid our understanding of muscle function further, as it has in other primate species (e.g. Ariano et al., 1973). Preliminary muscle fibre type data from captive animal cadavers indicates that most of the musculature associated with powerful leaping movements (e.g. hip and knee extensors) is composed of approximately 35-40% fast twitch (type II) muscle fibres. Conversely the Sartorius muscle, which is probably used in leg lift during brachiation, has a high proportion (~80%) of slow twitch (type I) muscle fibres, perhaps reflecting the necessity of a fatigue resistant muscle for long bouts of brachiation. A likely difficulty with collecting these data is that the majority (all of the data presented here) of gibbon cadavers are attained from zoos and wild animal parks, where the animals are not subject to the same exercise as wild gibbons (owing to an effectively smaller home range, Milton and May, 1976), which means that the muscle fibre distribution of captive gibbons might not be representative for wild populations (Pette and Staron, 1997, 2001). This is, however, an unavoidable constraint of working with captive animals. Yet, it can be assumed that this effect is limited if captive animals are held in a relatively large enclosure ('free ranging' as the case in this study).My interpretation of the importance of elastic energy storage in the hind limb would also benefit greatly from knowing the material properties of specific tendons in the hind limb (Ker et al., 1988; Alexander, 2002), some preliminary work has been conducted on the hind limb tendons of gibbons (Vereecke et al., 2008), indicating that the Achilles tendon possesses appropriate material properties to influence muscle performance during locomotion. More data and analyses are required to make firm conclusions about the propensity for energy storage in a larger range specific tendons and muscle groups.

Internal bone morphology (trabeculae, cortical bone thickness etc.) can also yield valuable insight into musculoskeletal function, by reflecting the loads placed upon it (Thomason, 1985, 1995; MacLatchy and Müller, 2002). Modern X-ray imaging techniques, such as microCT, are currently relatively readily available and can be conducted opportunistically on living animals during routine veterinary examinations as well as on museum specimens, substantially increasing the number and ecological diversity of available specimens.

Leaping biomechanics: are gibbons leaping specialists?

Gibbons posses an unusual morphology which can be used to improve leaping performance. Without doubt, the long and heavy forelimbs play a crucial role in both powering maximal leaps and facilitating a safe landing. The countermovement observed during the maximal leaps (Chapter 6) added substantially to the mechanical energy of the centre of mass during the push-off phase, and my calculations are almost certainly an underestimate. The forelimb-lead landings observed from the gibbons serve to minimise potentially damaging impact forces and translate downward kinetic energy into forward momentum, powering brachiation. There is, presumably, a limit reached during leaps with a large net height loss, where the gibbon's falling velocity is too great to be translated by rotating about a branch into forward momentum. This limit could be broached by the branch breaking as reported in wild siamang (McClure, 1964), or by exceeding the force production capabilities of the digital flexor muscles causing the gibbon to fall. The latter is particularly pertinent for larger gibbons (such as siamang), because the PCSA of a muscle scales with body mass raised to the power ⅔, meaning that body mass increases faster than the force available to support it (Alexander, 1981; Preuschoft and Demes, 1985). This theory raises the intriguing possibility that the resultant distance of gibbon leaps (including height loss) could be limited by landing forces and not take-off power production. However, this seems unlikely since the gibbons could (and reportedly do, Fleagle, 1976) land in bushes and flexible foliage, which dissipate landing energies effectively (Demes et al., 1999) when leaps with large height loss are conducted.

Despite the unusual body plan (and hence, mass distribution) of the gibbons, the hind limb kinematic patterns were typical of other leapers, utilising a proximo-distal joint extension pattern, with the hip extending first, followed by the knee then the ankle. As the joints extend the distal limb segment traces a circular outline around the joint centre, meaning that toward the end of joint

extension the translation of the centre of mass achieved for a given joint angle change is reduced (Van Ingen Schenau, 1989). Interestingly, the same extension sequence was found for the forelimbs (Fig. 4.7); further purporting them as important for maximising leap performance.

The gibbons observed during this study did not utilise take-off angles which minimised the required take-off velocity (Chapter 6), opting instead for a more acute take-off trajectory. Although only the most specialised leapers (e.g. *Galago moholi*) utilise such acute take-off angles during leaps of all distances, the take-off angles of other, less-specialised, species (e.g. *Microcebus murinus*, *Cheirogaleus major*, *Lemur catta*) tended toward those angles which minimised velocity only as the leaps became longer (Crompton et al., 1993). In light of this, my findings suggest that either: the leaps observed were not maximally performed, the gibbons are not 'specialised enough' to minimise the required take-off velocity, that some other constraint determined take-off angle in my study, or some combination of these. The muscle-mass specific powers measured during the observed leaps (of Chapter 6) suggest that the leaps were near maximal, eclipsing the muscle powers achieved by maximally leaping bonobos (Scholz et al., 2006). Further, the gibbons only utilised the two-footed leaps in their repertoire for these distances, suggesting that the power production from both limbs was needed or that the leap was challenging and so required a, more stable, two-footed propulsion phase (see, Chapter 4). There was some correlation between observed take-off angle and minimum velocity take-off angle found in my study (Fig. 6.5a), suggesting that the gibbons did modify their take-off angle with different leap orientations in the *direction* I would expect (i.e. lower leap angle, higher take-off angle), but not to the *extent* that I might expect. The gibbons for which near maximal leaps were attained, were usually playing during the leaps. The younger of the two animals chased the older one (her father) around the enclosure for approximately an hour each day. It therefore cannot be ruled out that the gibbons chose take-off angles by some other criteria associated with playing. I also found that the gibbons could execute different leap types, which might be utilised in different scenarios, e.g. squat leaps for obscured or difficult leaps or rapid pronograde leaps when running atop branches (Chapter 4). In addition, gibbons were observed to select the most appropriate leap type according to the situation. When leaping longer distances (Chapter 6), the gibbons avoided leaps with a single take-off foot, opting instead to use pronograde two-footed and pronograde-squat leaps. Conversely, when leaping from the compliant pole (Chapter 5), the gibbons avoided leaps requiring high powers of the centre of mass, using orthograde single-footed leaps and pronograde single-footed leaps only. Moreover, the gibbons could modify each leap type where necessary, by increasing the amount of back flexion and arm-swing during longer squat leaps, and including a

'preparatory-leap' during the long pronograde two-footed leaps (Chapter 6). The great versatility of leaping as a locomotor mode for gibbons reflects that of their terrestrial gaits (Vereecke et al., 2006), in being modifiable for a range of given scenarios, meaning that gibbons can not only choose an appropriate leap type for a given leap, but also modify that leap type to best suit each leap specifically.

Leaping is unusual as a locomotor mode, especially in the case of gibbons, in that failure to power or control the leap fully is more likely to result in serious injury or death than other cyclical modes such as bipedalism or brachiation. Leaping is used predominantly to cross large gaps in the canopy, where (by definition) there is less of a 'safety net' of branches below. In contrast, brachiation and bipedalism are utilised in areas of dense vegetation and during feeding (Sati and Alfred, 2002), where there are a number of alternative branches to grasp should a supporting structure fail, the gibbon's velocity is also much lower during these modes (I recorded velocities in excess of 7 ms^{-1} during leaps vs. ~3.5 ms^{-1} during bipedalism and brachiation, Bertram and Chang, 2001, Vereecke et al., 2006b). This incongruity of safety margin between locomotor modes could explain why the hind limb appears to present a, perhaps disproportionate, number of adaptations to leaping, given its relatively low prevalence as a locomotor mode (Fleagle, 1976; Gittins, 1983). Similarly, the variety and adaptability of leap techniques could be necessary, even though leaps are comparatively uncommon (20-25% of locomotor bouts in *Hylobates agilis* and *Bunopithecus hoolock*, Gittins, 1983, Sati and Alfred, 2002; 5% in *Symphalangus syndactylus*, Fleagle, 1976), because the cost of a failed leap is so high (Schultz, 1956).

The role of substrate compliance in gibbon locomotion

The gibbons in my study (Chapter 5) did not utilise the energy stored in the compliant pole for mechanical gain. They did, however, demonstrate an ability to modify their leap behaviour (e.g. by avoiding certain leap types) and biomechanics (e.g. by applying force to a relatively stiff portion of the pole) to minimise the negative effects of the compliant pole. There are several barriers to useful energy recovery from elastic substrates which might prevent wild arboreal leapers using their branches to this end. Firstly, the substrate needs to either be massive (in comparison to the animal), with a relatively low oscillation frequency (compared to the leg extension period, like a diving board), or be light weight, with a high oscillation frequency (Alexander, 1991). As discussed in Chapter 5, tree branches do not fall into either of these

categories, and so the potential number of suitable branches to perform this act is likely to be very low. Secondly, energy should not be wasted by damping effects within the branch. Thorpe et al. (2007a) demonstrated damping effects to be negligible for tree swaying orang-utans, suggesting that little energy was lost via air resistance attributable to the tree's foliage. However, during rapid leaping conducted from the terminal branches of the forest canopy (as most are, Fleagle, 1976), these effects are likely to be much more substantial, especially given the low inertia of the terminal branches, which are probably easily slowed by the air resistance of the attached foliage (McMahon and Kronauer, 1976). The animal must also carefully control the branch's movements in two dimensions, up-down and left-right (unlike a diving board which only deflects in one dimension, up-down), while propagating it further. Despite remarkable balance, gibbons can walk bipedally along slack ropes in captivity (AJC, pers. obs.), it is probable that large branch propagation presents an avoidable risk to wild gibbon, especially given the high cost of a fall (see above). Thus, opportunities for such behaviour in the wild are probably rare. It is also important to consider motive; why *would* the gibbons (or any arboreal leaper) want to use the internal compliance of the substrate for energetic gain? It is true that energy recovered from the branch can be used to amplify power used in a single leap, improving performance, and is probably more energetically efficient than equivalent leaps without using substrate compliance. The gibbons in my study (Chapter 6) leapt easily and repeatedly leapt up to 5 metres, and wild gibbons have been reported leaping up to 10 m (Gittins, 1983). For distances of this magnitude, identifying a safe landing target (with the required compromise of strength and compliance, given the high impact velocity), although hazardous, is probably possible for gibbons. For smaller leapers (tarsiers, galagos etc.) this risk is likely reduced (since their leaps are, in absolute terms, shorter) and might be justified to avoid predation, but propagating branches takes time (especially for a small animal), and during that time the prey follows a predictable trajectory. Therefore currently available data indicate that arboreal animals, rather than using branch elasticity, are more likely to try to avoid the negative effects of branch compliance by choosing substrates which are more appropriately angled or sized (Kinzey et al., 1975; Demes et al., 1995; Crompton et al. In press) or by using gaits which minimise branch oscillation (Schmitt, 1999; Thorpe et al., 2009). Yet theoretically, the propensity for useful elastic energy storage and recovery remains for arboreal leapers. In light of these issues, it would be erroneous to assume that the propagation movements reported for wild siamang (Fleagle, 1976, Fig. 1.1), demonstrate useful energy storage and recovery in the branches. Rather, the animal could be assessing the integrity of the take-off substrate before the leap, since a breakage during push-off could be fatal for the gibbon.

Alternatively, the gibbon could gain a better understanding of the hazards of the leap by viewing the landing target while propagating the branch. Squirrels actually do something analogous when faced with a long leap, moving the head up and down several times before leaping (AJC pers. obs.). Alternatively, the animal might simply enjoy propagating the branch playfully. While the data available on wild arboreal leapers is so limited, it remains difficult to further our understanding of these fascinating phenomena.

What is left to learn?

The biomechanics studies presented here (Chapters 4, 5 and 6) have enhanced our understanding about the mechanisms used by gibbons to attain such impressive leap performance and the coping strategies used by gibbons when confronted with compliant take-off supports. Nevertheless, data about the leaps that wild gibbons perform, the situations in which they are used and the substrates from which they occur remain largely lacking. Data from wild animals are crucial to substantiating my findings from captive populations, and so should be the foci of future work. Such field studies could utilise the video based analysis methods detailed in Chapter 6, which only require video footage of the animal and a relatively few calibration measurements to attain biomechanical parameters from wild populations.

Zoo and laboratory based studies have the benefit of being able to manipulate the animal's surroundings in a more controlled fashion than do field studies. Future captive population studies should focus on the effect of substrate properties on leap biomechanics. In reality, substrate compliance is a continuum, not a discrete variable as it was treated here, branches come in a number of different stiffnesses and so analysing the animals as they leap from substrates with a variety of stiffness properties would add greatly to our understanding of the coping mechanisms the animals utilise. Likewise, substrate orientation is crucial. Here I only examined horizontal substrates, but the canopy ecomorph is composed of branches aligned at a range of angles, which present varied biomechanical challenges. Leap orientation and distance are further crucial determinants of leap mechanics, neither of which were controlled here, and could be fascinating foci of future studies. Choice is another fundamental variable. Crompton et al. (In press) documented the substrates that wild Western tarsiers (*Tarsius bancanus*) chose to leap from, and inferred the reasoning behind those choices from biomechanics. In my studies, the gibbons had very limited or no choice but to leap from the substrates I presented them with, yet an

understanding of which substrates gibbons opt to use could highlight what, mechanically, are desirable substrate properties for gibbons and arboreal leapers as a whole.

In this thesis I have demonstrated anatomical specialisations to specific locomotor modes in the hind limb of gibbons, as well as behavioural and biomechanical adaptations of leaping. I showed that leaping is a complex, dynamic and adaptable locomotor task, which is doubtless invaluable to wild gibbons when traversing the canopy. My studies are not exhaustive and further work should build upon these foundations to better understand the mechanics and performance of leaping on a multitude of levels.

References

Ackland D. C. and Pandy M. G. (2009). Lines of action and stabilizing potential of the shoulder musculature. *Journal of Anatomy* **215**, 184-197.

Aerts P. (1998). Vertical jumping in Galago senegalensis: the quest for an obligate mechanical power amplifier. *Philosophical Transactions of the Royal Society B: Biological Sciences* **353**, 1607-1620.

Aerts P., Damme R. V., Elsacker L. V. and Duchêne V. (2000). Spatio-temporal gait characteristics of the hind-limb cycles during voluntary bipedal and quadrupedal walking in bonobos (*Pan paniscus*). *American Journal of Physical Anthropology* **111**, (4):503-517.

Ahlborn B. K., Blake R. W. and Megill W. M. (2006). Frequency tuning in animal locomotion. *Zoology* **109**, (1):43-53.

Alexander R. M. (1968). Animal mechanics. London, UK: Sidgwick and Jackson

Alexander R. M. and Vernon A. (1975). The dimensions of the knee and ankle muscles and the forces they exert. *Journal of Human Movement Studies* **1**, 115-123.

Alexander R. M. (1977). Allometry of the limbs of antelopes (*Bovidae*). *Journal of Zoology*, 183, 125-146.

Alexander R. M., Jayes A.S., Maloiy G.M. and Wathuta E. (1981). Allometry of the leg muscles of mammals. *Journal of Zoology*, 194, 227-267.

Alexander R. M. (1984). Elastic energy storage in running vertebrates. *American Zoology* **24**, 85-94.

Alexander R. M. (1985). Body size and limb design in primates and other mammals. In: Size and scale in primate biology. (ed. W. L. Jungers), pp. 337-344. New York: Plenum Press.

Alexander R. M. (1991). Elastic mechanisms in primate locomotion. *Zeitschrift fur Morphologie und Anthropologie* **78**, 315-320.

Alexander R. M. (1992). The work that muscles can do. *Nature* **357**, (6377):360-361.

Alexander R. M. (1995). Leg design and jumping technique for humans, other vertebrates and insects. *Philosophical Transactions of the Royal Society B: Biological Sciences* **347**, 235-248.

Alexander R. M. (1996). Principles of animal locomotion, Princeton University Press, Princeton.

Alexander R. M. (2002). Tendon elasticity and muscle function. *Comparative Biochemistry and Physiology - Part A: Molecular & Integrative Physiology* **133**, (4):1001-1011.

Altringham J. D. and Johnson I. A. (1990). Modelling muscle power output in a swimming fish. *Journal of Experimental Biology* **148**, 395-402.

Angilletta J. M. J. (2006). Estimating and comparing thermal performance curves. *Journal of Thermal Biology* **31**, 541-545.

Ariano M. A., Armstrong R. B. and Edgerton V. R. (1973). Hind limb muscle fiber populations of five mammals. *Journal of Histochemistry and Cytochemistry* **21**, 51-55

Askew G. N. and Marsh R. L. (2001). The mechanical power output of the pectoralis muscle of blue-breasted quail (*Coturnix chinensis*): the in-vivo length cycle and its implications for muscle performance. *Journal of Experimental Biology*, 204, (21):3587-3600.

Azizi E., Brainerd E. L. and Roberts T. J. (2008). Variable gearing in pennate muscles. *Proceedings of the National Academy of Sciences of the United States of America* **105**, (5):1745-1750.

Bennet-Clark H.C. and Lucey E.C.A. (1967). The Jump of the flea: a study of the energetics and a model of the mechanism. *Journal of Experimental Biology* **47**, 59-76.

Bennett M. B. (1987). Fast locomotion of some kangaroos. *Journal of Zoology* **212**, 457-464.

Bennett M. B. and Taylor G. C. (1995). Scaling of elastic strain energy in kangaroos and the benefits of being big. *Nature* **378**, 56-59.

Bertram J. E. A, Ruina A., Cannon C.E., Chang Y.H. and Coleman MJ. (1999). A point-mass model of gibbon locomotion. *Journal of Experimental Biology*, 202, 2609-2617.

Bertram J. E. A. and Chang Y. H. (2001). Mechanical energy oscillations of two brachiation gaits: measurement and simulation. *American Journal of Physical Anthropology* **115**, 319-326.

Biewener A. A. (1989). Scaling body support in mammals: limb posture and muscle mechanics. *Science* **245**, 45-48.

Biewener A. A. (1998a). Muscle-tendon stresses and elastic energy storage during locomotion in the horse. *Comparative Biochemistry and Physiology B. Biochemistry and Molecular Biology* **120**, 73-87.

Biewener A. A. (1998b). Muscle function in vivo: a comparison of muscles used for elastic energy savings versus muscles used to generate mechanical power. *American Zoologist* **38**, 703-717.

Biewener A. A. and Daley M. A. (2007). Unsteady locomotion: integrating muscle function with whole body dynamics and neuromuscular control. *Journal of Experimental Biology* **210**, (17):2949-2960.

Bischoff L. W. (1870). Beiträge zur anatomie des hylobates leuciscus und zu einer vergleichenden anatomie der muskeln der affen und des menschen. *Abhandlungen der Königlich Bayerischen Akademie der Wissenschaften. Mathematisch-physikalische Klasse* **10**, (3):, 198-297.

Blanchard M. L. (2007). Locomotor behavior and ecology of three sympatric lemur species in Mantadia National Park, Madagascar. PhD Thesis, Liverpool: University of Liverpool pp. 336-337.

Blundon J. A. (1988). Morphology and muscle stress of chelae of temperate and tropical stone crabs Minippe mercenaria. *Journal of Zoology* **215**, 663-73

Bramblett C. A. (1967). Pathology of the Darajani baboon. *American Journal of Physical Anthropology* **26**, 331-340.

Brand R. A., Pederson D. R. and Friederich J. A. (1986). The sensitivity of muscle force predictions to changes in physiological cross-sectional area. *Journal of Biomechanics*, 19, 589-596.

Britt A. (1996). Environmental Influences on the behavioural ecology of the black-and-white ruffed lemur (*Varecia variegata variegata*, Kerr 1792). PhD. Dissertation, The University of Liverpool.

Buickstra J. A. (1975). Healed fractures in *Macaca mulatta*: age, sex and symmetry. *Folia Primatologica* **23**, 140-148.

Burkholder T. J., Fingado B., Baron S. and Lieber R. L. (1994). Relationship between muscle fiber types and sizes and muscle architectural properties in the mouse hind limb. *Journal of Morphology* **221**, 177-190.

Byrnes G., Lim N. T. L. and Spence A. J. (2008). Take-off and landing kinetics of a free-ranging gliding mammal, the malayan colugo (*Galeopterus variegatus*). *Proceedings of the Royal Society B. Biological Sciences* **275**, (1638):1007-1013.

Caravaggi P., Pataky P., Goulermas J. Y., Savage R. and Crompton R. H. (2009). A dynamic model of the windlass mechanism of the foot: Evidence for early stance phase preloading of the plantar aponeurosis. *Journal of Experimental Biology* **212**, 2491-2499.

Carroll A. M., Lee D. V. and Biewener A. A. (2008). Differential muscle function between muscle synergists: long and lateral heads of the triceps in jumping and landing goats (Capra hircus). *Journal of Applied Physiology* **105**, 1262-1273

Cavangna G. A, Heglund N. C. and Taylor C. R. (1977). Mechanical work in terrestrial locomotion: two basic mechanisms for minimizing energy expenditure. *American Journal of Physiology-Regulatory and Integrative Comparative Physiology* **233**, 243-261.

Chandler R., Clauser C., McConville J., Reynolds H. and Young J. (1974). Investigation of inertial properties of the human body. Washington, U. S. Department of Transportation.

Chang Y. H., Bertram J. E. A. and Lee D. V. (2000). External forces and torques generated by the brachiating white-handed gibbon (*Hylobates lar*). *American Journal of Physical Anthropology* **113**, (2):201-216.

Channon A. J. Günther M. M., Crompton R. H. and Vereecke E. E. (2009). Mechanical constraints on the functional morphology of the gibbon hind limb. *Journal of Anatomy* **215**, (4):383-400.

Channon A. J., Crompton R. H., Gunther M. M. and Vereecke E. E. (2010). Muscle moment arms of the gibbon hind limb: implications for hylobatid locomotion. *Journal of Anatomy* **216**, (4):446-462.

Channon A. J., Crompton R. H., Günther M. M., D'Août K. and Vereecke E. E. (In press). The biomechanics of leaping in gibbons. *American Journal of Physical Anthropology.*

Cheng K. B. and Hubbard M. (2004). Optimal jumping strategies from compliant surfaces: A simple model of springboard standing jumps. *Human Movement Science* **23**, 35-48.

Cheng K. B. and Hubbard M. (2008). Role of arms in somersaulting from compliant surfaces: A simulation study of springboard standing dives. *Human Movement Science* **27**, 80-95.

Cheng K. B., Wang C. H., Chen H. C., Wu C. D. and Chiu H. T. (2008). The mechanisms that enable arm motion to enhance vertical jump performance – A simulation study. *Journal of Biomechanics* **41**, 1847-1854.

Clauser C., McConville J. and Young J. (1969). Weight, volume and centre of mass of segments of the human body. North American Space Agency.

Close R. I. (1972) Dynamic properties of mammalian skeletal muscles. *Physiological Reviews* **52**, 129-197.

Craven P. and Wahba G. (1978) Smoothing noisy data with spline functions. *Numerische Mathematik* **31**, 377-403.

Creel N. and Preuschoft H. (1984). Systematics of the lesser apes: a quantitative taxonomic analysis of craniometric and other variables. The lesser apes. Evolutionary and behavioural biology. Eds. Preuschoft, Chivers, Brockelman, Creel. Edinburgh, Edinburgh University Press. 562-614.

Crompton R. H., Blanchard M. L., Coward S., Alexander R. M. and Thorpe S. K. S. (In press). Vertical clinging and leaping revisited: Locomotion and habitat use in the western tarsier, *Tarsius bancanus* explored through loglinear modelling. *International Journal of Primatology.*

Crompton R. H., Sellers W. I., Günther M. M. (1993). Energetic efficiency and ecology as selective factors in the saltatory adaptation of prosimian primates. Proceedings of the Royal Society London B: Biological Sciences **254**, 41-45.

Crompton R. H., Li Y., Alexander R. M., Wang W. and Günther M. M. (1996) Segment inertial properties of primates: New techniques for laboratory and field studies of locomotion. *American Journal of Physical Anthropology* **99**, 547-570.

Crompton R. H., Weijie L. Y. W., Günther M. and Savage R. (1998). The mechanical effectiveness of erect and "bent-hip, bent-knee" bipedal walking in *Australopithecus afarensis*. *Journal of Human Evolution* **35**, (1):55-74.

Crompton R. H. and Sellers W. I. (2007). A consideration of leaping locomotion as a means of predator avoidance in prosimian primates. Primate Anti-Predator Strategies. Gursky, S. and Nekaris, K. Stuttgart, Springer: 127-145.

Crompton R. H., Vereecke E. E. and Thorpe S. K. S. (2008). Locomotion and Posture from the Common Hominoid Ancestor to Fully Modern Hominins, with Special Reference to the Last Common Panin/Hominin Ancestor. *Journal of Anatomy*. **212**, (4):501-543.

Daley M. A. and Biewener A. A. (2003). Muscle force–length dynamics during level versus incline locomotion: a comparison of in vivo performance of two guinea fowl ankle extensors. *Journal of Experimental Biology*, 206, 2941-2958.

Daley M. A., Usherwood J. R., Felix G. and Biewener A. A. (2006). Running over rough terrain: guinea fowl maintain dynamic stability despite a large unexpected change in substrate height. *Journal of Experimental Biology*, 209, (1):171-187.

D'Août K., Vereecke E. E., Schoonaert K., Clercq D. D., ElsackerL. V. and Aerts P. (2004). Locomotion in bonobos (*Pan paniscus*): differences and similarities between bipedal and quadrupedal terrestrial walking, and a comparison with other locomotor modes. *Journal of Anatomy*, 204, (5):353-361.

Delp S. L., Ringwelski D. A. and Carroll N. C. (1994) Transfer of the rectus femoris: effects of transfer site on moment arm about the knee and hip. *Journal of Biomechanics* **27**, 1201-1211.

Demes B. and Günther M. M. (1989). Biomechanics and allometric scaling in primate locomotion and morphology. *Folia Primatologica* **53**, 125-141.

Demes B., Forchap E. and Herwig H. (1991). They seem to glide. Are there aerodynamic effects in leaping prosimians. *Zeitschrift für Morphologie und Anthropologie* **78**, 373-385.

Demes B., Jungers W. L., Gross T. S. and Fleagle J. G. (1995). Kinetics of leaping primates: Influence of substrate orientation and compliance. *American Journal of Physical Anthropology* **96**, 419-429.

Demes B., Fleagle J. G. and Jungers W. L. (1999). Takeoff and landing forces of leaping strepsirrhine primates. *Journal of Human Evolution* **37**, 279-292.

DeSilva J.M. (2009). Revisiting the "midtarsal break". *American Journal of Physical Anthropology* **141**, 245-258.

Doran D. M. (1993). Comparative locomotor behavior of chimpanzees and bonobos: the influence of morphology on locomotion. *American Journal of Physical Anthropology* **91**, (1):83-98.

Eng C. M., Smallwood L. H., Rainiero M. P., Lahey M., Ward S. R. and Lieber, R. L. (2008). Scaling of muscle architecture and fiber types in the rat hind limb. *Journal of Experimental Biology* **211**, (14):2336-2345.

Epperson J. F. (1987) On the Runge example. *The American Mathematical Monthly* **94**, 329-341.

Essner R. L., Jr. (2002). Three-dimensional launch kinematics in leaping, parachuting and gliding squirrels. *Journal of Experimental Biology*, 205, (16):2469-2477.

Fleagle J. G. (1974). The dynamics of the brachiating siamang (*Hylobates* [*Symphalangus*] *syndactylus*). *Nature* **248**, 259-260.

Fleagle J. G. (1976). Locomotion and posture of the Malayan siamang and implications for hominoid evolution. *Folia Primatologica* **26**, 245-269.

Friederich J. A. and Brand R. A. (1990). Muscle fascicle architecture in the human lower limb. *Journal of Biomechanics* **23**, 91-95.

Fukunaga T., Miyatani M., Tachi M., Kouzaki M., Kawakami Y. and Kanehisa H. (2001). Muscle volume is a major determinant of joint torque in humans. *Acta Physiological Scandinavica* **172**, 249-255.

Fukunaga T., Roy R. R. and Shellock F. G. (1992). Physiological cross-sectional area of human leg muscles based on magnetic resonance imaging. *Journal of Orthopedic Research* **10**, 926-934.

Gans C. and Gaunt A. S. (1991). Muscle architecture in relation to function. *Journal of Biomechanics* **24**, 53-65.

Garner B. A. and Pandy M. G. (2001). Musculoskeletal model of the upper limb based on the visible human male dataset. *Computer Methods in Biomechanics and Biomedical Engineering* **4**, 93-126.

Gittins S. P. (1983) Use of the forest canopy by the agile gibbon. *Folia Primatologica* **40**, 134-144.

Graichen H., Englmeier K. H., Reiser M. and Eckstein F. (2001). An in vivo technique for determining 3D muscular moment arms in different joint positions and during muscular activation - application to the supraspinatus. *Clinical Biomechanics* **16**, 389-394.

Green J. A., HalseyL. G., Wilson R. P. and Frappell P. B. (2009). Estimating energy expenditure of animals using the accelerometry technique: activity, inactivity and comparison with the heart-rate technique. *Journal of Experimental Biology* **212**, (4):471-482.

Griffiths R. I. (1991). Shortening of muscle fibres during stretch of the active cat medial gastrocnemius muscle: the role of tendon compliance. *Journal of Physiology* **436**, 219–236.

Günther M. M. (1989). Funktionsmorphologische uuntersuchungen zum sprungverhalten an mehreren halbaffenarten. PhD Thesis, Berlin.

Günther M. M., Ishida H., Kumakura H. and Nakano Y. (1991). The jump as a fast mode of locomotion in arboreal and terrestrial biotopes. *Zeitschrift für Mophologie und Anthropologie* **78**, (3):341-372.

Hara M., Shibayama A., Arakawa H. and Fukashiro S. (2008). Effect of arms swing direction on forward and backward jump performance. *Journal of Biomechanics* **41**, 2806-2815.

Hase K. and Stein R. B. (1999). Turning strategies during human walking. *Journal of Neurophysiology* **81**, 2914-2922.

Hildebrand M. and Hurley J. (1985). Energy of the oscillating legs of a fast moving cheetah, pronghorn, jackrabbit and elephant. *Journal of Morphology*, 184, 23-31.

Hill T. L. (1968). On the Sliding-Filament Model of Muscular Contraction. *Proceedings of the National Academy of Sciences of the United States of America* **61**, (1):98-105.

Hirasaki E., Ogihara N. and Nakatsukasa M. (2006). Primates trained for bipedal locomotion as a model for studying the evolution of bipedal locomotion. In Human Origins and Environmental Backgrounds, pp. 149-155.

Hiroyuki A., Kozaburo H. and Masaaki S. (1996). Data Book on Mechanical Properties of Living Cells, Tissues, and Organs, Springer, Tokyo.

Hou H. and Andrews H. (1978) Cubic splines for image interpolation and digital filtering. *IEEE transactions on acoustics, speech and signal processing* **26**, 508-517.

Huang C. and Li Y. (2005). How does the white-headed langur (Trachypithecus leucocephalus) adapt locomotor behavior to its unique limestone hill habitat? *Primates* **46**, 261-267.

Hunt K. D. Cant J. G. H., Gebo D., Rose M. D., Walker S. E. and Youlatos D. (1996). Standardized descriptions of primate locomotor and postural modes. *Primates* **37**, 363-387.

Isler K. (2005). 3D-Kinematics of vertical climbing in hominoids. *American Journal of Physical Anthropology* **126**, 66-81.

Isler K., Payne R. C., Günther M. M., Thorpe S. K. S, Li Y., Savage R. and Crompton R. H. (2006) Inertial properties of hominoid limb segments. *Journal of Anatomy*, 209, 201-218.

IUCN. (2008). The IUCN red list of threatened species. www.iucnredlist.org

Jayes A. S. and Alexander R. M. (1982). Estimates of mechanical stresses in leg muscles of galloping greyhounds (*Canis familiaris*). *Journal of Zoology*, 198, 315-328.

Jeffrey A. (2005). Mathematics for engineers and scientists, sixth edition. London: Chapman and Hall.

Jones S., Martin R. and Pilbeam D. (1992). The cambridge encyclopedia of human evolution. Cambridge University Press, Cambridge.

Jungers W. L. (1985). Body Size and Scaling in Primate Biology. New York: Plenum Press. Edited by Jungers WL. pp. 345-382.

Jungers W. L. (1988). Relative Joint Size and Hominoid Locomotor Adaptations with Implications for the Evolution of Hominid Bipedalism. *Journal of Human Evolution* **17**, (1-2):247-265.

Jungk R. A., Snyder H. E., Goll D. E., and McConnell K. G. (1967). Isometric tension changes and shortening in muscle strips during post-mortem aging. *Journal of Food Science* **32**, 158-161.

Kanagsuntheram R. (1952). Observations on the anatomy of the hoolock gibbon. *Celyon Journal of Science* **5**, 11-64.

Kappeler M. (1984). Diet and Feeding Behaviour of the Moloch Gibbon. In The Lesser Apes, Evolutionary and Behavioral Biology. (eds. H. Preuschoft, D. Chivers, W. Brockelman and N. Creel), pp. 228-241. Edinburgh: Edinburgh University Press.

Kawakami Y., Muraoka T., Ito S., Kanehisa H. and Fukunaga T. (2002). In vivo muscle fibre behaviour during counter-movement exercise in humans reveals a significant role for tendon elasticity *Journal of Physiology* **540**, 635–646

Ker R. F., Alexander R. M. and Bennet M. (1988). Why Are Mammalian Tendons So Thick? *Journal of Zoology London* **216**, 309-324.

Kinzey W. G., Rosenberger A. L. and Ramirez M. (1975). Vertical clinging and leaping in a neotropical anthropoid. *Nature* **255**, (5506):327-328.

Kooi B. and Kuipers M. (1994). The Dynamics of Springboards. *Journal of Applied Biomechanics* **10**, 335-351.

Kramer P. A. (1999) Modelling the locomotor energetics of extinct hominids. *Journal of Experimental Biology* **202**, 2807-2818.

Krevolin J. K., Pandy M. G. and Pearce J. C. (2004). Moment arm of the patellar tendon in the human knee. *Journal of Biomechanics* **37**, 785-788

Legnani G., Zappa B., Casolo F., Adamini R. and Magnani P. L. (2000). A model of an electro-goniometer and its calibration for biomechanical applications. *Medical Engineering and Physics* **22**, 711-722.

Legreneur P., Thevenet F.-R., Libourel P.-A., Monteil K. M., Montuelle S., Pouydebat E. and Bels V. (2010). Hind limb interarticular coordinations in microcebus murinus in maximal leaping. *Journal of Experimental Biology* **213**, (8):1320-1327.

Lessels C. M. and Boag P. T. (1987). Unrepeatable repeatabilities: a common mistake. *The Auk* **104**, 116-121.

Lichtwark G. A. and Wilson A. M. (2005) In vivo mechanical properties of the human Achilles tendon during one-legged hopping. *Journal of Experimental Biology*, 208, 4715-4725.

Lichtwark G.A., Bougoulias K., and Wilson A.M. (2006). Muscle fibre and series elastic element length changes along the length of the gastrocnemius during walking and running. *Journal of Biomechanics* **40**, 157-164.

Lieber R. L. and Friden J. (2001). Clinical significance of skeletal muscle architecture. *Clinical Orthopaedics and Related Research* **383**, 140-151.

Lieberman D. E., Venkadesan M., Werbel W. A., Daoud A. I., D'Andrea S., Davis I. S., Mang'Eni R. O. and Pitsiladis Y. (2010). Foot strike patterns and collision forces in habitually barefoot versus shod runners. *Nature* **463**, (7280):531-535.

Linthorne N. P., Guzman M. S. and Bridgett L. A. (2005). Optimum take-off angle in the long jump. *Journal of Sport Science* **23**, 703-712

Lovell N. C. (1987). Skeletal pathology of pongids. *American Journal of Physical Anthropology* **72**, 227 (abstract).

Lutz G. J. and Rome L. C. (1994). Built for jumping: the design of the frog muscular system. *Science* **263**, (5145):370-372.

MacFadden L. N. and Brown N. A. T. (2007). Biarticular hip extensor and knee flexor muscle moment arms of the feline hind limb. *Journal of Biomechanics* **40**, 3448-3457.

MacLatchy L. and Müller R. (2002). A comparison of the femoral head and neck trabecular architecture of Galago and Perodicticus using micro-Computed Tomography ([Mu]Ct). *Journal of Human Evolution* **43**, (1):89-105.

Marey E. J. (1894). Des mouvements que certains animaux exécutent pour retomber sur leurs pieds lorsqu'ils sont précipités d'un lieu élevé. *Comptes rendus hebdomadaires des séances de l'Académie des Sciences* **119**, 714-717.

Marsh R. L. and Bennett A. F. (1986). Thermal dependence of contractile properties of skeletal muscle from the lizard Sceloporus occidentalis with comments on methods for fitting and comparing force-velocity curves. *Journal of Experimental Biology* **126**, 63-77

Maughan R. J., Watson J. S. and Weir J. (1983). Strength and cross-sectional area of human skeletal muscle. *Journal of Physiology* **338**, 37-47.

McClearn D. (1985). Anatomy of racoon (*Procyon lotor*) and coati (*Nasua narica* and *N. nasua*) forearm and leg muscles: relations between fiber length, moment-arm length, and joint angle excursion. *Journal of Morphology* **183**, 87-115.

McClure H. (1964). Some Observations of Primates in Climax Diptocarp Forest near Kuala Lumpur, Malaya. *Primates* **5**, (3):39-58.

McGowan C. P., Baudinette R. V., Usherwood J. R. and Biewener A. A. (2005). The mechanics of jumping versus steady hopping in yellow-footed rock wallabies. *Journal of Experimental Biology*, 208, 2741-2751.

McGowan C. P., Skinner J. and Biewener A. A. (2008). Hind limb scaling of kangaroos and wallabies (superfamily Macropodoidea): implications for hopping performance, safety factor and elastic savings. *Journal of Anatomy* **212**, 153-163.

McMahon T. A. and Kronauer R. E. (1976). Tree structures: deducing the principle of mechanical design. *Journal of Theoretical Biology* **59**, 443-466.

McMahon T. A. and Greene P. R. (1979). The influence of track compliance on running. *Journal of Biomechanics* **12**, (12):893-904.

McNitt-Gray J. L., Yokoi T. and Millward C. (1994). Landing strategies used by gymnasts on different surfaces. *Journal of Applied Biomechanics* **10**, 237-252.

Medler S. (2002). Comparative trends in shortening velocity and force production in skeletal muscles. *American Journal of Regulatory, Integrative and Comparative Physiology* **283**, 368-378.

Meershoek L., Van den Bogert A. and Schamhardt H. (2001). Model formulation and determination of in-vitro parameters of a non invasive method to calculate flexor tendon forces in the equine forelimb. *American Journal of Veterinary Research* **62**, 1585-1593.

Mendez J. and Keys A. (1960). Density and composition of mammalian muscle. *Metabolism* **9**, 184-188.

Michilsens F., Vereecke E., E. , D'Août K. and Aerts P. (2009). Functional anatomy of the gibbon forelimb: adaptations to a brachiating lifestyle. *Journal of Anatomy* **215**, (3):335-354.

Miller C. E., Basu C., Fritsch G., Hildebrand T., Hutchinson J. R. (2008). Ontogenetic scaling of foot musculoskeletal anatomy in elephants. *Journal of Royal Society Interface* **5**, 465-475.

Milton K. and May M. L. (1976). Body weight, diet and home range area in primates. *Nature* **259**, (5543):459-462.

Moritz C. T. and Farley C. T. (2005). Human hopping on very soft elastic surfaces: implications for muscle pre-stretch and elastic energy storage in locomotion. *Journal of Experimental Biology*, 208, (5):939-949.

Murray W. M., Delp S. L. and Buchanan T. S. (1995). Variation of muscle moment arms with elbow and forearm position. *Journal of Biomechanics* **28**, 513-525.

Muybridge E. (1887). An electro-photographic investigation of consecutive phases of animal movements. Philadelphia, University of Pennsylvania.

Nagy M., Akos Z., Biro D. and Vicsek T. (2010). Hierarchical group dynamics in pigeon flocks. *Nature* **464**, (7290):890-893.

National Instruments (2010). http://zone.ni.com/reference/en-XX/help/371361E-01/gmath/cubic_spline_fit/\

Nauwelaerts S. and Aerts P. (2006). Take-off and landing forces in jumping frogs. *Journal of Experimental Biology*, 209, 66-77.

Németh G. and Ohlsén H. (1985). In vivo moment arm lengths for hip extensor muscles at different angles of hip flexion. *Journal of Biomechanics*, 18, 129-140.

Oxnard C.E., Crompton R.H. and Lieberman S. S. (1990). Animal Lifestyles and Anatomies. Washington: Washington University Press.

Pandy M. G. (1999). Moment arm of a muscle force. *Exercise and Sport Sciences Reviews* **27**, 79-118.

Payne R. C., Hutchinson J. R., Robilliard J. J., Smith N. C. and Wilson A. M. (2005). Functional specialisation of pelvic limb anatomy in horses (*Equus caballus*). *Journal of Anatomy*, 206, 557-574.

Payne R. C., Crompton R. H., Isler K., Savage R., Vereecke E. E., Günther M. M., Thorpe S. K. S and D'Août K. (2006a). Morphological analysis of the hind limb in apes and humans. I. Muscle architecture. *Journal of Anatomy*, 208, 709-724.

Payne R. C., Crompton R. H., Isler K., Savage R., Vereecke E. E., Günther M. M., Thorpe S. K. S and D'Août K. (2006b). Morphological analysis of the hind limb in apes and humans. II. Moment arms. *Journal of Anatomy*, 208, 725-742.

Pelletier D., Guillemette M., Grandbois J.M. and Butler P. J. (2007). It is time to move: linking flight and foraging behaviour in a diving bird. *Biology Letters* **3**, (4):357-359.

Pette D. and Staron R. (2001). Transitions of muscle fiber phenotypic profiles. *Histochemistry and Cell Biology* **115**, (5):359-372.

Pette D. and Staron R. S. (1997). Mammalian skeletal muscle fiber type transitions. *International Review of Cytology* **170**, 143-223.

Pfau T., Ferrari M., Parsons K. and Wilson A. M. (2008). A Hidden Markov Model-based stride segmentation technique applied to equine inertial sensor trunk movement data. *Journal of Biomechanics* **41**, (1):216-220.

Pfau T., Spence A. J., Starke S., Ferrari M. and Wilson A. M. (2009). Modern riding style improves horse racing times. *Science* **325**, (5938):289.

Pollock C. M. and Shadwick R. E. (1994). Allometry of muscle, tendon, and elastic energy storage capacity in mammals. *American Journal of Regulatory, Integrative and Comparative Physiology* **266**, 1022-1031.

Prassas S., Kwon Y. H. and Sands W. A. (2006) Biomechanical research in artistic gymnastics: a review, *Sports Biomechanics* **5**, (2):261-291.

Preece S. J., Goulermas J. Y., Kenney L. P. J., Howard D., Meijer K. and Crompton R.H. (2009). Activity identification using body-mounted sensors—a review of classification techniques. *Physiological Measurements* **30**, R1–R33.

Preuschoft H. and Demes B. (1984). Biomechanics of brachiation. In The Lesser Apes (eds Preuschoft H, Chivers DJ, Brockelman WY, Creel N), pp. 96-118. Edinburgh: Edinburgh University Press.

Preuschoft H. (1985). On the quality and magnitude of mechanical stresses in the locomotor system during rapid movements. *Zeitschrift für Mophologie und Anthropologie* **75**, 245-262.

Preuschoft H. and Demes B. (1985). Influence of size and proportions on the biomechanics of brachiation. Size and Scaling in Primate Biology. Jungers, W. L. New York, Plenum Press.

Preuschoft H. and Witte H. (1991). Biomechanical reasons for the evolution of hominin body shape. Origines de la bipédie chez les hominids, Editions du CNRS, Paris, 59-77.

Preuschoft H., Witte H. and Demes B. (1992). Biomechanical factors the influence overall body shape of large apes and humans. Topics in Primatology Volume 3: Evolutionary Biology, Reproductive Endocrinology and Virology, University of Tokyo press, Tokyo.

Preuschoft H. and Günther M. M. (1994). Biomechanics and body shape in primates compared with horses. *Folia Primatologica* **53**, 125-141.

Preuschoft H., Witte H., Christian A. and Fischer M. (1996). Size influences on primate locomotion and body shape, with special emphasis on the locomotion of 'small mammals'. *Folia Primatologica* **66**, 93-112.

Preuschoft H., Günther M. M. and Christian A. (1998). Size dependence in prosimian locomotion and its implications for the distribution of body mass. *Folia Primatologica* **69**, 60-81.

Preuschoft H. (2002). What does "arboreal locomotion" mean exactly and what are the relationships between "climbing", environment and morphology? *Zeitschrift für Mophologie und Anthropologie* **83**, 171-188.

Reinsch C. (1967). Smoothing by spline functions. *Numerische Mathematik* **10**, 177-183.

Rubenson J. and Marsh R. L. (2009). Mechanical efficiency of limb swing during walking and running in guinea fowl (*Numida meleagris*). *Journal of Applied Physiology* **106**, 1618-1630.

Rugg S. G., Gregor R. J., Mandelbaum B. R. and Chiu L. (1990). In vivo moment arm calculations at the ankle using magnetic resonance imaging (MRI). *Journal of Biomechanics* **23**, 495-497.

Saltin B., Henriksson J., Nygaard E. and Andersen P. (1977). Fiber types and metabolic potentials of skeletal muscles in sedentary man and endurance runners. *Annals New York Academy of Sciences* **301**, 3-29

Sati J. and Alfred J. (2002). Locomotion and posture in hoolock gibbon. *Annals of Foresty* **10**, 298-306.

Schmitt D. (1994). Forelimb mechanics as a function of substrate type during quadrupedalism in two anthropoid primates. *Journal of Human Evolution* **26**, 441-458.

Schmitt D. (1999). Compliant walking in primates. *Journal of Zoology* **248**, (02):149-160.

Schmitt D. (2003). Insights into the evolution of human bipedalism from experimental studies of humans and other primates. *Journal of Experimental Biology*, 206, 1437-1448.

Scholz M. N., D'Août K., Bobbert M. F. and Aerts P. (2006). Vertical jumping performance of bonobo (*Pan paniscus*) suggests superior muscle properties. *Proceedings of the Royal Society B: Biological Sciences* **273**, 2177-2184.

Scholz M. N., Bobbert M. F., Van Soest A. J., Clark J. R. and Van Heerden J. (2008). Running biomechanics: shorter heels, better economy. *Journal of Experimental Biology* **211**, 3266-71.

Schultz A. H. (1936). Characters common to higher primates and characters specific to man. *Quarterly Reviews in Biology* **11**, 425-45.

Schultz A. H. (1956). The occurrence and frequency of pathological and teratological conditions and of winning among non-human primates. *Folia Primatologica* **1**, 965-1014.

Sellers W. I. (1992). A study of leaping prosimian primates. Department of Human Anatomy and Cell Biology. Liverpool, University of Liverpool. PhD Thesis.

Sellers W. I. and Crompton R. H. (1994). A system for 2- and 3D kinematic and kinetic analysis of locomotion, and its application to analysis of the energetic efficiency of jumping locomotion. *Zeitschrift für Mophologie und Anthropologie* **80**, (1):99-108.

Sellers W. I. and Crompton R. H. (2004). Automatic monitoring of primate locomotor behaviour using accelerometers. *Folia Primatologica* **75**, 279-293.

Sellers W. I., Cain G. M., Wang W. and Crompton R. H. (2005). Stride lengths, speeds and energy costs in walking of Australopithecus afarensis: using evolutionary robotics to predict locomotion of early human ancestors. *Journal of the Royal Society: Interface* **2**, 431-441.

Sellers W. I. and Manning P. L. (2007). Estimating dinosaur maximum running speeds using evolutionary robotics. *Proceedings of the Royal Society B: Biological Sciences* **274**, 2711-2716.

Sheehan F. T. (2007). The 3-D patellar tendon moment arm: Quantified in vivo during volitional activity. *Journal of Biomechanics* **40**, 1968-1974.

Sigmon B. A. and Farslow D. L. (1986). The primate hind limb. *Comparative Primate Biology* **1**, 671-718.

Späth H. and Meier J. (1988). Flexible smoothing with periodic cubic splines and fitting with closed curves. *Computing* **40**, 293-300.

Spoor C. W. and Van Leeuwen J. L. (1992). Knee muscle moment arms from MRI and from tendon travel. *Journal of Biomechanics* **25**, 201-206.

Stern J. T. (1972). Anatomical and functional specialisations of the human gluteus maximus. *American Journal of Physical Anthropology* **36**, 315-339.

Steudel K. (1990). The work and energetic cost of locomotion. I. The effects of limb mass distribution in quadrupeds. *Journal of Experimental Biology* **154**, 273-285.

Steudel K. (1996). Limb morphology, bipedal gait, and the energetics of hominid locomotion. *American Journal of Physical Anthropology* **99**, 345-355.

Stevens J. L., Mitton S. and Edgerton V. R. (1972). Gross anatomy of hind limb skeletal muscles of the Galago senegalensis. *Primates* **13**, (1):83-101.

Stevens N. (2008). Linking in-situ and ex-situ approaches for studying primate locomotor responses to support stability. *Abstract: International Primatological Society Meeting.* Edinburgh, UK. pp.762.

Thomason J. J. (1985). The relationship of trabecular architecture to inferred loading patterns in the third metacarpals of the extinct equids merychippus and mesohippus. *Paleobiology* **11**, (3):323-335.

Thomason J. J. (1995). To what extent can the mechanical environment of a bone be inferred from its internal architecture? Functional Morphology in Vertebrate Paleontology. Thomason, J. J. Cambridge, Cambridge University Press: 249-263.

Thorpe S. K. S, Crompton R. H., Gunther M. M., Ker R. F. and Alexander R. M. (1999). Dimensions and moment arms of the hind- and forelimb muscles of common chimpanzees (*Pan troglodytes*). *American Journal of Physical Anthropology* **110**, 179-199.

Thorpe S. K. S, Crompton R. H. and Wang W. J. (2004). Stresses exerted in the hind limb muscles of common chimpanzees (*Pan troglodytes*) during bipedal locomotion. *Folia Primatologica* **75**, 253-265.

Thorpe S. K. S and Crompton R. H. (2005). The locomotor ecology of wild orang-utans (*Pongo pygmaeus abelii*) in the Gunung Leuser ecosystem, Sumatra, Indonesia: a multivariate analysis using log-linear modelling. *American Journal of Physical Anthropology* **127**, 58-78.

Thorpe S. K. S and Crompton R. H. (2006). Orang-utan positional behavior and the nature of arboreal locomotion in Hominoidea. *American Journal of Physical Anthropology* **131**, 384-401.

Thorpe S. K. S, Crompton R. H. and Alexander R. M. (2007a). Orangutans utilize compliant branches to lower the energetic cost of locomotion. *Biology Letters* **3**, 253-256.

Thorpe S. K. S., Holder R. L. and Crompton R. H. (2007b). Origin of human bipedalism as an adaptation for locomotion on flexible branches. *Science* **316**, (5829):1328-1331.

Thorpe S. K. S., Holder R. and Crompton R. H. (2009). Orangutans employ unique strategies to control branch flexibility. *Proceedings of the National Academy of Sciences* **106**, (31):12646-12651.

Tuttle R. H. (1981). Evolution of hominid bipedalism and prehensile capabilities. *Philosophical Transactions of the Royal Society B: Biological Sciences* **292**, 89-94.

Usherwood J. R and Bertram J. E. A. (2003). Understanding brachiation: insight from a collisional perspective. *Journal of Experimental Biology*, 206, 1631-1642.

Usherwood J. R. (2008). Collared Doves Streptopelia Ecaocto Display with High, near-Maximal Muscle Powers, but at Low Energetic Cost. *Journal of Avian Biology* **39**, (1):19-23.

Van Ingen Schenau G. J. (1989). From rotation to translation: constraints on multi-joint movements and the unique action of bi-articular muscles. *Human Movement Science* **8**, (4):301-337.

Vereecke E. E., D'Août K., Payne R., Aerts P. (2005). Functional analysis of the foot and ankle myology of gibbons and bonobos. *Journal of Anatomy*, 206, 453-476.

Vereecke E. E., D'Août K. and Aerts P. (2006a). Locomotor versatility of the white-handed gibbon (*Hylobates lar*): a spatiotemporal analysis of the bipedal, tripedal and quadrupedal gaits. *Journal of Human Evolution* **50**, 552-567.

Vereecke E. E., D'Août K. and Aerts P. (2006b). The dynamics of hylobatid bipedalism: evidence for an energy-saving mechanism? *Journal of Experimental Biology*, 209, 2829-2838.

Vereecke E. E and Aerts P. (2008). The mechanics of the gibbon foot and its potential for elastic energy storage during bipedalism. *Journal of Experimental Biology* **211**, 3661-3670.

Vereecke E. E., Channon A. J. and Ker R. F. (2008). The mechanical properties of the gibbon Achilles tendon and its role in locomotion. *Comparative Biochemistry and Physiology A: Molecular and Integrative Physiology* **150**, (3, Supplement 1):S75-S75.

Visser J. J., Hoogkamer J. E., Bobbert M. F. and Huijing P. A. (1990). Length and moment arm of human leg muscles as a function of knee and hip-joint angles. *European Journal of Applied Physiology* **61**, 453-460.

Wakeling J. M., Uehli1 K. and Rozitis A. I. (2006). Muscle fibre recruitment can respond to the mechanics of the muscle contraction. *Journal of the Royal Society: Interface* **3**, 533–544

Warren R. D. and Crompton R. H. (1997). Locomotor ecology of Lepilemur edwardsi and Avahi occidentalis. *American Journal of Physical Anthropology* **104**, 471-486.

Wells J. B. (1965). Comparison of mechanical properties between slow and fast mammalian muscle. *Journal of Physiology* **178**, 252-269.

Westing S. H., Cresswell A. G. and Thorstensson A. (1991). Muscle activation during maximal voluntary eccentric and concentric knee extension. *European Journal of Applied Physiology* **62**, 104-108.

Whitmoor T. C. (1975). Tropical rain forests of the far-east. Clarendon Press, Oxford .

Wickiewicz T. L., Roy R. R., Powell P. L. and Edgerton V. R. (1983). Muscle architecture of the human lower limb. *Clinicial Orthopaedic Related Research* **179**, 275-283.

Widrick J. J., Trappe S. W., Costill D. L. and Fitts R. H. (1996). Force-velocity and force-power properties of single muscle fibers from elite master runners and sedentary men. *The American Journal of Physiology: Cell Physiology* **271**, 676-683.

Williams S. B., Payne R. C. and Wilson A. M. (2007). Functional specialisation of the pelvic limb of the hare (*Lepus europeus*). *Journal of Anatomy* **210**, 472-490.

Williams S. B., Wilson A. M., Rhodes L., Andrews J. and Payne R. C. (2008). Functional anatomy and muscle moment arms of the pelvic limb of an elite sprinting athlete: the racing greyhound (*Canis familiaris*). *Journal of Anatomy* **213**, 361-372.

Williams S. B., Usherwood J. R., Jespers K., Channon A. J. and Wilson A. M. (2009a). Exploring the mechanical basis for acceleration: pelvic limb locomotor function during accelerations in racing greyhounds (*Canis familiaris*). *Journal of Experimental Biology* **212**, 550-565.

Williams S. B., Tan H., Usherwood J. R. and Wilson A. M. (2009b). Pitch then power: limitations to acceleration in quadrupeds. *Biology Letters* **5**, (5):610-613.

Witte H., Preuschoft H. and Recknagel S. (1991). Human body proportions explained on the basis of biomechanical principles. *Funktionelle Morphologie* **3**, 407-423.

Wretenberg P., Németh G., Lamontagne M. and Lundin B. (1996). Passive knee muscle moment arms measured in vivo with MRI. *Clinical Biomechanics* **11**, 439-446.

Yamaguchi G. T. and Zajac F. E. (1989). A planar model of the knee joint to characterize the knee extensor mechanism. *Journal of Biomechanics* **22**, 1-10.

Zajac F. E. (1989). Muscle and tendon: properties, models, scaling and application to biomechanics and motor control. *Critical Reviews in Biomedical Engineering* **17**, 359-411.

Zajac F. E. (1992). How musculotendon architecture and joint geometry affect the capacity of muscles to move and exert force on objects: A review with application to arm and forearm tendon transfer design. *The Journal of Hand Surgery* **17**, 799-804.

Zihlman A. L. (1992) Locomotion as a life history character: the contribution of anatomy. *Journal of Human Evolution* **22**, 315-325.

Appendices

Appendix 2.1. Mean anatomical data on hind limb muscles collected for each species. A dash (-) represents where data was unavailable.

Appendix 3.1. Polynomial approximations to describe the scaled *MA* curves of *Hylobates lar*. Where the curve is described as a n^{th} order polynomial and describes y (scaled *MA*) in terms of $hx^7+gx^6+fx^5+ex^4+dx^3+cx^2+bx+a$ and x is joint angle in degrees. Where it was not possible to obtain a polynomial which minimized the RSS to within 5% of the range a linear curve is quoted, see text for curve fitting methodology.

Appendix 6.1. Sensitivity analysis showing calculation inputs and outputs from the video which was analysed twice. See text for parameter calculation.

Appendix 2.1a

H. lar

THIGH	Mass (g)	MTU Length (cm)	Tendon Length Origin	Tendon Length Insertion	Mean Fascicle Length (cm)	Ext. Tendon length (cm)	Belly Mass (g)
Gluteus superficialis	61.5	19.6	-	6.4	13.2	-	61.5
Gluteus medius	38.1	10.6	-	3.2	5.9	-	38.1
Gluteus minimus	7.4	5.3	-	1.6	3.5	-	7.4
Pectineus	2.8	6.5	-	0.7	5.3	-	2.8
Obturator internus	8.4	6.3	-	2.8	3.6	-	8.4
Obturator externus	7.4	6.5	-	2.2	4.4	-	7.4
Piriformis	6.7	7.8	-	2.1	6.2	-	4.5
Adductor magnus	78.6	21.1	-	8.2	13.8	-	78.5
Adductor longus	6.1	12.6	1.8	3.5	8.7	-	6.1
Adductor brevis	10.6	10.2	-	-	9.8	-	3.5
Quadratus femoris	4.8	4.7	-	-	3.8	-	4.8
Rectus femoris	17.1	20.7	6.3	10.9	9.1	2.8	16.9
Vastus medialis	19.3	18.8	-	8.2	8.4	2.6	19.2
Vastus intermedius	42.1	23.0	-	11.6	8.0	-	42.1
Vastus lateralis	63.2	19.1	7.0	10.8	8.2	3.1	62.9
Gracilis	9.1	23.6	0.8	4.4	21.7	-	9.1
Sartorius	15.3	25.7	2.2	-	24.8	-	15.3
Semimembranosus	9.8	23.5	9.0	7.6	13.1	4.7	9.5
Semitendinosus	17.2	27.0	6.4	6.2	19.0	3.8	17.0
Biceps femoris (Long head)	10.0	23.2	6.4	8.5	9.7	1.6	9.5
Biceps femoris (Short head)	6.5	9.3	-	3.5	5.3	-	6.5
SHANK							
Tibialis anterior	8.7	15.7	-	9.5	7.9	3.2	8.3
Extensor digitorum longus	4.2	24.6	-	19.9	7.6	3.8	3.9
Extensor hallucis longus	2.8	20.4	-	12.9	7.9	5.8	2.7
Peroneus longus	5.8	22.0	-	18.7	5.4	9.7	5.6
Peroneus brevis	2.2	12.3	-	9.6	4.0	-	1.3
Soleus	10.5	17.5	14.7	7.1	5.9	2.4	10.2
Gastrocnemius medialis	12.7	20.0	6.3	15.6	5.9	-	11.8
Gastrocnemius lateralis	16.8	19.1	4.3	14.7	6.4	-	16.8
Plantaris	6.9	18.1	-	15.3	5.0	-	2.3
Tibialis posterior	6.4	20.0	-	16.3	4.7	6.0	6.1
Flexor tibialis	6.1	23.6	-	16.7	7.3	5.0	5.8
Flexor fibularis	21.2	26.7	-	18.7	7.9	6.6	20.6
Popliteus	3.1	5.6	1.7	2.0	2.6	-	3.1

Appendix 2.1b.

H. pileatus

THIGH	Mass (g)	MTU Length (cm)	Tendon Length Origin	Tendon Length Insertion	Mean Fascicle Length (cm)	Ext. Tendon length (cm)	Est. Belly Mass (g)
Gluteus superficialis	38.0	16.1	-	4.4	10.9	-	38.0
Gluteus medius	27.7	11.3	-	6.8	6.3	-	27.7
Gluteus minimus	5.0	7.5	-	1.4	5.4	-	5.0
Pectineus	2.5	5.1	-	-	4.9	-	2.5
Obturator internus	7.8	6.9	-	4.4	3.2	-	7.8
Obturator externus	5.2	5.1	-	2.0	2.8	-	2.6
Piriformis	5.6	8.0	-	3.8	4.4	-	5.6
Adductor magnus	49.0	21.5	-	10.3	13.0	5.8	48.9
Adductor longus	11.3	11.7	-	4.4	8.7	-	11.3
Adductor brevis	3.7	7.2	-	-	5.7	-	1.9
Quadratus femoris	2.4	3.3	-	-	3.3	-	2.4
Rectus femoris	11.7	20.8	14.7	16.4	8.3	1.8	10.2
Vastus medialis	19.8	21.8	-	17.2	8.3	2.4	9.4
Vastus intermedius	33.7	23.6	-	17.3	7.7	-	33.7
Vastus lateralis	37.9	23.1	12.5	10.8	8.3	-	37.9
Gracilis	6.8	20.7	-	4.5	17.3	4.4	6.7
Sartorius	9.8	23.6	4.1	-	21.7	-	9.8
Semimembranosus	9.1	22.7	9.5	9.9	11.7	6.6	8.8
Semitendinosus	10.5	23.6	-	9.9	18.6	4.5	10.2
Biceps femoris (Long head)	8.4	22.4	8.6	10.3	11.0	2.7	8.1
Biceps femoris (Short head)	4.2	11.0	6.1	5.4	6.1	-	4.2
SHANK							
Tibialis anterior	5.9	20.4	-	13.4	7.6	3.9	5.4
Extensor digitorum longus	3.9	23.6	-	18.1	9.0	5.0	3.4
Extensor hallucis longus	1.8	17.8	-	9.2	8.0	5.1	1.7
Peroneus longus	2.7	11.8	3.9	17.7	4.5	9.2	2.2
Peroneus brevis	1.5	13.1	-	11.1	6.1	2.4	1.2
Soleus	5.3	16.9	-	11.5	5.8	4.7	5.2
Gastrocnemius medialis	8.3	19.9	9.0	14.8	6.2	5.0	6.9
Gastrocnemius lateralis	11.8	20.4	8.0	10.9	6.7	5.0	11.8
Plantaris	-	-	-	-	-	-	-
Tibialis posterior	6.1	19.6	-	17.9	4.9	13.1	5.3
Flexor tibialis	4.1	21.7	-	13.6	6.4	6.4	3.5
Flexor fibularis	15.4	22.9	-	17.4	8.3	6.3	13.6
Popliteus	3.2	7.8	5.6	-	3.1	1.4	3.2

Appendix 2.1c.

H. moloch

THIGH	Mass (g)	MTU Length (cm)	Tendon Length Origin	Tendon Length Insertion	Mean Fascicle Length (cm)	Ext. Tendon length (cm)	Est. Belly Mass (g)
Gluteus superficialis	41.1	14.7	-	3.1	10.0	-	41.1
Gluteus medius	24.4	10.0	-	5.3	5.6	-	24.4
Gluteus minimus	5.5	4.9	-	1.5	3.5	-	5.5
Pectineus	2.3	5.1	-	-	4.3	-	2.3
Obturator internus	6.2	5.8	-	3.6	3.1	-	6.2
Obturator externus	4.8	4.9	-	2.5	2.7	-	4.8
Piriformis	3.9	7.0	-	3.3	4.7	-	3.9
Adductor magnus	53.5	18.6	-	7.1	11.9	-	53.5
Adductor longus	5.0	11.4	1.5	4.1	7.7	-	5.0
Adductor brevis	2.3	6.2	-	-	6.2	-	1.2
Quadratus femoris	3.6	4.5	-	-	3.6	-	3.6
Rectus femoris	9.9	18.8	11.6	12.9	7.0	2.8	9.6
Vastus medialis	15.4	21.1	-	13.6	7.5	-	15.2
Vastus intermedius	21.5	20.2	-	16.3	7.3	-	21.5
Vastus lateralis	23.9	17.5	8.9	12.2	7.5	3.1	23.4
Gracilis	8.4	20.0	-	4.4	17.0	-	8.4
Sartorius	12.1	22.5	3.6	4.4	19.4	-	12.1
Semimembranosus	8.2	22.3	8.6	8.8	10.1	4.7	8.2
Semitendinosus	13.9	22.5	2.9	6.1	15.5	3.8	13.7
Biceps femoris (Long head)	9.5	22.4	9.4	8.9	10.4	1.6	9.1
Biceps femoris (Short head)	4.7	7.0	-	7.5	4.6	-	4.7
SHANK							
Tibialis anterior	6.5	18.3	-	12.8	6.3	3.2	6.2
Extensor digitorum longus	3.1	21.0	-	9.5	7.3	3.8	3.1
Extensor hallucis longus	1.6	16.7	-	8.6	7.3	5.8	1.6
Peroneus longus	4.6	20.0	-	16.9	4.5	9.7	4.2
Peroneus brevis	1.7	14.2	-	10.2	3.8	-	1.7
Soleus	8.6	16.9	13.8	-	5.9	2.4	8.1
Gastrocnemius medialis	8.1	19.6	7.6	15.9	5.8	9.3	6.7
Gastrocnemius lateralis	11.1	19.7	6.7	14.2	6.4	11.1	11.1
Plantaris	2.4	7.5	-	-	2.9	-	1.2
Tibialis posterior	5.6	19.5	-	16.1	5.3	5.6	5.2
Flexor tibialis	3.3	18.5	-	14.2	6.0	5.0	3.0
Flexor fibularis	12.2	22.0	-	16.6	7.4	6.6	11.1
Popliteus	2.7	5.7	3.9	-	2.3	-	2.7

Appendix 2.1d.

S. syndactylus

THIGH	Mass (g)	MTU Length (cm)	Tendon Length Origin	Tendon Length Insertion	Mean Fascicle Length (cm)	Ext. Tendon length (cm)	Est. Belly Mass (g)
Gluteus superficialis	78.2	18.5	6.0	7.9	11.0	-	78.2
Gluteus medius	52.8	13.7	-	7.9	7.1	-	52.8
Gluteus minimus	8.3	6.5	-	3.4	4.3	-	8.3
Pectineus	6.8	7.1	-	6.5	6.5	-	5.1
Obturator internus	13.7	7.7	-	4.9	4.3	-	13.7
Obturator externus	13.1	7.0	-	3.8	4.0	-	13.1
Piriformis	8.2	9.9	-	4.7	5.5	-	8.2
Adductor magnus	101.9	20.6	3.1	8.5	13.8	5.1	101.6
Adductor longus	10.1	12.1	2.4	1.4	10.0	-	10.1
Adductor brevis	6.2	8.3	-	2.3	7.3	-	3.1
Quadratus femoris	7.5	5.3	-	1.0	4.8	-	7.5
Rectus femoris	22.9	21.3	13.4	14.4	9.4	1.5	22.1
Vastus medialis	24.0	19.1	-	12.8	8.6	-	12.0
Vastus intermedius	52.6	21.4	-	10.8	8.3	-	39.5
Vastus lateralis	56.4	19.2	8.0	13.6	8.5	-	28.2
Gracilis	20.7	24.2	1.4	5.3	20.0	3.2	20.6
Sartorius	22.4	25.2	4.9	5.7	21.7	4.6	22.3
Semimembranosus	15.5	23.6	10.5	8.2	11.4	6.6	15.0
Semitendinosus	29.6	26.3	-	8.5	19.0	4.3	29.2
Biceps femoris (Long head)	18.2	24.7	11.0	9.7	11.4	4.8	17.9
Biceps femoris (Short head)	8.7	12.0	-	6.5	6.7	-	8.7
SHANK							
Tibialis anterior	15.8	19.1	-	12.0	8.0	2.7	15.1
Extensor digitorum longus	7.3	25.8	-	18.7	9.3	12.3	6.3
Extensor hallucis longus	3.4	19.0	-	12.1	7.4	9.0	3.1
Peroneus longus	10.5	21.9	-	17.8	6.8	7.5	9.6
Peroneus brevis	3.9	11.4	-	9.1	3.9	4.0	3.6
Soleus	19.3	17.3	13.4	-	6.6	3.8	18.7
Gastrocnemius medialis	25.8	20.1	7.8	14.3	7.0	4.7	23.3
Gastrocnemius lateralis	25.7	20.5	9.5	14.5	7.2	5.5	18.7
Plantaris	-	-	-	-		-	0.0
Tibialis posterior	11.2	20.0	-	12.6	6.5	4.9	10.4
Flexor tibialis	12.3	22.9	-	17.5	8.2	11.2	11.5
Flexor fibularis	25.5	26.6	-	20.2	9.4	14.3	23.6
Popliteus	11.1	10.9	4.0	11.4	4.3	-	11.1

Appendix 3.1a.

Hip

Muscle	Polynomial Order	RSS/Range (%)	Coefficients g	f	e	d	c	b	a
Adductor magnus	3	3.2					-4.7E-06	2.3E-03	-1.3E-01
Gluteus medius	4	1.2				-9.7E-08	2.8E-05	-2.5E-03	8.4E-02
Gluteus superficialis	6	1.2		2.8E-10	-1.1E-07	1.6E-05	-1.1E-03	3.2E-02	-3.3E-01
Rectus femoris	4	3.1				1.4E-07	-3.8E-05	2.9E-03	-1.1E-01
Gracilis	6	1.1		2.6E-10	-1.2E-07	2.2E-05	-1.7E-03	6.0E-02	-7.3E-01
Sartorius	4	2.8				-2.9E-07	9.4E-05	-1.0E-02	2.8E-01
Biceps femoris	Lin.	2.7						-5.9E-04	1.8E-01
Semimembranosus	6	4.7		1.7E-11	-8.0E-09	1.4E-06	-1.0E-04	3.1E-03	1.0E-01
Semitendinosus	Lin.	41.7						2.4E-04	7.9E-02

Knee

Rectus femoris	3	1.9					-3.5E-06	6.3E-04	4.0E-04
Vastus lateralis	4	2.2				8.0E-08	-3.0E-05	3.5E-03	-6.2E-02
Gracilis	7	1.1	-2.0E-12	1.2E-09	-3.0E-07	3.6E-05	-2.2E-03	6.4E-02	-7.1E-01
Sartorius	5	1.9			-3.1E-09	1.1E-06	-1.1E-04	3.0E-03	-6.0E-02
Biceps femoris	4	4.0				-1.0E-07	3.1E-05	-2.4E-03	1.6E-02
Semimembranosus	3	4.2					1.9E-06	-2.7E-04	-2.1E-02
Semitendinosus	4	1.2				1.2E-07	-1.8E-05	-1.2E-04	-1.0E-01
Gastrocnemius lat.	6	3.1		-7.1E-11	3.0E-08	-4.6E-06	3.4E-04	-1.3E-02	1.4E-01
Gastrocnemius med.	3	2.0					1.2E-05	-2.5E-03	7.2E-02

Ankle

Gastrocnemius lat.	6	3.8		1.8E-10	-7.3E-08	9.7E-06	-4.4E-04	-1.1E-03	3.6E-01
Gastrocnemius med.	5	3.1			1.3E-08	-4.7E-06	5.8E-04	-2.5E-02	3.8E-01
Soleus	6	4.4		-5.3E-10	2.4E-07	-4.0E-05	3.0E-03	-9.9E-02	1.2E+00

Appendix 3.1b. Polynomial approximations to describe the *MA* curves of *Hylobates moloch*

Muscle	Polynomial Order	RSS/Range (%)	Coefficients g	f	e	d	c	b	a
Hip									
Adductor magnus	4	2.4				-1.2E-07	3.6E-05	-2.4E-03	4.3E-02
Gluteus medius	Lin.	4.8						4.0E-04	-2.5E-02
Gluteus superficialis	4	3.6				1.2E-07	-5.3E-05	7.6E-03	-3.5E-01
Rectus femoris	5	4.5			-5.6E-09	2.2E-06	-3.6E-04	2.6E-02	-7.9E-01
Gracilis	4	1.4				-6.1E-07	1.4E-04	-6.9E-03	-8.9E-02
Sartorius	3	2.1					1.1E-05	-1.6E-03	-4.3E-02
Biceps femoris	4	4.5				-7.2E-08	-1.0E-05	4.3E-03	-9.8E-02
Semimembranosus	5	0.6			6.1E-09	-2.4E-06	3.0E-04	-1.3E-02	2.2E-01
Semitendinosus	3	1.9					-2.6E-05	6.0E-03	-1.8E-01
Knee									
Rectus femoris	3	4.6					-4.4E-06	9.3E-04	-1.2E-02
Vastus lateralis	3	3.4					-3.3E-06	6.2E-04	1.7E-02
Gracilis	5	2.1			-1.9E-09	8.5E-07	-1.2E-04	3.8E-03	-2.4E-02
Sartorius	4	3.8				3.8E-08	2.5E-06	-1.8E-03	-7.3E-03
Biceps femoris	4	3.4				3.0E-08	-1.1E-05	1.5E-03	-7.6E-02
Semimembranosus	5	1.2			-9.0E-10	3.9E-07	-5.7E-05	3.2E-03	-8.7E-02
Semitendinosus	4	2.4				-7.4E-08	4.6E-05	-8.1E-03	2.5E-01
Gastrocnemius lat.	6	2.7		1.6E-11	-1.0E-08	2.2E-06	-2.0E-04	7.8E-03	-1.5E-01
Gastrocnemius med.	5	1.3			-1.3E-09	5.9E-07	-8.8E-05	4.7E-03	-9.0E-02
Ankle									
Gastrocnemius lat.	6	2.0		1.9E-10	-6.8E-08	7.7E-06	-3.0E-04	1.6E-03	1.4E-01
Gastrocnemius med.	5	0.9			1.2E-08	-3.8E-06	4.0E-04	-1.3E-02	1.5E-01
Soleus	7	4.3	-1.6E-11	8.5E-09	-1.7E-06	1.8E-04	-9.5E-03	2.4E-01	-1.9E+00
Tibialis anterior	6	3.3		-3.6E-10	1.2E-07	-1.4E-05	7.3E-04	-1.6E-02	-1.6E-03

Appendix 3.1c. Polynomial approximations to describe the *MA* curves of *Hylobates syndactylus* 1

Muscle	Polynomial Order	RSS/Range (%)	Coefficients f	e	d	c	b	a
Hip								
Adductor magnus	3	4.8				-9.3E-06	2.8E-03	-1.8E-01
Gluteus superficialis	4	4.8			-4.6E-07	1.1E-04	-8.4E-03	2.2E-01
Rectus femoris	5	2.2		-1.5E-08	4.8E-06	-5.2E-04	2.2E-02	-3.7E-01
Gracilis	4	4.4			-2.6E-07	4.5E-05	4.9E-04	-2.4E-01
Sartorius	5	0.6		-1.0E-08	3.3E-06	-3.4E-04	1.1E-02	-9.9E-02
Biceps femoris	5	4.0		2.6E-09	-4.2E-07	-5.5E-05	1.1E-02	-2.2E-01
Semitendinosus	5	0.8		5.7E-09	-1.8E-06	1.6E-04	-1.7E-03	-7.4E-02
Knee								
Rectus femoris	Lin.	4.0					3.0E-04	-1.3E-03
Vastus lateralis	5	2.0		3.1E-09	-1.4E-06	2.2E-04	-1.4E-02	3.3E-01
Gracilis	3	4.8				2.0E-05	-5.3E-03	1.3E-01
Sartorius	6	0.3	5.4E-10	-2.7E-07	5.1E-05	-4.5E-03	1.9E-01	-2.8E+00
Biceps femoris	4	3.3			-2.6E-07	6.8E-05	-5.8E-03	1.5E-01
Semitendinosus	5	2.8		-4.4E-09	2.1E-06	-3.2E-04	1.8E-02	-4.2E-01
Gastrocnemius lat.	4	3.9			-3.5E-07	1.3E-04	-1.5E-02	4.6E-01
Gastrocnemius med.	3	4.4				1.2E-05	-2.4E-03	6.1E-02
Ankle								
Gastrocnemius lat.	5	1.3		1.3E-08	-5.6E-06	8.5E-04	-5.1E-02	1.1E+00
Gastrocnemius med.	5	4.1		2.4E-08	-1.0E-05	1.5E-03	-9.5E-02	2.1E+00
Soleus	5	3.3		2.4E-08	-8.9E-06	1.1E-03	-5.6E-02	8.7E-01
Tibialis anterior	4	1.4			-1.9E-07	5.7E-05	-5.1E-03	1.2E-01

Appendix 3.1d. Polynomial approximations to describe the *MA* curves of *Hylobates syndactylus* 2

Muscle	Polynomial Order	RSS/Range (%)	Coefficients							
			h	g	f	e	d	c	b	a
Hip										
Adductor magnus	Lin.	4.3							8.8E-04	-8.1E-02
Gluteus superficialis	5	2.4				7.0E-09	-2.6E-06	3.4E-04	-1.8E-02	3.6E-01
Rectus femoris	7	3.3		7.8E-12	-3.7E-09	6.8E-07	-5.9E-05	2.4E-03	-3.2E-02	-2.4E-01
Gracilis	3	2.2						-1.9E-05	4.9E-03	-3.0E-01
Sartorius	5	1.3				-1.4E-08	4.0E-06	-3.8E-04	1.1E-02	-1.1E-01
Biceps femoris	5	1.6				4.5E-09	-1.2E-06	8.2E-05	1.1E-03	-2.4E-02
Semimembranosus	5	1.9				3.8E-09	-1.2E-06	1.1E-04	-1.9E-03	5.0E-02
Semitendinosus	5	3.3				1.1E-08	-3.2E-06	2.9E-04	-7.4E-03	8.0E-02
Knee										
Rectus femoris	8	1.8	2.0E-13	-1.6E-10	5.3E-08	-9.5E-06	1.0E-03	-6.0E-02	1.9E+00	-2.5E+01
Vastus lateralis	4	3.1					9.6E-08	-3.9E-05	5.0E-03	-1.5E-01
Gracilis	3	3.9						1.5E-05	-2.4E-03	-1.5E-01
Sartorius	5	0.5				-5.1E-09	2.2E-06	-3.1E-04	1.6E-02	-3.7E-01
Biceps femoris	4	3.1					-1.3E-07	3.7E-05	-2.5E-03	-2.5E-02
Semimembranosus	4	2.2					-1.6E-07	5.1E-05	-4.7E-03	8.1E-02
Semitendinosus	3	3.8						2.7E-05	-4.5E-03	-2.1E-02
Gastrocnemius lat.	4	3.6					-2.7E-07	6.7E-05	-4.8E-03	5.3E-02
Gastrocnemius med.	Lin.	69.5							-4.6E-05	-3.1E-02
Ankle										
Gastrocnemius lat.	5	1.5				4.0E-09	-1.7E-06	2.5E-04	-1.4E-02	2.8E-01
Gastrocnemius med.	6	1.3			8.6E-11	-4.0E-08	6.7E-06	-5.1E-04	1.8E-02	-2.3E-01
Soleus	5	4.7				4.9E-09	-2.3E-06	3.8E-04	-2.5E-02	6.1E-01
Tibialis anterior	3	3.0						2.3E-05	-3.9E-03	8.5E-02

RSS, residual sum of squares; Lin., linear curve fit.

Appendix 6.1.

Inputs	A	B	% difference
Leap distance (R, m)	5.41	5.37	0.60
Leap angle (α, °)	-30.75	-30.22	1.76
PE loss (Jkg^{-1})	23.43	23.02	1.80
Take-off angle (φ, °)	17.00	15.18	12.02
Resultant velocity (U, ms^{-1})	6.74	8.55	-22.25
Outputs			
Optimum take-off angle (φ_{OPT}, °)	29.62	29.89	-0.90
Total energy, measured (E_M, Jkg^{-1})	42.16	55.70	-24.31
Total energy at $KE_{M\Phi}$ ($E_{M\Phi}$, Jkg^{-1})	37.26	37.34	-0.21
Total energy at KE_{Mmin} (E_{Mmin}, Jkg^{-1})	36.39	36.11	0.77
Total energy at $KE_{45°}$ ($E_{M45°}$, Jkg^{-1})	23.79	23.71	0.30
Peak power, measured (P_{MPeak}, Wkg^{-1})	260.86	176.59	32.31
Mean power, measured (P_{Mmean}, Wkg^{-1})	85.35	76.14	10.80
Mean power at $KE_{M\Phi}$ ($P_{Mmean\Phi}$, Wkg^{-1})	38.41	39.78	-3.44
Mean power at KE_{Mmin} ($P_{Mmean\text{-}min}$, Wkg^{-1})	35.99	36.37	-1.04
Mean power at $KE_{45°}$ ($P_{Mmean\text{-}45°}$, Wkg^{-1})	66.07	65.87	0.30